

**EFFECTS OF CHEMICAL ADDITIVES
ON THE LIGHT WEIGHT PAPER**

A Dissertation

Presented to

The Academic Faculty

By

Jin Liu

In Partial Fulfillment

Of the Requirements for the Degree

Doctor of Philosophy in Chemical Engineering

Georgia Institute of Technology

October 2004

Copyright 2004 by Jin Liu

EFFECTS OF CHEMICAL ADDITIVES
ON THE LIGHT WEIGHT PAPER

Approved by:

Dr. Jeffery S. Hsieh, Advisor

Dr. Jeff Empie

Dr. Peter Ludovice

Dr. Hiroki Nanko

Dr. Arthur Ragauskas

Dr. Matthew Realff

October 12, 2004

ACKNOWLEDGEMENTS

I would like to express my sincere gratitude to my thesis advisor, Dr. Jeffery S. Hsieh, who gave me many good suggestions during my Ph.D. study. I also want to thank Dr. Hsieh for sharing his industrial experience, and for the opportunities provided for my professional growth. My thanks are expressed to the thesis committee members, Dr. Jeff Empie, Dr. Peter Ludovice, Dr. Jeffery Morris, Dr. Hiroki Nanko, Dr. Arthur Ragauskas and Dr. Matthew Realff for their valuable discussions and suggestions.

The technical discussions and guidance from Julie Yoh, Bob Schiesser, Paul Hoffman, Jeffery Herman, Giff Scarborough and Nicholas Lazorisak are sincerely appreciated. Gratitude is also extended to Craig Poffenberger and William Zeman of Goldschmidt Chemical Corporation for providing the debonding agent samples and technical insights. I am thankful to Jennifer Meeks and Chris Gilbert, who made great contributions to the project in the fall 1997.

I am grateful to Chai Xinsheng and Luo Qi who offered critical help on the chemical analysis using the UV method. Xinsheng's passion for the scientific research gave me inspiration, and I have greatly benefited from the discussions with him. Bill Anderson generously taught me how to use the profilometer, and Cheng Jianchun is acknowledged for sharing his expertise on digital signal processing. Alice Gu provided help on the measurement of the zeta potential of the pulp solutions. I also had the privilege of

discussing many technical problems with Yan Zegui in the field of wet end chemistry. I am grateful toward Steve Woodard for his help using the laser scanning confocal microscope.

The encouragement and fellowship of friends in the Pulp and Paper Engineering group at Georgia Tech are greatly appreciated. The individuals are Jason Smith, Wei Wang, Ahmed Baosman, Peter Long, Jeff Stevens, Chhaya Agrawal and Sam Fanday. The following undergraduate students are acknowledged for their help on some of the experiments: Nathan McGowan, Tim Otchy and Felton Corbert. Especially worth mentioning are Nathan and his wife Sharon went beyond their duty and finished the wicking test early one Saturday morning.

I would like to thank Ray Dunbrack, Anita Woodruff of M/K Systems Inc., and Anthony Linares, Jr. of Pro-Tech Instruments, Inc. for their help on the start-up of the M/K automatic sheet former. I want to thank Calvin Brock of the Georgia Power Company for his significant contribution to the setup of the sheet former. Without his help, the success of the former installation would be unimaginable. Dennis Gunderson of Mu Measurement Inc. provided great help on the measurement of tissue surface friction measurement. I would like to acknowledge his constant support and patience through out this project.

I want to thank my dear friends at the Technology Applications Center of Georgia Power Company for their friendship and support of my study: Gary Birdwell, Gloria Walters, Jane Hill, Bill Pasley, Jim Leben, Bill Studstill, Rick Ranhotra, Jack Ballard and

David Hood. A special acknowledgement goes to Gary Birdwell who provided the generous support for the on-going projects. Thanks go to Bill Pasley for his witness for the LORD, his encouragement, love and prayer; I am truly thankful for his trust and support. Thanks go to Gloria Walters for being one of my buddies and for sharing in my joys and sorrows.

Thanks go to Yu Wenbing, Li Yawei, Feng Hua, Zhang Jing, Lin Yimeng, Sun Song, Shi Bing, Chen Yue, Liu Tao, Wang Duyuan, Yang Ning, and Xu Yufeng for their friendship and delightful discussions.

Sincere thanks are also extended to many friends in my home Church: Jeremy Noonan, Archie Parrish, Al Lacour, Joel and Weese Whitworth, Doug and Margie Mallow, Scott Stephenson, Bill Hollberg, Bo Simpson, Steve Marcs, Ronald Huges, Thad Persons, John Gunter, Phil Autry and many others. I thank them for their fellowship, guidance and prayer during my spiritual pilgrimage. Thanks to Jennifer Meeks for her beautiful testimony for Christ, and thanks to Trudy Walker and Shirley Whitfield for their solid faith in the LORD and for sharing faith with me. I would like to thank Elizabeth Bolton and Keith Green for proofreading the thesis and correcting grammars.

My parents, Duanlin Liu and Xurong Guo, my younger brother and sister-in-law, Xun Liu and Ke Zhao, have given me constant encouragement. Their love and faith have helped me to endure the difficulties, to develop optimistic attitude when it has been hard, and to always do my best.

My deepest appreciation goes to the LORD, whose infinite wisdom has become more and more visible to me during my final Doctorate research. I thank Him who brought the men and women aforementioned into my life to help the thesis completion in many wonderful ways. All the glory and honor belong to Him.

TABLE OF CONTENTS

| | |
|---------------------------|-----------|
| Thesis Approval Page | ii |
| Acknowledgement | iii |
| Table of Contents | vii |
| List of Tables | xii |
| List of Figures | xiv |
| Summary | xx |
| 1. Introduction | 1 |
| 1.1 Introduction | 1 |
| 1.2 Thesis Objectives | 5 |
| 1.3 Research Significance | 6 |
| 1.4 Thesis Structure | 7 |
| 1.5 References | 8 |
| 2. Background | 12 |

| | |
|---------------------------------------|--------|
| 2.1 Introduction | 12 |
| 2.2 Tissue Properties | 13 |
| 2.3 Tissue Manufacturing | 29 |
| 2.4 Fundamentals of wood fiber | 35 |
| 2.5 Tissue Chemical Additives | 40 |
| 2.6 References | 50 |
| 3. Experimental | 59 |
| 3.1 Introduction | 59 |
| 3.2 Chemical Adsorption Study | 60 |
| 3.3 Preparations for Making Handsheet | 71 |
| 3.4 TAPPI Handsheet Making | 75 |
| 3.5 Sheet Physical Testing | 79 |
| 3.6 Zeta Potential Measurement | 83 |
| 3.7 Confocal Microscopy | 85 |
| 3.8 References | 86 |

| | |
|---|----------------|
| 4. Adsorption of Wet Strength Resin and Debonding Agents on Cellulose Fibers | 88 |
| 4.1 Introduction | 88 |
| 4.2 Results and Discussion | 89 |
| 4.2.1. Adsorption of Kymene [®] 1500 on cellulose fiber | 89 |
| 4.2.2. Adsorption of Softrite [®] 7516 on cellulose fiber | 107 |
| 4.2.3. Simultaneous competitive adsorption of Kymene and Softrite | 119 |
| 4.3 Conclusions | 125 |
| 4.4 References | 126 |
| 5. Chemical Additive Effects on Sheet Properties | 129 |
| 5.1 Introduction | 129 |
| 5.2 Results and Discussions | 130 |
| 5.2.1 Confocal microscopy | 130 |
| 5.2.2. Handsheet softness | 135 |
| 5.2.3 Effects of wet strength resin on sheet properties | 137 |
| 5.2.4 Effects of debonding agent on sheet properties | 154 |
| 5.2.5. Effects of dual additives on sheet properties | 170 |

| | |
|---|-----|
| 5.3 Conclusions | 184 |
| 5.4 References | 185 |
| 6. Effects of New Debonding Agents on Sheet properties | 187 |
| 6.1 Introduction | 187 |
| 6.2 Results | 191 |
| 6.2.1 Effects of fatty acids on debonder's function | 191 |
| 6.2.2 Effects of ethoxylation degree on debonder's function | 200 |
| 6.3 Discussion | 210 |
| 6.4. Conclusions | 217 |
| 6.5 References | 218 |
| 7. Conclusions and Recommendations | 220 |
| 7.1 Conclusions | 220 |
| 7.2 Recommendations | 222 |
| Appendix A: Characterization of Tissue Softness | 225 |

| | |
|---|-----|
| Appendix B: Matlab Code for Tissue Surface Profile | 268 |
| Appendix C: Fiber Quality Analysis Results | 272 |
| Appendix D: Effects of Pulp Quality Variation on Tissue Qualities | 278 |
| Appendix E: M/K Automatic Sheetformer Operation Procedure | 295 |
| Vita | 308 |

LIST OF TABLES

| Table | | Page |
|-------|--|------|
| 3.1 | The experimental design for the chemical adsorption study | 69 |
| 3.2 | Physical properties of the wet strength resin, Kymene [®] 1500 | 74 |
| 3.3 | Physical properties of Softrite [®] 7516 | 74 |
| 3.4 | The experimental design for chemical application unto handsheet | 76 |
| 3.5 | The conditions used for zeta potential measurement | 84 |
| 6.1 | ANOVA results for sheet water absorbency property | 213 |
| 6.2 | ANOVA results for sheet tensile strength | 213 |
| 6.3 | ANOVA results for sheet bulk | 214 |
| 6.4 | ANOVA results for sheet stiffness | 214 |
| 6.5 | ANOVA results for sheet reduced softness | 215 |
| A2.1 | Power function exponents from group averaged subjective magnitude estimation | 234 |
| A3.1 | Parameters used in the tissue profile scanning by the HommelWerke LV-50 Surface Profilometer | 237 |
| A3.2 | Settings of TA Model89-100 electronic thickness tester | 239 |
| A4.1 | Correlation between measured physical properties and softness ranking | 242 |

| | | |
|------|---|-----|
| A4.2 | The correlation results of tissue softness with modulus | 243 |
| A4.3 | The correlation results of the tissue softness with surface profile parameters | 248 |
| A4.4 | The correlation results of the tissue softness with tissue Handle-O-Meter readings | 255 |
| A4.5 | The correlation results of the tissue softness with thickness values | 256 |
| A4.6 | The correlation results of compressibility factors with tissue softness | 257 |
| A4.7 | The correlation results of the thermal flux with tissue softness | 260 |
| A4.8 | The results of multi-variable softness correlation | 261 |
| D.1 | Parameters used in the data statistical analysis | 288 |
| D.2 | Correlation of tissue properties with pulp testing data only | 289 |
| D.3 | Correlation of tissue properties with pulp and process data | 290 |
| D.4 | Correlation of tissue properties with pulp testing data selected in the best subset regression of study (B) | 291 |

LIST OF FIGURES

| Figure | | Page |
|---------|---|------|
| 2.1 (a) | Surface softness evaluation | 14 |
| 2.1 (b) | Bulk softness evaluation | 14 |
| 2.2 | Schematic showing the formation of hydrogen bonds between two adjacent fibers | 25 |
| 2.3 | The diagram showing the commercial tissue production | 34 |
| 2.4 | Schematic that illustrates the wood fiber wall | 36 |
| 2.5 | Schematic of the electrical double layer on a negatively charged particle | 39 |
| 2.6 | The chemical reactions to retain the wet strength of cellulose web | 43 |
| 2.7 | The structure of traditional debonding agent | 47 |
| 2.8 (a) | Two extreme structures of imidazolinium compound | 48 |
| 2.8 (b) | Diester dialkyl dimethyl quaternary ammonium compound | 48 |
| 2.9 | The biodegradation of debonding agent containing ester functionalities | 49 |
| 3.1 | Calibration curve for Kymene [®] 1500 solution | 66 |
| 3.2 | Calibration curve for Softrite [®] 7516 solution | 67 |

| | | |
|------|--|-----|
| 3.3 | Schematic of experimental apparatus for chemical adsorption study | 68 |
| 3.4 | Typical time-dependent UV/Vis absorption spectra for the wet strength resin solution | 70 |
| 3.5 | Series of confocal images showing the cross sectioning of a tissue sample | 87 |
| 4.1 | Graph of adsorbed amount of Kymene [®] 1500 versus time | 90 |
| 4.2 | Graph of Kymene [®] 1500 adsorption versus time | 91 |
| 4.3 | Graph showing model predictions at 0.25 percent Kymene concentration | 95 |
| 4.4 | Graph showing model predictions at 0.5 percent Kymene concentration | 96 |
| 4.5 | Graph showing model predictions at 1.0 percent Kymene concentration | 97 |
| 4.6 | Effects of Kymene [®] 1500 on system's zeta potential | 102 |
| 4.7 | Graph of $k_d N_0$ and k_d versus initial Kymene concentration | 105 |
| 4.8 | Graph of adsorption percentage prediction versus time for infinite dilution | 106 |
| 4.9 | Graph of Softrite [®] 7516 adsorption versus time at 0.6 percent fiber consistency | 108 |
| 4.10 | Graph of adsorbed amount of Softrite [®] 7516 versus time | 109 |
| 4.11 | Graph of Softrite [®] 7516 adsorption versus time at 1.2 percent fiber consistency | 110 |
| 4.12 | Graph of $-\ln(1-A_d)$ versus time for Softrite [®] 7516 adsorption at 0.25, 0.75 percent and 0.6 percent consistency | 112 |
| 4.13 | The orientation of ionic surfactants on the negatively charged surface | 115 |
| 4.14 | Effects of Softrite [®] 7516 on the system's zeta potential | 117 |

| | | |
|------|--|-------|
| 4.15 | Graph of simultaneous competitive adsorption of Kymene and Softrite onto fibers at 1.2 percent consistency | 120 |
| 4.16 | Graph of simultaneous competitive adsorption of Kymene and Softrite at 0.6percent consistency (S=30ppm) | 121 |
| 4.17 | Graph of simultaneous competitive adsorption of Kymene and Softrite at 0.6percent consistency (S=90ppm) | 123 |
| 5.1 | Confocal optical slice showing the fiber structure of control and those with chemical treatment | 132-4 |
| 5.2 | The sheet softness in reduced form as a function of reduced tensile strength and reduced Handle-O-Meter stiffness. | 136 |
| 5.3 | Effects of Kymene [®] 1500 addition on sheet wet tensile index | 142 |
| 5.4 | Effects of Kymene [®] 1500 addition on handsheet dry tensile index | 143 |
| 5.5 | Effects of Kymene [®] 1500 addition on the ratio of handsheet wet tensile index to dry tensile index. | 144 |
| 5.6 | Effects of Kymene [®] 1500 addition on the handsheet wet and dry tensile index in reduced form. | 145 |
| 5.7 | Effects of Kymene [®] 1500 addition on the Handle-O-Meter stiffness of handsheet | 147 |
| 5.8 | Effects of Kymene [®] 1500 addition on the bulk of handsheet | 148 |
| 5.9 | Effects of Kymene [®] 1500 addition on the total water absorbency of handsheet | 151 |
| 5.10 | Effects of Kymene [®] 1500 addition on the sheet reduced softness | 152 |
| 5.11 | Effects of Softrite [®] 7516 application on the sheet wet tensile index | 158 |
| 5.12 | Effects of Softrite [®] 7516 application on sheet dry tensile index | 159 |
| 5.13 | Effects of Softrite [®] 7516 addition on the reduced wet tensile index and reduced dry tensile index. | 160 |
| 5.14 | Effects of Softrite [®] 7516 addition on the sheet Handle-O-Meter stiffness | 163 |

| | | |
|------|--|--------|
| 5.15 | Effects of Softrite®7516 addition on sheet bulk | 164 |
| 5.16 | Effects of Softrite®7516 addition on the sheet total water absorbency | 167 |
| 5.17 | Effects of Softrite®7516 addition on reduced sheet softness | 168 |
| 5.18 | Effects of combined application of Softrite®7516 and Kymene®1500 on the sheet wet tensile strength | 174 |
| 5.19 | Effects of combined application of Softrite®7516 and Kymene®1500 on sheet dry strength | 175 |
| 5.20 | Effects of combined application of Softrite®7516 and Kymene®1500 on sheet Handle-O-Meter stiffness | 177 |
| 5.21 | Effects of combined application of Softrite®7516 and Kymene®1500 on sheet bulk | 178 |
| 5.22 | Effects of combined application of Softrite®7516 and Kymene®1500 on sheet water absorbency | 182 |
| 5.23 | Effects of combined application of Softrite®7516 and Kymene®1500 on sheet reduced softness | 183 |
| 6.1 | The preparation steps of the new class of debonding agent | 189-90 |
| 6.2 | Effects of fatty acid on the sheet TWA property | 194 |
| 6.3 | Effects of fatty acid in the debonder structure on the sheet tensile strength | 195 |
| 6.4 | Effects of fatty acid in the softener structure on the sheet bulk | 196 |
| 6.5 | Effects of fatty acid in the debonder on the sheet Handle-O-Meter stiffness | 198 |
| 6.6 | Effects of fatty acid in the debonder on sheet reduced softness | 199 |
| 6.7 | Effects of degree of ethoxylation of debonder on sheet total water absorbency property | 204 |
| 6.8 | Effects of degree of ethoxylation of debonder on sheet tensile strength | 205 |

| | | |
|------|--|-----|
| 6.9 | Effects of degree of ethoxylation of debonder on the sheet bulk | 206 |
| 6.10 | Effects of degree of ethoxylation on the sheet Handle-O-Meter stiffness | 208 |
| 6.11 | Effects of degree of ethoxylation of debonder on the sheet reduced softness | 209 |
| A4.1 | The correlation of tissue softness with the tensile index in machine direction and tensile index ratio | 244 |
| A4.2 | The power law correlation of tissue softness with elastic modulus in the machine direction | 245 |
| A4.3 | The facial tissue surface profile obtained by stylus profilometry and the filtered profile | 249 |
| A4.4 | The power law correlation of tissue softness with arithmetic mean roughness and mean square roughness | 250 |
| A4.5 | Facial tissue surface profiles with filtering treatment | 251 |
| A4.6 | The power law correlation of tissue softness with PAAREA_EQ | 252 |
| A4.7 | Comparison of tissue softness by the panelists and by the 3-parameter softness model | 263 |
| A4.8 | Testing of softness model for samples by creping and through-air drying technologies | 264 |
| B.1 | The filter values as a function of the finger motion frequency | 271 |
| C.1 | Softwood fiber length histogram | 274 |
| C.2 | Softwood fiber curl index histogram | 275 |
| C.3 | Hardwood fiber length histogram | 276 |
| C.4 | Hardwood fiber curl index histogram | 277 |
| D.1 | Pulp tensile data for within-a-lot variation | 285 |

| | | |
|-----|--|-----|
| D.2 | Pulp freeness data for within-a-lot variation | 285 |
| D.3 | Pulp bulk data for within-a-lot variation | 286 |
| D.4 | Pulp tensile data for inter-lot variation | 286 |
| D.5 | Pulp freeness data for inter-lot variation | 287 |
| D.6 | Pulp bulk data for inter-lot data | 287 |
| D.7 | Pulp factor weight for tissue product properties | 292 |
| E.1 | M/K 9000 Fully Automatic Sheetformer | 297 |

SUMMARY

Tissue, among the highest value added paper products, finds extensive application in modern society. Continued efforts are being made to further improve tissue properties, such as strength, softness and water absorbency. Besides the efforts on characterizing facial tissue softness, this study focuses on tissue quality improvement through chemical means. The application of a wet strength resin, Kymene[®]1500 and a debonding agent, Softrite[®]7516 onto cellulose fibers is considered.

First, the adsorption kinetics of the two chemical additives onto cellulose fibers was studied. The adsorption mechanisms were proposed and validated by kinetic data. A novel apparatus was designed in this study, and represented the first in the field to collect real-time data, which has the potential to be applied to the adsorption kinetic study of other types of paper additives.

Second, the effects of Kymene[®]1500 and Softrite[®]7516 on various sheet properties were studied. The results provide quantitative information on tissue additives' effects on sheet properties. It is shown that the combined application of the additives can overcome the disadvantages of individual species and produce sheets with both wet strength and softness.

Finally, environmental-benign debonding agents with polyoxyethylene chains were applied to the sheets, and the effects of two design parameters, i.e., fatty acid and degree of ethoxylation, on tissue properties were investigated.

CHAPTER I

INTRODUCTION

1.1. Introduction

1.1.1. Tissue product

Tissue products consist of various grades, including facial tissue, bath tissue, paper towels, napkins and diapers. The desired tissue product should be strong, soft, and absorbent. Most tissue products belong to the lightweight paper, and low basis weight is one of their characteristics. For example, the basis weight of a typical single-ply bath tissue is from 20 to 22.8 g/m² (12-14 lb/3,000 ft²), and for a typical single-ply paper towel, the basis weight ranges from 47 to 52 g/m² (29 to 32 lb/3,000ft²) [P&P Mag., 1997, 1999].

The tissue market is large and estimated to be \$17 billion per year worldwide. With stable growth in the developed countries, the potential consumption growth of tissue products in the developing countries is tremendous. In the competitive market, there is strong motivation for tissue manufacturers to improve the tissue product quality although many technological breakthroughs have been achieved [Cody et al., 1998]. To make tissue with premium quality, one or more tissue properties must be improved.

1.1.2. Tissue properties

The important tissue properties include strength, water absorbency, softness and lint resistance [Phan et al., 1993a, 1993b, 1994, 1995a, 1995b, 1996].

- Tissue strength refers to its ability to maintain its integrity under use conditions. The wet tissue strength is particularly important.
- Water absorbency property is the water absorbency capacity per unit mass of tissue, which is often referred to as Total Water Absorbency (TWA) by the tissue industry. Another aspect of water absorbency involves the rate of absorbency.
- Softness is the tactile sensation perceived by the customer when he rubs the tissue across his skin or crumbles the tissue in his hand. Softness is the most desired property for the facial tissue.
- Lint resistance is the tissue's ability to bind fibers and fines together with its bulk constituent under use conditions. High lint resistance of tissue is preferred since it indicates low tendency to lint.

For different grades of tissue, the priority of tissue properties is ranked differently by the consumer. For example, the most desired property for facial tissue is the softness, while water absorbency becomes the most important for the paper towels [Poffenberger, 2000]. The quality of the tissue product is reflected in tissue properties, and the industry has established reliable testing methods for various tissue properties. However, tissue softness is quite subjective, therefore, remains difficult to quantify. Traditionally, tissue softness is evaluated by a group of experienced panelists. However, the evaluation is

time-consuming, subjective, and influenced by various human factors [Pan, 1989]. Increasingly high-speed modern tissue machines require less machine downtime, and therefore, faster and more reliable tissue quality characterization methods are needed. Significant research efforts have been made to quantify the softness with other tissue physical properties [Brown, 1939; Lashof, 1960; Pearlman, 1962; Stewart et al., 1965; Ampulski, 1991]. However, to date, there is no satisfactory method to objectively measure the tissue softness with high accuracy.

1.1.3. Tissue manufacturing technologies

There are two major technologies widely used by the tissue industry, i.e., creping and through-air-drying. Both technologies consist of four stages, i.e., forming, draining, pressing, and drying. These two technologies are essentially mechanical. While the modification of the mechanical process is an effective way to improve tissue quality, the cost of tissue machinery is often prohibitively expensive. As an alternative, chemical additives can be applied to improve the tissue quality at much lower cost and offer more flexibility. In the field of tissue making, rich information exists concerning tissue property improvement through the application of chemical additives. The techniques are described in various patents [Reynolds, 1954; Sanford et al., 1967; Hervery et al., 1971; Ayers, 1976; Morgan, et al., 1976; Emanuelsson et al., 1979; Becker et al., 1979; Trokhan, 1980, 1985; Carstens, 1981; Laursen, 1981; Osborn, 1982, 1984; May et al., 1984].

The two most frequently used chemical additives in tissue production are wet strength resins and debonding agents. The addition of wet strength resins is necessary for many tissue grades, since it can render tissue enough strength to remain integrated and applicable under wet conditions [Bjorkquist, 1991]. The addition of debonding agents (also called “softeners” and “debonders”) can improve tissue softness and its bulk. Usually the additives are added in the wet end of the tissue machine. The papermaking process is dynamic, and the contact time between the additives and pulp fiber is quite short. Therefore, the adsorption kinetics of the two kinds of additives is important. However, the adsorption kinetic study of wet strength resins and debonders is very limited with little information on the adsorption mechanism. Furthermore, the competitive adsorption for this binary system has not been reported.

Although an enormous number of patents teach how to produce strong, soft and absorbent tissue by the application of debonding agents and wet strength resins, there is very little information available that quantitatively describes the effects of the additives on tissue physical properties, especially on the softness improvement. The mechanisms of the wet strength resin and the debonding agent’s function for tissue application have not been fully studied. To overcome the negative impacts on water absorbency caused by traditional debonding agents, a new type of biodegradable softener with the polyoxyethylene chains has been recently developed. However, there is little published information on the effects of the molecular structure of the debonder on sheet properties [Poffenberger et al., 2000].

1.2. Thesis objectives

The main objective of this thesis is to improve tissue properties by the application of chemical additives. In order to monitor the improvement of tissue quality, the tissue properties need to be characterized. Important properties that significantly contribute to the tissue softness are to be identified and a softness model is to be developed for the commercial creped facial tissue. Based on the commercial tissue softness characterization, a softness model will be applied to the handsheet so that its physical properties can be translated into the softness sensation.

Since the chemical additive must adsorb onto the wood fiber surface to be effective, the individual adsorption kinetics of wet strength resin and debonding agent on the cellulose fibers must be studied. Moreover, the competitive adsorption of the two additives will be investigated so that the effects of their interaction on sheet properties can be better understood. Since one important goal of this study is to design the tissue properties with the application of chemical additives, the effects of debonding agents as well as wet strength resin on various sheet properties are to be investigated. In addition, the interaction of the wet strength resin and the debonder will be discussed. Finally, the effects of a new type of biodegradable debonding agent with a polyoxyethylene chain on sheet properties are also to be investigated. The effects of the molecular structure of the

debonder on the sheet properties will be discussed, and the understanding will provide guidance to the application of debonder in commercial tissue production.

1.3. Research significance

First, this study addresses the lack of information on tissue softness quantification. The softness model for commercial facial tissue is of practical value, and the subjective human factors can be eliminated from the evaluation process. The model involves tissue properties that can be measured on line and opens the prospect of real time tissue softness monitoring in the manufacturing process. The softness model proposed for handsheets makes it possible to predict handsheet softness with routine paper physical properties in the laboratory, which will facilitate the chemical screening process.

Second, the investigation of the adsorption kinetics of two types of chemical additives, the wet strength resin and the debonding agent, onto the cellulose fibers represents the first detailed study of the adsorption mechanism in aqueous fiber system. The competitive adsorption of this binary system will shed light on the additives' adsorption affinity on cellulose fibers and provide guidance to commercial production. The adsorption system design in this study is unique and overcomes the drawbacks of the traditional chemical adsorption method. The system can be extended to the adsorption study of other paper chemicals and help the mechanism study with quality data.

Third, the study of the effects of the wet strength resin and the debonding agent on various sheet properties shows the quantitative results. Detailed analysis of the application of individual chemicals and combined chemical applications illustrates that the tissue properties can be engineered to meet customer need by chemical modifications. The study shows not only how, but also why the combined additive application can produce strong, soft, and absorbent sheets for tissue application.

Finally, the study of a new class of environmentally benign debonding agents with polyoxyethylene chains provides valuable information on the effects of debonder design parameters and generates the understanding to further optimize the new class of debonding agents.

1.4. Thesis structure

Chapter 2 provides the background of tissue properties, commercial tissue production, and tissue chemical additives. The experimental is presented in Chapter 3.

The results and discussion of adsorption kinetics of the wet strength resin and the debonding agent onto pulp fiber are given in Chapter 4. In Chapter 5, the effects of a wet strength resin and a debonding agent on sheet properties are presented. The results of combined application of tissue additives are also included in this chapter. The effects of new debonding agents that incorporate the ester functionality and polyoxyethylene chain

on sheet properties are discussed in Chapter 6. The conclusions and recommendations are presented in Chapter 7.

The characterization of commercial tissue softness is included in Appendix A. A comprehensive and systematic study is performed, and a three-parameter softness model for conventional facial tissue is developed, which has the potential to be used for the on-line application. Appendix B is the code used for calculating tissue surface texture factors. Appendix C gives the properties of the hardwood and softwood fibers used in this study. Appendix D is a research summary on the effects of fiber quality variation on tissue properties. Finally, the installation and the operation procedure of the M/K automatic sheet former are included in Appendix E.

1.5. Reference

Ampulski, R. S., Albert H. Sawdai, Wolfgang U. Spindel and Ben Weinstein, Methods for the measurement of the mechanical properties of tissue paper, *Proceedings of 1991 International Paper Physics Conference*, 19-29 (1991)

Ayers, P. G., U.S. Patent: 3,974,025: Absorbent paper having imprinted thereon a semi-twill, fabric knuckle pattern prior to final drying, August 1976.

Becker, Henry F., Albert L. McConnell and Richard W. Schutte, *U. S. Patent 4,158,594*: Bonded, differentially creped, fibrous webs and method and apparatus for making same, June 1979.

Bjorkquist, David W., Temporary wet strength resins with nitrogen heterocyclic nonnucleophilic functionalities and paper products containing same, U.S. Patent: 4,981,557, January 1991.

Brown, T. M., A method for determining the softness of soft papers, *Paper Mill* 92, Vol.23, 19-21, June 10 (1939)

Carstens, J. E., *U. S. Patent 4,300,981*: Layered paper having a soft and smooth velutinous surface, and method of making such paper, November 1981.

Cody, H. M., and Kelly H. Ferguson, Tissue, towel producers conquer market with form and function, *Pulp & Paper*, 41-48, April 1998.

Emanuelsson, J. G. and S. L. Wahlen, *U.S. Patent 4,144,122*: Quaternary ammonium compounds and treatment of cellulose pulp and paper therewith, March 1979.

Hervy, L. R. B., and D. K. George, *U.S. Patent: 3,554,863*: Cellulose fiber pulp sheet impregnated with a long chain cationic debonding agent, January 1971.

Lashof, T. W., Note on the performance of the Handle-O-Meter as a physical test instrument for measuring the softness of paper, *TAPPI Journal* vol.43, no.5: 175-178A (1960)

Laursen, B. L., *U. S. Patent: 4,303,471*: Method of producing fluffed pulp, December 1981.

May, Oscar W. and Philip M. Hoekstra, *U. S. Patent: 4,425,186*: Dimethylamide and cationic surfactant debonding compositions and the use thereof in the production of fluff pulp, January 1984.

Morgan, G. Jr. and T. F. Rich, *U.S. Patent: 3,994,771*: Process for forming a layered paper web having improved bulk, tactile impression and absorbency and paper thereof, November 1976.

Osborn, III, T. W., *U. S. Patent: 4,351,699*: Soft, absorbent tissue paper, September 1982.

Osborn, III, T. W., *U. S. Patent 4,441,962*: Soft, absorbent tissue paper, April 1984.

Pan, Y., C. Habeger and J. Biasca, Empirical relationships between tissue softness and out-of-plane ultrasonic measurements, *TAPPI Journal*, 95-100, November (1989)

P&P Magazine, *Tissue, Pulp & Paper 1997 North American Fact book* - Paper grade, 235-245 (1997)

P&P Magazine, *Tissue, Pulp & Paper 1999 North American Fact book* – Paper grade, 359-370 (1999)

Pearlman, J., *U.S. Patent: 3,060,719*: Testing paper tissues and the like, Oct. 30, 1962.

Phan, Dean V. and Paul D. Trokhan, *U.S. Patent 5,264,082*: Soft absorbent tissue paper containing a biodegradable quaternized amine-ester softening compound and a permanent wet strength resin, November (1993a).

Phan, Dean V., *U.S. Patent 5,217,576*: Soft absorbent tissue paper with high temporary wet strength, June (1993b).

Phan, Dean V., Paul D. Trokhan and Toan Trinh, *U.S. Patent 5,312,522*: Paper products containing a biodegradable chemical softening composition, May 1994.

Phan, D. V., Paul D. Trokhan, *United States Patent: 5,405,501*, Multi-layered tissue paper web comprising chemical softening compositions and binder materials and process for making the same, April 11 (1995a).

Phan, Dean V., Paul D. Trokhan, Stephen R. Kelly, Ward W. Ostendorf and Bart S. Hersko, *U.S. Patent 5,437,766*: Multi-ply facial tissue paper product comprising biodegradable chemical softening compositions and binder materials, August (1995b).

Phan, Dean V., Paul D. Trokhan, Robert G Laughlin and Toan Trinh, *U.S. Patent: 5,543,067*: Waterless self-emulsifiable biodegradable chemical softening composition useful in fibrous cellulosic materials, August 1996.

Poffenberger, C., Yvonne Deac and William Zeman, Novel hydrophilic softeners for tissue and towel applications, *Proceeding of 2000 TAPPI Papermakers Conference and Trade fair*, vol.1, 85-93 (2000)

Reynolds, W. F., *U.S. Patent: 2,683,087*: Absorbent cellulosic products, July 1954.

Sanford, L. H. and J. B. Sisson, *U.S. Patent: 3,301,746*: Process for forming absorbent paper by imprinting a fabric knuckle pattern thereon prior to drying and paper thereof, January, 1967.

Stewart, R., R. J. Volkman, Thickness measurement of sanitary tissues in relation to softness, *TAPPI Journal* vol.48, no.4: 54-56A (1965)

Trokhan, P. D., *U. S. Patent 4,191,609*: Soft absorbent imprinted paper sheet and method of manufacture thereof, March 1980.

Trokhan, Paul D., *U. S. Patent 4,529,480*: Tissue Paper, July 1985.

CHAPTER II

BACKGROUND

2.1. Introduction

Tissue manufacturing research is multi-disciplinary in nature and this chapter provides some background information most relevant to the study. First, this chapter introduces each of the important tissue properties--strength, softness and water absorbency. More attention has been paid to the softness since it is quite subjective and difficult to define. The current understanding of tissue softness is reviewed and some softness models are introduced. Second, commercial tissue manufacturing technologies, i.e., creping and through-air drying, are introduced. Creping effectively develops tissue properties by liberating fibers from bonding and creating surface characteristics, while through-air-drying technology employs hot air to dewater the tissue web so that high bulk can be achieved. These two technologies essentially employ mechanical methods to improve various tissue properties including softness and set the framework within which the study of chemical additive effects on tissue can be performed. At the end of the

chapter, the fundamentals of wet end chemistry and the review of two kinds of tissue additives, i.e., the wet strength resin and the debonding agent, are provided.

2.2. Tissue properties

2.2.1 Tissue softness

2.2.1.1. Introduction to tissue softness

Tissue softness has been extensively studied by the tissue industry [Andersson, 1988; Greenfield, 1994; Carr et al., 1997]. It has long been realized that tissue softness is a complex function of various physical and psychological interactions [Stevens et al., 1960; Bates, 1965]. It is believed that the softness sensation has two components: surface softness and bulk softness [Hollmark, 1983a, 1983b]. Surface softness is the softness perception generated when the consumer gently brushes his/her fingertips over the tissue surface. Bulk softness is the perception of softness obtained when the tissue sample is crumbled in the hands. The consumer evaluation of these two tissue softness components is illustrated in Figures 2-1 (a) and (b).

2.2.1.2. Tissue softness evaluation methods

There are two commonly used methods in performing the tissue softness evaluation, i.e., direct comparison and pair-comparison. In the direct comparison method, the standard tissue samples are carefully selected and softness scores from 0 to 100 are

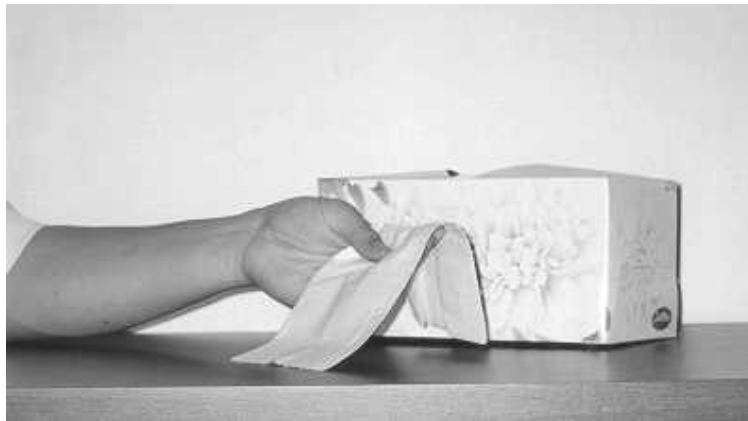


FIGURE 2-1 (a) Surface softness evaluation



FIGURE 2-1(b) Bulk softness evaluation

assigned. The test sample is compared to a series of standard tissue samples. If the panelist senses that the test sample is softer than the tissue standard with the softness score of X , but is harsher than the tissue standard with a score of Y , the test sample is assigned a softness score between X and Y .

In the pair-comparison method, the panelists compare a pair of tissue samples (A and B), and the scores are given in Panel Score Units (PSU) according to the following rules [Trokhan et al., 1996]:

- If the sample A is judged to be a little softer than B with some uncertainty, then A is given the score of plus one;
- if sample A is judged surely to be a little softer than B, the sample A is given the score of plus two;
- if sample A is judged to be a lot softer than sample B, the sample A is given the score of plus three;
- if sample A is surely to be much softer than sample B, sample A is given the score of plus four.

2.2.1.3. Multi-dimensional Sensation

It is believed that the nature of the softness sensation is multi-dimensional [Lyne et al., 1983, 1984]. The sensations, such as sight, sound and tactile, are all involved in the softness evaluation process. The visual factors, such as color and embossing patterns, affect the customer's softness sensation and decision-making process. The sound of the

tissue sheet friction is also found to relate to tissue softness [Pearlman, 1962]. Efforts have been devoted to quantifying the sound emission due to tissue friction. In Pearlman's study, the tissue sample placed on a knob-like head containing a sensitive microphone was rubbed against another sample over a similar head with a predetermined force and motion. The sound of the tissue friction was recorded and found to be a function of tissue handfeel.

Although the hearing and sight are involved in the softness evaluation process, the research on the softness understanding is usually focused on the study of important factors affecting the human tactile sensation. The interference from hearing and sight can be eliminated by such techniques as using earplugs and blindfolds [Bates, 1965].

2.2.1.4. Physical properties related with softness

The following physical properties are believed to be important factors that affect the tissue softness sensation:

(A) Specific volume

Specific volume is defined as the volume of unit mass of materials (cm^3/g). In the tissue industry, specific volume is often referred to as bulk. It is calculated as the ratio of tissue basis weight to its thickness. Bulk is an important factor contributing to tissue's bulk softness component. If other properties remain same, a bulkier sheet usually generates a higher softness sensation. Since tissue deforms easily under pressure, bulk values vary dramatically with the measurement pressure. In Technical Association of

Pulp and Paper Industry (TAPPI) standard method, the pressure applied by the measuring foot of a micrometer is 50 ± 2 kPa [TAPPI, 1989]. Since low measurement pressure simulates the practical application more realistically, bulk values under low pressures are of more interest.

(B) Compressibility

As mentioned above, the tissue thickness varies with measurement pressures. Compressibility is defined as the ratio of the bulk measured at a lower pressure to that at a higher pressure. Tissue thickness was measured under the pressures of 0.0207 kPa and 0.207 kPa, and the compressibility factors were calculated [Eperen et al., 1965]. It is shown that the compressibility factors at higher loading pressures are more strongly correlated with tissue softness.

(C) Modulus

It is generally believed that tissue stiffness is inversely related to tissue softness [Ampulski et al., 1991]. A power relationship between tissue stiffness and softness has been established [Hollmark, 1983b]. Lower stiffness usually leads to higher softness sensation. One measure of stiffness is Young's modulus of tissue. Generally speaking, at the same breaking elongation, tissue with low Young's modulus also has low tensile strength.

Other forms of the modulus, such as bending stiffness and tensile stiffness, have also been used to correlate with tissue softness. Tensile stiffness, E_T , is the product of Young's

modulus and tissue thickness, while bending stiffness, E_b , is defined as the product of Young's modulus and the cube of tissue thickness [Hollmark, 1983a].

(D) Surface texture

Tissue surface texture plays an important role in human tactile sensation. It is pointed out that a large number of free fiber ends protruding from the tissue surface can simulate the velvety surface of a cloth, which gives customer the sense of surface softness [Carstens, 1981].

Stylus profilometry is one of the most commonly used methods to investigate tissue surface texture [Lindsay, 1997]. The stylus tip scans the tissue surface at a specified speed, and the information of the tissue surface profile is picked up, and then subject to further data processing.

HTR (Human Tactile Response) has been developed to quantify the surface softness component, and is defined as the area under the amplitude frequency curve, above the 2.54 μm base line, and between 10 cycles per inch and 50 cycles per inch [Carstens, 1981]. A normalizing procedure is taken to adjust the HTR values between 0 and 1. It is suggested that tissue samples with the HTR of less than 0.7 usually give good tactile sensation [Carstens, 1981]. However, it is later pointed out that the 0.5mm hemispherical stylus tip in Carstens' study is too wide to resolve important tissue surface features [Lindsay, 1997].

Ampulski et al. define the factor PAAREA (Physiological Amplitude Area) to describe the tissue surface texture. PAAREA is obtained by integrating the Verillo-adjusted frequency amplitude spectrum from 0 to 10 cycles per mm (0-254 cycles per inch) [Ampulski et al., 1991]. Thus the PAAREA is integrated over quite a wider frequency spectrum than the HTR.

FITS (Frequency Index of Tactile Softness) and HTR-EQ [Rust et al., 1994a, 1994b] have been developed and based on similar concepts. Fourier-transform is performed on the filtered data to generate the power frequency spectrum. Assuming the panelist's finger velocity is about 65 mm/s, the FITS value is obtained by integrating the amplitude frequency spectrum from 0 to 650 cycles per second. Since the filters and normalizing factors used by Carstens are not available, Rust et al. fail to reproduce the HTR data although other guidelines set up by Carstens have been carefully followed; thus, their parameter is named HTR-EQ.

2.2.1.5. Tissue softness models

Tissue softness models are the mathematical equations that predict softness with tissue physical properties. The softness models provide the guidance to identify important physical properties, which are significantly relevant to tissue softness. The modification of those physical properties can help to improve tissue softness. Therefore, the task of improving a subjective quality (softness) can be translated into modulating tangible tissue properties. In addition, a reliable tissue softness model helps the efforts of tissue quality

monitoring and can reduce the effects of subjective ranking and feedback time. As a result, higher productivity can be realized. Various softness models have been developed by tissue manufacturers to predict tissue softness. Due to the confidential nature of the industry, few models are accessible to the public. However, information in literature provides a rich body of knowledge on this topic, since many fundamental aspects of tissue tactile sensation have been explored.

The bulk softness of tissue and towel samples has been studied [Hollmark, 1983b], and a power relationship is developed between the tensile stiffness ($E \cdot t$) and softness. The model coefficient of correlation is 0.88. The data from the STFI surface softness analyzer is incorporated into the model, which does not improve the correlation (the correlation coefficient is down to 0.86). Since heavily embossed tissue samples give unreliable surface softness analyzer readings and are also found to have low tensile stiffness, such samples are excluded from the model construction. As a result, the degree of correlation is improved greatly. The R^2 of bulk softness with tensile stiffness alone is 0.92. With the addition of a surface factor, the R^2 is further improved to 0.98. Thus the surface softness contributes to bulk softness and that the two softness components are dependent on each other to some degree.

Eperen et al. have correlated tissue and towel softness using the paired comparison method [Eperen, et al., 1965]. Tensile stiffness, thickness, and the sum of tissue stretch at machine and cross machine directions are used to predict tissue softness. The three-parameter-model has a correlation coefficient of 0.92. The tissue thickness is measured

under the pressure of 8.62kPa, which is higher than actual tissue application pressure. The thickness value at lower pressure may have been able to improve the correlation.

HTR (Human Tactile Response) is developed to quantify the surface softness component, and it is suggested that tissue samples with the HTR of less than 0.7 usually give good tactile sensation [Carstens, 1981]. It has been pointed out later that the 0.5mm hemispherical stylus tip in Carstens' study is too wide to resolve important tissue surface features [Lindsay, 1997].

Rust et al. have performed a study on the softness of bathroom tissue. Only the parameters contributing to the surface softness are considered [Rust et al., 1994a, 1994b]. Similar methods used by Ampulski and Carstens are employed to develop the FITS (Frequency Index of Tactile Softness) and HTR-EQ factors. Another factor, the loosely bonded surface fibers (LBSF), has also been developed and measured using a laser imaging system with the capability of optical image analysis (OIA). The R^2 of softness with FITS is 0.785, although the softness models are not disclosed. The addition of LBSF does not improve the degree of correlation; the correlation of softness with HTR-EQ and LBSF has a much lower R^2 of 0.542.

Certain techniques used by the textile industry have been adapted to quantify paper towel softness. Kawabatta Evaluation System (KES) is widely used in the textile industry to evaluate fabric handling. The instrument settings have been modified to measure the mechanical properties of towels, such as bending, surface roughness, shear, tensile and compression [Kim, et. al, 1994]. The extensibility and surface roughness have been

identified as the most important parameters for the softness sensation. A linear relationship between towel softness and the two parameters is established with the correlation coefficient of 0.90.

The softness of facial tissue made by conventional creping technology has been systematically studied and the results are included in Appendix A. Various tissue physical properties are considered in the correlation. Factors describing tissue surface textures are correlated with softness, and a new parameter PAAREA_EQ is defined, which has been demonstrated to have better correlation with tissue softness than similar parameters. A softness model based on three parameters, i.e., R (cross machine to machine direction tensile index ratio), R_a (arithmetic surface roughness), and E_{avg} (mean elastic modulus), is shown in Equation 2.1

$$S = 1164.4 \left(\frac{R}{R_a^{1.220} E_{avg}^{0.793}} \right)^{0.387} \quad (2.1)$$

This model is demonstrated to be able to predict the softness of creped facial tissue with high accuracy. The facial tissue softness model coupled with enabling technologies, such as acoustical and optical techniques [Waterhouse, 1993; Lindsay, 1997], open the prospect of the instrument development with on-line monitoring capabilities.

2.2.2. Paper strength

Strength is another important property for tissue products. The tissue must have functional strength in both dry and wet applications. In the papermaking process, surface tension plays an important role in bringing fibers together. As water is removed, the surface tension generates a tremendous force, which draws the fibers into more intimate contact. The force of surface tension acts in a direction normal to the fiber surface, resulting in a thickness change up to 200%, while the change in area is relatively small [Pierce, 1953]. As the web consistency increases, inter-fiber capillary water is replaced by air, but leaves a film of water around the fibers. Inter-fiber bonding takes place when no free water remains and the associated water of fiber is being removed [Robertson, 1959].

It is believed that hydrogen bonding provides inter-fiber bond energy. Experiments show that the energy necessary to rupture the bonds in paper is comparable to the energy liberated from hydrogen bonds formed during paper drying [Corte et al., 1955]. Figure 2.2 provides a schematic that shows the formation of hydrogen bonds between two cellulose fibers.

Paper strength is generally believed to consist of two components, i.e., the intrinsic fiber strength and the inter-fiber strength [Page, 1969]. Equation 2.2 is often used to describe the paper strength

$$\frac{1}{T} \propto \frac{1}{F} + \frac{1}{B} \quad (2.2)$$

In the above equation, T is the tensile strength, F is the strength of individual fiber, and B is the inter-fiber bond strength. Equation 2-2 suggests that paper strength is dependent on both intrinsic fiber strength and inter-fiber bonding. Intrinsic fiber strength is usually characterized by zero-span tensile [Cowan, 1975], and is dependent on the wood species and the specific pulping method employed. In the papermaking process, it is the inter-fiber bonding that can be controlled and improved. Important factors that affect inter-fiber bonding are fiber length, fibrillation, hemicellulose content and chemical additives. The following section will discuss these factors in order:

(A) Fiber length

Fiber length was once considered the most important measure of pulp quality, and is still a property to be considered in papermaking. When the inter-fiber bonding reaches its maximum for unit length, the strength of inter-fiber bonding parts depends on the length of its fibers. Longer fiber has less chance of slippage between the fibers when the paper is subject to stress. In addition, the probability of fibril formation is higher for longer fibers, which leads to higher capacity for inter-fiber bonding.

(B) Fibrillation

The primary wall of a fiber is a deterrent to fiber bonding. With mechanical treatment, such as refining¹, the primary wall is removed, and the fibrils from the secondary wall are

¹ A mechanical treatment of pulp fibers to develop their optimum papermaking properties [Biermann, 1996]

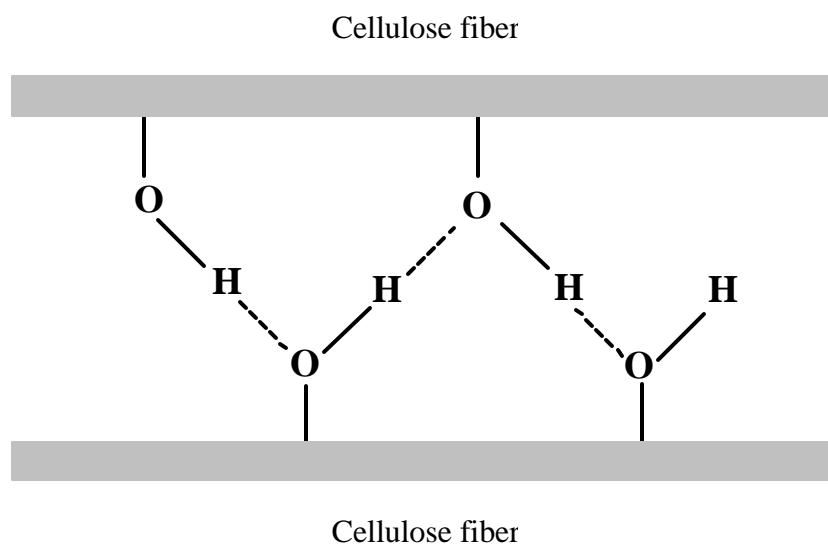


FIGURE 2.2 Schematic showing the formation of hydrogen bonds between two adjacent fibers [Forbess, 1997]. The hydrogen atom is shared by two different oxygen atoms. Fibers are held together through hydrogen bonding of the hydroxyl groups of cellulose and hemicellulose. In addition to hydroxyl groups, the carboxylic acid groups of hemicellulose also play an important role. Although an individual hydrogen bond is weak, relatively high paper strength can be developed through a large amount of bonds.

caused to protrude from the fiber surfaces. As a result of fibrillation, the effect area for the inter-fiber bonding is increased and the fiber becomes less rigid. The surface tension is increased significantly due to the raised surface elements and tends to bring the fine fibrils into contact. The finer fibrils lie in parallel contact, and are joined by hydrogen bonding when the water is removed. Therefore the dry strength of paper is increased by fibrillation under most conditions.

(C) Hemicellulose

The importance of hemicellulose in paper strength development is well recognized, and is believed to play a more important role than fibrillation [Rance, 1953]. When the fiber structure is loosened, additional water is more easily attracted by the large surface of the amorphous, hydrophilic hemicellulose material. In comparison, the cellulose is hydrophilic itself by nature, though part of it is crystalline and not available for hydration. Therefore, hemicellulose contributes strongly to swelling. Furthermore, the carboxyl groups on xylan glucuronic acid groups are identified to be the main source of negative fiber surface charge [Scott, 1996].

(D) Chemical additives

Most chemical additives used in the paper industry carry cationic charges and can adsorb onto pulp fiber surface through the electrostatic mechanism. The additives not only change the amount of bonding between adjacent fibers, but also modify the strength of the individual bond. Usually, the additives have a minimal effect on the intrinsic fiber

strength. In the low basis weight paper, such as tissue, the inter-fiber bonding plays a much more significant role than the fiber strength [Hollmark et al., 1978].

2.2.3. Water absorbency

For various tissue products, water absorbency includes two aspects; one is the water absorbency capacity and the other is the rate of absorbency. Absorbency is the most important criterion for certain types of tissues, such as paper towels. It is pointed out that to a large extent, tissue absorbency is governed by the surface chemistry of its fibers [Hollmark, 1983a].

The water in the pulp fiber exists in three forms: (A) colloidal water, which is held on the cellulose crystalline regions by adsorption; (B) capillary water, which is in the narrow capillaries of the fiber in excess of colloidal water; and (C) imbibed water, which can be absorbed by fiber through contact with the liquid phase. Colloidal water causes fiber swelling and opens up new areas so that more water can enter. Due to strong interaction with the cellulose, colloidal water does not exhibit the properties of “free” water. Capillary water keeps its liquid properties, has less influence on fiber swelling, and is responsive to the changing humidity of the environment. Imbibed water fills in the lumen and coarse visible pores of the fiber and remains there as free water.

The paper web is often treated as a porous body that consists of a series of interconnected pores [Peek et al., 1934]. Therefore, in considering the water absorbency phenomena, most attention has been paid to capillary flow with no external pressure

differential applied (spontaneous flow). Derived from the Poiseuille and Laplace Equations, the Lucas-Washburn equation (Equation 2.3) is often used to describe the wetting kinetics:

$$\frac{dh}{dt} = \frac{r\gamma_L \cos \theta}{4\eta h} \quad (2.3)$$

where h is the length of the filled portion of capillary, η is the liquid viscosity, r is the capillary radius, γ_L is the surface free energy, and θ is the contact angle between liquid and capillary walls. The Lucas-Washburn Equation applies to the situation where the effects of gravity can be neglected. When the mean cross-sectional areas of flow channels are small, the weight of raised liquid volume is relatively small compared to the driving force, and the effects of gravity can be neglected. Although the equation has some theoretical limitations [Lyne, 1978], it yields results that reasonably match experimental data [Hoffman, 1994a, 1994b].

In order to enhance the water absorbency capacity, the pulp fibers have been treated chemically. Excellent fiber absorbency properties have been achieved when fiber is treated with a solution of glycol and dialdehyde [Ona et al., 1994] and N, N'-methylene bis-acrylamide [Box, 1990]. An order of magnitude of absorbency increase is observed for the hydrolyzed methyl acrylate or acrylonitrile-grafted fibers, and the enhanced absorbency is partially attributed to the increased fiber osmotic forces [Rezai, et al., 1997; Warner et al., 1997a, 1997b].

There are various methods in evaluating the rate and capacity of water absorbency. The methods of measuring absorbency rate include the orifice method [Choksi et al., 1977], the floating time method [Kimmel et al., 1970], and the capillary rise method [SCAN, 1964]. Among these absorption rate evaluation methods, it is generally believed that the capillary rise method provides a simple and reliable way for the tissue absorbency characterization. The absorbency capacity measurement is to determine the amount of liquid absorbed after an infinite amount of time.

2.3. Tissue manufacturing

In this section, the entire tissue manufacturing process is reviewed. First of all, the fundamental knowledge of the wood fiber is introduced. Then commercial tissue production is reviewed. The production usually consists of two sections, i.e., the pulping and the tissue making sections. In the pulping section, the wood chips go through a combination of mechanical and/or chemical processes, and individual fibers are liberated to provide the raw material for tissue production. In the tissue making section, the dilute cellulose fiber slurry is dewatered and processed so that a soft and absorbent tissue product is produced at the end of the production line.

2.3.1. Pulping

The main purpose of pulping is to make cellulose fibers ready for papermaking. In the pulping process, individual wood fibers or other lignocellulosic materials are liberated by physical or chemical means. The fibers can then be dispersed in water, formed into a web, and ultimately made into paper. In the mechanical pulping process, lignin is not removed. This kind of pulping is often referred to as high-yield pulping. Chemical pulping, especially kraft pulping, is the dominant pulping method due to its superior papermaking properties. In chemical pulping, wood chips are cooked at high temperatures with various chemicals to remove lignin from the fibers. In the kraft pulping process, a solution of sodium sulfide and sodium hydroxide cooks the wood chips at temperatures up to 180°C. The alkaline cooking solution makes the lignin molecules fragmented and soluble, which helps the subsequent washing process [Smook, 1992]. The kraft pulp is much stronger than that of any other pulping process, and the kraft pulping process can recover all the pulping chemicals.

2.3.2 Commercial tissue making

Two major technologies are widely used by the tissue industry, i.e., creping and through-air-drying. Both technologies consist of four major steps: (A) forming, in which the pulp slurry is formed on a screen; (B) draining, in which the water in the pulp slurry is drained by the mechanism of either gravity or an applied vacuum; (C) pressing, in which the mechanical pressure is applied to further dewater the wet sheet, and (D) drying, in which the final product moisture specification is reached through heat exchange.

Figure 2.3 is a diagram of a typical commercial tissue production process. In the following sections, the two technologies will be discussed in more detail.

2.3.2.1. Creping technology

In the creping technology, a pressurized headbox delivers the low consistency pulp slurry through a thin slice onto a forming wire, for example, a Fourdrinier wire to form a wet paper web. The Fourdrinier wire (also called “forming fabric”) forms a continuous belt that picks up fiber at the breast roll from the headbox, runs over the table rolls, foils, suction boxes, and then over a couch roll [Strauss, 1969]. The design parameters of the forming fabric, such as mesh, weaves, wear patterns, void volumes, have significant impacts on the important tissue properties [Ayers, 1975; Trokhan, 1980; Kobayashi, 1990; Adanur, 1994; Liu et al., 1999]. The wet web is dewatered by gravity or vacuum, and reaches the consistency of 7 to 25% in the forming section. At the couch roll, the paper web leaves the forming fabric and the fabric returns to the breast roll. The water is further removed from the sheet by pressing generated by two opposing press rolls. After pressing, the sheet consistency reaches 25 to 50% before the sheet is transferred to a steam-heated dryer, which is called a Yankee dryer.

The Yankee dryer is a large, cast iron, steam heated dryer drum with the diameter of 3.5-4.5 meters [Corboy, 1986]. An air cap (a hood mounted close to the Yankee dryer surface) blows heated air on the paper web and increases the drying efficiency, contributing up to 70 percent of the drying on the tissue machine [Poirier et al., 1996].

The tissue web is pressed by a pressure roll onto the Yankee dryer surface. The adhesion of the web on the dryer depends highly on the formation of an organic coating on the dryer surface, which is formed by the organic material (hemicellulose, lignin, etc.) from the pulp or the chemical additives applied to the dryer through spraying [Sloan, 1991; Oliver, 1993]. Within less than one turn, the paper web is creped off by a creping blade at the other side of the dryer. The creping blade is loaded on the dryer surface at a certain angle (from 15° to 25°) and a sufficiently high pressure is applied to the blade so that the adhesive bond between the light-weight web and the dryer can be destroyed. As a result of creping, the flexibility of the paper in the machine direction is increased. Because part of the inter-fiber bonds is broken by the creping, the tissue bulk is improved and the water absorbency is enhanced [Cozzens, 1997]. Since the conventional creped tissue is pressed at a significant pressure at the wet state and dried at the compressed state, the tissue produced in this manner is strong and has an even density distribution. However, the tissue's bulk, absorbency, and softness are adversely affected by the operation of the wet press [Phan et al., 1995].

2.3.2.2. Through-air-drying technology

The through-air-drying (TAD) technology is similar to that of the creped tissue except that the water in the wet web is removed without mechanical compression until the sheet reaches the consistency of about 80%. In order to remove water from the web without mechanical pressing, the through-air dryer is used in the process. The sidewall of the through-air dryer has at least a 75% open area [Sisson, 1967]. Ambient air is drawn into

the inlet of a fan and forced at high speeds through a heater to provide a source for drying air. The flow rate of the hot air depends on the air temperature, web speed, and the inlet and outlet web consistencies. While the wet web is carried in a circular path from one side to the other side of the dryer, hot air is blown through the wet web to evaporate the water contained in the web. The water-enriched air is discharged by an exhaust fan or is fed into the heater of through-air dryer at the next stage. The web, at a higher fiber consistency, is then creped on the Yankee dryer. Compared with tissue by traditional creping technology, tissue made by through-air-drying technology has higher bulk, water absorbency, and lower strength, since the sheet is not significantly pressed during the process [Salvucci et al., 1974; Becker et al., 1980].

The comparison of creping and through-air drying is performed for 35 g/m² two-ply and 28 g/m² single-ply tissues. The results show that through-air dried tissue has lower production costs, although it incurs higher investment costs and has slightly lower machine efficiency [Leffler, 1998].

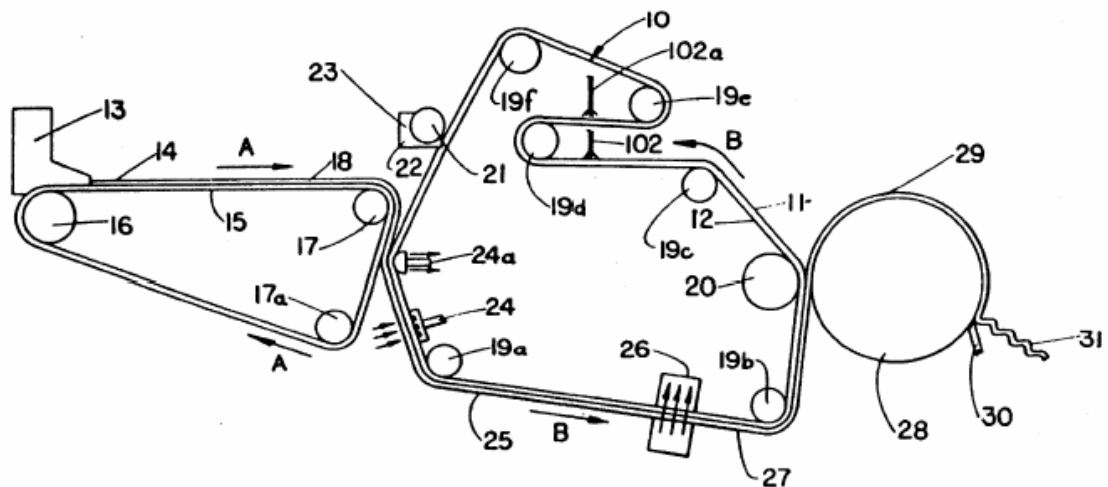


FIGURE 2.3 The diagram showing the commercial tissue production [Trokhan et al., 1996]. The Fourdrinier machine is used to illustrate the process. The dilute fiber slurry is ejected at high speed through the slice of the headbox 13, and forms a continuous cellulose web on the forming fabric 15. After the drainage in the forming stage, the cellulose web is picked up by the couch roll 24a, and transferred to the felt. In the creping technology, the tissue web is pressed onto the Yankee dryer 28, creped off by the creping blade 30, and the final tissue product 31 is made. In the through-air-drying technology, the tissue is dried by one or more through-air dryers, and then creped at a higher fiber consistency on the Yankee dryer.

2.4. Fundamentals of wood fiber

This section briefly introduces the fundamentals of wood fiber. First the physical structure of fiber is introduced. Then the background information about the fiber surface is provided. Finally, the zeta potential of the papermaking fibers is included at the end of the section.

2.4.1 Fiber structure

The fiber structure of different tree species is usually different. The wood is generally classified into two major categories, i.e., softwood and hardwood [Clark, 1985]. Softwoods typically have longer fibers than hardwood and include southern pine, spruce, redwood and jack pine. Hardwoods include aspen, oak, birch etc., and the fibers are relatively short. The tensile and tear strength of hardwood pulp are lower than those of the softwood, but hardwood pulp renders good formation to the paper. On the other hand, softwood pulp is often used to enhance paper strength [Filed, 1982].

The wood fibers are separated by the middle lamella, which is mostly made up of lignin. The fiber contains the primary layer and a three-layered secondary layer [Biermann, 1996]. The void space in the middle of the fiber is the lumen, which provides wood with buoyancy and bulk. The primary wall consists of cellulose, hemicellulose and extractives completely embedded in lignin. The secondary layer consists of S1, S2 and S3

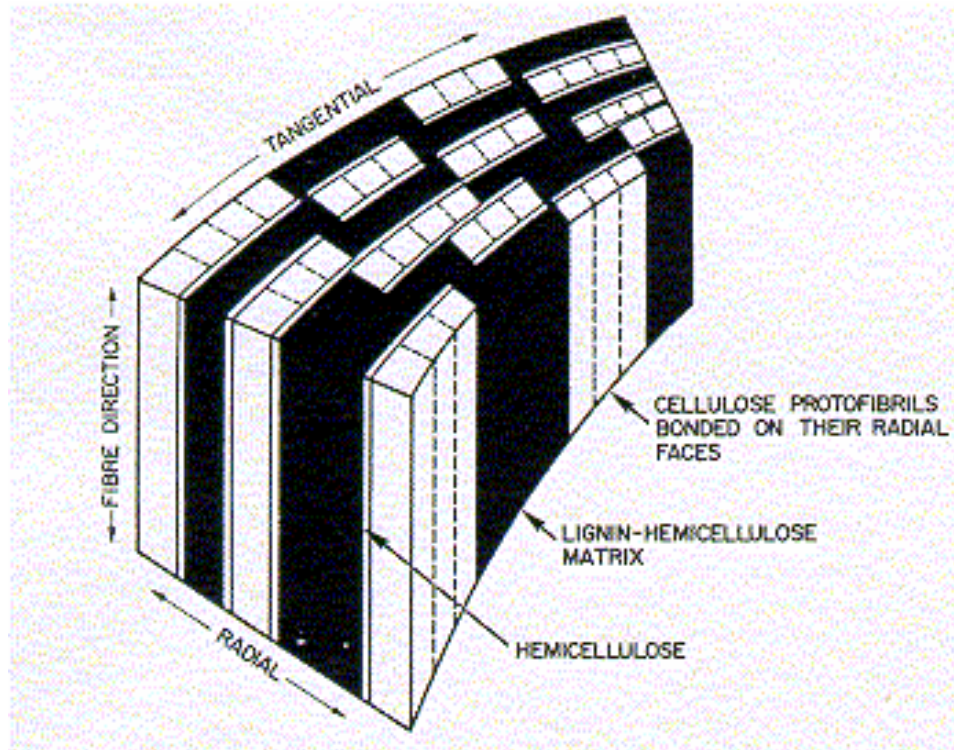


FIGURE 2.4 This schematic illustrates the wood fiber wall [Kerr et al., 1975]. Cellulose in a fiber wall forms elementary fibrils that are about 35 Angstroms in diameter and aggregate together to form microfibrils. The fibrils exist as sheets of parallel fibrils with different layers orientated relative to the fiber's longitudinal axis. The crystalline cellulose fibrils are embedded in a matrix of lignin and hemicellulose.

layers with different thickness. The inner secondary wall, S2, forms the main body of the fiber with thickness of 2 to 8 microns.

The main chemical composition of wood fibers includes cellulose, hemicellulose, and lignin. Figure 2.4 shows a schematic of the wood fiber wall. Cellulose is a white solid material that makes up the backbone of the wood fiber. It is a polysaccharide carbohydrate made up of polymerized glucose units. The degree of polymerization of the cellulose is a chemical property that determines the pulp strength. For untreated wood fiber, the degree of polymerization of cellulose is usually more than 10,000. Unlike cellulose, hemicellulose occurs at about 100-200 degrees of polymerization, and is not fibrous in nature [Smook, 1992]. Cellulose and hemicellulose make up the entire carbohydrate content of wood fibers. Lignin is an amorphous, highly polymerized substance with a three-dimensional structure comprised of phenylpropane units for the most part and many inter-unit ether and carbon-carbon bonds. Lignin's main function is to hold the cellulose fibers together in the wood. In addition to lignin and carbohydrates, there are other chemical substances, collectively called extractives, which impart color, odor, taste, and decay resistance to the wood.

2.4.2. Fiber surface

The fiber surface is coated with a layer of hydrated and negatively charged hydrophilic polymers, which originate either from the wood fiber (hemicellulose or soluble lignin fragments) or from chemical additives put into the process. It is suggested

that wood pulp fibers are rough, porous, complicated surfaces exhibiting behavior characteristics of both a hydrogel and a micro-porous solid [Pelton, 1993].

The wood fibers are negatively charged during the whole pH range of paper manufacturing. The ionizable groups on the cellulose fibers can be carboxyl groups, hydroxyl groups, and/or sulfonic acid and phenolic groups. For carboxyl groups, there are three sources: (A) the uronic acid residues in the form of 4-O-methyl- α -D-glucopyranosyluronic acid, which account for most carboxyl groups; (B) the pectic substances localized in the middle lamella; and (C) the fatty acids and resin acids in the extractives [Fengel et al., 1989]. The carboxyl group of hemicellulose is the largest source of surface charge for kraft fibers, and a typical range of carboxyl content in wood fiber is from 50 to 100 μeq per gram pulp [Scott, 1996].

2.4.3. Zeta potential of papermaking fiber

Although the electro-neutrality is maintained for colloidal suspension, the developed potential at local areas near the charged solid surface is observed. The potential distribution determines the interaction energy between particles, which is responsible for the stability of particles toward coagulation. The measurement of the Zeta potential, ζ , is one of the most valuable tools for obtaining information of surface potential, and has been used extensively in the paper industry.

Figure 2.5 illustrates the charge distribution on an anionic surface. It is recommended that in the papermaking system, the Zeta potential should be kept close to zero, but on the

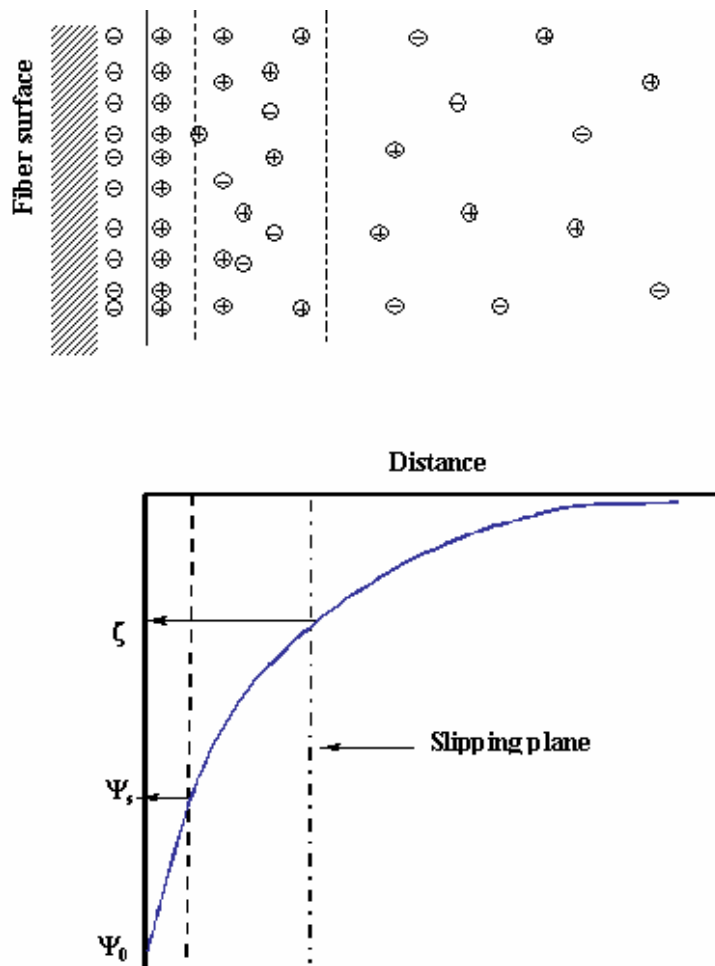


FIGURE 2.5 Schematic of the electrical double layer on a negatively charged particle. In the Stern layer, which is adjacent to the charged surface, the ions of opposite charge are held tightly to the surface by electrostatic forces and Van der Waals forces. In the Gouy-Chapman region, the opposite charges are less ordered. The slipping plane is the plane within which counter ions are bound to the particle and travel with it, outside which the counter ions move independently of the particle. The Zeta potential is defined as the potential of the slipping plane.

negative side [King, 1992]. The reason is that in this situation, the cationic additives are not overdosed. If the Zeta potential target is set to be zero, the possibility of overshooting exists, and the swing of Zeta potential across zero has a well-known adverse effect on the paper machine retention and operation efficiency.

2.5. Tissue chemical additives

Various tissue chemical additives are designed and applied in manufacturing according to different needs. In this section, two classes of tissue additives, i.e., wet strength resins and debonding agents, are introduced. They are cationic in nature, since fiber systems carry negative charges; cationic additives are effective at much lower concentration than anionic polymers [Swanson, 1961; Linke, 1968].

2.5.1. Wet strength resin

As mentioned in 2.2.2, paper strength depends on the strength of individual fibers and that of the inter-fiber bonding. At low basis weight, the strength of the cellulose network is more dependent on the inter-fiber bonding, which is hydrogen bonding in nature [Biermann, 1996]. The hydrogen bonds formed among the cellulose fibers are water sensitive and can be easily disrupted by water molecules. Upon contact with water, paper structure tends to lose integrity and more than 90 percent of its original strength. The

application of wet strength resin can retain 10 to 30 percent of paper's original dry strength.

There are several types of wet-strength resins available commercially. The urea-formaldehyde resins and melamine-formaldehyde resins are the first synthetic polymers, which reached commercial success in wet-strength paper application, and were used extensively under acid papermaking conditions [Chan et al., 1994]. The mechanism of wet strength development by urea-formaldehyde or melamine-formaldehyde proposes that during the curing process, the crosslinked polymer forms a network which protects the existing fiber-to-fiber bonds, making them resistant to water and retarding the loosening of the bonds by water [Fineman, 1952; Dalheim et al., 1956; Hazard et al., 1961; Kennedy, 1962]. Most formaldehyde based wet strength resins contain about 2-5 percent free formaldehyde, which will lead to its emission during paper curing and from the finished products on storage. Due to the environmental concerns of formaldehyde and the reduced need for its application in acidic medium, the usage of these polymers has declined significantly in the past decade [Peters, 2000].

Because of the paper industry's major trend of converting to the alkaline papermaking operations, the wet-strength resins applied under the neutral and alkaline conditions have gradually gained acceptance [Espy et al., 1988; Cates, 1992; Bi et al., 1993; Emerson, 1995]. The poly (amido-amine)-epichlorohydrin (PAE) resins are the most widely used wet strength agents, and have optimum performance under neutral and alkaline conditions. The PAE resins are used extensively in almost all types of wet strength

papers, for example, various tissue products (paper towels, napkins and facial tissue), packaging materials (liquid packaging, tea bags), and specialties (photographic papers).

The synthesis of PAE resins is similar to that of making Nylon-6, 6 and consists of (1) the formation of a pre-polymer with secondary or tertiary amine functionality, and (2) the reaction of the pre-polymer with epichlorohydrin. The resin precursors are made by a poly-condensation reaction of a polyalkylenepolyamine with a polycarboxylic acid. Typical examples are the resin made from polyethylenepolyamine, such as diethylenetriamine (DETA) with a dibasic acid, such as adipic acid [Keim, 1960]. The precursor is then alkylated and cross-linked with epichlorohydrin. The amine groups of the resin precursor may be primary, secondary, or tertiary. The most important PAE resins are derived from secondary amino polyamides, in which the 3-hydroxyazetidinium rings are the principal reactive functional groups [Carr et. al, 1973; Bates, 1969a, 1969b; Fischer, 1996]. Secondary amines react with epichlorohydrin to form tertiary aminochlorohydrins, which cyclize to form reactive 3-hydroxy-azetidinium salts [Ross et. al, 1964; Gaertner, 1966, 1967a, 1967b, 1968]. The final product consists of polyamide backbones with many reactive side chains. The azetidinium groups can (1) react with residual amines to form cross links and increase the molecular weight of the resin as shown in Figure 5.4(a); and (2) react with the carboxyl groups of cellulose surface as shown in Figure 5.4(b). The mechanism of the PAE resin is classified into two categories:

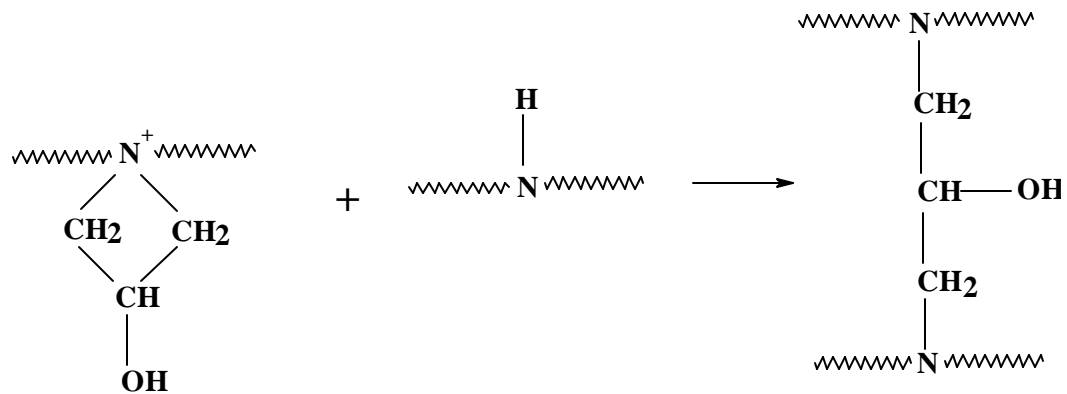


Figure 2.6 (A)

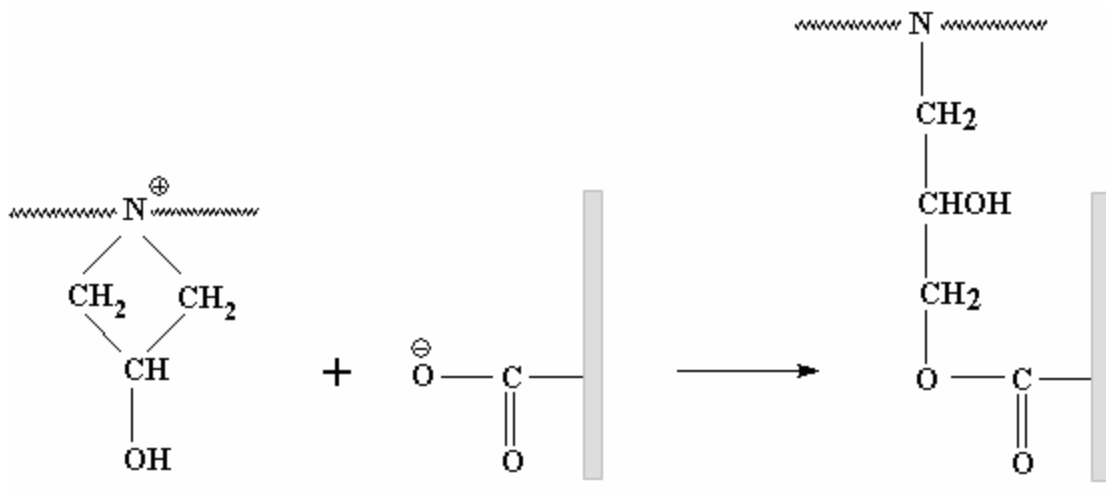


Figure 2.6(B)

FIGURE 2.6 (A) and (B) The chemical reactions to retain the wet strength of the cellulose web. (A) The azetidinium group in the wet strength resin reacts with residual amines to form cross links and increase the resin's molecular weight; (B) wet strength resin molecule reacts with the carboxyl group of cellulose surface.

(1) the preservation mechanism, which suggests that the cross-linking of the resin with itself occurs within the cellulose or surrounding the fiber-fiber contacts, impeding cellulose fiber swelling and holding the fibers with hydrogen-bonding distance; and (2) the reinforcement mechanism, which suggests that more direct covalent linking of cellulose to cellulose is achieved through a resin molecule or the resin network [Jurecic, 1958, 1960; Fredholm et al., 1983; Espy, 1988; Devore et al., 1993].

2.5.2. Debonding agent

The traditional cationic debonders usually are quaternary ammonium compounds, which have the structure shown in Figure 5.5. In practice, the long fatty alkyl chain in the debonder structure consists of 16-18 carbon atoms, which can be provided by the fatty acid in tallow or coconut oil [Phan et al, 1994a, 1994b]. The long fatty alkyl groups in the debonding agents disrupt the fiber-fiber bonding, which weakens the tissue sheet strength and increases the sheet bulk. The anionic group can be halide, i.e., chloride or bromide. The more popular anionic group is methyl sulfate. Interestingly, the optimum bactericidal activity of completely aliphatic compounds is achieved when the higher aliphatic group contains a chain of 16-18 carbon atoms.

The dialkyl dimethyl ammonium quaternaries are widely used as debonding agents by textile and tissue industries. Some examples of the dimethyldialkyl quaternary ammonium compounds include ditallow dimethyl ammonium chloride, di (hydrogenated tallow) dimethyl ammonium chloride, ditallow dimethyl ammonium methyl sulfate, and

di (hydrogenated tallow) dimethyl methyl Sulfate [Phan et al., 1997]. Poffenberger et al. have studied the debonding effects of the quaternaries with various fatty aliphatic groups (monoalkyl trimethyl ammonium quaternaries, dialkyl dimethyl ammonium quaternaries and the trialkyl monomethyl ammonium quaternaries) [1996]. It is found that among the quaternaries, the dialkyl dimethyl quaternaries have the best debonding effects for the blend of Northern Softwood kraft pulp and Southern Hardwood kraft pulp. This phenomenon can be explained as the result of the competition of two factors, i.e., debonder adsorption and the debonding effect per molecule [Liu et al., 2000].

Quaternary ammonium compounds often have strong germicidal effects. It is concluded [Baleux, 1977] that environmental bacteria, which are mainly involved in biodegradation, are much less susceptible to the bactericidal action of cationic surfactants than the pathogenic bacteria, which are the main targets of germicides. The biodegradation of cationic quaternary compounds, however, is relatively low, which causes environmental concerns [Cruz, 1979a, 1979b]. For most quaternaries today, their biodegradation profiles are reported to be below 40 percent [Poffenberger et al., 2000]. In response to increasingly stringent environmental regulations, the trend has shifted toward using the more biodegradable debonding agents.

The imidazolinium quaternaries are more readily biodegradable than the traditional quaternaries. The monododecyl imidazolinium compounds are shown to have speedier biodegradation than traditional quaternaries [Cruz, 1979a, 1979b]. The usual imidazolinium quaternary structure is shown in Figure 2.8 (A), which is a resonance

hybrid between the two extreme structures [Wysocki, 1970; Takano 1983]. Again the R in the formula refers to the long aliphatic hydrocarbon chain consisting from 11 to 21 carbon atoms. R1, R2 are usually smaller groups, or one of them hydrogen.

Quaternaries that incorporate ester functionality are rapidly biodegradable, and impart tissue with desirable properties [Phan et al., 1993a-d, 1994a,b, 1996, 1997]. The hydrolysis of ester-functional quaternary ammonium compounds can be catalyzed by acids or bases. Chain cleavage at ester bond level is auto-catalyzed by carboxyl end groups initially present or generated by the degradation reaction [Li et al., 1995]. Figure 2.8 (B) gives the structure of diester dialkyl dimethyl quaternaries, and Figure 2.9 illustrates the biodegradation reaction of the compounds. Some examples of the ester-functional quaternary ammonium compounds are monoester ditallow dimethyl ammonium chloride, diester di (hydrogenated) tallow dimethyl quaternary ammonium chloride, diester ditallow dimethyl quaternary ammonium chloride, and diester di (hydrogenated) tallow dimethyl quaternary ammonium methyl sulfate.

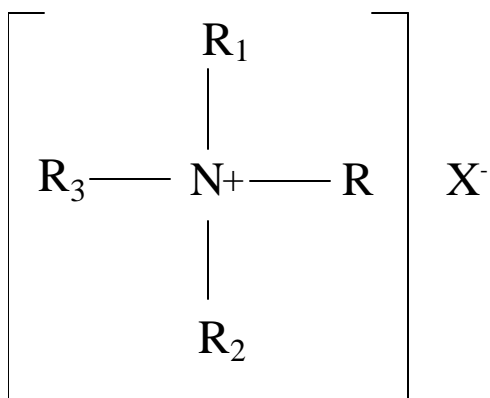


FIGURE 2.7 The structure of traditional debonding agent. In the above structure, the R is an aliphatic hydrocarbon C1-C6 chain, and usually methyl group is selected. Among R1, R2 and R3, at least there is one long fatty alkyl group, which is from C11 to C21, saturated or unsaturated.

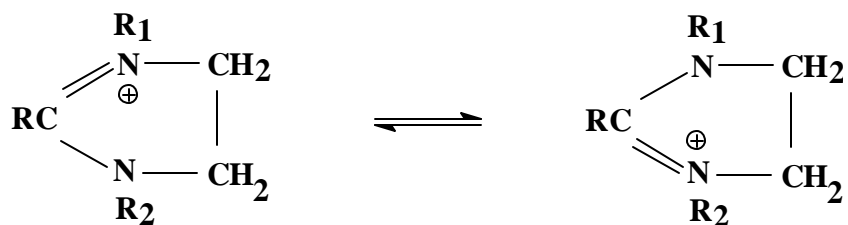


FIGURE 2.8 (A) Two extreme structures of imidazolinium compound

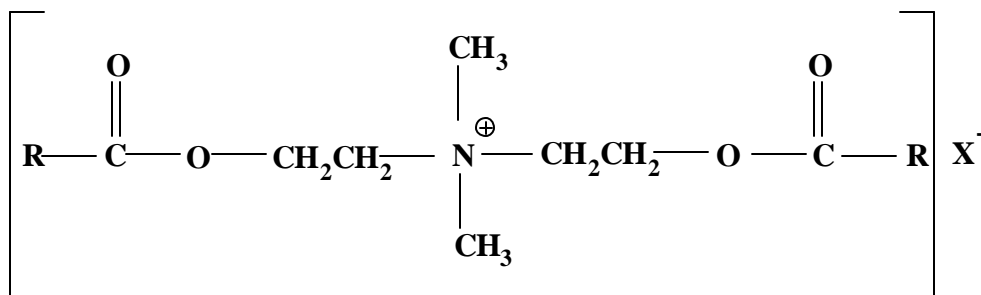


FIGURE 2.8 (B) Diester dialkyl dimethyl quaternary ammonium compound

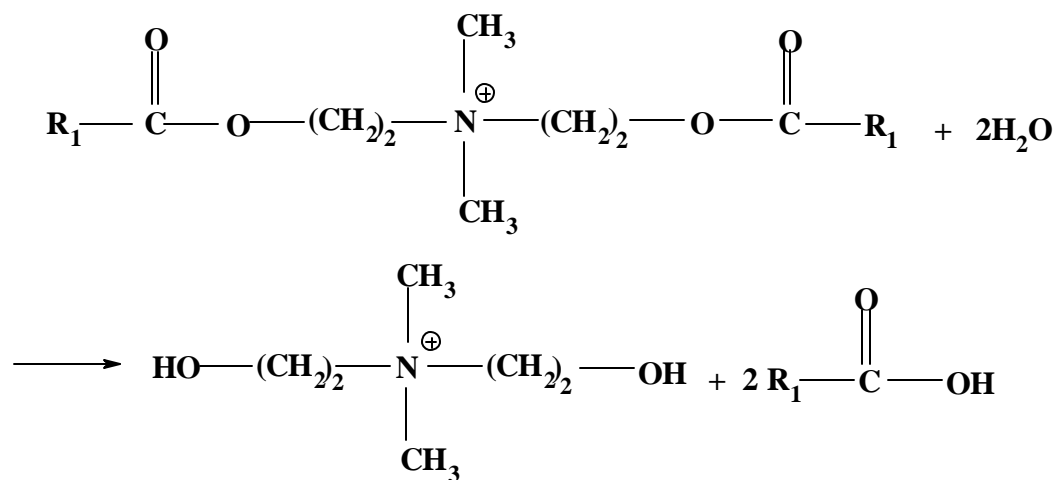


FIGURE 2.9 The biodegradation of debonding agent containing ester functionalities. Chain cleavage at ester bond level is auto-catalyzed by carboxyl end groups, and generates readily biodegradable fatty acids.

2.6. References

- Adanur, S., Effects of forming fabric structural parameters on sheet properties, *TAPPI Journal*, vol. **77**, no.10: 187-195 (1994)
- Ampulski, R. S., W. U. Spindel, A. H. Sawdai and B. Weinstein, Methods for the measurement of the mechanical properties of tissue paper, *Proceedings of 1991 TAPPI International Paper Physics Conference*, TAPPI Press, Atlanta, GA Vol. 1: 19-30 (1991)
- Andersson, I., Multilayer forming and the sheet properties of tissue, *Paper Technology & Industry*, vol.**29**, no.1: 28, 30-31 (1988)
- Ayers, P. G., *U.S. Patent 3,905,863*: Process for forming absorbent paper by imprinting a semi-twill fabric knuckle pattern thereon prior to final drying and paper thereof, Sept. 16, 1975.
- Baleux, B. and P. Caumette, Biodegradation of some cationic surfactants, *Water Research* **11**: 833-841 (1977)
- Bates, J. D., Softness index: fact or mirage, *TAPPI Journal* vol. **48**, no.4: 63-64 (1965)
- Bates, N. A., Polyamide-epichlorohydrin wet strength resin, part I: retention by pulp, *TAPPI Journal*, vol. **52**, no.6: 1157-1161 (1969a)
- Bates, N. A., Polyamide-epichlorohydrin wet strength resin, II: a study of mechanism of wet-strength development in paper, *TAPPI Journal*, vol. **52**, no.6: 1162-1168 (1969b)
- Becker, H. E., A. L. McConnell and R. W. Schutte, U. S. Patent 4,208,459: Bonded differentially creped fibrous webs and method and apparatus for making same, Jun. 17, 1980.
- Bi, S. L., P. C. Wu, H. Q. Dai, Z. Z. Li and B. Qian, Application of polyamide polyamine epichlorohydrin resin to wheat-straw pulp, *China Pulp Paper* **12**, no. 1: 32-37 (1993)
- Biermann, C.J., *Handbook of Pulping and Papermaking*, 2nd Edition, 41 (1996)
- Box, L., *U.S. Patent 4,908,097*: Modified cellulosic fibers, March 13, 1990.

Carr, C., and P. Knight, How to be objective about softness, *Pulp & Paper Europe* vol. **2**, no. 6: 32-35 (1997)

Carr, M. E., Doane, W. M., Hamerstrand, G. E., and Hofreiter, B. T., Interpolymer from starch xanthate and polyamide-polyamine-epichlorohydrin resin: structure and papermaking application, *Journal of Applied Polymer Science*, **17**(3): 721-735 (1973)

Carstens, J. E., *U. S. Patent 4300981*: Layered paper having a soft and smooth velutinous surface, and method of making such paper, November 17, 1981.

Cates, R. E., Wet-strength resins, *Chemical processing aids in papermaking: practical guide* (K. J. Hipolit, ed.), Chap. 9: 129-148, TAPPI Press, Atlanta, GA (1992)

Chan, L.L., and P.W.K. Lau, *Wet Strength Resin and Their Application*, TAPPI Press, Atlanta, GA, 3 (1994)

Choksi, P. V., E. E. Spaeth and J. A. Shiff, Adsorption characteristics of woven and nonwoven laparotomy sponges as measured by a novel device, *INDA Technical Symposium on Nonwoven Technology*, Washington, D.C., vol. **5**:29-41 (1977)

Clark, J. d'A., *Pulp technology and treatment for paper*, 2nd edition, Miller Freeman Publications, San Francisco, 119-140 (1985)

Corboy, W. G., Jr., *Guidelines for safe operation of Yankee dryers*, TAPPI Press, Atlanta, GA (1986)

Corte, H. and H. Schaschek, The physical nature of paper strength, *Papier, Das*, vol.**9**, no.21/22: 519-530 (1955)

Cowan, W. F., Short span tensile analysis, Pulmac Instrument Ltd., Montreal, 67p (1975)

Cozzens, D. E., Yankee doctors as a tool for tissue making, *Course notes of 1997 TAPPI tissue runnability short course*, 295-322, Cincinnati, OH, (1997)

Cruz, R., Influence of surfactant concentration and bacterial acclimation on biodegradation of cationic surfactants in river water, *Grasas Aceites* **30**: 293-299 (1979a)

Cruz, R., M. C. Dobarganes Garcia, Relation between structure and biodegradation of cationic surfactants in river water, *Grasas Aceites* **30**: 67-74 (1979b)

Dalheim, S., F. W. O'Neil and V. Stannett, The curing of paper-resin combinations with radiant heat, *TAPPI Journal*, vol.**39**: 234 (1956)

Devore, D. I. and S. A. Fischer, Wet strength mechanism of polyaminoamide-epichlorohydrin resins, *TAPPI Journal*, vol.**76**, no.8: 121-128 (1993)

Emerson, M. M., Impact of regulatory, worker safety, and end-product considerations in the selection of polyamide-epichlorohydrin wet strength resin technology, *Proceedings of 1995 TAPPI Papermakers Conference*, 153-156, TAPPI Press, Atlanta, GA (1995)

Eperen, V. and W. A. Winck, *IPC Project 2220*, Report 5, The Institute of Paper Chemistry, Appleton, Wis., June (1965)

Espy, H. H. and R. W. Rave, Mechanism of wet strength development by alkaline-curing amino polymer-epichlorohydrin resins, *TAPPI Journal*, vol. **71**, no.5: 133-137 (1988)

Fengel, D. and Wegener, G., *Wood-Chemistry: Ultra-structure, Reactions*, Walter de Gruyter, Berlin, New York (1989)

Field, J. H., Pulp parameters affecting product performance, *TAPPI Journal*, vol. **65**, no.7: 93-97 (1982)

Fineman, M.N., The role of hemicelluloses in the mechanism of wet strength, *TAPPI Journal*, vol. **35**, no.7: 320 (1952)

Fischer, S. A., Structure and wet-strength activity of polyaminoamide epichlorohydrin resins having azetidinium functionality, *TAPPI Journal*, vol. **79**, no.11: 100, 107, 116, 179-186 (1996)

Forbess, D. L., Wet end chemistry in towel and tissue, *Course notes: 1997 TAPPI tissue runnability short course*, 25-36 (1997)

Fredholm, B., Samuelsson, B., Wesfelt, A., and Westfelt, L., Chemistry of paper wet-strength (7) Effect of model polymers on wet-strength, water absorbency, and dry strength, *Cellulose Chem. and Technol.*, vol. **17**, no.3: 279-296 (1983)

Gaertner, V. R., Cyclization of 1-alkylamino-3-halo-2-alkanols to 1-alkyl-3-azetidinols, *Tetrahedron Letters*, no.**39**: 4691-4694 (1966)

Gaertner, V. R., Cyclization of 1-alkylamino-3-halo-2-alkanols to 1-alkyl-3-azetidinols, *Journal of Organic Chemistry*, **32**: 2972 (1967a)

Gaertner, V. R., Ring-opening alkylations of 1,1-dialkyl-3-substituted azetidinium cations, *Tetrahedron Letters*, no.**4**: 343-347 (1967b)

Gaertner, V. R., Ring-opening alkylations of 1,1-dialkyl-3-substituted azetidinium cations: substituent entropy controlled strained ring-chain equilibrium, *Journal of Organic Chemistry*, **33**: 523-530 (1968)

Greenfield, S. H., Testing tissue in the crumple zone, *World Paper*, vol. **219**, no.3: 28-29 (1994)

Hazard, S.J., F. W. O'Neil, and V. Stannett, Studies on the mechanism of wet strength development, part III, *TAPPI Journal*, vol.**44**, no.1: 35 (1961)

Hoffman, P., Horizontal wicking in non-pressed and pressed handsheets, *Scott Paper Co. Internal Report* (1994a)

Hoffman, P., The effect of inter-ply gap on wicking rate for Bounty, *Scott Paper Co. Internal Report* (1994b)

Hollmark, H., Chap. 20: Absorbency of tissue and toweling, *Handbook of physical and mechanical testing of paper and paperboard* (R. E. Mark and K. Murakami ed.), Marcel Dekker Inc., NY, vol.**2**: 143-168 (1983a)

Hollmark, H., Evaluation of tissue paper softness, *TAPPI Journal*, vol.**66**, no.2: 97-99, (1983b)

Hollmark, H., H. Andersson and R. W. Perkins, Mechanical properties of low density sheets, *TAPPI Journal*, vol.61, No.9, 69-71 (1978)

Jurecic, A., T. Lindh, S. E. Church and V. Stannett, Studies on the mechanism of wet-strength development I., *TAPPI Journal* vol. **41**: 465 (1958)

Jurecic, A., C. M. Hou, C. P. Donofrio, K. Sarkanen and V. Stannett, Studies on mechanism of wet strength development II, *TAPPI Journal* vol.**43**, 861 (1960)

Keim, G. I., *U.S. Patent 1,926,154*: Wet strength paper and method of making same, February 23, 1960.

Kennedy, R.J., Some observations on the mechanism of resin-cellulose interactions, *TAPPI Journal*, vol.**45**, no.9: 738 (1962)

- Kerr, A. J. and D. A. I. Goring, Ultrastructure arrangement of the wood cell wall, *Cellulose Chem. Tech.*, vol. **9**, 563-573 (1975)
- Kim, J. J., I. Shalev and R. L. Barker, Softness properties of fabric like tissues, *Proceedings of 1994 Nonwoven Conference*, 143-154 (1994)
- Kimmel, J. M. and F. H. Steiger, Effect of temperature on the surface wetting rate of cellulose fibers, *Ind. Eng. Chem. Prod. Res. Devt.*, vol. **9**, no. 2: 259-264 (1970)
- King, C. A., Charge and paper machine application, *Proceedings of 1992 TAPPI Papermakers Conference*, TAPPI Press, Atlanta, GA, 507-512 (1992)
- Kobayashi, T., Latest trend of forming fabric for paper machine, *Japan Pulp Paper*, vol. **27**, no.4: 73-87 (1990)
- Leffler, M., Through-air drying technology for absorbent, soft and high-bulk tissue, *Paper technology*, September 41-45 (1998)
- Li, S.M. and M. Vert, IV: Biodegradation of aliphatic polyesters, *Degradable polymers*, Edited by G. Scott and D. Gilead, Chapman & Hall, 43-87 (1995)
- Lindsay, J. D., and Leonard, H. B., Exploring tactile properties of tissue with Moirè Interferometry, *Proceedings of 1997 TAPPI Engineering & Papermakers Conference*, TAPPI Press, Atlanta, GA, Vol.2: 979-992 (1997)
- Linke, W. F., *TAPPI Journal* Vol. **51**, 59A(1968)
- Liu, J. and J. Hsieh, Effect of Scapa forming fabrics on the physical properties of handsheets, *Irving Tissue Inc. Internal Report*, p20 (1999)
- Liu, J., and Jeffery Hsieh, Application of debonding agent in tissue manufacturing, *Proceedings of 2000 TAPPI Papermaker Conference*, TAPPI Press, Atlanta, GA, Vol.1, 71-83 (2000)
- Lyne, M. B., A., Whiteman, D. C. Donderi, Multidimensional scaling of tissue quality, *Proceedings of TAPPI International Paper Physical Conference*, TAPPI Press, Atlanta, GA, 213-219 (1983)
- Lyne, M. B., A. Whiteman, D. C. Donderi, Multidimensional scaling of tissue quality, *Pulp Paper Canada*, vol.**85**, no.10: 43-46, 48-50 (1984)

Lyne, M. B., The effect of moisture and moisture gradients on the calendering of paper. In *Fiber-water interactions in papermaking*, F. Bolam, ed., British Paper and Board Industry Federation, London, 641-665 (1978)

Oliver, J. F., Dry creping of tissue paper- review of basic factors, *Yankee dryer and drying anthology of published papers*, W. G. Corboy, Jr., ed., TAPPI Press, Atlanta, GA, Chap. 4: 215-219 (1993)

Ona, I., and M. Ozaki, *U.S. Patent 5,281,658*: Fiber treatment agent composition, January 25, 1994.

Page, D. H., A theory for the tensile strength of paper, *TAPPI Journal*, vol.52, no.4: 674-681 (1969)

Pearlman, J., *U. S. Patent 3,060,719*: Testing paper tissues and the like, October 30, 1962.

Peek, R. L., Jr., and D. A. McLean, Capillary penetration of fibrous materials, *Ind. Eng. Chem.*, vol. 6, no.2: 85-90 (1934)

Pelton, R., Model of the external surface of wood pulp fiber, *Nordic Pulp and Paper Research Journal*, vol.8, no.1: 113-119 (1993)

Peters, J. C., Formaldehyde Based Wet-Strength Resins, *Proceedings of 2000 TAPPI Papermaker Conference*, 287-303, TAPPI Press, Atlanta, GA (2000)

Phan, D. V. and B. S. Hersko, *U.S. Patent 5,262,007*: Soft absorbent tissue paper containing a biodegradable quaternized amine-ester softening compound and a temporary wet strength resin, November 16 (1993a).

Phan, D. V. and P. D. Trokhan, *U.S. Patent 5,223,096*: Soft absorbent tissue paper with high permanent wet strength, Jun. 29 (1993b).

Phan, D. V. and P. D. Trokhan, *United States Patent 5,264,082*: Soft absorbent tissue paper containing a biodegradable quaternized amine-ester softening compound and a permanent wet strength resin, November 23 (1993c).

Phan, D. V., and P.D. Trokhan, *U.S. Patent 5,240,562*: Paper products containing a chemical softening composition, Aug.31 (1993d).

Phan, D. V. and P. D. Trokhan, *United States Patent 5,279,767*: Chemical softening composition useful in fibrous cellulosic materials, January 18 (1994a).

Phan, D. V., P. D. Trokhan and T. Trinh, *United States Patent 5,312,522*: Paper products containing a biodegradable chemical softening composition, May 17 (1994b).

Phan, D. V. and P. D. Trokhan, *U. S. Patent 5,405,501*: Multi-layered tissue paper web comprising chemical softening composition and binder materials and process for making the same, Apr. 11, 1995.

Phan, D. V., P.D. Trokhan, R.G. Laughlin and T. Trinh, *U.S. Patent 5,543,067*: Waterless self-emulsifiable biodegradable chemical softening composition useful in fibrous cellulosic materials, Aug.6, 1996.

Phan, D. V. and P. D. Trokhan, *U.S. Patent 5,698,076*: Tissue Paper Containing a Vegetable Oil Based Quaternary Ammonium Compound, December 16, 1997.

Pierce, C. J., Computation of pore sizes from physical adsorption data, *Journal of Physical chemistry*, vol.**57**, 149 (1953)

Poirier, D., J. Guadagno and C. Tourigny, Methods of evaluating hood drying rates, *TAPPI Journal*, vol.**79**, no.8: 361-365 (1996)

Poffenberger, C., Yvonne Deac and William Zeman, Novel hydrophilic softeners for tissue and towel applications, *Proceeding of 2000 TAPPI Papermakers Conference and Trade fair*, vol.**1**, 85-93 (2000)

Poffenberger, C. and N. Jenny, Evaluation of cationic debonding agents in recycled paper feedstocks, *1996 TAPPI Recycling Symposium*, 289-304 (1996).

Rance, H. F., *Paper-Maker*, vol. **126**, no.1: 31-34 (1953)

Rezai, E., and R. R. Warner, Polymer-grafted cellulose fibers: I. Enhanced water absorbency and tensile strength, *Journal of Applied Polymer Science*, vol. **65**: 1463-1469 (1997)

Robertson, A. A., The physical properties of wet webs, I. Fiber-water association and wet-web behavior, *TAPPI Journal*, vol. **42**, no.12: 969-978 (1959)

Ross, J. H., D. Baker, and A. T. Coscia, Some reactions of epichlorohydrin with amines, *Journal of Organic Chemistry*, **29**: 824-826 (1964)

Rust, J. P., Keadle, T. L., Allen, D. B., Shalev, I., and Barker, R. L., Tissue Softness Evaluation by Mechanical Stylus Scanning, *Textile Res. J.*, vol. **64**, no.3: 163-168 (1994a)

Rust, J. P., T. L. Keadle, I. Shalev and R. L. Barker, Evaluation of surface softness of tissue paper products using mechanical stylus scanning, optical image analysis, and fuzzy sets, *Proceedings of 1994 TAPPI Nonwoven Conference*, 139-142 (1994b)

Salvucci, J. L. and P. N. Yiannos, *U. S. Patent 3,812,000*: Soft, absorbent, fibrous, sheet material formed by avoiding mechanical compression of the elastomer containing fiber furnished until the sheet is at least 80% dry, May 21, 1974.

Scandinavian Pulp, Paper and Board Testing Committee, *SCAN-PI3*: 64, Capillary rise of water in paper and paperboard by the Klemm method (1964)

Scott, W. E., *Principles of wet end chemistry*, TAPPI Press, Atlanta, GA, Chap. 3: Basic properties of papermaking fibers and fiber fines important to wet end chemistry, 11-17 (1996)

Sisson, J. B., *U. S. Patent 3,303,576*: Apparatus for drying porous paper, Feb. 14, 1967.

Sloan, J. H., Yankee dryer coatings, *TAPPI Journal*, vol. **74**, no.8: 123-126 (1991)

Smook, G.A., *Handbook for Pulp and Paper Technologists*, Angus Wilde, Vancouver, B.C., 5-7 (1992)

Stevens, J. C. and S. S. Stevens, Warmth and cold: Dynamics of sensory intensity, *Journal of Experimental Psychology*, vol. **60**, no.3: 183-192 (1960)

Strauss, R. W., Papermaking machines: the Fourdrinier, *Pulp and Paper Manufacture*, MacDonald, R. G. Ed., McGraw-Hill, New York, Vol. **3**, 245-297 (1969)

Swanson, J. W., The science of chemical additives in papermaking, *TAPPI Journal*, vol. **44**, no.1: 142 (1961)

Takano, S., and K. Tsuji, Structural analysis of imidazolinium cationic surfactants, *Journal of the American Oil Chemists' Society*, vol. **60**: 870-874 (1983)

TAPPI Standard T411 om-89, Thickness (caliper) of paper, paperboard, and combined board, p3 (1989)

Trokhan, P. D. and D. V. Phan, *U.S. Patent 5,575,891*: Soft tissue paper containing an oil and a polyhydroxy compound, Nov. 19, 1996.

Trokhan, P. D., *U. S. Patent 4,191,609*: Soft absorbent imprinted paper sheet and method of manufacture thereof, March 4, 1980.

Warner, R. R. and E. Rezai, Polymer grafted cellulose fibers. III. Interactions of grafted and ungrafted fibers in handsheets, *Journal of Applied Polymer Science*, vol. **65**: 1487-1492 (1997a)

Warner, R. R. and E. Rezai, Polymer-grafted cellulose fibers, II Polymer localization and induced alterations in fiber morphology, *Journal of Applied Polymer Science*, vol. **65**: 1471-1485 (1997b)

Waterhouse, J. F., Ultrasonic testing of paper and paperboard: principles and applications, IPST Tech. Pap. Ser. No. 495: 13p (1993)

Wysocki, A. J., and D. Tabler, *Cyclical alkylammonium compounds*, pp.71-146 (1970)

CHAPTER III

EXPERIMENTAL

3.1. Introduction

Chapter 3 presents the experimental procedures used in this study. First, the experimental setup for the adsorption kinetics of Kymene[®]1500 and Softrite[®]7516 onto cellulose fibers is described. The methodology is established for the chemical adsorption via UV/Vis measurement. The method developed in this study represents the first that is capable of collecting accurate chemical adsorption data in the cellulose system and has the potential to generate more fundamental understanding of the important subject. Second, a detailed description is given on the procedures of applying the tissue chemical additives into handsheets, including the preparation steps, the making of the TAPPI handsheet, and the testing of the sheet physical properties. This chapter also includes the procedures of making electrokinetic measurements of the fiber system. Finally, the confocal microscopy technique for observation of internal paper structure is introduced at the end of the chapter. Other experimental procedures and instrument installations, such

as the automatic sheet former operation, commercial tissue softness characterization, and pulp quality study, are included in the appendices.

3.2. Chemical Adsorption Study

3.2.1. Methodology of chemical adsorption via UV/Vis measurement

In the chemical adsorption experiment, suppose the initial chemical concentration is C_0 , and C_t is the concentration in the bulk solution after time t . The chemical adsorption percentage is defined as

$$Adsorption = \frac{C_0 - C_t}{C_0} \quad (3.1)$$

According to Beer's Law, the absorption is proportional to the concentration of the test sample. Thus we have

$$A_0 = \epsilon \cdot l \cdot C_0 \quad (3.2)$$

$$A_t = \epsilon \cdot l \cdot C_t \quad (3.3)$$

where A_0 and A_t are the spectral intensity of the solution in the beginning and the time t of the absorption, and ϵ and l are the molar absorptivity of the solution and the optical path-length of the cell, respectively. Substituting Equations 3.2 and 3.3 into Equation 3.1, the

chemical adsorption percentage can be calculated from the solution's spectral intensity by Equation 3.4

$$Adsorption = 1 - \frac{A_0}{A_t} \quad (3.4)$$

3.2.2. Chemical calibration

A series of standard samples were prepared for a wet strength resin, Kymene[®]1500 and a debonder, Softrite[®]7516, respectively. The UV/Vis spectrum for each sample was collected by a spectrophotometer (UV-8453, Hewlett-Packard, Palo Alto, CA).

3.2.2.1 Kymene[®] 1500 concentration calibration

The UV spectra intensity was measured for the standard Kymene[®]1500 samples with concentration from 0 to 120 ppm and the calibration curve of the wet strength resin was obtained and shown in Figure 3.1. The linear calibration curve showed that the Beer's Law was applicable to Kymene solution at the studied concentration range. The correlation between the spectra intensity at 315 nm and Kymene concentration was fit by the following equation:

$$A=0.0014C \ (R^2=0.994) \quad (3.5)$$

where A is the spectra intensity of Kymene solution at 315 nm, and

C is the Kymene concentration in ppm.

3.2.2.2. Softrite[®] 7516 concentration calibration

The UV spectra intensity was measured for the standard Softrite[®]7516 samples with concentrations from 0 to 90 ppm and the calibration curve was obtained as shown in Figure 3.2. The calibration curve suggests that Beer's Law was applicable to the Softrite solution at the concentration range considered. The linear correlation equation between the softener spectra intensity at 330 nm and the debonder concentration was found to be

$$A=0.00097C \ (R^2=0.9966) \quad (3.6)$$

where A is the spectra intensity of softener solution at 330 nm, and C is the Softrite concentration in ppm.

3.2.3. Adsorption study of Kymene[®] 1500 and Softrite[®] 7516

The chemical adsorption experiments were conducted with an adsorption apparatus as shown in Figure 3-3. The flow loop consisted of a peristaltic pump (RP-1, Rainin Woburn, MA), nature Teflon tubing (0.762 mm ID, 1.588 mm OD, Optimize Technologies, Inc., Oregon City, OR), connectors, a 25mL beaker (30 mm ID, VWR), a net filter of 200 mesh (McMaster-Carr, Atlanta, GA), which was capable of separating the fibers from the chemical solution, and a UV/Vis optical flow cell. All adsorption measurements were continuously performed over the whole UV/Vis range by a

spectrophotometer (UV-8453, Hewlett-Packard, Palo Alto, CA) equipped with a HP ChemStation for real-time data collection and analysis.

The chemical solution was well mixed by magnetic stirring during the experiment. Distilled water was used as a blank solution for the UV/Vis measurements. 20 ml of Kymene[®] 1500 or Softrite[®] 7516 solution of a certain concentration was added to a 25 ml beaker under strong magnetic stirring. The mixing was provided by a Teflon-coated stir bar (length of 7 mm and width of 2 mm, VWR). The stirring speed of the KMO 2 basic magnetic stirrer (VWR) was set at 500 rpm. The net filter was positioned at the beaker center and 5 mm above the upper surface level of the stir bar. After fibers were filtered by the net, the filtrate was circulated through the optical flow cell of the spectrophotometer by the peristaltic pump. The flow rate of the pump was set to be 5 ml per minute. The total dead volume of the Teflon tubing and the flow cell was 0.21 ml or 1.05 percent of the solution volume in the beaker. The spectra signals collected by the spectrophotometer had a time lag of 1.3 seconds compared to those in the bulk solution. Therefore, the filtrate had higher chemical concentration than that of the bulk solution when it was re-circulated into the beaker. However, the potential increase in the bulk concentration caused by this effect was determined to be negligible; since even the filtrate concentration was twice as high as the bulk concentration, the bulk concentration was raised by less than 0.5 percent².

² From the adsorption data, the highest bulk concentration increase due to the time lag of the filtrate was less than 0.07 percent.

A pulp sample of 1.2 ± 0.02 g with 10 percent consistency was weighed. In the beginning of each adsorption experiment, the peristaltic pump was started and the chemical solution was circulated in the loop. The pre-weighted pulp was added to the bulk solution after the spectral signal of filtrate was stable for 15 seconds. Under the stirring speed of 500 rpm, complete mixing of the pulp with the solution was achieved after two seconds. The time-dependent spectra data of the filtrate were recorded by the ChemStation for four minutes with a time interval of 1 second. The spectra recorded were the average of 50 spectra measurements with the typical relative standard deviation of 0.1 percent. Therefore, a relative error in the ratio of the absorption spectral intensities in Equation 3.4 was 0.2 percent. Figure 3.4 shows the typical time-dependent UV/Vis absorption spectra of Kymene[®] 1500 solution, and Table 3.1 lists the experimental design for the chemical adsorption study.

The adsorption apparatus designed in this study was shown to be a valuable tool in gathering accurate kinetic data conveniently and in a relatively short period of time. Despite the advantages of the instrument, it did have its own limitations-- it was only capable of handling fiber consistency up to 0.6 percent. When the consistency was further increased, it tended to generate air bubbles in the filtering process, which led to the invalidity of spectroscopic data. Therefore, traditional chemical adsorption techniques using the dynamic drainage jar were adopted for the study at 1.2 percent fiber consistency.

The dynamic drainage jar (Paper Chemistry Laboratory, Inc., Carmel, NY) consisted of a vaned plexiglass jar and the base separated by a wire screen of 200 mesh and a support screen. A 63.5 mm diameter variable speed impeller was positioned in the jar just above the screen. The base of the jar had a valve to control the fluid flow from the jar. A total volume of 20 ml of chemical solution of desired levels was added to the fiber slurry, and the timer was started. The 10 ml samples were collected at 0.5, 1, 2, 7, 15 and 20 minutes of adsorption. In order to avoid collecting the liquid accumulated in the base, the valve was opened three seconds before the sampling time to release the accumulated liquid, which was then poured back into the drainage jar. Throughout the experiment, the stirring speed was 500 rpm and rotation of the propeller was set to be counter-clockwise. The Kymene and Softrite concentration was determined by charge titration with PVSK (poly-vinyl sulfate potassium, Nalco Chemical Company, Naperville, IL), and the toluidine blue (Aldrich Chemical Company, Milwaukee, WI) was used as the indicator dye.

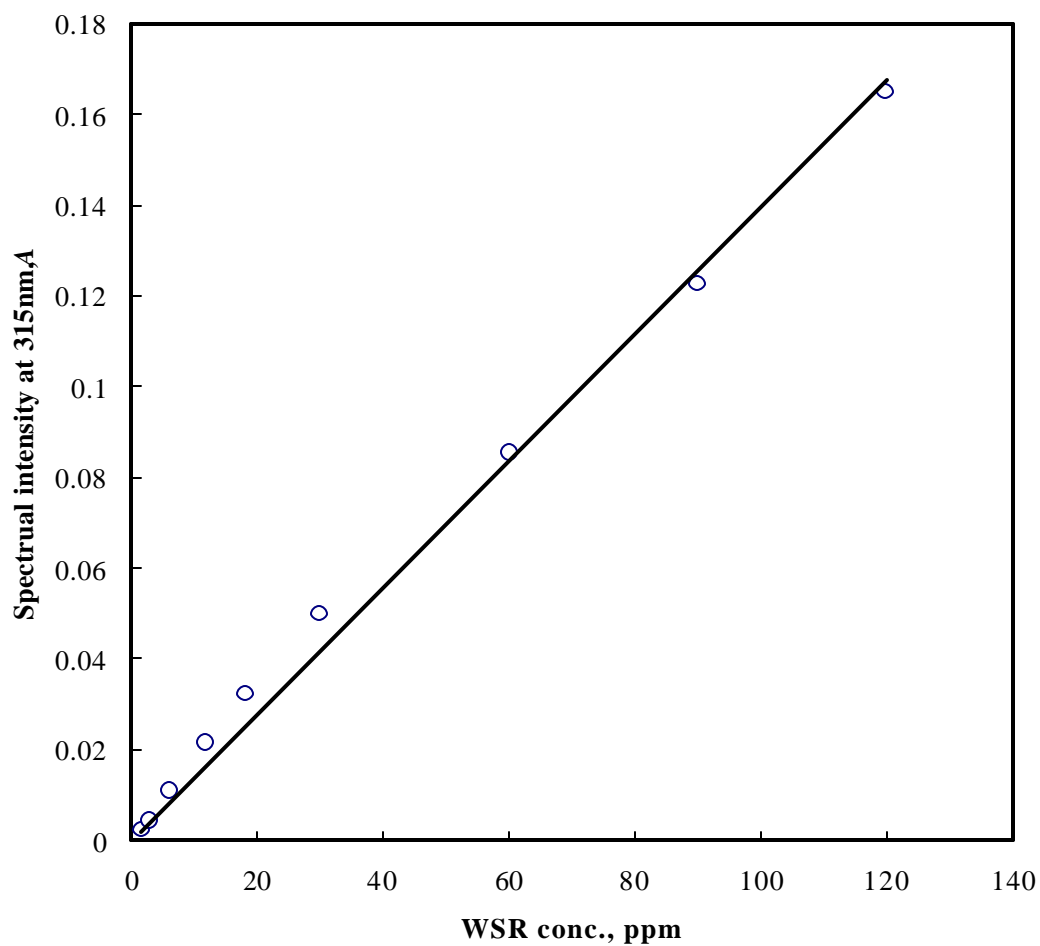


FIGURE 31 Calibration curve for Kymene[®] 1500. As shown in the figure, a linear relationship existed between the spectral intensity at 315 nm and wet strength resin concentration ($0 \leq c \leq 120$ ppm): $Y=0.0014x$ ($R^2=0.994$), where Y is the spectral intensity and x is the wet strength resin concentration in ppm.

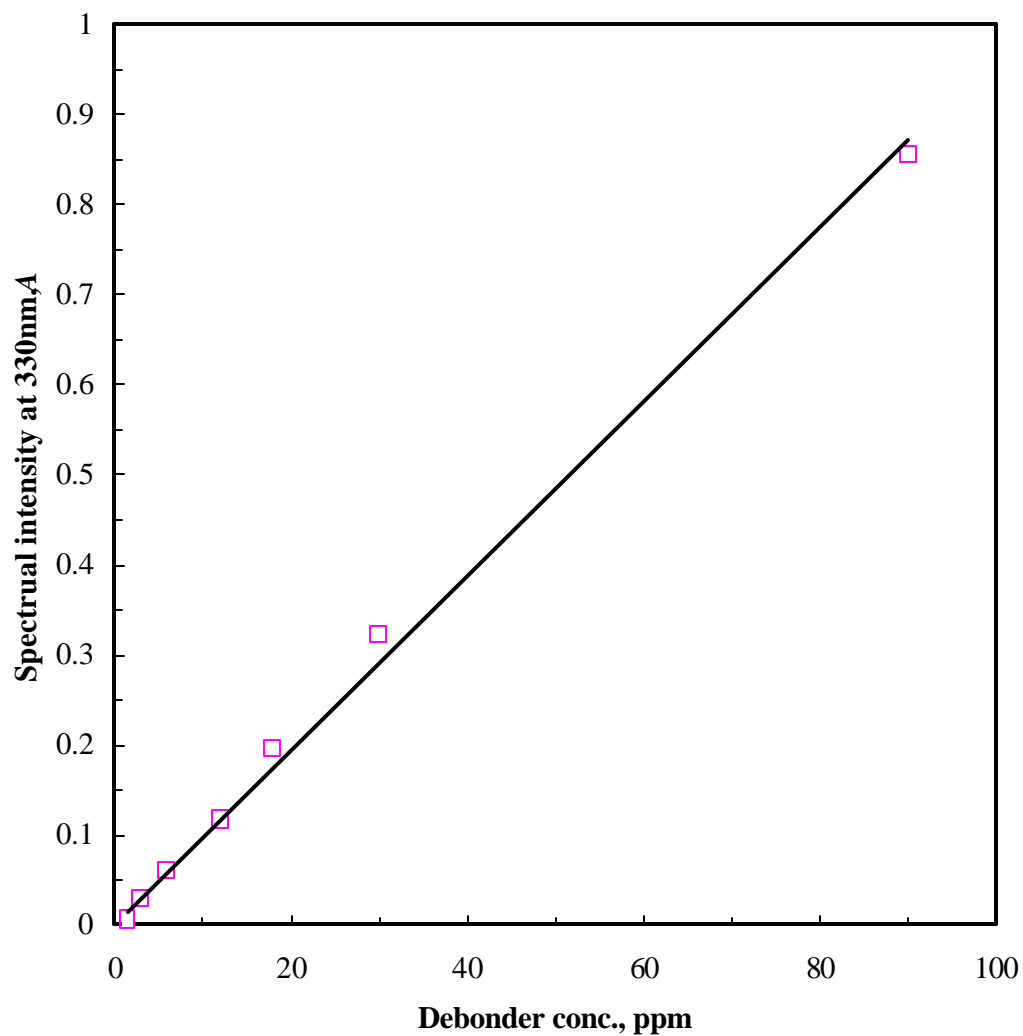


FIGURE 3.2 Calibration curve for Softrite® 7516. As shown in the figure, a linear relationship existed between the spectral intensity at 330 nm and debonder concentration ($0 \leq c \leq 90$ ppm): $Y=0.0097x$ ($R^2=0.9966$), where Y is the spectral intensity and x is the debonder concentration in ppm.

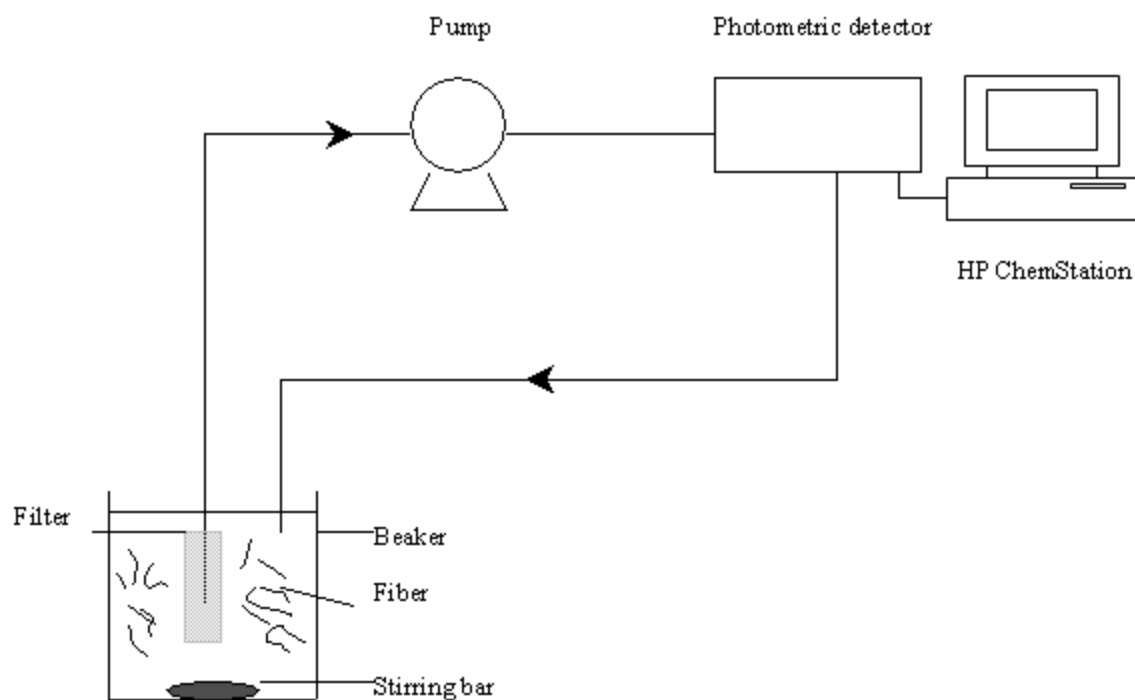


FIGURE 3.3 Schematic of experimental apparatus for chemical adsorption study. The solution in the beaker was well stirred by magnetic stirring. A mesh screen was used to filter out pulp fibers. The filtrate was transferred by a peristaltic pump to a photometric detector for UV/Vis measurement and re-circulated to the beaker.

TABLE 3.1 The experimental design for the chemical adsorption study

| | Wet strength resin, % | Debonder, % |
|---------------------------|-----------------------|-------------|
| Wet strength resin effect | 0.25 | 0 |
| | 0.50 | 0 |
| | 1.00 | 0 |
| Effect of the debonder | 0 | 0.25 |
| | 0 | 0.75 |
| Effect of the interaction | 0.25 | 0.25 |
| | 0.25 | 0.75 |

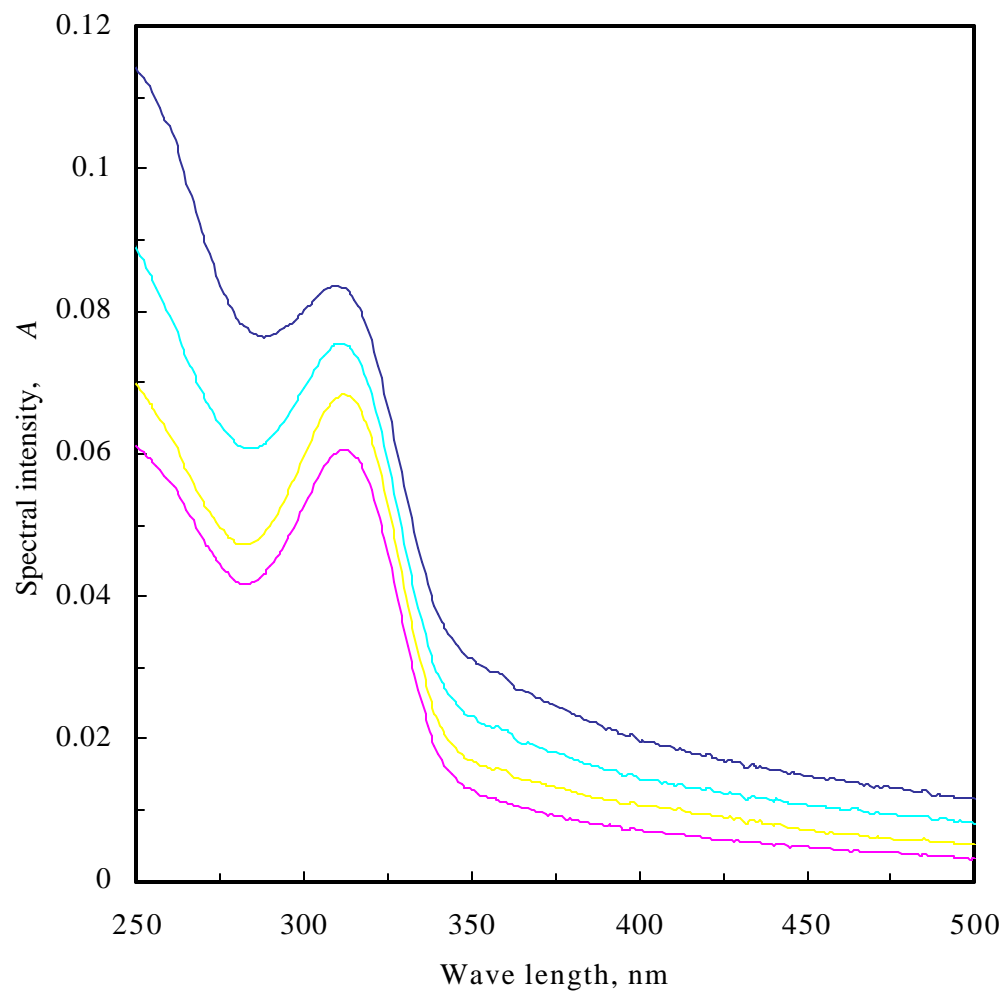


FIGURE 3.4 Typical time-dependent UV/Vis absorption spectra of Kymene[®] 1500 solution.

3.3. Preparations for making handsheets

3.3.1. Pulp wetting

Dry laps of kraft bleached hardwood and kraft bleached softwood pulp were soaked in deionized water for 5 minutes. The wet pulp lap was torn to equal pieces of about 30 mm² and then soaked in water for at least four hours.

3.3.2. Pulp consistency determination

Pulp consistency is defined as the mass percentage of the dry fiber in the pulp slurry. A certain mass (M_0) of partially dewatered pulp was taken, and put into a measuring cup (VWR) of mass M_1 . The pulp sample was torn further into very small and thin pulp pieces, and put into a forced ventilation oven for 30 minutes. The combined mass of the cup and pulp sample, M_2 , was recorded immediately after taken out of oven. The consistency of the wet pulp sample was calculated using Equation 3.7

$$C = \frac{M_2 - M_1}{M_0} \quad (3.7)$$

where C is the pulp consistency,

M_0 is the original mass of pulp sample, g,

M_1 is the mass of the measuring cup, g, and

M_2 is the mass of the oven-dried pulp sample and measuring cup, g.

The process was repeated for both hardwood and softwood pulp samples. The wet pulp was stored in sealed plastic bags in a dark cold room (at 4°C) for future experiments.

3.3.3. Pulp disintegration

The pulp slurry was a blend of both hardwood and softwood pulps. The amount of the hardwood and softwood pulp, m_k , was calculated by Equation 3.8

$$m_k = \frac{24 \cdot x_k}{C_k} \quad (3.8)$$

where m_k is the wet mass of pulp k, g,

X_k is the percentage of pulp k in the pulp blend, and

C_k is the consistency of pulp k.

In the study, the pulp slurry was the blend of 65 percent bleached hardwood kraft and 35 percent bleached softwood kraft pulp. Appropriate amounts of wet pulps were taken from the storage room and diluted to 2000 ml with water at $20 \pm 2^\circ\text{C}$. The pulp and water mixture was disintegrated in a TAPPI standard disintegrator at 3000 rpm to 40,000 revolutions. After disintegration, the pulp slurry was equally divided into two 1000 ml plastic beakers. The 1000 ml pulp slurry was transferred to a dynamic drainage jar (DDJ).

3.3.4. Chemical addition

3.3.4.1. Determination of chemical active solid content

The chemicals obtained from manufacturer usually contained a certain amount of solvent (water in this study). In the experiment, the calculation of chemical addition amount was always based on the active chemical content applied to the pulp slurry. The active solid content was measured in the following procedure: a chemical of certain mass M_1 was weighed on an aluminum pan of mass M_2 . The aluminum pan with the chemical was then put into a forced ventilation oven at 105°C for two hours to exhaust the solvent (water) in the chemical. The pan was taken out of the oven quickly and the combined mass of the pan and the chemical was measured. The active content was calculated as the ratio of the chemical dry mass to the wet mass.

3.3.4.2. Wet strength resin

The wet strength resin used in this study was Kymene[®] 1500 (Hercules Inc., Wilmington, DE), a polyamide-epichlorohydrin resin. The average molecular weight was about 500,000. The physical properties of Kymene[®] 1500 are summarized in Table 3.2.

3.3.4.3. Debonder

The debonder used was Softrite[®] 7516 (Southwest Engineers Paper Science, Slidell, LA). Its active chemical component was methyl-1 tallow-amidoethyl-2-tallow imidazolinium methyl sulfate. The physical properties of the debonder are summarized in Table 3.3.

TABLE 3.2 Physical properties of the wet strength resin, Kymene® 1500³

| Property | | Property | |
|---------------------|---------------------|------------------|------------------|
| Boiling point | 100°C | Evaporation rate | Similar to water |
| Freezing point | 0°C | Specific gravity | 1.03 |
| Vapor density | Lighter than air | Solids, % | 12.5 |
| pH | 2.8-3.2 | Appearance | liquid |
| Solubility in water | Miscible with water | Color | Light amber |

TABLE 3.3 Physical properties of Softrite® 7516

| Property | | Property | |
|---------------|---------|---------------------|--------------------------|
| Boiling point | N/A | Solubility in water | Dispersible |
| Melting point | 44-47°C | Appearance and odor | Light tan, viscous fluid |
| Vapor density | N/A | Specific gravity | 1.0 |
| pH | 4.5-5.6 | Flash point | >200°F |

³ The physical properties refer to those of commercially available Kymene® resin, which is the aqueous solution of 12.5 percent (wt.) Kymene®.

3.3.4.4. Application of chemical additives to pulp slurry

The pH of the pulp slurry was adjusted to 7.5 ± 0.1 using 0.1N Sodium hydroxide (NaOH) and 0.1N sulfuric acid (H_2SO_4). A pH meter (Corning, VWR) was used to monitor the pH of pulp slurry. The mixing speed of the dynamic drainage jar was set at 750 rpm. 1.2 percent polymer solution was added. Equation 3.9 was used to calculate the addition volume of the polymer solution:

$$V = 10 \cdot C \quad (3.9)$$

where V is the volume of 1.2% chemical solution, ml, and C is the chemical addition based on the dry fiber mass, percent.

The proper amount of polymer solution was added to the pulp slurry by a 20 ml syringe (VWR). Upon the polymer addition, a lab timer (Control Company, Texas) was started. The mixing was stopped after 20 minutes. The experimental conditions are listed in Table 3.4.

3.4. TAPPI handsheet making

The pulp slurry was transferred from the dynamic drainage jar and diluted with water of $20 \pm 2^\circ\text{C}$ to 4000 ml (0.30% consistency). The diluted pulp stock was well stirred. For each handsheet, 400 ml of the stock slurry was measured.

TABLE 3.4 The experimental design for chemical application unto handsheet

| | Wet strength resin, % | Debonder, % |
|---------------------------|-----------------------|-------------|
| Control | 0 | 0 |
| Wet strength resin effect | 0.25 | 0 |
| | 0.50 | 0 |
| | 1.00 | 0 |
| Effect of debonder | 0 | 0.25 |
| | 0 | 0.50 |
| | 0 | 0.75 |
| Effect of interaction | 0.25 | 0.25 |
| | 0.25 | 0.50 |
| | 0.25 | 0.75 |

Before making each handsheet, the water supply of the sheet mold (Essex International Inc., Custom Machinery, Lancaster, Ohio) was turned on and the wire surface of the handsheet mold was gently rubbed with fingers to remove any fibers and fines from previous experiment. The sheet mold was closed and when the mold was half filled with water, the pre-measured pulp stock was poured into the sheet mold. The water supply was shut off when the water level reached the line inscribed around the inside of the cylinder (349.3 mm above the wire surface).

A perforated stirrer was inserted into the handsheet mold and moved down and up five times within 6 ± 1 seconds. After a 5 second pause, when the liquid surface became motionless, the drain cock of the sheet mold was quickly and fully opened so that all the water could be drained. After all the water was drained, the pulp fibers were retained on the stainless wire to form a handsheet.

Two pieces of standard 8 inch by 8 inch blotting paper (Testing Machines Inc., Amityville, New York) were centrally placed upon the wet handsheet with the smoother side of blotting paper in contact with the handsheet. A flat stainless steel couch plate was centrally laid on the blotting paper, and the brass couch roll was gently placed in the middle of the plate. The roll was rotated forward and backward four times on the couch plate, and finally stopped in the middle of the plate. After the couch roll was lifted up, the wet handsheet, blotting paper and couch plate were removed from the wire. The couch filler (the blotting paper contacting couch roll) was discarded, and the couch blotting paper (the blotting paper contacting handsheet) was placed in the handsheet press with

the wet handsheet facing up. The wet handsheet was then covered with a polished metal plate with the polished side facing down. Another piece of fresh blotting paper was centrally put on the metal plate. The process was repeated. No more than 10 sheets were required for a complete sheet press operation. Finally a single piece of blotting paper was laid on the uppermost plate.

The cover of the handsheet press (Essex International Inc., Custom Machinery, Lancaster, Ohio) was placed in position and the wing nuts were screwed tightly. The first press switch was turned on so that the pressure of the press could be raised from 0 psig to 50 psig (345 kPa) within 30 seconds. The pressure was maintained for 5 minutes. After the pressure was released, the press cover was removed.

The stack of metal press plates and blotting paper was taken out from the press. Using a press template as a guide, the plate and sheet on the top of the stack were laid in the press followed by the second sheet and plate from the top of the plate and sheet stack. Therefore, in the second pressing, the sheet order was reversed. The press cover was put into place, and the switch of the second press was turned on. Again, within 30 seconds, the press pressure was raised from 0 psig to 50 psig as indicated by the pressure gauge and maintained for 2 minutes.

At the end of the second press, the plate and sheet stack were taken out of the press. The wet handsheet should have adhered to the polished side of the metal plate. Each plate with the wet handsheet was then fitted into the drying rings. The rings were assembled in a way that each handsheet was in contact with the rubber of the next ring above it. The

wet handsheets were dried under the standard conditions at $50.0 \pm 2.0\%$ relative humidity and $23.0 \pm 1.0^{\circ}\text{C}$ ($73.4 \pm 1.8^{\circ}\text{F}$). Before removing the handsheets from the metal plates, the handsheets were fully dried in the rings.

3.5. Sheet physical testing

3.5.1. Conditioning

Before physical testing, all handsheets were placed in a conditioning room overnight. The room was kept at $50.0 \pm 2.0\%$ relative humidity and $23.0 \pm 1.0^{\circ}\text{C}$ ($73.4 \pm 1.8^{\circ}\text{F}$) as required by TAPPI standard 402 om-88.

3.5.2. Basis weight

The mass of each handsheet was measured using Ohaus electronic balance (model GT 210, Precision Advanced, Florham Park, New Jersey). The basis weight of the handsheet was calculated using Equation 3.10

$$W = 48m \tag{3.10}$$

where W is the basis weight of the handsheet, g/m^2 , and

M is the mass of the handsheet, g.

3.5.3. Thickness

The thickness of handsheet was measured using an Electronic Thickness Tester (Model 89-100, Thwing-Albert Instrument Company, Philadelphia, PA). Although the thickness tester could operate at various pressures, the applied pressure was set to be 0.1 psi. The handsheet bulk was calculated with Equation 3.11

$$B = \frac{19.76t}{m} \quad (3.11)$$

where B is the handsheet bulk, cm³/g,

T is handsheet thickness, mm, and

M is handsheet mass, g.

3.5.4. Dry tensile strength

For each sample, 10 test specimens were cut with the width of 25.4 ± 1 mm (1.00 ± 0.04 in.). The test strips were free of wrinkles, creases and etc. The specimen was first aligned and clamped in the upper jaw of the QC-1000 Tensile tester (Thwing-Albert Instrument Company, Philadelphia, PA). After carefully removing noticeable slack, the specimen was clamped in the lower jaw. The purpose of the proper specimen alignment was to prevent the jaw tear type breaks. The tensile tester was started by pressing the “start” button, and the tensile and percentage of elongation were recorded when the strip was broken.

3.5.5. Wet tensile strength

The testing procedure of the sheet wet tensile strength was similar to that of the dry tensile testing except for the following:

After a 1.0 inch strip was cut from the sheet, the strip was folded in half (not creased) and dipped into distilled water for 30 seconds so that only the center (approximately 1 inch) of the sample was fully saturated with water. Both sides of the strip were put into contact with a blotting paper surface to completely remove the free water on the strip surface.

3.5.6. Handle-O-Meter stiffness

A Handle-O-Meter (Thwing-Albert Instrument Company, Philadelphia, PA) consisted of a penetrating arm pivoted to ride on an eccentric cam engaging the test specimen and forcing it into a slot. In this study, the slot width was adjusted to 6.35 mm (0.25 in.). A 3.5 inch by 1.0 inch handsheet squared was cut from the sample and placed across the platform over the slot. The slot width was still set to 6.35 mm (0.25 in.). The Handle-O-Meter was turned on to set the penetration arm in motion, and the force necessary to push the specimen into the slot to form a “U” shaped strip was recorded.

3.5.7. TWA (Total water absorbency)

The TWA test measured sheet water absorbency capacity. A 3 inch by 3 inch sample was cut from the handsheet. The sample was put into a weighing container and its mass

was measured on an Ohaus electronic balance (model GT 210, Precision Advanced, Florham Park, New Jersey). The dry weight was recorded to the nearest thousandth of a gram. The sample was attached to the alligator clips of the hunger. The sample was immersed into distilled water at room temperature for one minute. After removed from the water bath, the sample was allowed a few seconds to drain its free water. A 1/8 inch by 1-1/2 inch drainage strip of the same handsheet was attached to the bottom center point of the sample. The wet sample was hung in the drainage tank, and as the drainage tank lid was closed, the timer was started. To ensure valid results, the drainage tank must have at least 1 inch of water and water in the bath must be changed daily. The bottom of the water bath should not be slimy; otherwise the water's condition would affect the testing results. After draining for 2 minutes, the wet sample was removed from the tank, and the drainage strip was discarded. The wet sample was released from the alligator clips into the original weighing container and the lid of the container was closed. The mass of sample and container was measured again. The Total Water Absorbency (TWA) was calculated from the wet and dry sample mass using Equation 3.12

$$TWA = \frac{m - m_0}{m_0} \quad (3.12)$$

where TWA is the amount of water absorbed by paper of unit mass, g/g,

M is the wet mass of the sample, g, and

M₀ is the dry mass of the sample, g.

3.6. Zeta potential measurement

The Zeta potential of the pulp fiber solution, ζ , was measured with a System Zeta Potential meter (SZP 04, Mutek Analytical GmbH Herrsching, Germany). For each measurement, 500 ml of pulp slurry at one percent pulp consistency was used. The pulp slurry was prepared in the distilled water. Solutions of Softrite[®]7516 and Kymene[®]1500 with known concentrations were prepared. According to the oven dry fiber based chemical concentration (shown in Table 3.5), a proper amount of chemical solutions was added to the pulp slurry and mixed with a magnetic stirrer for 5 minutes.

The pulp sample was then placed under the intake tube of SZP 04. The intake tube was completely immersed into the pulp to avoid the interference of air bubbles. A sample portion was extracted by vacuum through the intake tube and a fiber plug was formed at the screen electrode. By varying the vacuum pressure, a streaming potential was induced and detected at the electrodes. With the sample viscosity, dielectric constant, electric conductivity, pressure differential, and streaming potential, the Zeta potential was obtained by the Helmholtz-Smoluchowski Equation

$$\zeta = \frac{4\eta h}{e} \bullet \frac{V_c}{\Delta p} \quad (3.13)$$

where ζ is the zeta potential, mV,

TABLE 3.5 The conditions used for zeta potential measurement

| | Wet strength resin, % | Debonder, % |
|--------------------|-----------------------|-------------|
| Control | 0 | 0 |
| Effect of Kymene | 0.05 | 0 |
| | 0.10 | 0 |
| | 0.15 | 0 |
| | 0.20 | 0 |
| | 0.25 | 0 |
| | 0.50 | 0 |
| | 1.00 | 0 |
| Effect of Softrite | 0 | 0.25 |
| | 0 | 0.50 |
| | 0 | 0.75 |

ϵ is the dielectric constant,

V is the streaming potential, mV,

χ is the electric conductivity, mS, and

Δp is the pressure difference, bar.

The reproducibility of zeta potential measurement by SZP 04 was ± 1.0 mV (Mutek Analytical GmbH, Herrsching, Germany).

3.7. Confocal microscopy

To qualitatively observe the effects of chemical additives on sheet structures, confocal microscopy was used to visualize the fiber structures within the sheet. Confocal microscopy has been increasingly applied in the fields of biology, medicine, and material sciences [Shotton, 1989; Verhoogt et al., 1993]. In this study, it allowed for the noninvasive optical sectioning of three-dimensional paper sheet to show the fiber network at certain depth within the sample. The basic principle is that light at a certain wavelength is used to excite a sample that is auto-fluorescent or contains fluorescent molecules. A set of filters and mirrors are then used to block out emitted light that is not in the focal plane. With this method, cross-sections (x, yplane) can be obtained for various imaging depths (z-planes).

The Zeiss LSM-510 was used in this study. A tissue sample of approximately 2 cm by 2 cm was cut from a commercial product and placed upon a glass slide (VWR). The

sample was placed beneath a cover slip (VWR). In order to overcome sample waviness, Scotch tape (3M, St. Paul, MN) was used to secure the position of the cover slip.

Figure 3.5 shows a series of the confocal images of tissue sample cross sectioning. As the figure shows, the internal tissue structure over its whole thickness was visible. This was due to the auto-fluorescent nature of the cellulose fiber and the loose fiber structure by the special tissue manufacturing processes. The laser scanning microscopy of the handsheet was performed in the same procedure as that for commercial tissue product. However, the observation of the handsheet structure over the entire depth was difficult due to the increased basis weight and the compact fiber structure of the handsheet. It is expected that advances in confocal systems, such as laser and light path configuration, will soon allow the reconstruction of the entire three-dimensional structure of conventional paper sheets [Béland et al., 1995].

3.8. References

Shotton, D. M., Confocal scanning optical microscopy and its applications for biological specimens, *J. of Cell Science* **94**, 175-206 (1989)

Verhoogt, H. Van Dam, A. Posthuma de Boer, A. Draaijer and P. M. Houpt, Confocal laser scanning microscopy: A new method for determination of the morphology of polymer belnds, *Polymer* **34**(6), 1325-1329 (1993)

Béland, M. C. and P. J. Mangin, Chap. 1: Three-dimensional evaluation of paper surfaces using confocal microscopy, Surface analysis of paper (edited by T. E. Connors, S. Banerjee), CRC Press, Boca Raton, FL (1995)

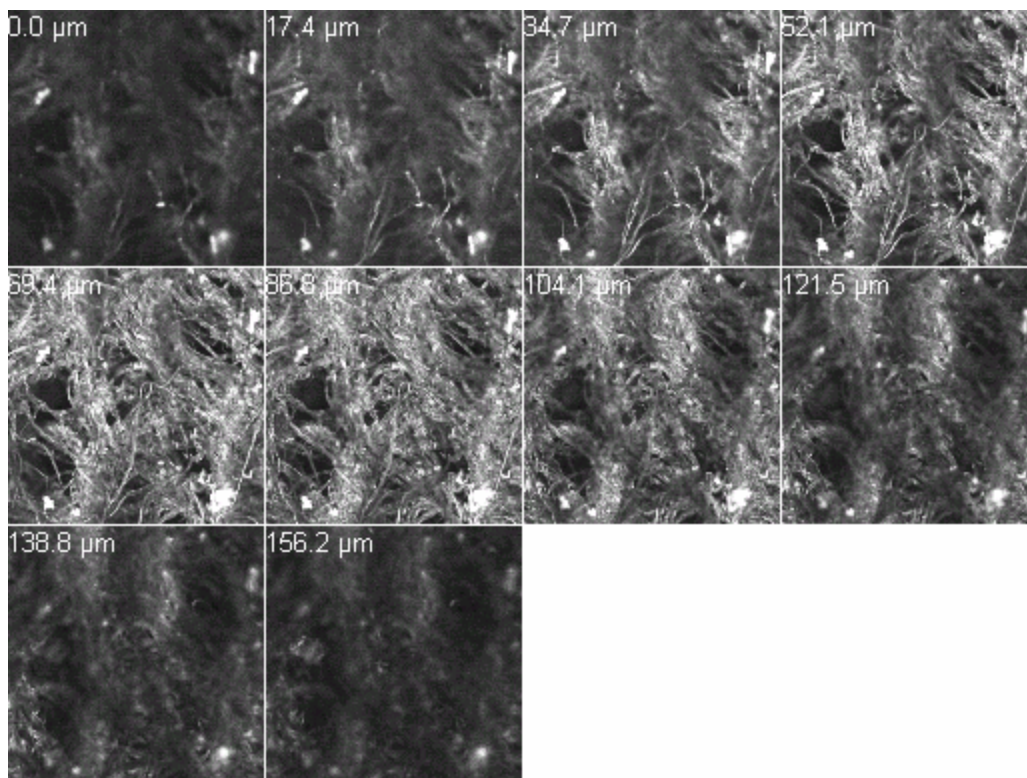


FIGURE 3.5 Series of confocal images showing the cross sectioning of a tissue sample over an area of $920\ \mu\text{m}$ by $920\ \mu\text{m}$ with the thickness of $156.2\ \mu\text{m}$. The fiber structure of the tissue over whole range of thickness was visible, because (1) the pulp fibers were auto-fluorescent, and (2) the fiber structure was loose due to special tissue manufacturing processes. However, for the $60\ \text{g/m}^2$ TAPPI handsheet, it was difficult to observe the sheet internal structure over the whole range of its thickness due to the compact fiber structure.

CHAPTER IV

ADSORPTION OF WET STRENGTH RESIN AND DEBONDING AGENT ON CELLULOSE FIBERS

4.1. Introduction

In order to be effective in modifying sheet properties, the chemical additives must first adsorb onto the cellulose fiber surface. In the papermaking research, the study of polymer adsorption kinetics is more important than the equilibrium study since the timeframes in the dynamic production are much shorter than the time needed for reaching equilibrium [Scott, 1996; Most, 1957]. In this chapter, the adsorption kinetics of a wet strength resin, Kymene[®]1500, and a debonding agent, Softrite[®]7516, onto cellulose fibers at two consistencies are investigated, and the adsorption mechanisms are proposed. The zeta potential of the fiber system is measured in order to provide valuable information on the polymer adsorption onto cellulose fibers. The study utilizes a novel experimental setup so that the chemical adsorption on the cellulose can be monitored reliably. Besides the individual chemical's adsorption kinetics, the simultaneous competitive adsorption of Kymene[®]1500 and Softrite[®]7516 is also investigated.

4.2. Results and discussion

4.2.1. Adsorption of Kymene[®]1500 on cellulose fiber

Figure 4.1 shows the Kymene adsorption kinetics over a period of 260 seconds at 0.6 percent fiber consistency. Three Kymene concentrations were studied at 0.25, 0.5 and 1 percent. The absolute Kymene amount adsorbed on fiber increased in the order of dry fiber based chemical concentration.

Figure 4.2 shows the adsorption of Kymene on the cellulose fiber at 1.2 percent fiber consistency. Compared to the adsorption at 0.6 percent consistency, the adsorption percentage increased much faster at all Kymene concentrations. At the 0.25 percent level, the Kymene adsorption reached 95 percent at 7 minutes, and more than 99 percent was adsorbed on the fiber after 20 minutes. The adsorption kinetics at 0.5 percent was similar to those of the 0.25 percent Kymene addition, except that the adsorption percentage was several points lower. At the highest Kymene level, 1.0 percent, the increase in adsorption percentage was the lowest. At the end of 20 minutes, the chemical adsorption reached 92 percent.

The more rapid and complete adsorption at a higher consistency is consistent with previous observations on the effect of fiber consistency on chemical adsorption [Scott,

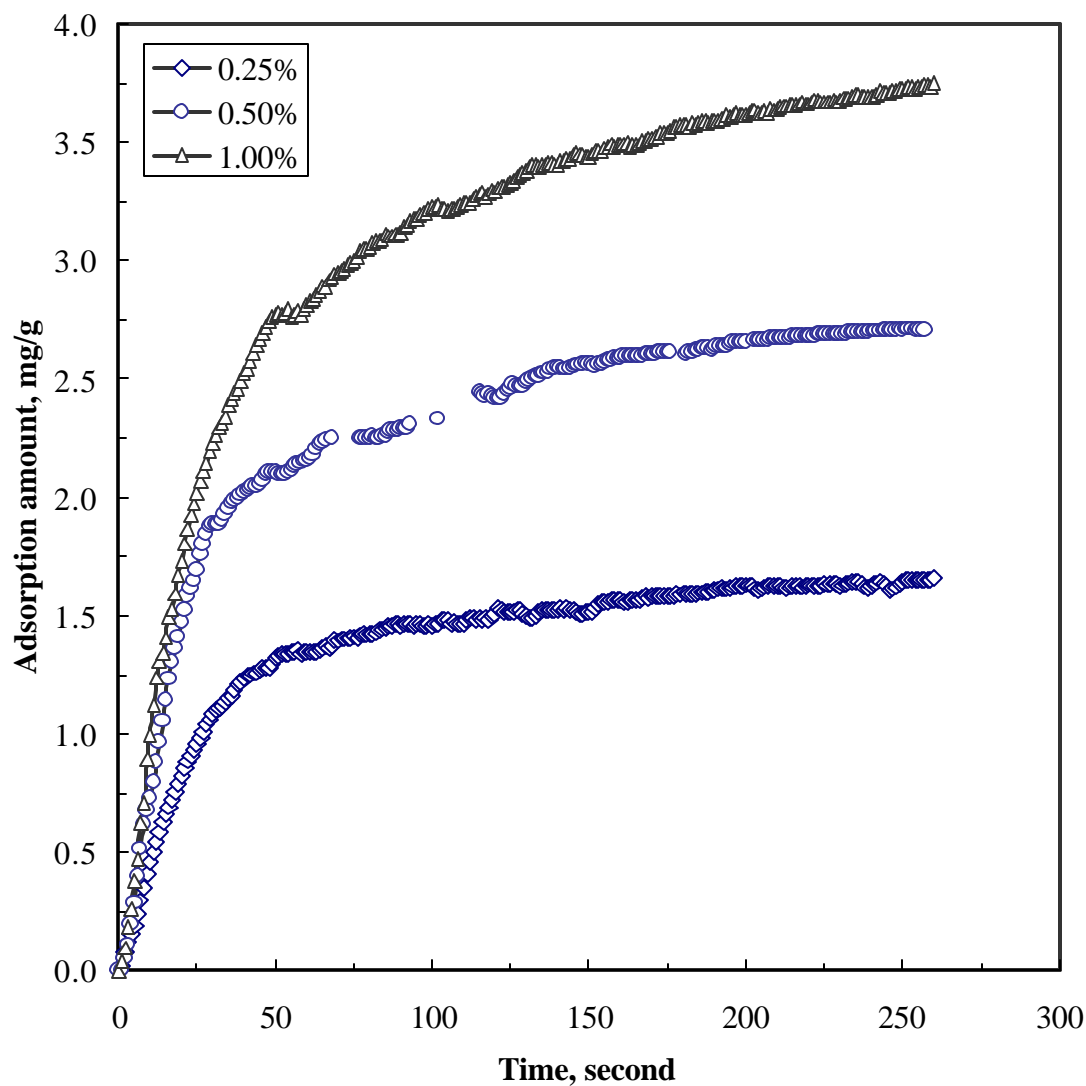


FIGURE 4.1 Graph of adsorbed amount of Kymene®1500 versus time. Three levels of wet strength resin addition, i.e., 0.25, 0.5 and 1.0 percents, were investigated in the study. The fiber consistency of the system was 0.6 percent. The spectroscopic data were collected from 0 to 260 seconds to determine the concentration of Kymene®1500.

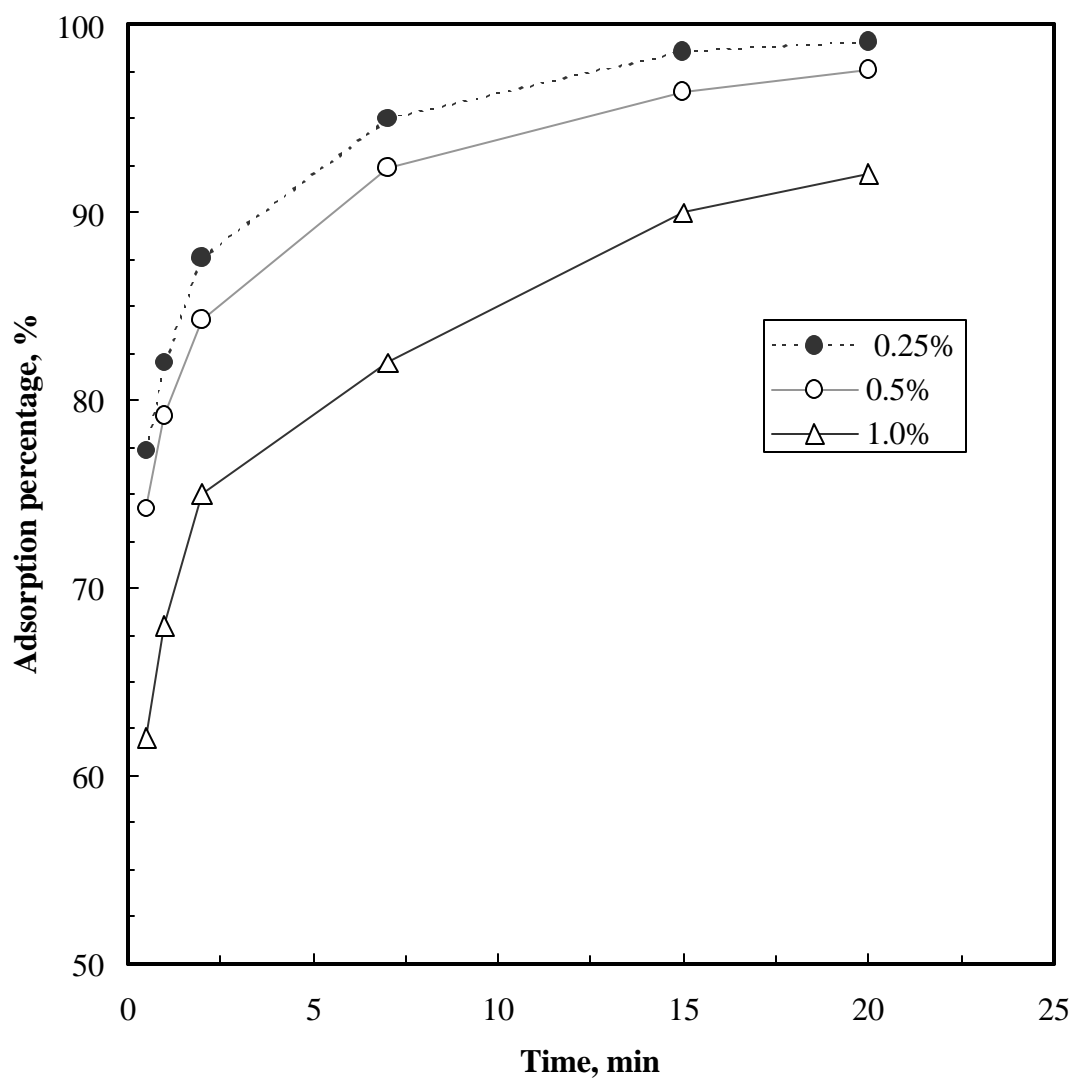


FIGURE 4.2 Graph of Kymene[®]1500 adsorption versus time. Three levels of wet strength resin were studied. The fiber consistency of the system was 1.2 percent. The concentration of Kymene[®]1500 was determined by charge titration.

1996]. The explanation is that with a higher surface area per unit volume at higher fiber consistencies, the probability of contact between polymer and fiber is enhanced. The implication for production is that the polymer needs to be added at thick stock box so that the adsorption of the wet strength resin can be more complete.

The adsorption kinetics at 0.6 percent fiber consistency was studied using the novel experimental setup, which had been shown to be a valuable tool in gathering adsorption kinetic data in a relatively short period of time. Due to reasons given in Chapter 3, the apparatus could not be used in the adsorption study at higher fiber consistencies. The adsorption mechanism analysis is, therefore, based on the result at 0.6 percent fiber consistency, since there are much more kinetic data available.

At all three Kymene concentrations, the initial adsorption was always the fastest. The adsorption rate became lower as the process continued. At the long time, the adsorption percentage varied at three Kymene concentrations. In the paper industry, the collision model is often used to describe the adsorption of a polymer on colloidal particles [Falk, 1989; Pelssers et al., 1990; Tanaka et al., 1999]. The collision model suggests that if the particle number density does not change significantly and only part of the particle surface is coated with the polymer, the adsorption rate is essentially determined by the effective collisions among polymers and particles. The collision model assumes the format of an irreversible adsorption and leads to a complete adsorption over the long time. It seems that at the studied conditions, the Kymene adsorption data can not be explained by the collision model.

The examination of the adsorption data show that the process could be modeled by the mathematical format of a reversible adsorption, which suggests that

$$\frac{dc}{dt} = -k_a N_0 c + k_d (c_0 - c) \quad (4.1)$$

where C is the solute bulk concentration, Kmol/m_f³,

k_a is adsorption rate constant, m_f³/(#• s),

N_0 is volumetric fiber density, #/ m_f³

k_d is the desorption rate constant, s⁻¹, and

t is the time, s.

The adsorption percentage is:

$$A = \left(\frac{k_a N_0}{k_a N_0 + k_d} \right) \left[1 - e^{-(k_a N_0 + k_d)t} \right] \quad (4.2)$$

Therefore in the long time, the adsorption percentage at equilibrium is

$$A_e = \frac{k_a N_0}{k_a N_0 + k_d} \quad (t \rightarrow \infty) \quad (4.3)$$

The following equations show the correlation results at three Kymene concentrations:

At 0.25 percent:

$$A = 0.679[1 - e^{-0.0172t}] \quad R^2 = 0.89 \quad (4.4)$$

At 0.75 percent:

$$A = 0.543[1 - e^{-0.0206t}] \quad R^2 = 0.94 \quad (4.5)$$

At 1.0 percent:

$$A = 0.378[1 - e^{-0.0168t}] \quad R^2 = 0.96 \quad (4.6)$$

Figures 4.3-5 compare the adsorption data and the model predictions at different Kymene concentrations. For all concentrations, the reversible adsorption format fits the latter stage of the adsorption better than the beginning. Another observation is the adsorption kinetics can be modeled better with a reversible adsorption as the initial Kymene concentration increases. At 0.25 percent Kymene concentration, the R^2 value is 0.89. As initial Kymene concentration is increased to 1.0 percent, the R^2 value increases to 0.96.

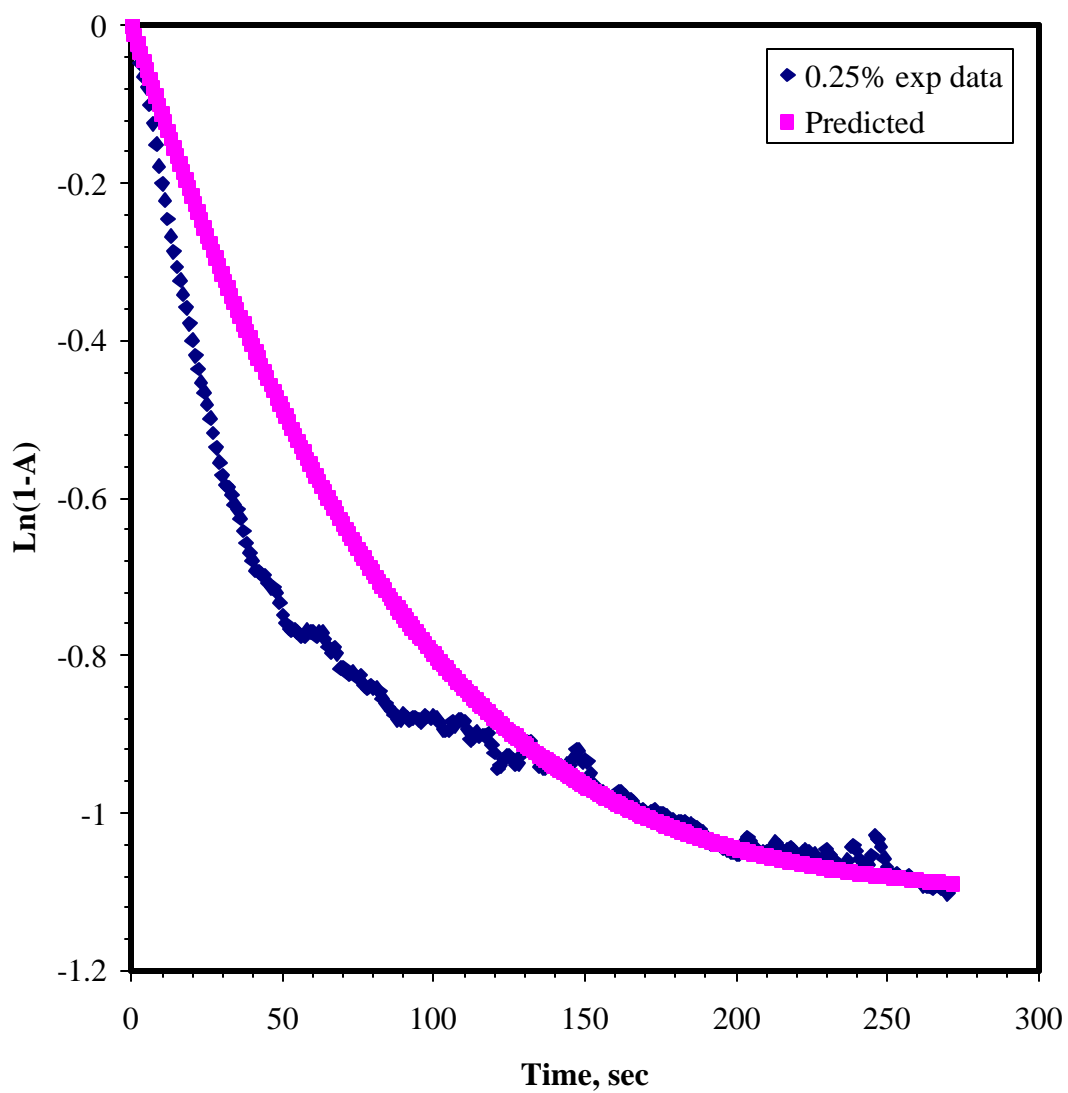


FIGURE 4.3 Graph showing model predictions at 0.25 percent Kymene concentration. $R^2=0.89$. The blue diamonds and pink squares represent the experimental data and the model prediction respectively.

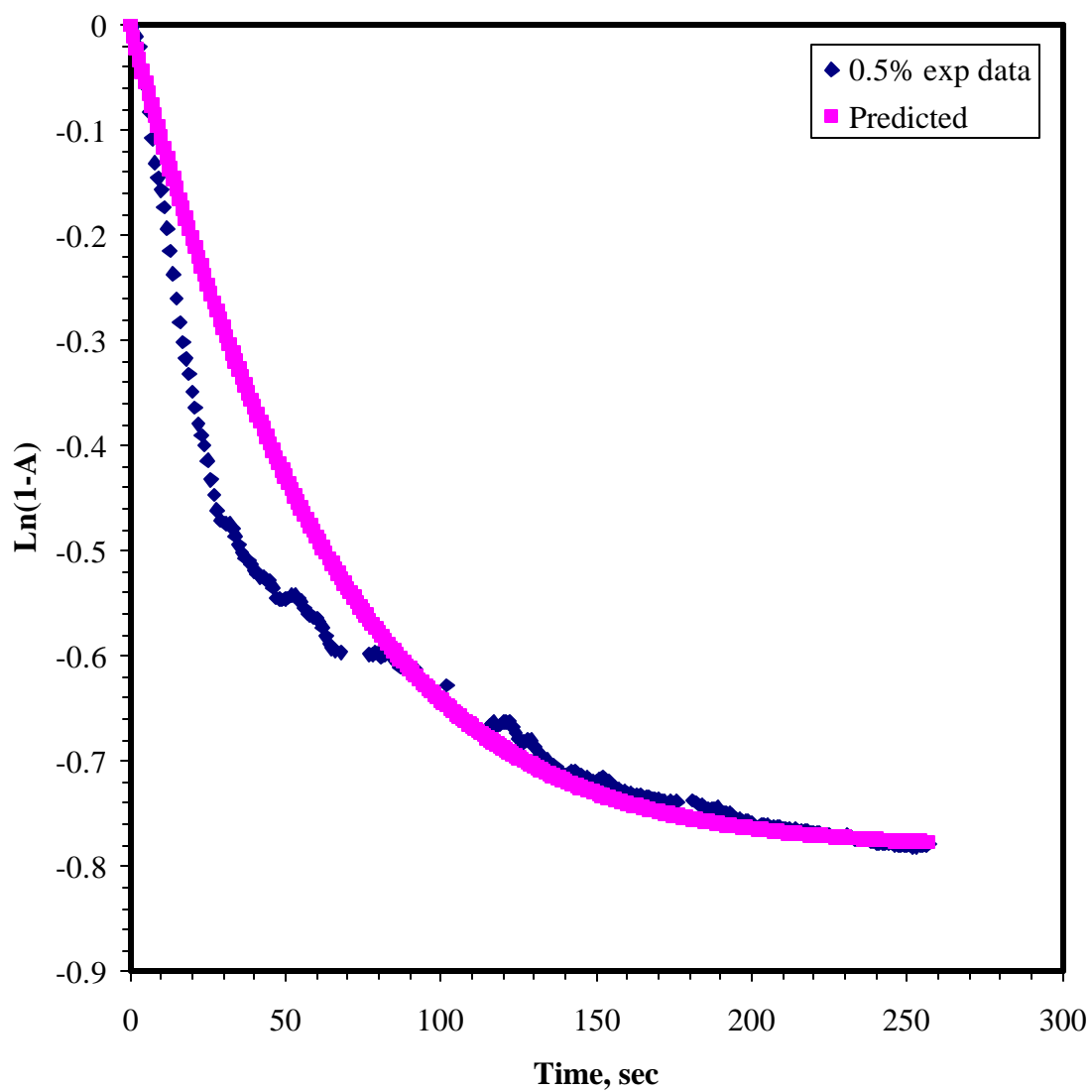


FIGURE 4.4 Graph showing model predictions at 0.5 percent Kymene concentration. $R^2=0.94$. The blue diamonds and pink squares represent the experimental data and the model prediction respectively.

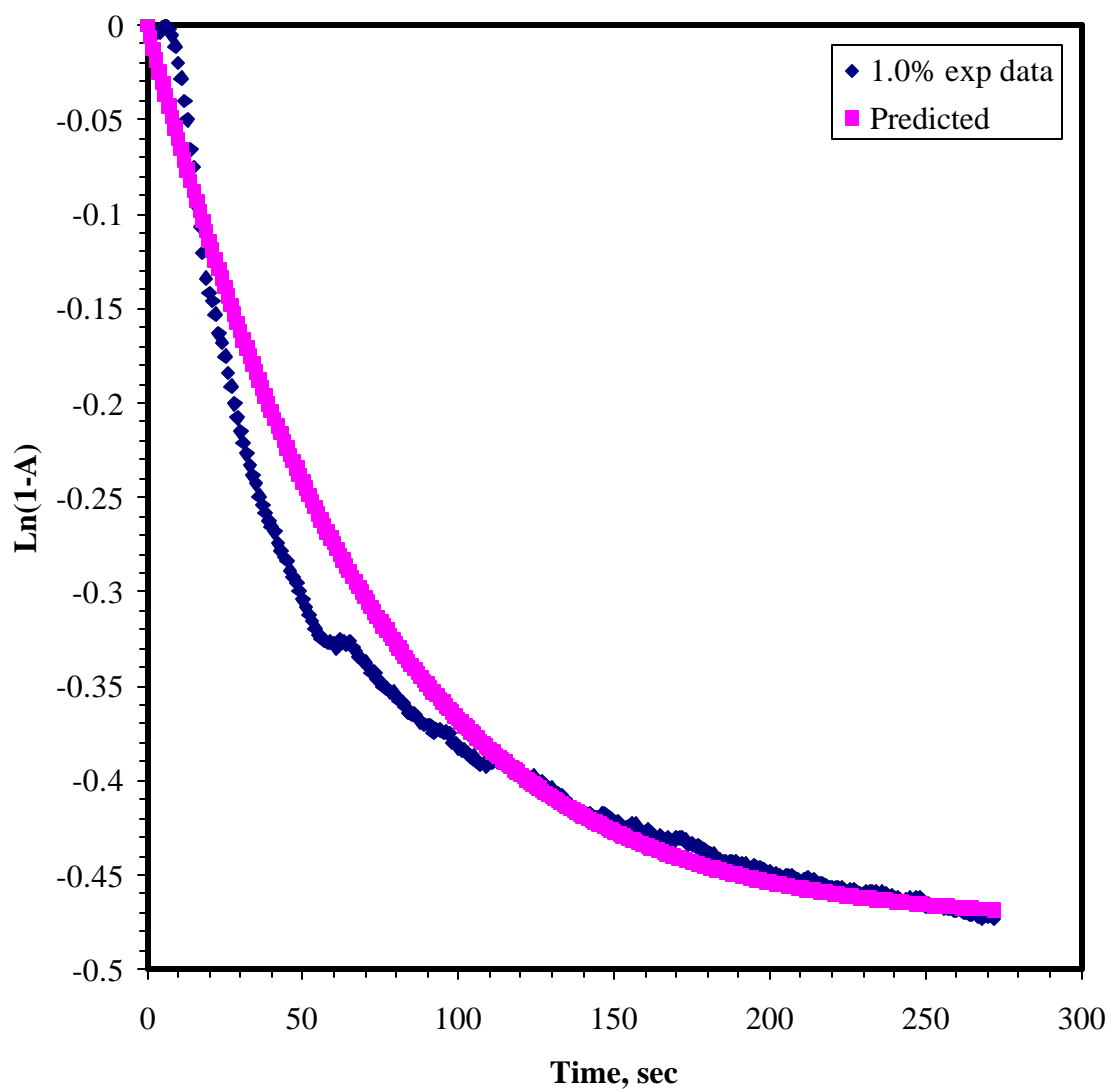


FIGURE 4.5 Graph showing model predictions at 1.0 percent Kymene concentration. $R^2=0.96$. The blue diamonds and pink squares represent the experimental data and the model prediction respectively.

Although the reversible adsorption model can simulate the adsorption data well, a further examination of the physical meaning of the adsorption model is needed. It is generally believed that the polymer adsorption onto a porous fibrous material consists of the following steps [Ratte, et al., 1974; Wagberg, 1988; Alince, 1990]: (A) transport from the bulk solution to the interfacial region; (B) polymer transport across the interface; (C) rearrangement of the polymer on the fiber surfaces; and (D) migration of the polymer into the porous fiber.

Due to the turbulent flow of the adsorption system, the step A is relatively fast. Once Kymene molecules diffuse across the boundary layer, three possible scenarios exist: (1) the Kymene molecules adsorb onto the fiber surface; (2) the molecules desorb from the surface; and (3) the molecules rearrange and diffuse through the porous surface into the fiber interior. In the following two paragraphs, the Kymene desorption and its rearrangement and diffusion through fiber is discussed.

The polymer desorption from substrate is generally believed to be a very slow process. The slow polymer desorption is due to a large number of polymer segment-surface contacts, and therefore, a large energy to remove a polymer chain from the surface [Santore, 1999; DeGennes, 1991]. It is extremely unlikely that all polymer segments release simultaneously from the surface, giving the polymer adsorption the appearance of irreversible binding [Obey et al., 1999; Dijt et al., 1992]. Radiotracer studies show that the adsorbed polymer layers are dynamic-there is a continuous exchange of the polymer segment in trains and those in loops and tails as well as the

chains in the adsorbed layer and those in solution [Dijt et al., 1992]. The exchange is a segment-by-segment process and the competition is at the segmental level. The exchange rate of a polymer is found to decrease with the residence time on the surface due to the chain entanglement or the pinning of a molecule to the surface by loops of another chain [Frantz et al., 1991; Johnson et al., 1992]. To date, limited experimental studies on polymer exchange kinetics suggest it is a very slow process. For example, the exchange rate between protonated and deuterated samples of poly (methyl methacrylate) with molecular weight of 60,000 on a single silicon oxide substrate is found to be about 1% of the mass adsorbed per hour [Johnson et al., 1990]. Another study by Santore [1999] shows that the adsorbed poly (ethylene-oxide) (MW=33,000) layer on silica surface of a slit-shearing cell are stable in flowing solvents for at least 10 hours. In this study, because (A) the adsorption surface is porous and not flat; (B) timescale is within minutes; and (C) higher molecular weight of Kymene (500,000) and stronger binding to surface due to electrostatic interactions and potential covalent bonding, the Kymene desorption can be neglected.

Next, we need to consider the diffusion of Kymene molecules through the fiber surface. The cellulose fiber made by kraft pulping is porous and has pores of 5 to 10nm on the surface [Swerin, 1990]. The radius of gyration of the Kymene molecule is estimated to be 9.3 nm^4 , but the possibility of Kymene migration into fiber still exists. It is argued that polymer molecules can enter an aperture smaller than their hydrodynamic

⁴ Estimated by the Einstein-Stokes Equation.

size, because the polymer chain is loosely packed and deformable [Alince, 1990]. When initially adsorbed onto the fiber, the polymers are attached to the fiber surface by a few chain segments and take a more coiled form, and with time the polymer molecules rearrange themselves and assume flatter configurations [Einarson et al., 1991]. Though the reptation of the polymers into the fiber interior is likely, the process is relatively slow. For the adsorption of a cationic-polyacrylamide (MW=700,000) onto cellulose fibers, the adsorption percentage rate due to reptation is less than 1.2 percent per minute [Lindstrom, 1976]. In this study, it is less likely that significant amount of Kymene molecules migrate into the fiber due to potential chemical reaction between azetidinium groups of Kymene and the carboxyl groups on the fiber surface. Therefore, it is reasonable to propose that once the Kymene molecule adsorbs on the fiber surface, it may undergo some configuration changes, but will be limited to the location as patches. In fact, this hypothesis is consistent with the observations of recent microscopic studies [Nanko, 2000].

Since the rate of Kymene desorption can be neglected, the seemingly desorption term from the reversible adsorption model is probably due to some other mechanism. The electrostatic repulsion may explain the slowed adsorption rate in the long time. In the beginning of the adsorption process, the adsorption and polymer relaxation steps are rapid compared to the polymer diffusion from bulk solution to the interface. In this mass-transfer-limited adsorption, the polymers at the interface are adsorbed rapidly when they arrive. As the adsorption process continues, the fiber surface becomes more crowded,

and the electrostatic repulsion between adsorbed molecules and those in solution starts to play an important role in the adsorption kinetics. The zeta potential data of the pulp solution can be used to validate the impact of electrostatic interaction on the adsorption rate. The results of the electrostatic measurement show that the zeta potential of pulp slurry without additives was -27 mV, which is in agreement with that reported in the literature [Muetek Analytical Inc., 1998]. Figure 4.6 shows that the addition of Kymene to pulp solution caused a rapid increase in the zeta potential and its sign reversal. At 0.25 percent Kymene concentration, the pulp slurry zeta potential was close to 0 mV. At 0.5 and 1.0 percent, the zeta potential was 13.1 and 16.1 mV, respectively. These results suggest that as more Kymene molecules were adsorbed, the initial electrostatic attraction between Kymene molecules and the fiber surface quickly diminished, which eventually led to the electrostatic repulsion between the adlayer and Kymene molecules in the solution. Since the adsorption rate was elevated at higher initial chemical concentration, the adsorption process became electrostatic-disfavored sooner.

At a given initial Kymene concentration, the electrostatic repulsion term plays an increasingly significant role as the adsorption process continues to the long time. This could also help explain for all three concentrations, the latter stage of adsorption is simulated better by using a reversible adsorption format. The same argument could also be used to explain the better fit of adsorption data with a reversible adsorption format at higher initial Kymene concentrations.

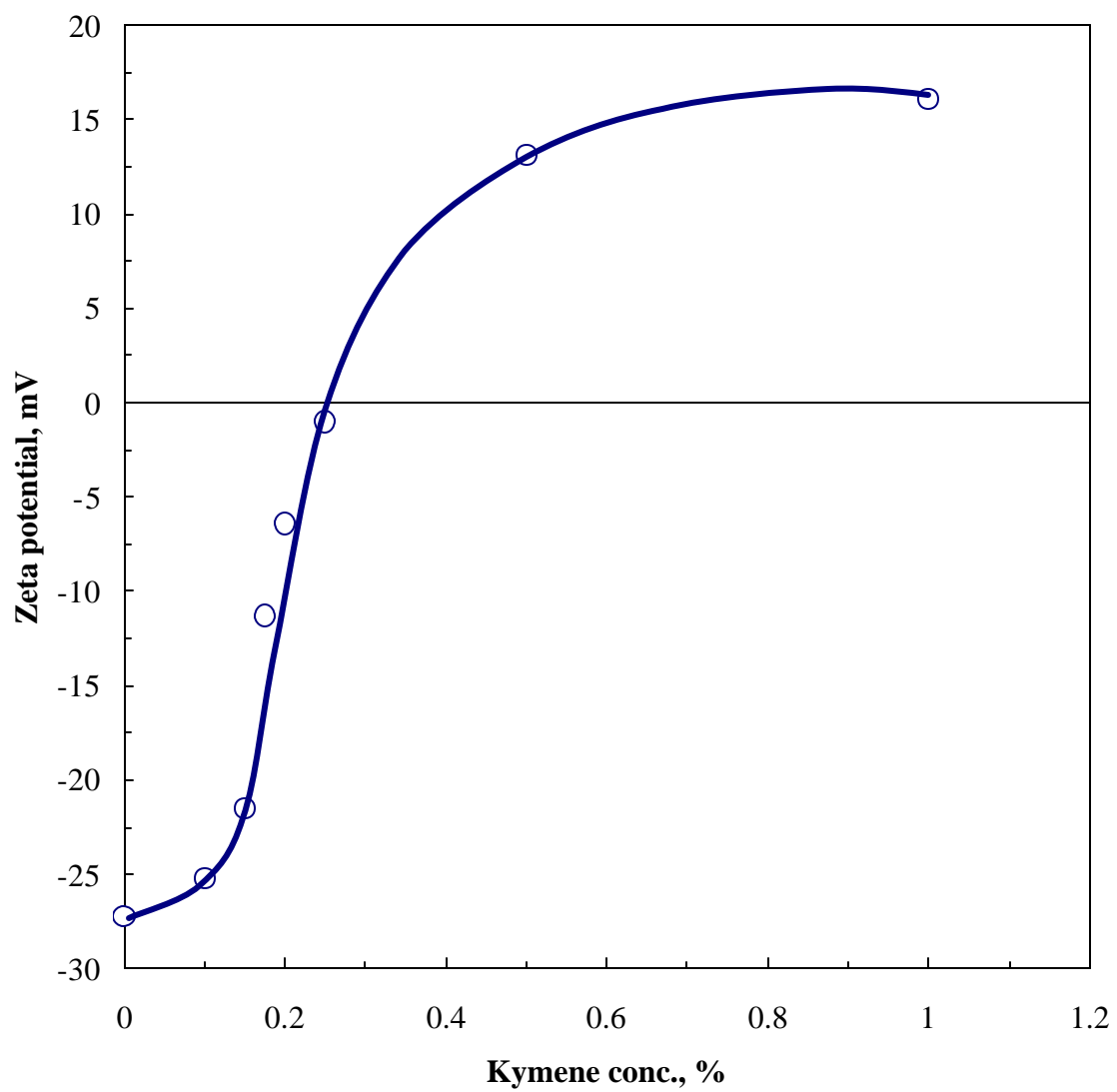


FIGURE 4.6 Effects of Kymene[®]1500 on system's zeta potential. The Kymene concentration was based on the dry mass of fiber.

In this study, the adsorption process is fast in the beginning and becomes slower as the electrostatic repulsion plays an increasingly significant role. The similar adsorption kinetics is observed in other studies of cationic polymer adsorption onto negatively charged surfaces [Shubin, 1994]. It is argued that the first, rapid stage of the adsorption process corresponds to the electrostatics-favored situation, while the repulsive electrostatic field inhibits the polymer adsorption in the second, slow stage.

Using the above adsorption correlation results, the Kymene adsorption at the condition of infinite Kymene dilution can be predicted. Adsorption constant values at infinite dilution are extrapolated from $k_a N_0$ and k_d values correlated from the experimental data. From Figure 4.7, $k_a N_0$ and k_d values are estimated to be 0.0126 and 0 respectively. Therefore, the adsorption percentage can be predicted by the following equation:

$$A_{C_0 \rightarrow 0} = 1 - e^{-0.0126t} \quad (4.7)$$

Figure 4.7 illustrates that at a very dilute concentration, the Kymene adsorption to the cellulose fibers is close to irreversible. It is reasonable to argue that the adsorption at infinite dilution is electrostatic-favored for the whole process and the effect of electrostatic repulsion is negligible.

At a very low initial chemical concentration, although the adsorption percentage is beneficial in terms of operation cost, the amount of Kymene adsorbed onto fiber is out of the practical range to effectively enhance paper web property. One observation from this study is that at 0.6 percent fiber consistency and practical Kymene concentrations, the

Kymene adsorption is far from being complete even as the time prolongs. This is economically and environmentally undesirable, since a significant portion of chemicals will be lost to the aqueous phase. Considering the short contact time between polymer additives and cellulose fibers on the commercial paper machine, the addition of Kymene at high-consistency locations in the stock preparation is beneficial for higher chemical efficiency and therefore strongly recommended.

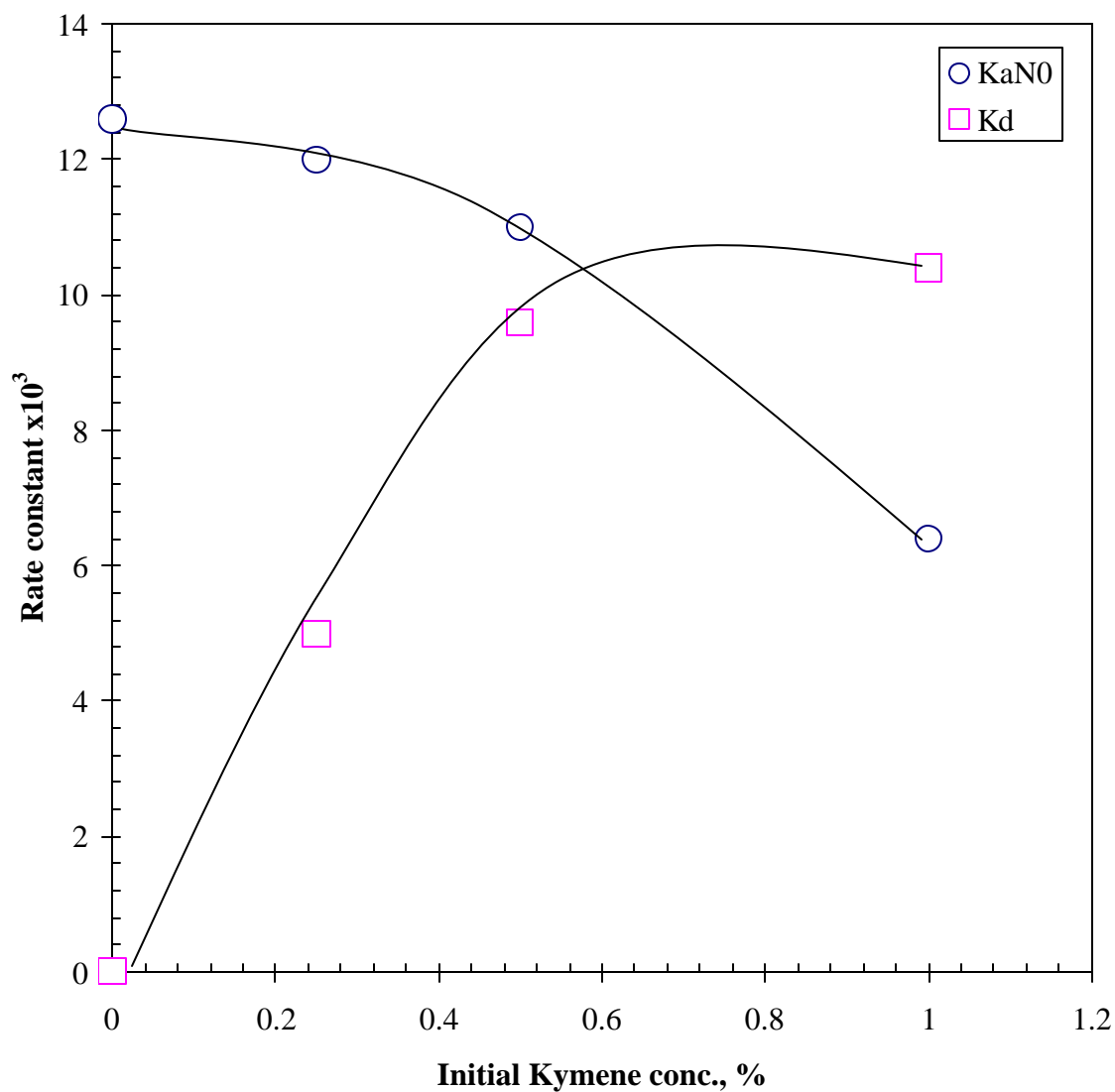


FIGURE 4.7 Graph of $k_a N_0$ and k_d versus initial Kymene concentration. The $k_a N_0$ and k_d values at infinite Kymene dilution are extrapolated to be 0.0126 and 0 respectively.

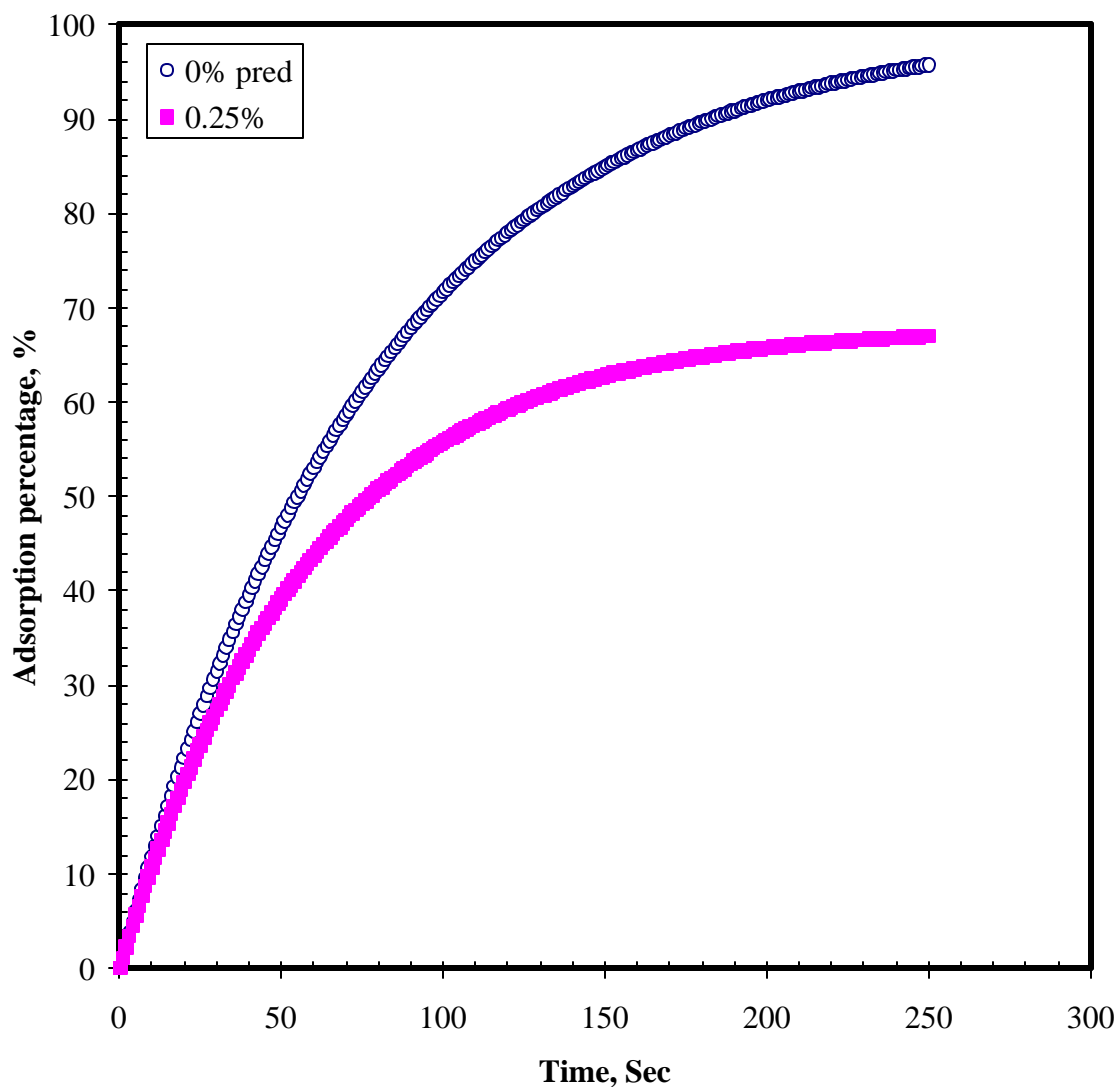


FIGURE 4.8 Graph of adsorption percentage prediction versus time for infinite Kymene dilution. The adsorption percentage of 0.25% initial Kymene concentration was also plotted in comparison. For infinite dilution, the adsorption tended to be irreversible. As time prolonged, the adsorption would be complete. For 0.25% Kymene concentration, the adsorption percentage at equilibrium was about 67%.

4.2.2. Adsorption of Softrite[®] 7516 on cellulose fiber

Figure 4.9 shows the kinetics of Softrite adsorption onto fiber over a period of 200 seconds at 0.6 percent fiber consistency. Two Softrite concentrations, i.e., 0.25 and 0.75 percent, were studied. Compared to the Kymene adsorption, the Softrite adsorption proceeded much faster. At 0.25 percent, it took merely 80 seconds for the Softrite molecules to completely adsorb onto the fibers (more than 99 percent adsorbed). The increase in adsorption percentage was slower at a higher Softrite concentration, 0.75 percent; 99 percent adsorption was reached after 120 seconds. The amounts of Softrite adsorption at the two concentrations are shown in Figure 4.10. The absolute Kymene amount adsorbed at 0.75 percent was higher than that at 0.25 percent.

Figure 4.11 shows the adsorption of Softrite on the cellulose fiber at 1.2 percent fiber consistency. The adsorption reached completion faster than that at 0.6 percent fiber consistency. At 0.25 percent, more than 92 percent of Softrite was adsorbed during the first 30 seconds compared to 80 percent adsorption at lower fiber consistency. Almost 99 percent adsorption was reached after 60 seconds. At 0.75 percent, 87 percent of Softrite was adsorbed during the first 30 seconds of adsorption compared to 60 percent adsorption during the same amount of time at the lower consistency. The higher Softrite adsorption percentage at higher fiber consistency can be explained by the larger fiber surface area available for the chemical adsorption.

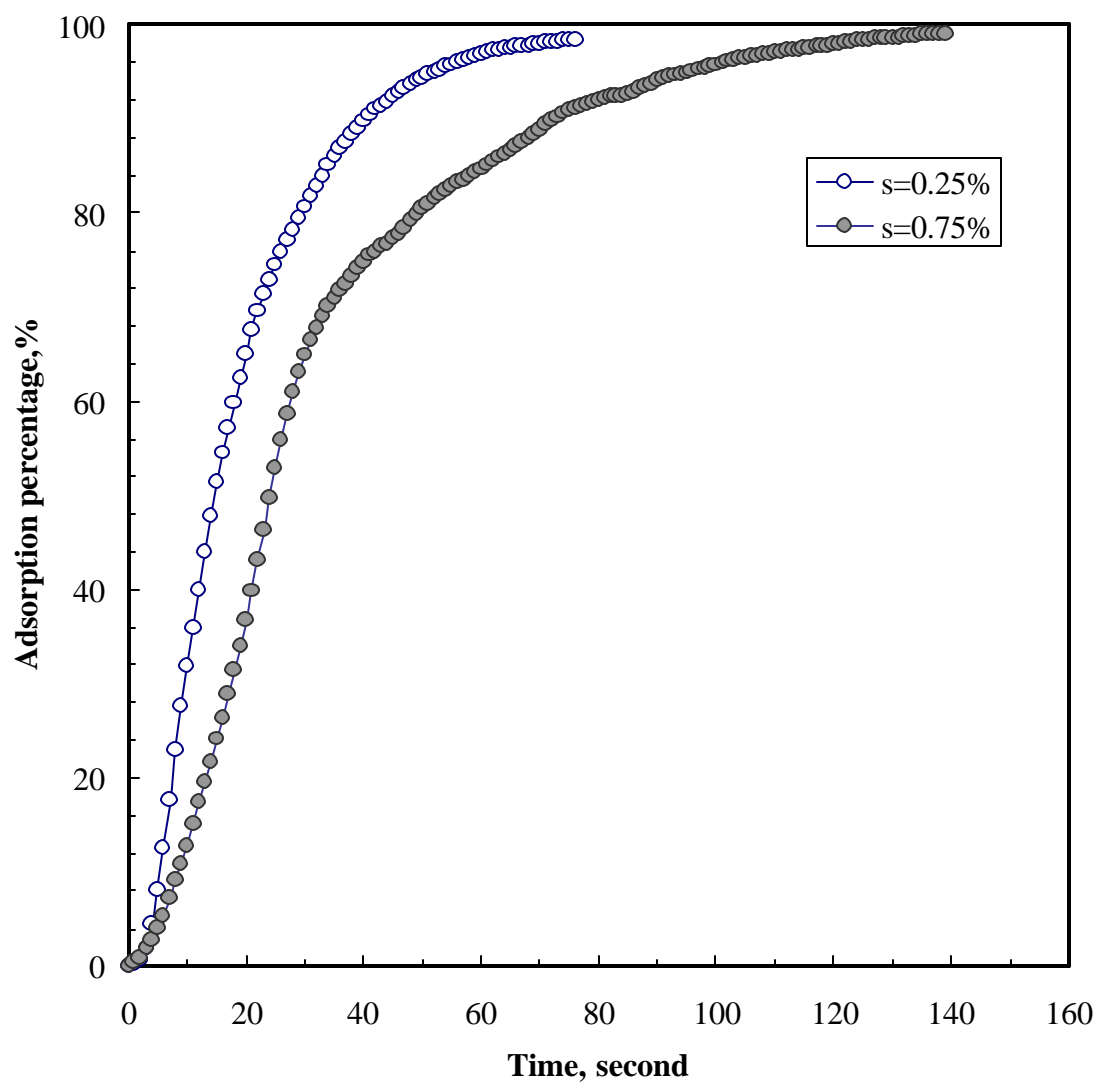


FIGURE 4.9 Graph of Sofrite adsorption versus time. Two levels of debonding agent addition, i.e., 0.25 and 0.75 percent, were investigated in the study. The fiber consistency of the system was 0.6 percent. The spectroscopic data were collected from 0 to 200 seconds to determine the debonding agent concentration.

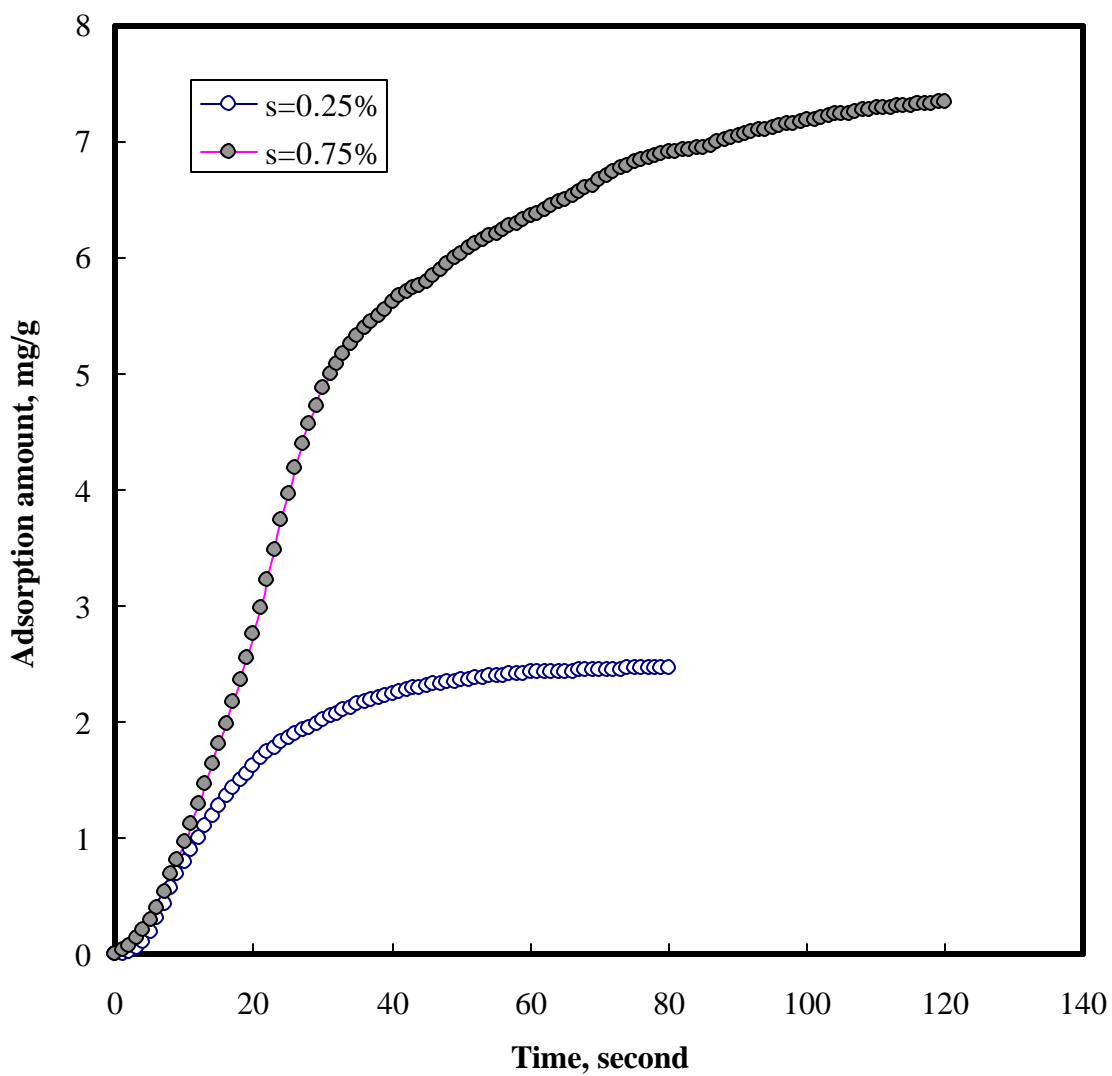


FIGURE 4.10 Graph of adsorbed amount of Softrite® 7516 versus time. Two levels of Softrite addition, i.e., 0.25 and 0.75 percent, were investigated in the study. The fiber consistency of the system was 0.6 percent.

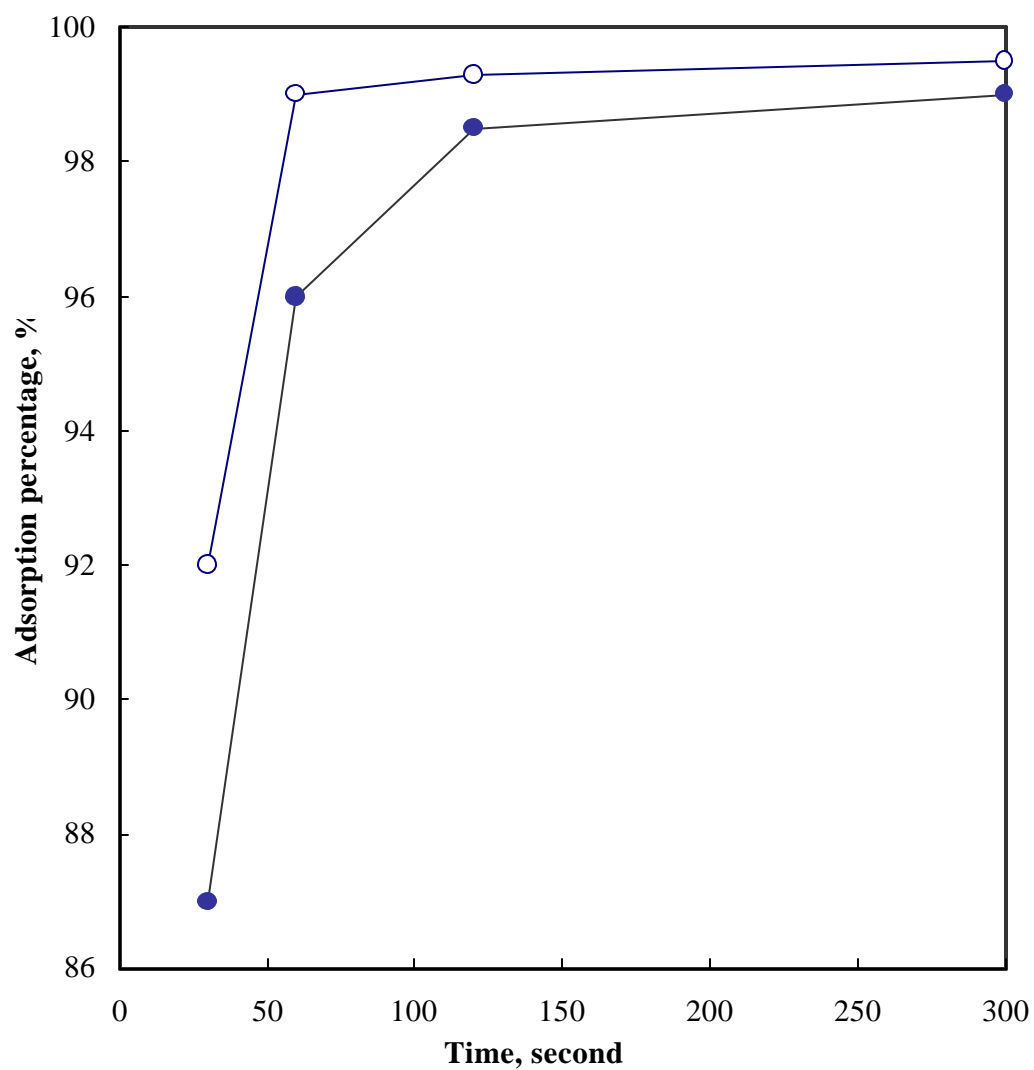


FIGURE 4.11 Graph of Sofrite[®]7516 adsorption onto cellulose fibers versus time. Two levels of Sofrite were studied. The fiber consistency of the system was 1.2 percent. The Sofrite[®]7516 concentration was determined by charge titration. The circles (o) and solid dots (•) represent the data at the 0.25 and 0.75 percent Sofrite levels respectively.

The Softrite adsorption analysis is again based on the result at 0.6 percent fiber consistency. The adsorption data are fitted at two Softrite concentration levels, i.e., 0.25 and 0.75 percent. Since the adsorption was complete at both concentration levels, the process could be simulated by an irreversible adsorption:

$$-\frac{dC}{dt} = kc \quad (4.8)$$

Where C is the concentration, Kmol/m^3 , k is the adsorption rate constant in second^{-1} and t is time in second.

Indeed, the correlation results show that $\ln(1-A_d)$ is a linear function of time throughout the whole adsorption process. The Softrite adsorption at 0.25 percent addition is correlated by Equation 4.9 ($0 < t < 76$ s):

$$A_d = 1 - e^{-0.0565t} \quad (4.9)$$

where A_d is the adsorption percentage and t is the time in second. Equation 4.9 has excellent correlation with the adsorption data (adjusted $R^2 = 0.995$ and $p\text{-value} < 0.01$).

Similarly, the Softrite adsorption is simulated at 0.75 percent by Equation 4.10 ($0 < t < 139$ s):

$$A_d = 1 - e^{-0.0319t} \quad (4.10)$$

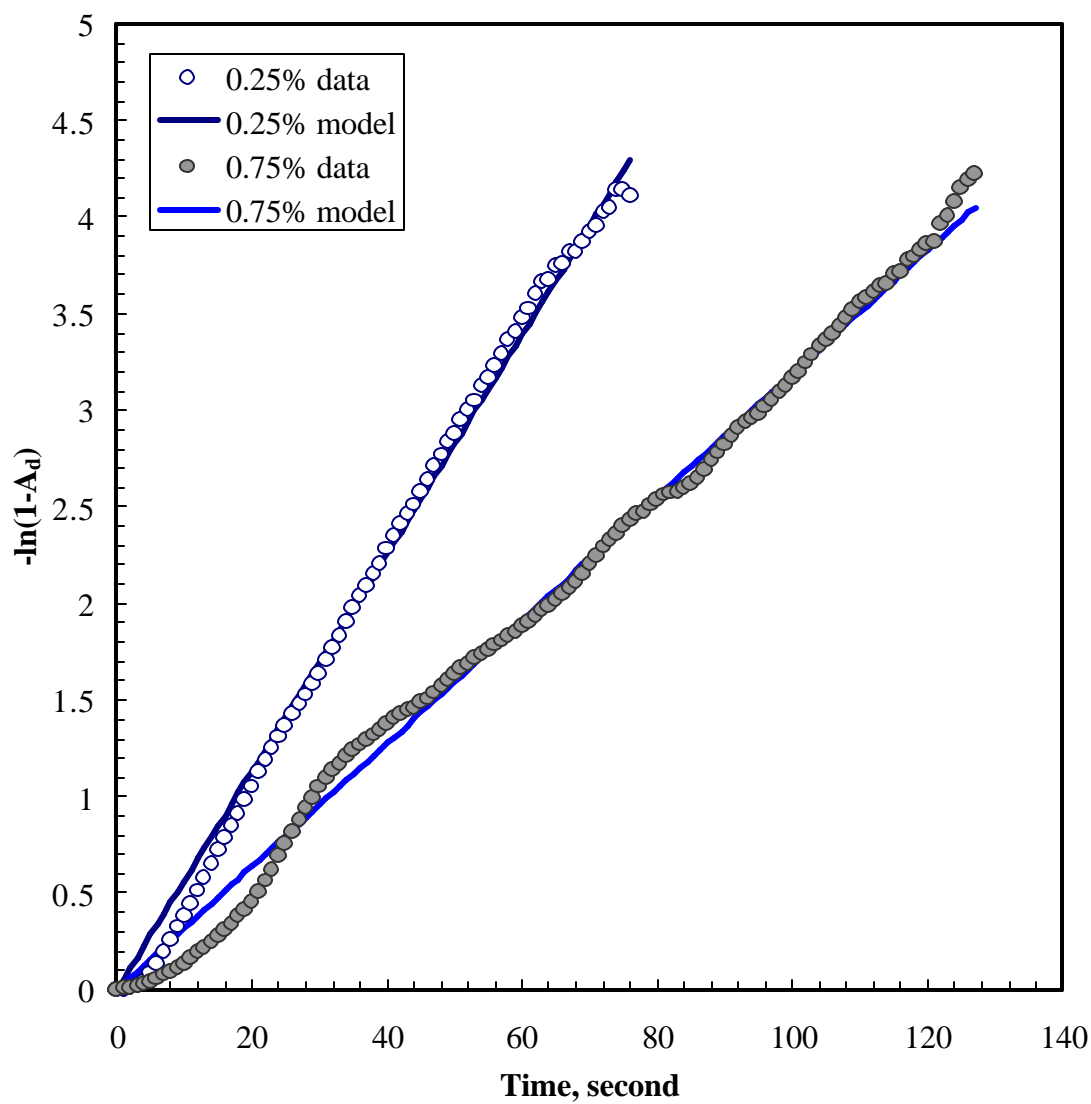


FIGURE 4.12 Graph of $-\ln(1-A_d)$ versus time for Sofrite adsorption. It shows good agreement between the experimental data and the model prediction at the two Sofrite addition levels, 0.25 and 0.75 percent.

where A_d is the adsorption percentage and t is the time in seconds. Again, the correlation fits the experimental data well with the adjusted R^2 of 0.994 and p -value<0.01. The model predictions are compared with experimental data in Figure 4.12. Since the adsorption constant is dependent on Softrite concentration, the adsorption kinetics can not be described by a simple first order equation.

At both concentration levels, the characteristic adsorption time ($\tau=1/k$) remains constant during the whole adsorption process, and is determined to be 17.7 and 31.3 seconds respectively. The half time, $t_{1/2}$, is defined as the time needed for 50 percent of chemical adsorption, and can be used to test the model's ability of correlating adsorption data. It is calculated as follows:

$$t_{1/2} = \frac{\ln 2}{k} \quad (4.11)$$

where k is the rate constant in Equation 4.8. The half times predicted by the adsorption model are in close agreement with those by the experimental data. At 0.25 percent, the half time is predicted to be 12.3 seconds compared with 14.6 seconds by the adsorption data. At 0.75 percent, the half time is determined experimentally to be 24.1 seconds and predicted to be 21.7 seconds.

The adsorption results show that similar to Kymene's adsorption, although the absolute adsorption amount is increased, the rate of Softrite adsorption percentage is lower at a higher initial chemical concentration. The lower adsorption percentage may be

explained by the lower diffusivity and more intense competition for adsorption sites at a higher chemical concentration.

Although the collision model also suggests a linear relationship between $\ln(1-A_d)$ and adsorption time, it does not consider the diffusion resistance in the boundary layer and can not be validated. Instead, the adsorption can be interpreted by traditional chemical engineering concepts. The diffusion through the boundary layer is the rate-determining step, and the adsorption onto the fiber occurs rather quickly. When the Sofrite concentration at the solution-fiber interface is so low that it can be neglected, a linear relationship between $\ln(1-A_d)$ and the adsorption time is obtained.

For the low molecular weight paper additives, the available adsorption area (including fiber surface, microfibrils on fiber surface, and fiber interior) is large [Alinec, B., 1990]. In addition, Sofrite does not take the configuration of high molecular weight polymers on the fiber surface. For the adsorption of ionic surfactants onto an oppositely charged surface, the charged headgroups of the surfactant prefer contact with the surface by electrostatic attraction [Connor et al., 1971]. Below the isoelectric point (iep), the “monolayer” adsorption prevails, while the “bilayer” adsorption starts above the isoelectric point as shown in Figure 4.13 [Iler, 1979]. At 0.25 and 0.75 percent concentrations, the adsorbed Sofrite charge is less than 10.7 and 32.3 percent of the fiber charge, respectively, far less than that needed for charge neutralization. Therefore, Sofrite molecules are expected to take the “head-on” orientation on the fiber surface.

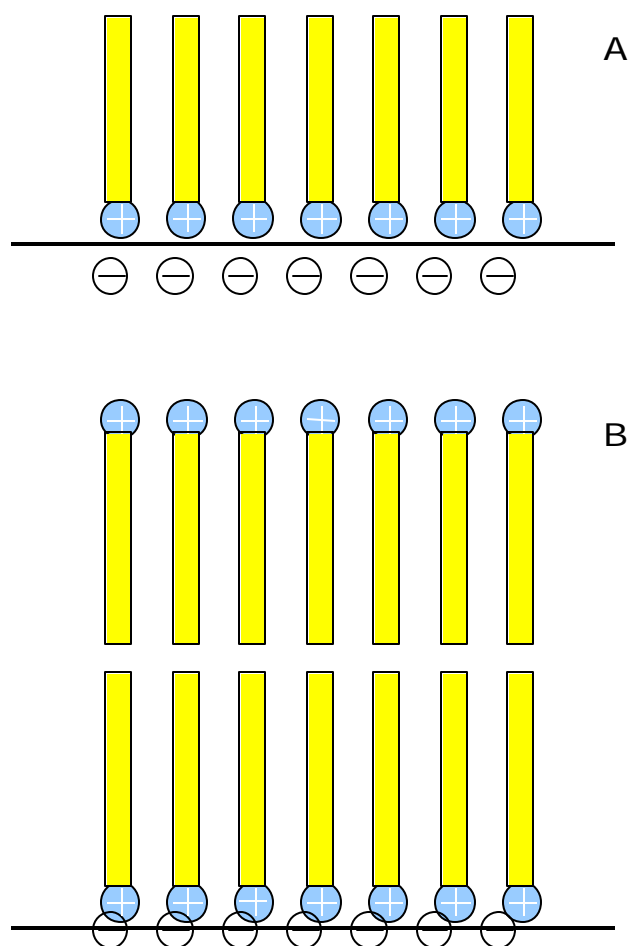


FIGURE 4.13 A, B The orientation of ionic surfactants on the negatively charged surface. (A) Below the isoelectric point, the surfactant adopts the “head-on” adsorption with its charged headgroups contacting the oppositely charged surface. (B) Further increase of surfactant concentration beyond iep leads to the “bilayer” adsorption of the surfactants.

Unlike multi-segmental polymer molecules, desorption of small molecules, such as Softrite, from fiber surface is likely to happen. However, the adsorption data suggest that the Softrite desorption from the fiber surface to the solution is negligible, since the adsorption was complete within several minutes. The irreversible Softrite adsorption is probably due to the large accessible fiber surface and the favorable electrostatic interaction between Softrite molecules and the fiber throughout the whole process.

To illustrate the electrostatic interaction, zeta potential measurement was taken at different Softrite concentrations. The electrokinetic information provides important clues to understanding the adsorption of cationic Softrite onto the anionic cellulose surface. The zeta potential results illustrated in Figure 4.14 show that the addition of Softrite only slightly increased the zeta potential of the fiber surface. The zeta potential of fiber slurry alone was -27 mV. The addition of 1 percent of Softrite increased the slurry's zeta potential by less than 7 mV. The zeta potential results suggest the electrostatic attraction between the anionic fiber surface and the cationic Softrite molecule decreased slightly during the adsorption process. The negative zeta potential values indicate that the process is electrostatics-favored to the adsorption of the cationic Softrite at studied conditions.

It is interesting to note the contrast of the zeta potential change by the addition of Kymene and Softrite. The zeta potential increase by Kymene is much higher than that by Softrite. The charge density of the additives can only partly explain the difference; the charge density ratio of Kymene to Softrite was 1.5, while the ratios in the zeta potential increase were much larger. For example, the zeta potential ratio was about 20 at 0.5

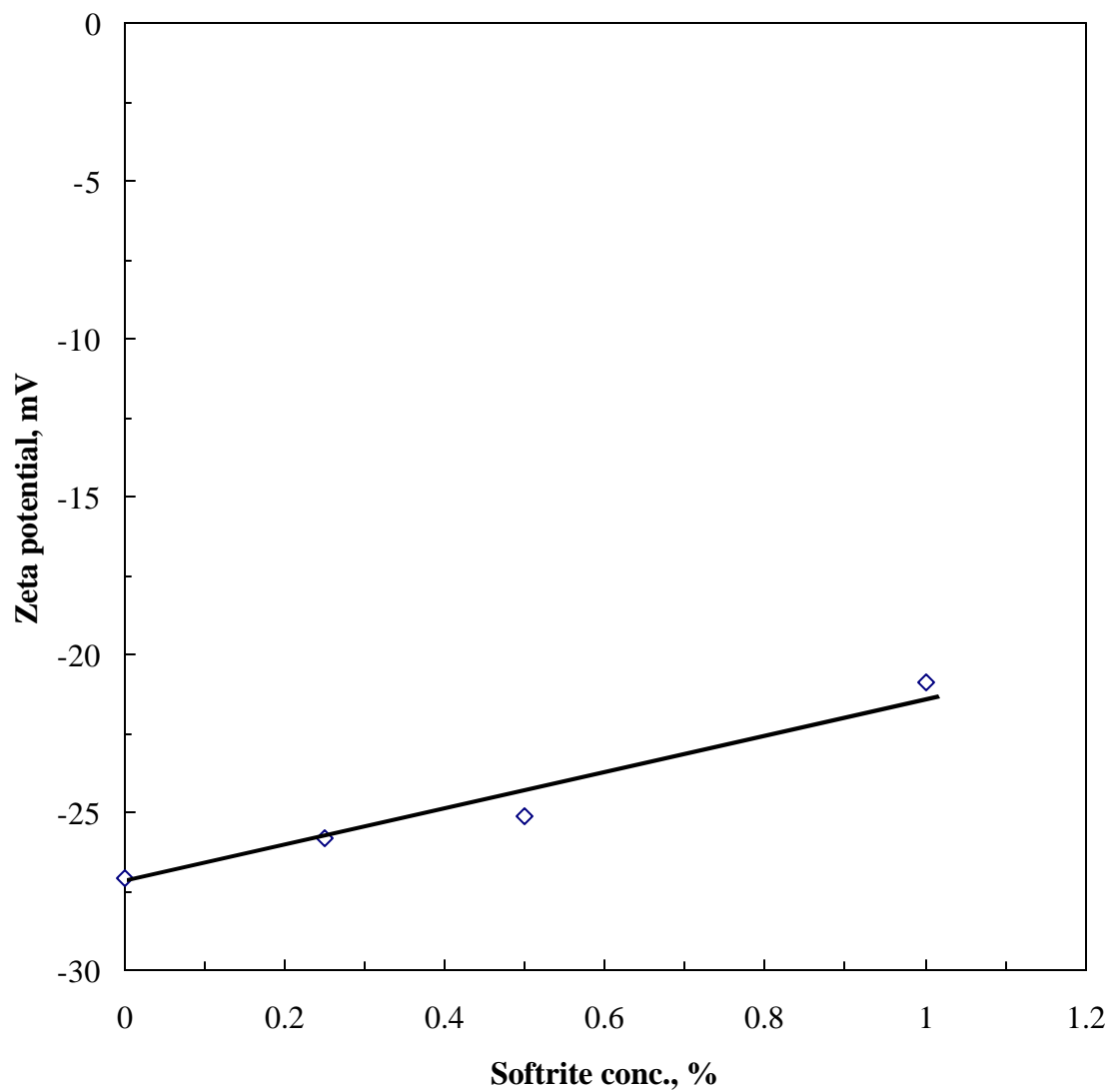


FIGURE 4.14 Effects of Softrite[®] 7516 on the system's zeta potential. The Softrite concentration was based on the dry mass of fiber.

percent chemical addition. The rest of the potential increase may be due to the excluded volume effect on the free energy of the double layer ions [Brooks, 1973]. The adsorption of the cationic polymer on an anionic surface is also believed to lead to the double layer expansion and the zeta potential increase [Jones, 1979; Onabe, 1979]. The larger zeta potential increase by the higher molecular weight polymer could probably be explained by the more extended polymer segments on the fiber surface.

It is noticed that the adsorption behavior of Softrite and Kymene are quite different. Softrite adsorption is fast and complete within minutes. The overall process can be simulated by an irreversible adsorption. In comparison, adsorption of Kymene is slower and the process is best fit by a reversible adsorption. The slower Kymene adsorption can be explained in part by the factors in its diffusion through the boundary layer. Due to its higher molecular weight, Kymene's diffusivity is lower than that of Softrite. In addition, the specific surface area available for Kymene is lower than that for Softrite. Softrite can quickly penetrate into the porous cellulose fibers (fiber interior and microfibrils on fiber surface), most of which is not available to Kymene in the timeframe studied. The electrostatic interaction between additives and the fibers also plays an important role: Softrite's adsorption is electrostatics-favored in the whole process, while the adsorption of Kymene quickly becomes electro-statically disfavored as the adsorption continues.

It is important to point out the progress made by this study. The current method makes it convenient to collect kinetic data of paper additive adsorption onto cellulose fibers below 0.6 percent fiber consistency. In literature, few kinetic data are available for

the mathematical validation of adsorption mechanisms in an aqueous cellulose system. A study claims the validity of an adsorption mechanism with the support of only one data point [Tanaka et al., 1999]. The experimental setup in this study is able to collect UV/Vis spectroscopic data automatically during the whole adsorption process, which is helpful in the mechanism investigation of adsorption kinetics.

4.2.3. Simultaneous competitive adsorption of Kymene[®] 1500 and Sofrite[®] 7516

The competitive adsorption of Kymene[®] 1500 and Sofrite[®] 7516 was studied at 0.6 and 1.2 percent fiber consistencies. Two sets of initial chemical concentrations were selected. The ChemMatrix software was used to solve for the concentrations of the two chemicals. Figure 4.15 shows the individual chemical adsorption percentage at 1.2 percent fiber consistency. The increase of adsorption percentage for both additives was decreased compared to that in the individual adsorption; however, with prolonged time, more than 90 percent of adsorption was reached for both chemicals. At 0.6 percent fiber consistency, the adsorption for both species was decreased considerably.

Figure 4.16 shows the competitive adsorption of the chemical additives with both initial concentrations of Kymene[®] 1500 and Sofrite[®] 7516 at 30 ppm. The figure indicates that the adsorption level of each chemical was reduced by the presence of a competing polymeric species; however, the adsorption of the two additives was affected to a different degree.

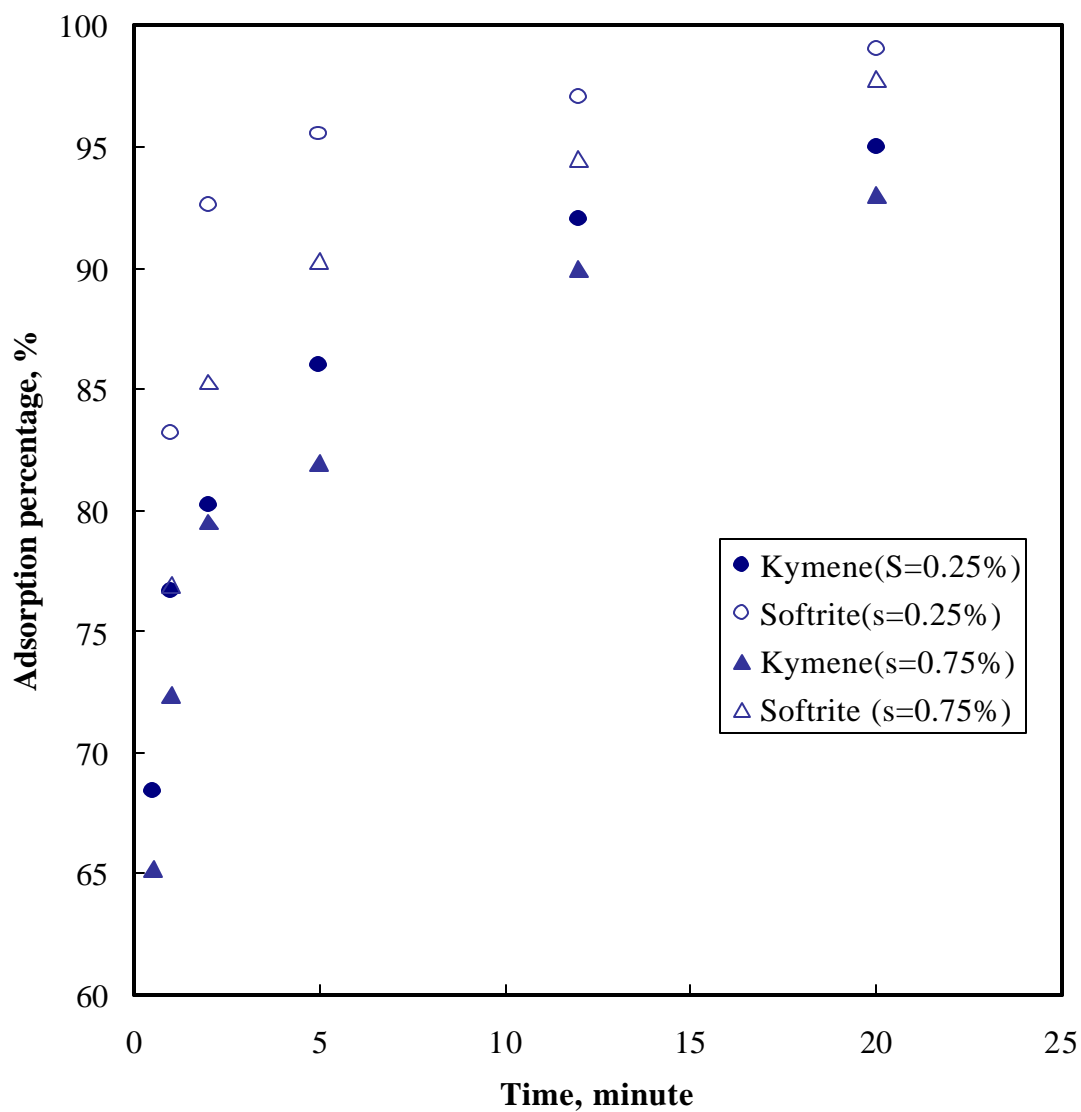


FIGURE 4.15 Graph of simultaneous competitive adsorption of Kymene[®]1500 and Softrite[®]7516 onto cellulose fibers versus time. The fiber consistency of the system was 1.2 percent. The Kymene[®]1500 concentration was 0.25 percent, and two levels of Softrite[®]7516 concentrations were selected: 0.25 and 0.75 percent.

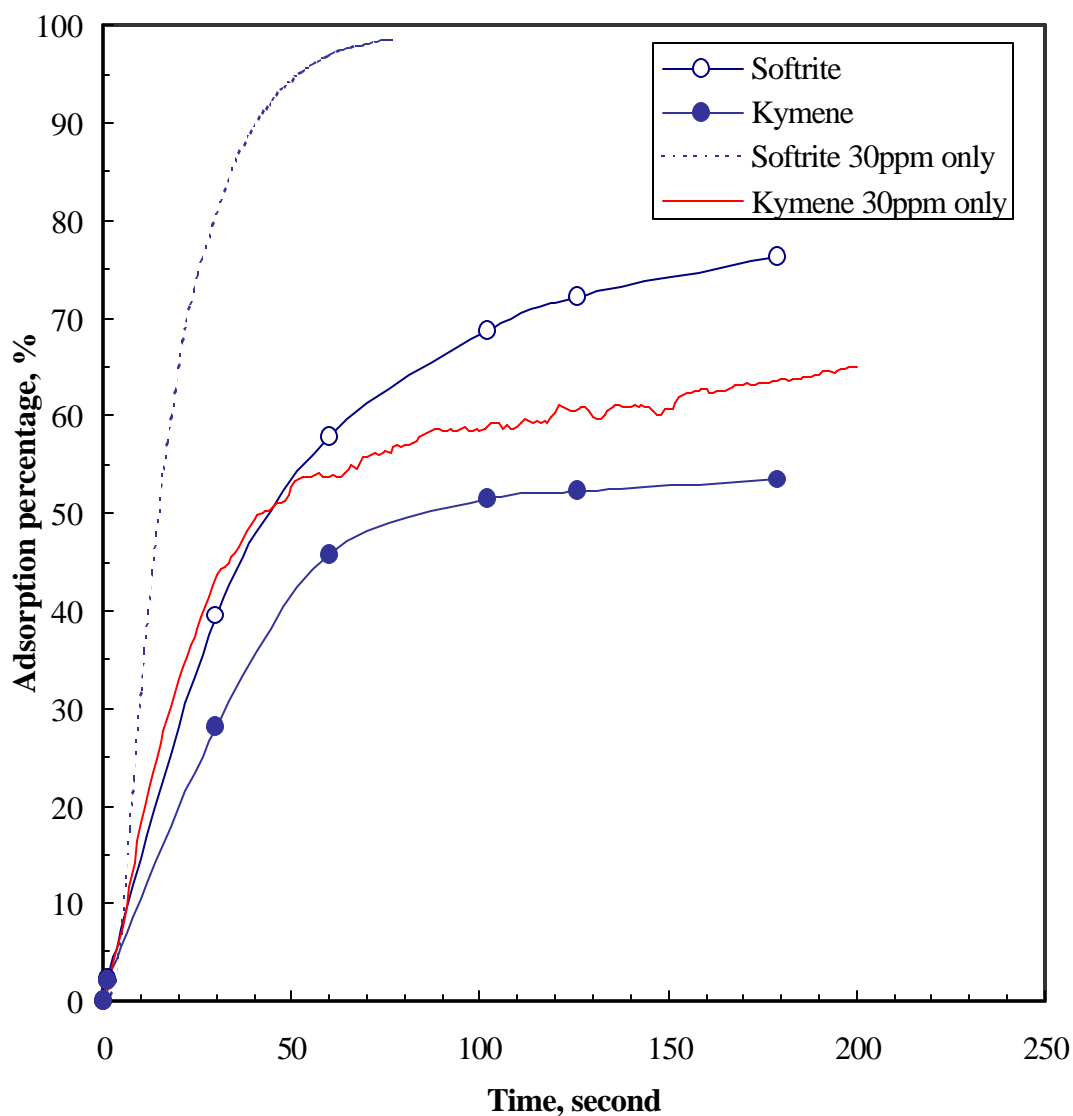


FIGURE 4.16 Graph of simultaneous competitive adsorption of Kymene[®]1500 and Softrite[®]7516 onto cellulose fibers versus time. The fiber consistency of the system was 0.6 percent. The Kymene[®]1500 concentration was 0.25 percent, and the initial Softrite[®]7516 concentration was 0.25 percent (30 ppm).

A significant difference exists between the adsorption characteristics of Softrite[®]7516 alone and its competitive adsorption with Kymene[®]1500. For individual Softrite[®]7516 adsorption, it reached completion at the end of 80 seconds. In contrast, its adsorption became slower in the competitive adsorption; only 62 percent of Softrite was adsorbed during the same period of time. At the end of 3 minutes, its adsorption only reached 76 percent. For Kymene, the difference between individual and competitive adsorption was relatively small. In the competitive adsorption, the amount of Kymene adsorbed was slightly reduced. At the end of 3 minutes, 53 percent of Kymene was adsorbed compared with 63.5 percent in individual adsorption.

In another set of experiments, the initial concentration of Kymene was kept at 30 ppm, while the concentration of Softrite was increased to 90 ppm. The adsorption results are shown in Figure 4.17, which shows that the same pattern was followed at this condition. The amount adsorbed of both chemicals was reduced, but the adsorption of Softrite was reduced to a larger degree. It is also observed that although the adsorbed amount of the individual component was reduced, the combined adsorbed charge was increased. For example, at the end of 3 minutes of adsorption, the adsorbed charge for Kymene with initial concentration of 30 ppm was 6.72 μeq per gram fiber. In the case of Softrite with an initial concentration of 30 ppm, the adsorbed charge was 6.88 μeq per gram fiber. In a simultaneous adsorption, the adsorbed charge of Kymene and Softrite was 9.83 μeq per gram fiber.

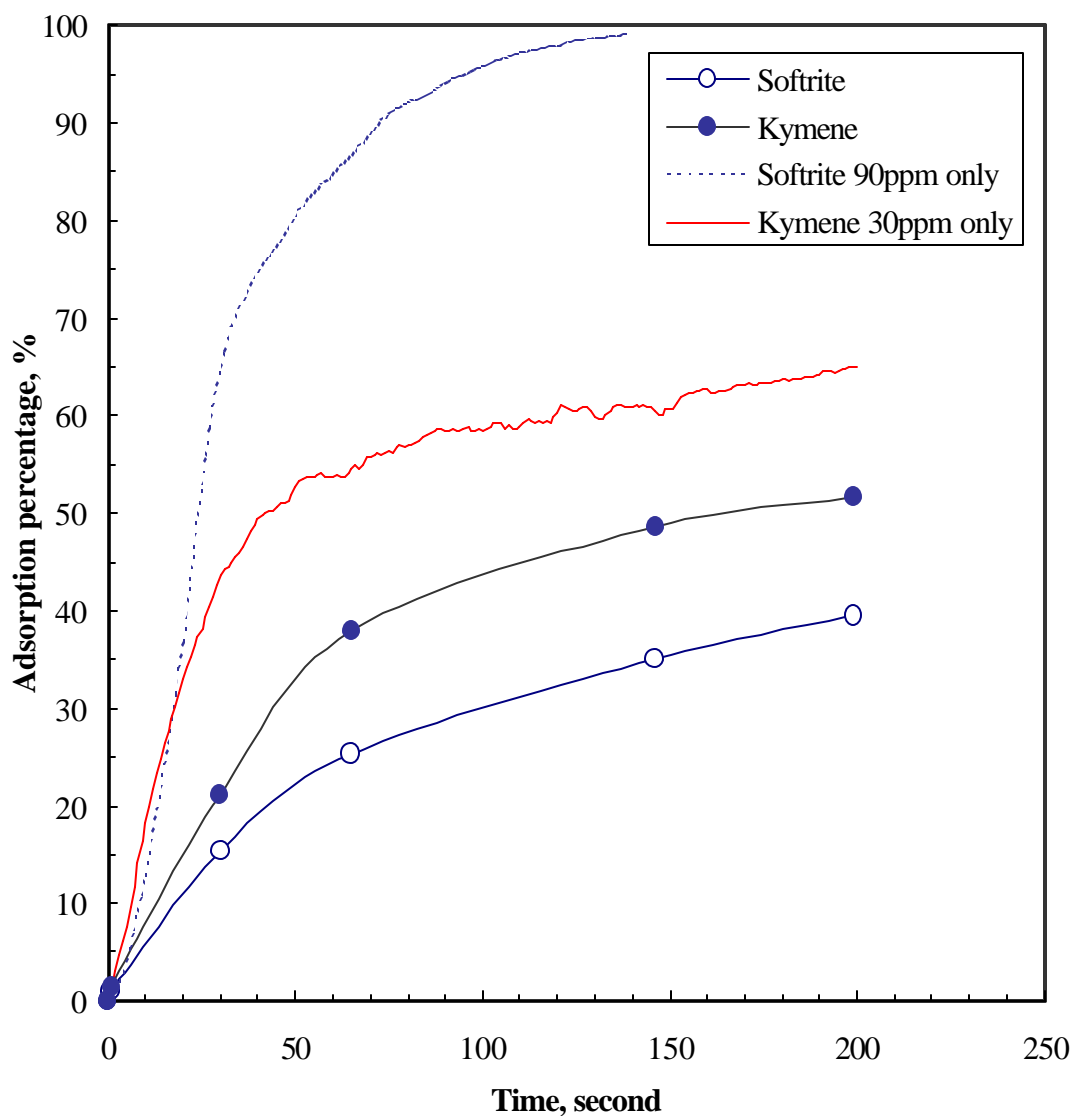


FIGURE 4.17 Graph of simultaneous competitive adsorption of Kymene[®]1500 and Softrite[®]7516 onto cellulose fibers versus time. The fiber consistency of the system was 0.6 percent. The Kymene[®]1500 concentration was 0.25 percent, and the Softrite[®]7516 concentration was 0.75 percent (90 ppm).

The adsorption decrease for both chemicals can be explained partly by the site-blocking effects of the competing additive since less anionic sites are left for adsorption [Stemme et al., 1999]. The relative larger reduction in Softrite adsorption could be partly explained by the reduction in its diffusivity due to the interference of cationic Kymene molecules. Another factor that might contribute to the more dramatically reduced Softrite adsorption is the different adsorption areas available to the additives. It is argued that the available surface area is larger for low MW chemicals due to the porous nature of cellulose fibers [Falk et al., 1989]. The adsorption of high molecular weight cationic polymers is believed to be limited to the fiber surface and external pores [Pelton, 1985]. Therefore, the decrease in adsorption area will have a bigger effect on the adsorption of Softrite. The decreasing electrostatic driving force in the competitive adsorption may also account for a more dramatic reduction in Softrite adsorption. The fact that the adsorption of Kymene was not affected too much when the initial concentration of Softrite was tripled seems to suggest that the adsorption affinity of Kymene to the cellulose fiber is greater than that of Softrite. In order to test the hypothesis, experiments with sequential additions of Kymene and Softrite to the fiber slurry are needed. The study of the adsorption kinetics suggests that (1) the chemical additives should be added to the thick stock to achieve optimum adsorption, and (2) Softrite needs to be first added to the upper stream of the tissue-making process to utilize the available larger surface area.

4.3. Conclusions

The adsorption kinetics and mechanism of two tissue chemical additives, Kymene[®] 1500 and Softrite[®] 7516, onto cellulose fibers were studied. At 0.6 percent consistency, the UV/Vis spectroscopic data of the additive adsorption were collected and analyzed. The data showed that the adsorption of Softrite on the fiber was fast, completed within 2 minutes, and could be simulated well by a first order irreversible adsorption. In contrast, the adsorption of Kymene was slower, and could be predicted by a reversible adsorption. Kymene's adsorption can be divided into two stages: the first stage was fast and electrostatics-favored, while the second, slow stage may be the result of increasing electrostatic repulsion. The simultaneous competitive adsorption of the binary system was also studied, which showed that the adsorbed amount of each additive was reduced in the presence of a competing species. The adsorption of the two chemical additives at 1.2 percent fiber consistency was studied by the traditional method, and was shown to proceed much faster and more completely than at a lower fiber consistency.

In addition, this study developed a novel experimental setup for the chemical adsorption on cellulose fibers at medium fiber consistency. The apparatus is the first of such instruments used in the field of paper chemical adsorption study, and has the potential to generate more fundamental understanding on the important subject.

4.4. References

- Abson, D., Brooks, D. F., Wet end behavior of dry strength additives, *TAPPI Journal*, vol. **68**, 76-78 (1985)
- Alinec, B., The roles of porosity in polyethylenimine adsorption onto cellulosic fibers, *Journal of Applied Polymer Science*, vol.**39**, 355-362 (1990)
- Brooks, D. E., The effect of neutral polymers on the electrokinetic potential of cells and other charged particles II: A model for the effect of adsorbed polymer on the diffuse double layer, *J. Colloid Interface Science*, vol. **43**, 68-699 (1973)
- Connor, P., and R. H. Ottewill, The adsorption of cationic surface active agents on polystyrene surfaces, *Journal of Colloid Interface and Science*, Vol. **37**: 642 (1971)
- DeGennes, P. G., *Adv. Colloid Interface Sci.*, vol. **27**, 190 (1991)
- Dijt, J. C., Cohen Stuart, M. A., Fleer, G. J., Kinetics of polymer adsorption and desorption in capillary flow, *Macromolecules*, vol. **25**: 5416-5423 (1992)
- Einarson M, R. Aksberg, L. Odberg and J. C. Berg, Adsorption and reconfiguration of a series of cationic polyacrylamides on charged surfaces, *Colloids and Surfaces*, vol. **53**, 183-191 (1991)
- Falk, M., L. Odberg, L. Wagberg and G. Risinger, Adsorption kinetics for cationic polyelectrolytes onto pulp fibers in turbulent flow, *Colloids and Surfaces*, vol. **40**, 115-124 (1989)
- Frantz, P., Granick, S., Kinetics of polymer adsorption and desorption, *Physical Review Letters*, vol. **66**, no.7, 899-902 (1991)
- Goossens, J. W. S., Luner, P., Flocculation of microcrystalline cellulose suspensions with cationic polymers: effect of agitation, *TAPPI Journal*, vol. **59**, 89-94 (1976)
- Iler, R. K., *The Chemistry of Silica*, John Wiley and Sons, New York, 1979, p. 683.

Johnson, H. E., Granick, S., Exchange kinetics between the adsorbed state and free solution. Poly (methyl methacrylate) in carbon tetrachloride, *Macromolecules*, vol. **23**, 3367-3374 (1990)

Johnson, H. E., Granick, S., New mechanism of nonequilibrium polymer adsorption, *Science*, vol. **255**, 966-968 (1992)

Jones, I. S., A theory of electrophoresis of large colloid particles with adsorbed polyelectrolyte, *J. Colloid Interface Sci.*, vol. **68**, 451 (1979)

Lindstrom T., Soremark, C., Adsorption of cationic polyacrylamides on cellulose, *Journal of Colloid and Interface Science*, vol.**55**, no.2, May 1976, 305-312.

Luce, J. E., Robertson, A. A., The sorption of polymers on cellulose, *J. Polym. Sci.*, vol.**51**, 317 (1961)

Most, D. S., The sorption of certain slash pine hemicellulose fractions by cellulose fibers, Doctor's Dissertation, 127p, Appleton, Wisconsin, The Institute of Paper Chemistry (1957)

Muetek Analytical Inc., brochure of SZP 04, 1998.

Nanko, H., private discussion, October 2000.

Obey, T. M. and P. C. Griffiths, Chapter 2: Polymer Adsorption: Fundamentals, *Principles of Polymer Science and Technology in Cosmetics and Personal Care*, edited by E. D. Goddard and J. V. Gruber, Marcel Dekker, NY, 1999.

Onabe, F., Interfacial properties of polyelectrolyte-cellulose systems, II: Electrokinetic properties of cellulose fibers with adsorbed monolayer of cationic polyelectrolyte, *Journal of Applied Polymer Science*, Vol. **23**, 2909-2922 (1979)

Pelssers, E. G. M., M A Cohen Stuart, G J Fleer, *J. Chem. Soc Faraday Trans Vol.* **86**: 1355-1361 (1990)

Pelton, R. H., Electrolyte effects in the adsorption and desorption of a cationic polyacrylamide on cellulose fibers, *Journal of Colloid and Interface Science*, Vol.**111** (2): 475-485 (1985)

Ratte, I. B., and M. M. Brever, *The physical chemistry of dye adsorption*, Academic Press, New York/London (1974)

Santore, M. M., Chapter 5: Diffusion-controlled phenomena in adsorbed polymer dynamics, *Colloid-polymer interactions from fundamentals to practice*, edited by Rarinato, R. S. and Dublin, P. L., John Wiley & Sons, 1999.

Scott, William E., *Principles of Wet End Chemistry*, 66, TAPPI Press, Atlanta, GA 1996.

Shubin, Victor, Adsorption of cationic polymer onto negatively charged surfaces in the presence of anionic surfactant, *Langmuir*, vol. **10**, 1093-1100 (1994)

Stemme, S., L. Odberg, Layer thickness for high molecular weight cationic polyacrylamides adsorbed on a surface with a preadsorbed poly-diallyl dimethyl ammonium chloride, *Colloids and Surfaces A: Physiochemical and Engineering Aspects*, vol. **157**, 307-313 (1999)

Swerin, A., Lars Odberg and Tom Lindstrom, Deswelling of hardwood kraft pulp fibers by cationic polymers, *Nordic Pulp and Paper Research Journal*, vol. **4**, 188-196 (1990)

Tanaka, H., A. Swerin, L. Ödberg and S. B. Park, Competitive adsorption of cationic polyacrylamides with different charge densities onto polystyrene latex, cellulose beads and cellulose fibers, *Journal of Pulp and Paper Science*, vol.**25**, no.8: 283-288 (1999).

Wagberg, Lars, Lars Odberg, Tom Lindstrom and Rein Aksberg, Kinetics of Adsorption and Ion-Exchange Reactions during Adsorption of Cationic Polyelectrolytes onto Cellulosic fibers, *Colloids and Surfaces*, vol. **31**, 119-124 (1988)

CHAPTER V

CHEMICAL ADDITIVE EFFECTS ON SHEET PROPERTIES

5.1. Introduction

As discussed in Chapter 1, tissue products have several important physical properties, such as strength, water absorbency, softness and lint resistance. To produce superior tissue, tissue manufacturers need to improve one or more of the above-mentioned tissue properties. The softness characterization result of commercial facial tissue is applied to handsheets. The softness in reduced form will facilitate the quantification of softness improvement in the laboratory.

Although there are mechanical as well as chemical methods to improve tissue properties, this study focuses on the tissue property improvement via chemical means. Two chemical additives are investigated in the study, i.e., Kymene[®]1500, a wet strength resin, and Softrite[®]7516, a debonding agent. The application of dual chemical additives in the tissue manufacturing has been reported in various patents [Trokhan et al., 1980, 1996; Phan et al., 1996, 1997]. However, to date, there is no systematic study to quantitatively describe the chemical effects on sheet properties. Moreover, there has been

no reported study on the quantitative response of handsheet softness to the chemical application. In this chapter, the individual effects of a wet strength resin, Kymene[®]1500 and a debonding agent, Softrite[®]7516, on various sheet properties are studied, and the combined effects of the two chemicals are also presented. The concept of design and engineer tissue properties via chemical methods has been applied in this study.

5.2. Results and discussion

5.2.1. Confocal microscopy

In order to visualize the changes of fiber structure by the chemical application, confocal microscopy was used to section the sheet samples. Three sheet samples made under different conditions were selected: (A) control, no chemical additive applied; (B) wet strength resin treated sample--the addition level of the wet strength resin was 1 percent; and (C) debonder treated sample; the debonder addition level was 0.75 percent. Accordingly, the representative confocal slices are given as Figures 5.1 (A), (B) and (C).

In the confocal slices, the cellulose fibers were visible due to their auto-fluorescence. The chemical additives, unfortunately, could not be observed. Although the chemical additives were invisible, their effects on sheet structures could be qualitatively visualized from the confocal images.

Figure 5.1 (A) shows the fiber structure of a control sample, and is suggestive of a three-dimensional sheet structure. The thin hardwood fibers and the thick softwood fibers

were clearly seen in the photograph. The fiber-fiber crossings, where inter-fiber bonding occurred, were also visible. Notice that in the confocal slice, all three kinds of fiber crossings were observed: (1) hardwood fiber with hardwood fiber; (2) hardwood fiber with softwood fiber; and (3) softwood fiber with softwood fiber. The fiber structure of a sample treated with 1 percent wet strength resin is shown in Figure 5.1 (B). The structural differences between the samples treated with wet strength resin and the control were not obvious. Since the wet strength resin was not fluorescent, its location on the fiber surface could not be identified. Figure 5.1 (C) represents the internal fiber structure of the sheet treated with 0.75 percent debonding agent. Similar to wet strength resin, the debonding agent could not be visualized in the fiber network. The sheet structure was much looser and weaker than that of the control, and the fiber density seemed lower.

Confocal microscopy made it possible to non-invasively examine the handsheet internal structure, but the visualization was only qualitative. In order to obtain quantitative conclusions on the effects of chemical additives, the sheet physical properties must be measured.

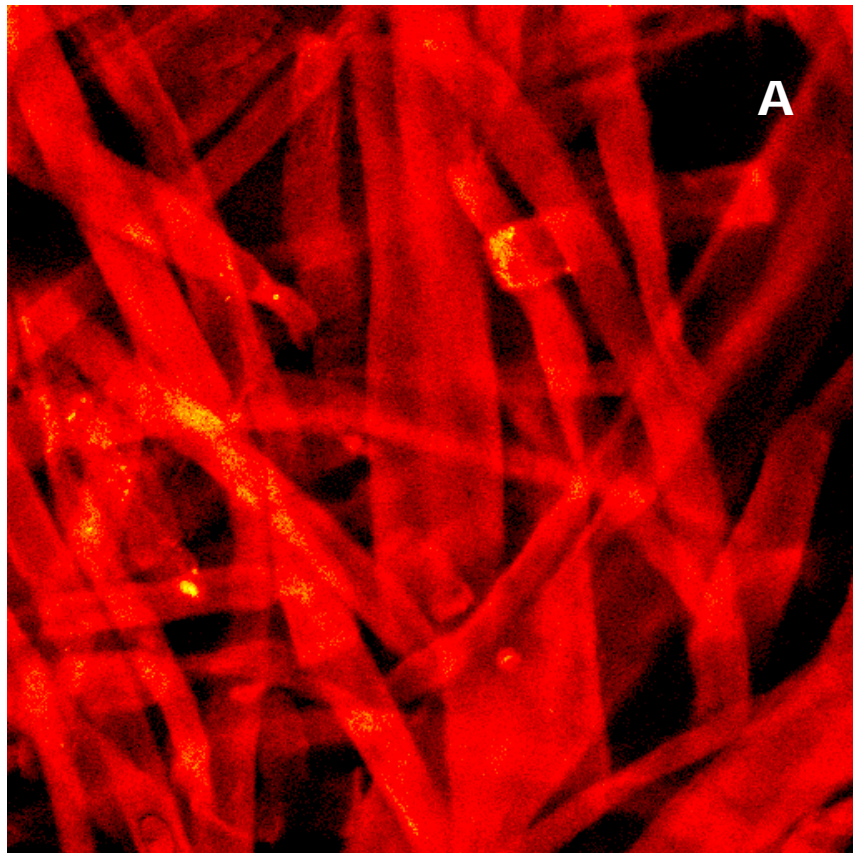


FIGURE 5.1 (A) Confocal optical slice showing the fiber structure of a control sample. The control sheet was made of 65% hardwood and 35% softwood fibers. The sliced area was 230 μm by 230 μm , and the slice was 12 μm deep from the sample surface. In the control sample, no chemicals were applied.

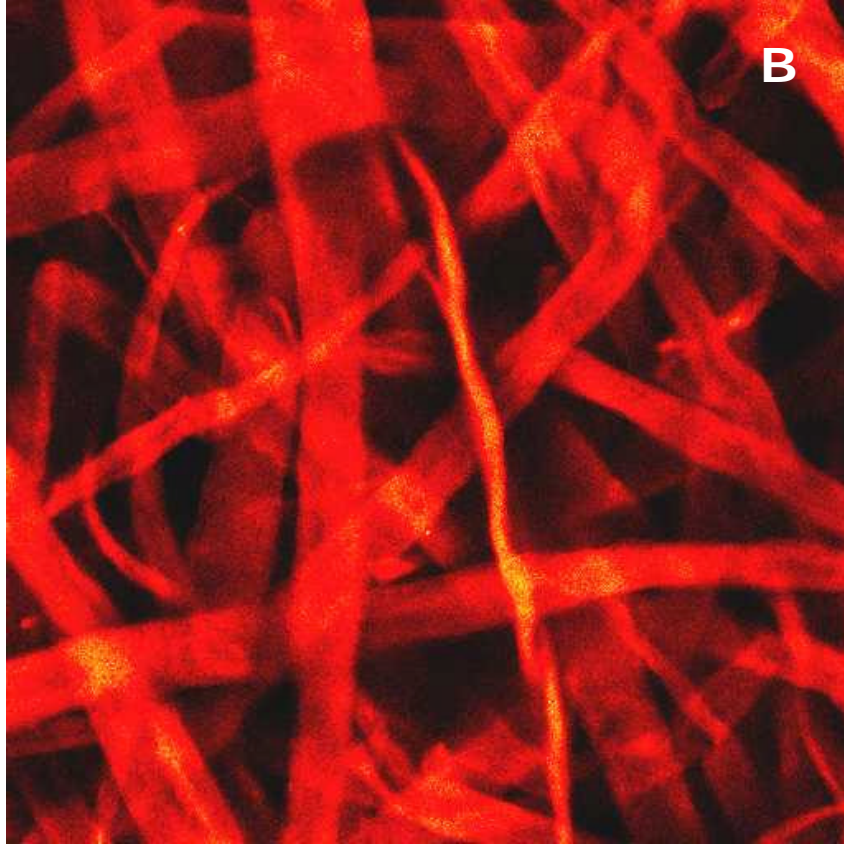


FIGURE 5.1 (B) Confocal optical slice showing the fiber structure of a sample treated with 1 percent wet strength resin. The sample was made of 65% hardwood and 35% softwood fibers. The sliced area was 230 μm by 230 μm , and the slice was 12 μm down from the sample surface.

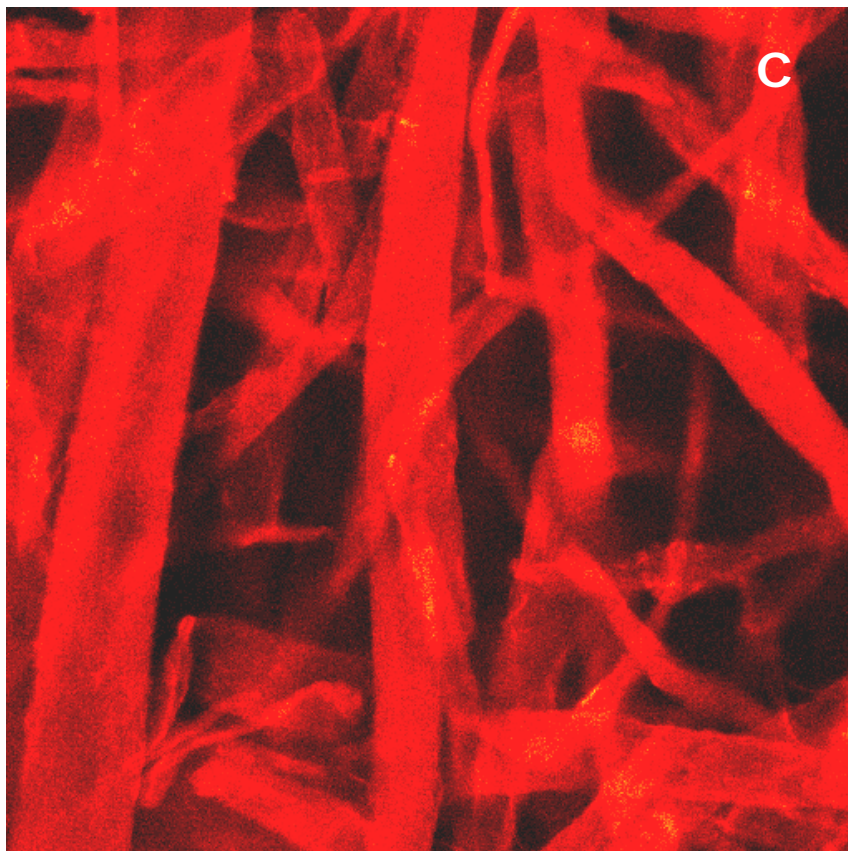


FIGURE 5.1 (C) Confocal optical slice showing the fiber structure of a sample treated with 0.75 percent debonding agent. The control was made of 65% hardwood and 35% softwood fibers. The sliced area was 230 μm by 230 μm , and the slice was 12 μm down from the sample surface.

5.2.2. Handsheet softness

The softness of commercial facial tissue made by creping technology has been systematically studied [Liu et al, 2001], and the multi-variable regression technique is used to develop softness models. Although the softness model could predict tissue softness with accuracy, it cannot be readily applied to the handsheet made in the laboratory due to two major reasons. First, the handsheet made in the laboratory does not have machine and cross-machine directions; therefore, it does not have directionality. In comparison, the commercial tissue has directionality and its physical properties are directionality dependent. Second, the handsheet is not creped; thus, the fiber ends do not protrude at the paper surface as the commercial tissue does. Therefore, modifications must be made to the softness models developed for the commercial tissue. A softness model in reduced form is developed based on two sheet properties, tensile and Handle-O-Meter stiffness:

$$S' = (T'_{avg})^{-1.16} (MH)^{-0.122} \quad (5.1)$$

where S' is reduced softness, the softness ratio of sheet to that of control,

T'_{avg} is the average tensile strength ratio of sheet to that of control, and

MH is the average Handle-O-Meter stiffness ratio of sheet to that of control.

The reduced softness uses two commonly measured sheet physical properties and gives the estimates of softness improvement.

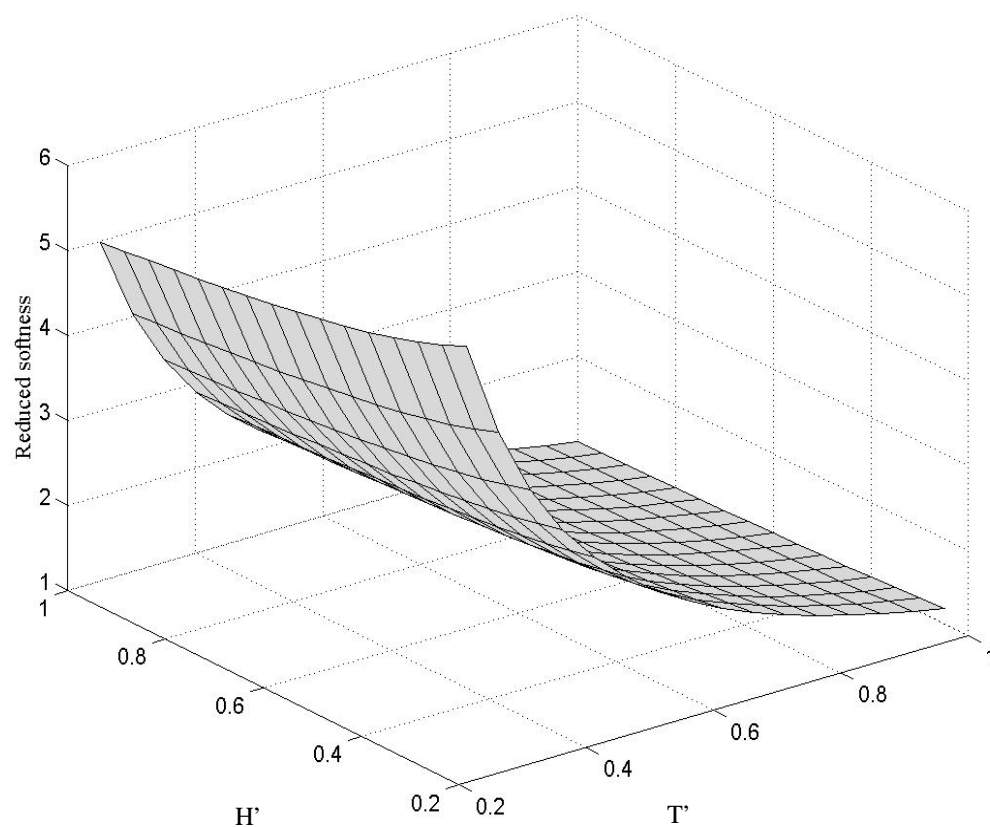


FIGURE 5.2 The sheet softness in reduced form as a function of reduced tensile strength and reduced Handle-O-Meter stiffness. The reduced softness can give an estimation of chemical effects on sheet softness based on the two commonly measured sheet physical properties in the laboratory.

5.2.3. Effects of wet strength resin on sheet properties

In this section, the effects of a wet strength resin, Kymene[®] 1500, on various sheet properties are presented. Sheet properties considered were wet and dry tensile strength, stiffness, bulk, total water absorbency (TWA) and softness. The pulp stock for making the handsheet was the blend of 65% bleached hardwood kraft (BHK) pulp and 35% bleached softwood kraft (BSK) pulp. Three wet strength resin addition levels were applied, i.e., 0.25%, 0.5% and 1%. The stock pH was adjusted to 7.5±0.1, and the experiments were performed at 20°C.

5.2.3.1. Wet strength

The effects of Kymene[®] 1500 on handsheet wet strength are shown in Figure 5.3. For the handsheet without wet strength resin treatment, it lost most of its strength when saturated in water. The wet tensile was only 1.35 Nm/g, about 4.5 percent of its dry strength. From Figure 5.3, it is observed that the addition of wet strength resin significantly increased sheet wet tensile strength. The initial application of Kymene[®] 1500 led to much faster wet strength increase than at higher dosages. The response of sheet wet strength to Kymene[®] 1500 can be predicted by the following equation:

$$T_w = T_{w0} + \frac{33.89C}{1 + 2.66C} \quad (5.2)$$

where T_{w0} is the wet tensile strength of control, 1.35 N m/g.

Equation 5.2 fits well with experimental data and has a correlation coefficient of 0.981. The improvement in sheet wet strength can be explained by two factors: (A) by the patch mechanism--the resin increases the fiber-fiber bonding area; and (B) the polymeric network reinforces the inter-fiber bonding [Bates, 1969; Chan et al., 1994]. It is beneficial to discuss the mechanisms by which the wet strength resin Kymene increases sheet wet strength. As discussed in Chapter 2, under wet conditions, hydrogen bonds between fibers will be lost for the control sheet. For the Kymene treated sheets, Kymene may deposit on the fiber surface through patch mechanism and interact with the neighboring fibers. Therefore, new interfiber bonds are formed. When located in the pulp fiber crossings, the Kymene patch is also likely to protect the existing hydrogen bonds by excluding water molecules. Finally, the wet strength resin molecules can form a polymeric network and provide additional strength for the cellulose fiber structure.

The next question is why the wet strength did not increase as quickly as at low Kymene concentrations. The phenomena may be explained by the effects of Kymene on the inter-fiber bonding. At low Kymene levels, the zeta potential of the fiber system was increased as its absolute value decreased. As discussed in Chapter 4, for the fiber system, the slightly negative zeta potential is preferred since the inter-fiber force is minimized. In addition to the bonding provided by Kymene, the fibers were allowed more intimate contact with each other, which led to better inter-fiber bonding. As pointed out in Chapter 4, the fiber system's zeta potential became positive when the Kymene concentration was

above 0.25 percent. The increasing colloidal forces among fibers prevented effective fiber-fiber bonding, although Kymene provided more strength through above-mentioned mechanisms.

5.2.3.2. Dry strength

Figure 5.4 shows the effects of Kymene[®] 1500 on the handsheet dry strength. The figure indicates that Kymene also moderately improved sheet dry strength property. For the control sheet, its dry tensile index was 30 Nm/g. Similar to that of wet strength, the dry strength exhibited a quick increase to initial chemical addition and plateaued at higher dosages. The addition of 0.25 percent Kymene resulted in an increase of 7 Nm/g in dry tensile index. At the addition levels of 0.5 and 1 percent, the sheet dry tensile indexes were increased to 39.6 and 42.7 Nm/g, respectively. The effects of Kymene on sheet dry strength can be described by an equation similar to Equation 5.2

$$T_d = T_{d0} + \frac{45.66C}{1 + 2.65C} \quad (5.3)$$

where T_{d0} is the dry tensile strength of the control, 30 N m/g.

The results suggest that Kymene not only improves sheet strength under wet conditions, but also moderately increases sheet dry strength. The increase in dry strength by the application of wet strength resin indicates that additional strength is provided by the resin and that the preservation mechanism is not the sole mechanism by wet strength

resin, which is in agreement with the observations of Fredholm et al. [1983]. The mechanisms for the dry strength increase by wet strength resin are the same for the wet strength improvement. Equation 5.3 shows that the increase of sheet dry strength follows a similar trend as the wet strength.

To gain more understanding of the effect of Kymene on sheet strength, two parameters, i.e., the ratio of wet to dry tensile and the reduced tensile, are considered. The ratio of wet to dry tensile is indicative of the balance of sheet strength at wet and dry conditions, while reduced tensile strength is defined as the ratio of sheet tensile strength to that of control, which is useful in describing chemical effectiveness.

The ratio of wet to dry tensile index was increased by the addition of wet strength resin as shown in Figure 5.5. For the control, the ratio was only 0.045 and the addition of 0.25 percent wet strength resin increased the sheet ratio to 0.17. Further increases in the wet strength resin concentration led to a smaller increase of the ratio. At the 0.5 and 1 percent addition levels, the ratios were 0.227 and 0.239, respectively.

The effects of wet strength resin on reduced tensile strength are shown in Figure 5.6. The addition of wet strength resin led to a significant increase in reduced wet tensile, which was almost four upon the addition of 0.25 percent Kymene[®]. At the 1 percent level, sheet wet strength was 7.6 times of that of the control. In comparison, the increase of the reduced dry tensile index was relatively small, which could be explained by the much higher dry strength of the control than its wet strength.

The azetidinium functional groups reacted with the carboxyl groups on the fiber surface; therefore, the wet strength resin was adsorbed by chemical bonding on the cellulose fiber. As discussed in Chapter 4, the wet strength resin deposited like a patch on the fiber surface. The wet strength resin patch connected one fiber with another, which reinforced the fiber-fiber bonding. The wet strength resin self cross-linked by dehydration in the curing process, formed a polymer network, and protected the hydrogen bonding between the fibers. Under wet conditions, paper strength was quickly lost because of the disruption of the inter-fiber hydrogen bonding by water molecules. The wet strength resin network maintained most of its strength in water, which was slowly decreased since the resin was hydrolyzed in the presence of water.

At 0.25 percent level, the sheet wet tensile index was increased from 1.35 Nm/g by 5 Nm/g to 6.35 Nm/g, while the increase in the sheet dry tensile index was about 7 Nm/g. At 1 percent addition level, the increase in the wet tensile index was 8.85 Nm/g, while the increase in the dry tensile index was 12.7 Nm/g. The slightly higher dry strength increase in absolute value is probably due to loss of hydrogen bonds among fibers and the slow hydrolyzation reaction between Kymene and water.

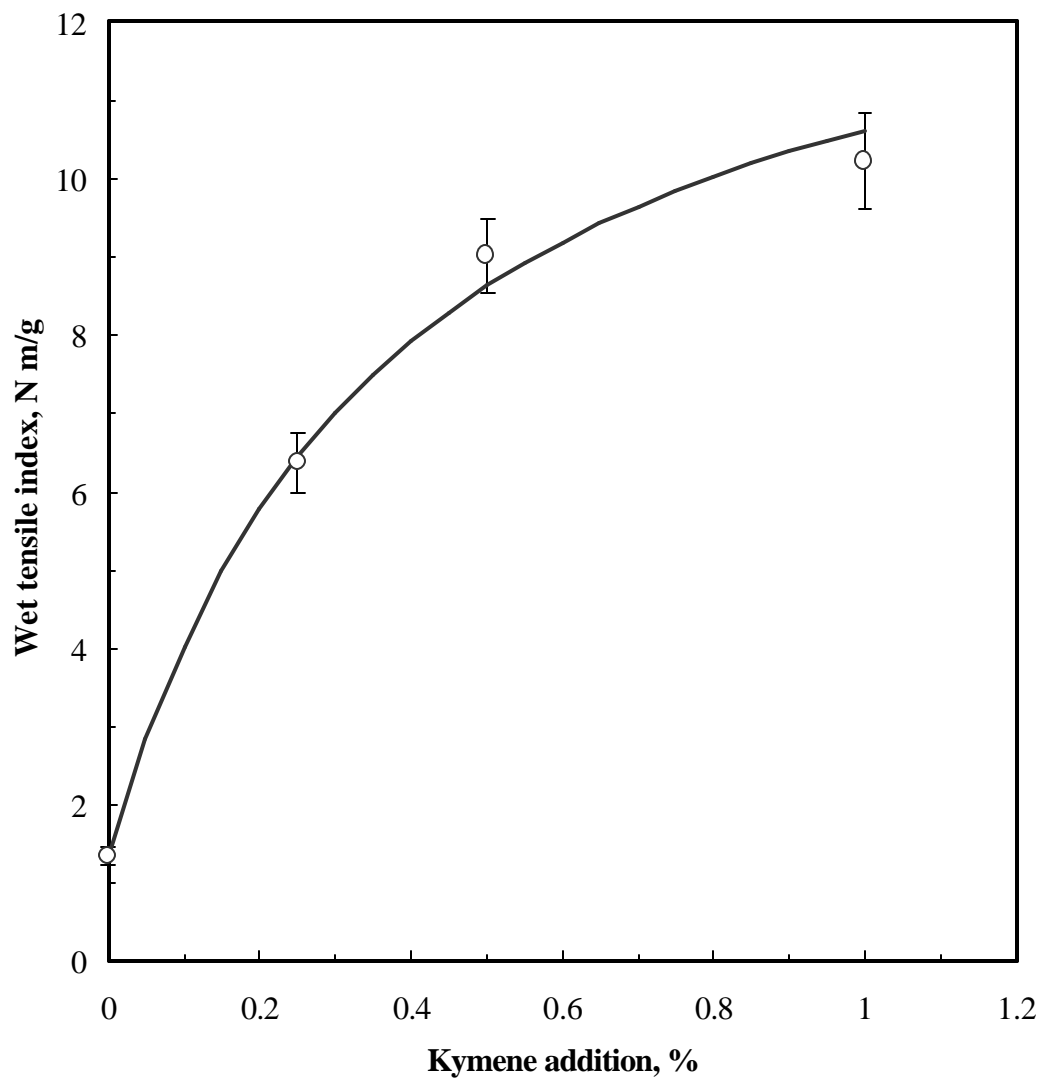


FIGURE 5.3 Effects of Kymene[®]1500 addition on sheet wet tensile index. All data points represent the average of 5 measurements. Points represent experimental data and the error bars are the 91% confidence interval. The solid curve represents the prediction of Equation 5.2.

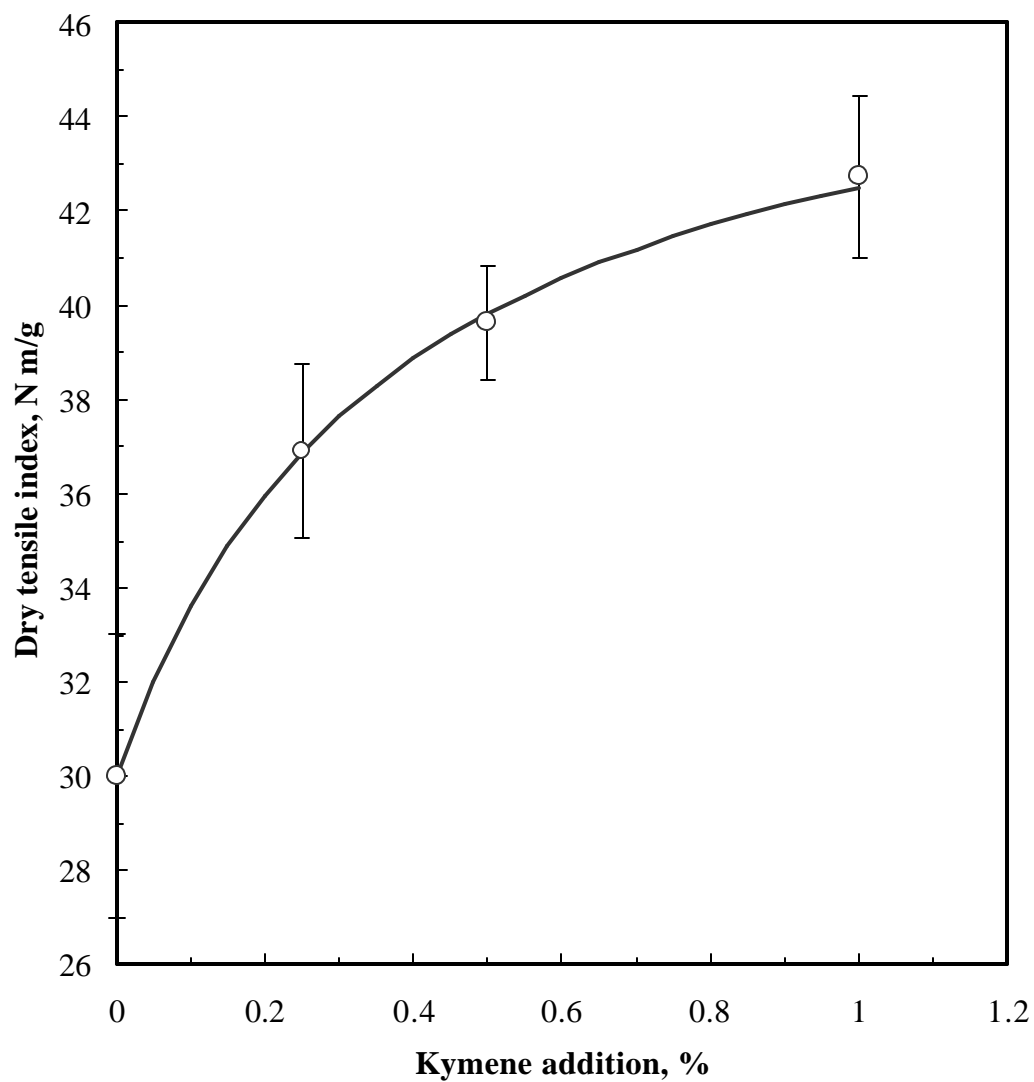


FIGURE 5.4 Effects of Kymene[®]1500 addition on the handsheet dry tensile index. All data points represent the average of 5 measurements. Points represent experimental data and the error bars are the 91% confidence interval. The solid curve represents the prediction of Equation 5.3.

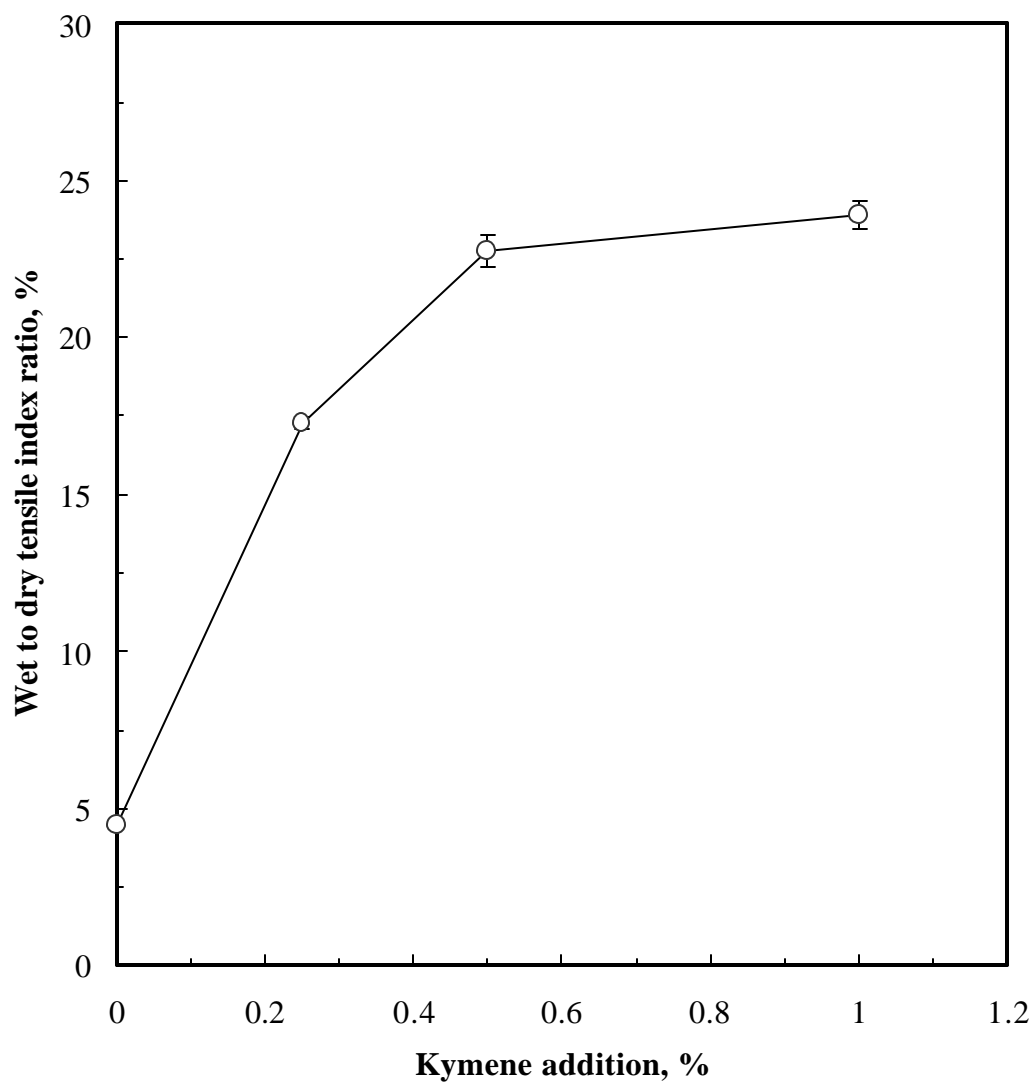


FIGURE 5.5 Effects of Kymene[®]1500 addition on the ratio of handsheet wet tensile index to dry tensile index. All data points represent the average of 5 measurements. Points represent experimental data and the error bars are the 91% confidence interval.

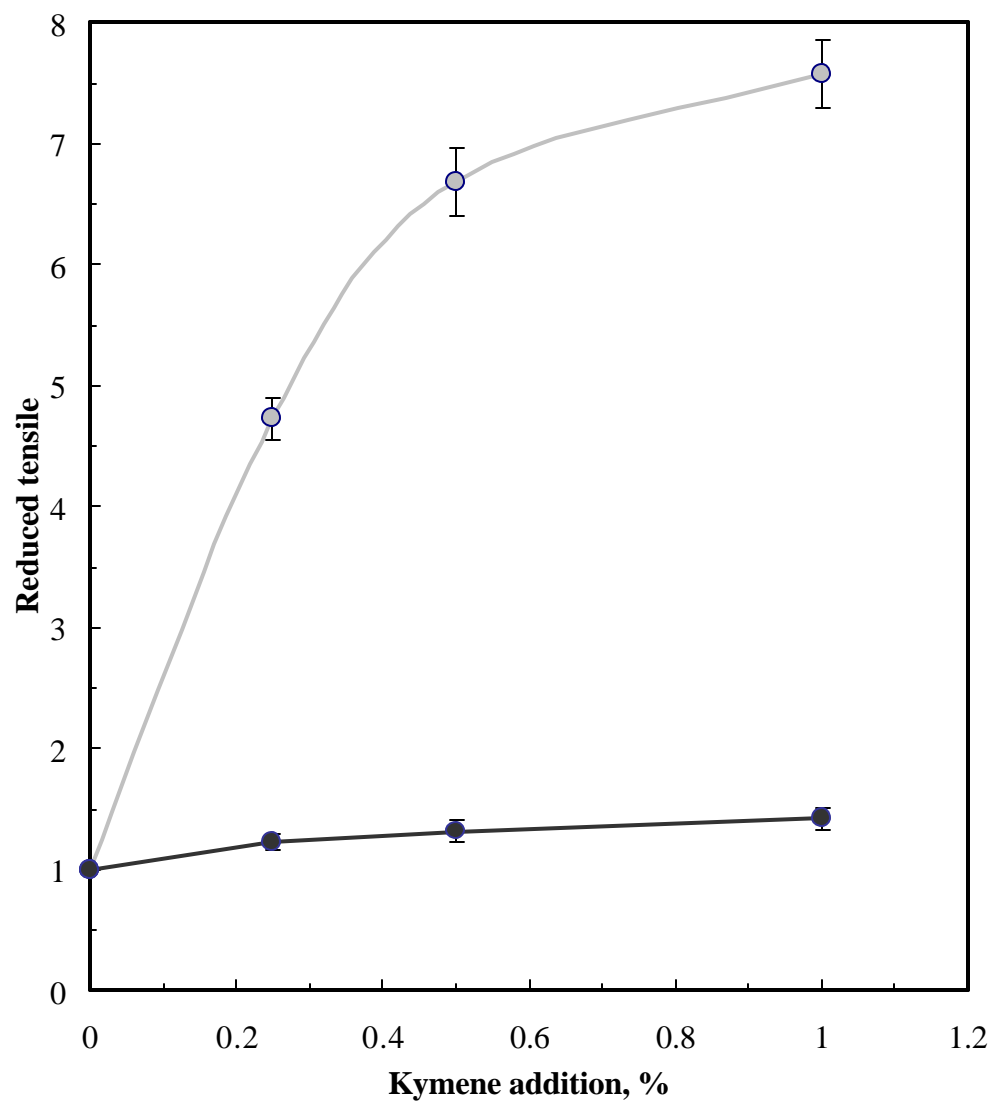


FIGURE 5.6 Effects of Kymene[®]1500 addition on the handsheet wet and dry tensile index in reduced form. All the data points represent the average of 5 measurements, and the error bars are the 91% confidence interval. The black line and the gray line represent the response of reduced wet and dry tensile index to wet strength resin addition, respectively.

5.2.3.3. Stiffness

As discussed in Chapter 2, stiffness is an important sheet property that contributes to the bulk softness component of the softness sensation. The effects of wet strength resin on the sheet Handle-O-Meter stiffness are shown in Figure 5.7. The data indicate that the addition of wet strength resin increased the sheet stiffness at all addition levels. For the control, the sheet Handle-O-Meter stiffness was about 0.23 N. At the 0.25 percent level, the sheet stiffness increased to 0.28 N (p -value<0.01). At the 0.5 and 1 percent Kymene addition levels, the sheet stiffness was increased to 0.31 and 0.33 N, respectively. The stiffness increase was expected, since higher tensile strength by Kymene suggests stronger inter-fiber bonds, and thus a stiffer fiber network. The addition of wet strength resin increased the sheet rigidity, indicating the reduced sheet softness if other properties remained the same.

5.2.3.4. Bulk

The effects of wet strength resin on sheet bulk are shown in Figure 5.8. The figure indicates that sheet bulk is slightly decreased by Kymene addition. At the 0.25 percent level, the data seems to suggest that the addition of Kymene reduced the sheet bulk to some extent; however, the decrease was determined to be statistically insignificant due to the large error bars (p -value>0.1). At higher Kymene concentration levels, the sheet bulk was decreased (p -value<0.05). The addition of the wet strength resin made the fiber-

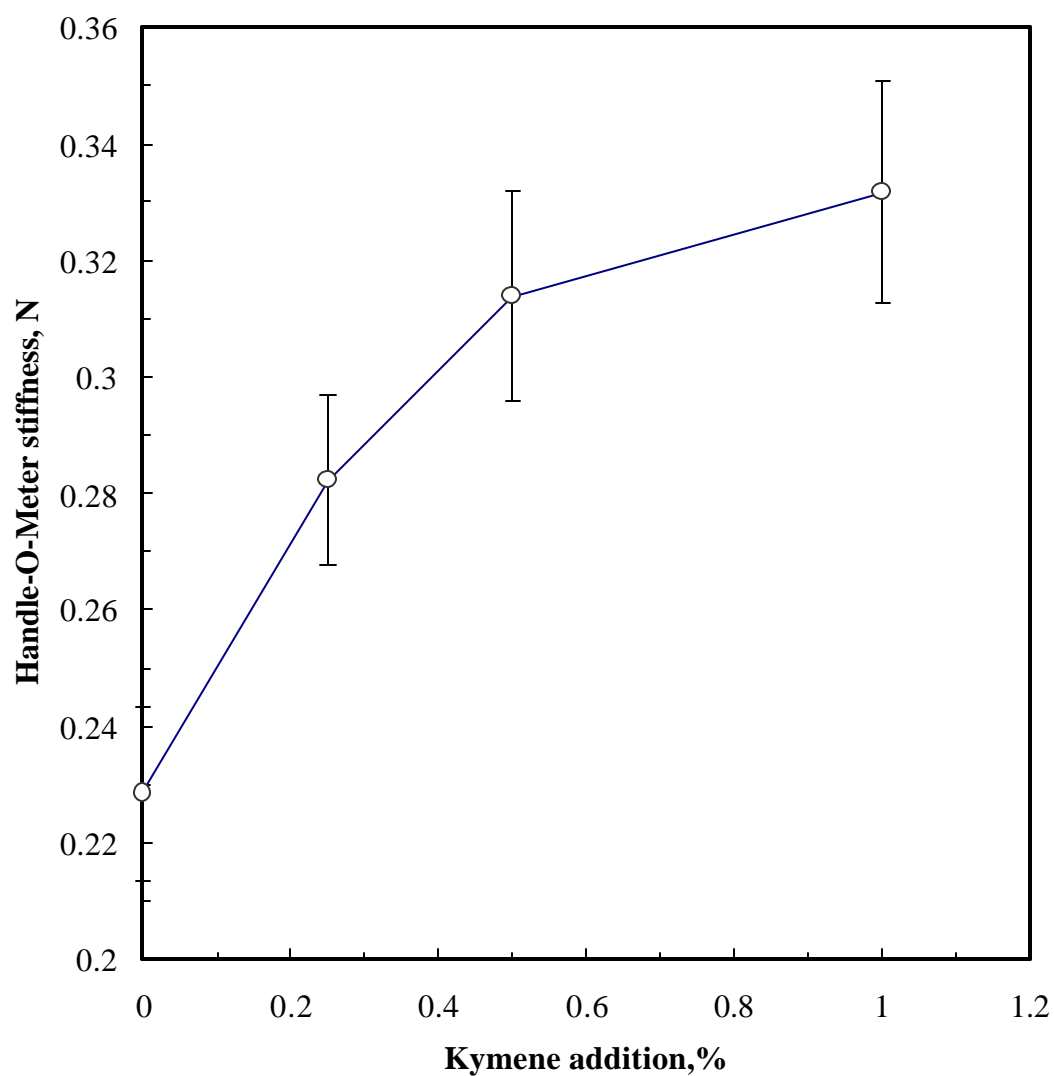


FIGURE 5.7 Effects of Kymene[®]1500 addition on the Handle-O-Meter stiffness of handsheet. All data points represent the average of 5 measurements. Points represent experimental data and the error bars are the 91% confidence interval.

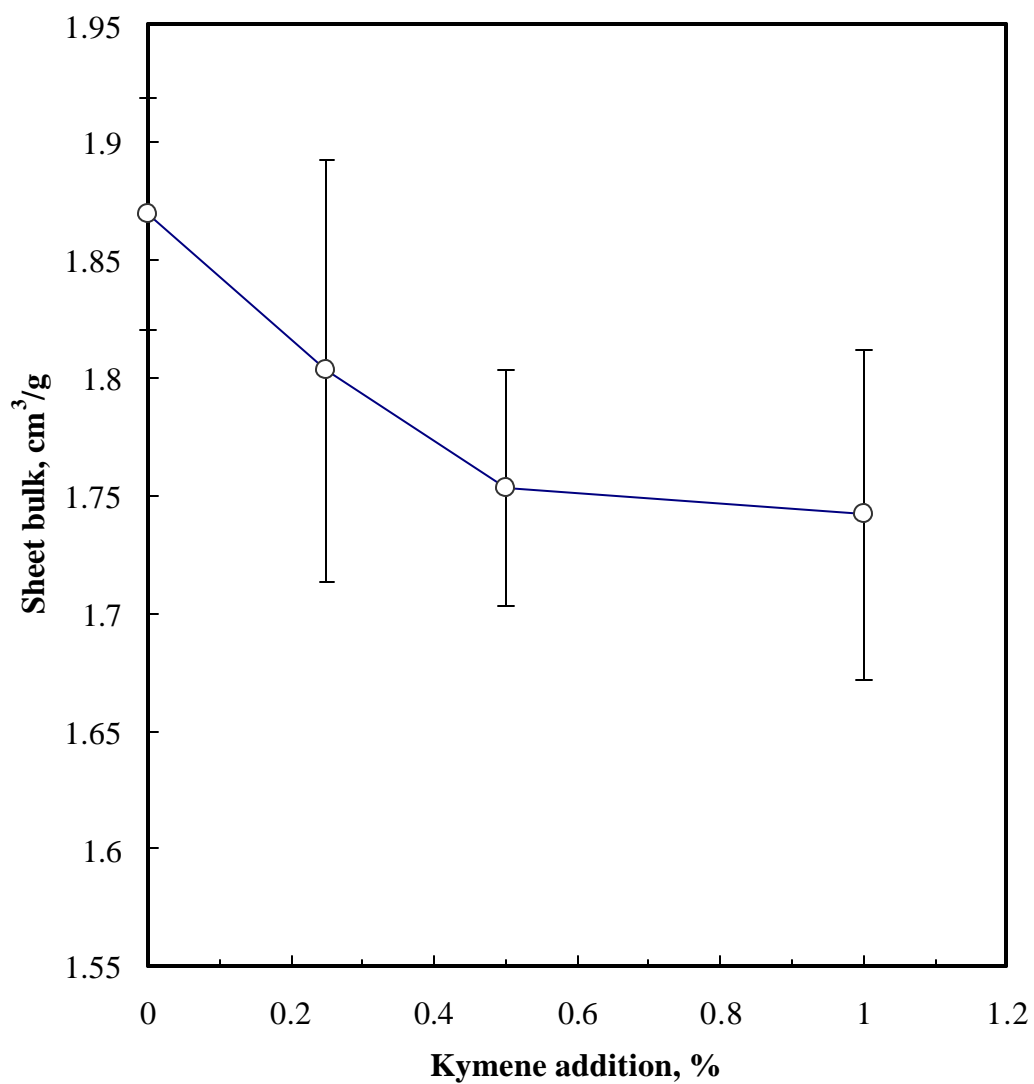


FIGURE 5.8 Effects of Kymene[®]1500 addition on the bulk of the handsheet. The measurement pressure of the electronic bulk tester was 0.687 kPa. All data points represent the average of 5 measurements. Points represent experimental data and the error bars are the 91% confidence interval.

fiber structure more compact; therefore, the fibers had more intimate contact, which led to the reduction of sheet bulk.

5.2.3.5. Total water absorbency (TWA)

The effects of wet strength resin on sheet TWA are shown in Figure 5.9. As the figure indicates, Kymene reduced the sheet water absorbency capacity at all addition levels. The TWA for the control was 2.9 gH₂O/g fiber. At the 0.25 percent level, the sheet TWA was reduced to 1.8 gH₂O/g fiber, which was a 38 percent decrease in absorbency capacity. Further increase in the wet strength resin addition only slightly reduced the sheet water absorbency. At the addition levels of 0.5 and 1 percent, the sheet TWA values were 1.6 and 1.5 gH₂O/g fiber, respectively. The response of TWA to Kymene addition can be simulated by the following equation

$$TWA = TWA_0 - \frac{17.3C}{1+11.46C} \quad (5.4)$$

where TWA_0 is the water absorbency of the control sheet, gH₂O/g fiber.

Equation 5.4 represents the data well and has a correlation coefficient of 0.994. The decrease in sheet water absorbency is expected and can be explained by the preservation mechanism of the wet strength resin. The preservation mechanism suggests that the resin crosslinks with itself surrounding the fiber-fiber contact area (volume), impeding fiber swelling and excluding water molecules so that a significant portion of hydrogen bonds

can be preserved [Fredholm, 1983]. The water absorbency decrease is not desirable; however, the compromise must be made in order to make sheet strong under wet conditions.

5.2.3.6. Softness

The effects of Kymene[®] on the sheet softness are shown in Figure 5.10. The reduced softness refers to the softness ratio of an additive-treated handsheet to control. The reduced softness combined the factors of tensile strength and stiffness, and allowed the qualitative assessment on the tissue softness, which is usually determined in a subjective way.

Figure 5.10 suggests that the addition of Kymene significantly reduced the sheet softness. As defined in the study, the reduced softness for the control was 1. The reduced softness decreased to 0.78 at the 0.25 percent level (p -value<0.01). When the concentration was 0.5 percent, the reduced softness was lowered to 0.7. Finally, the reduced softness was reduced to 0.64 at 1 percent Kymene concentration. The initial 0.25 percent wet strength resin led to most significant softness reduction, i.e., 22 percent, and subsequent Kymene addition resulted in relatively smaller reductions. The decrease in sheet softness was also in agreement with the results of the “handfeel” test by the panelists. It can be seen that the softness decrease by the wet strength resin addition was the result of the changes in several critical sheet properties.

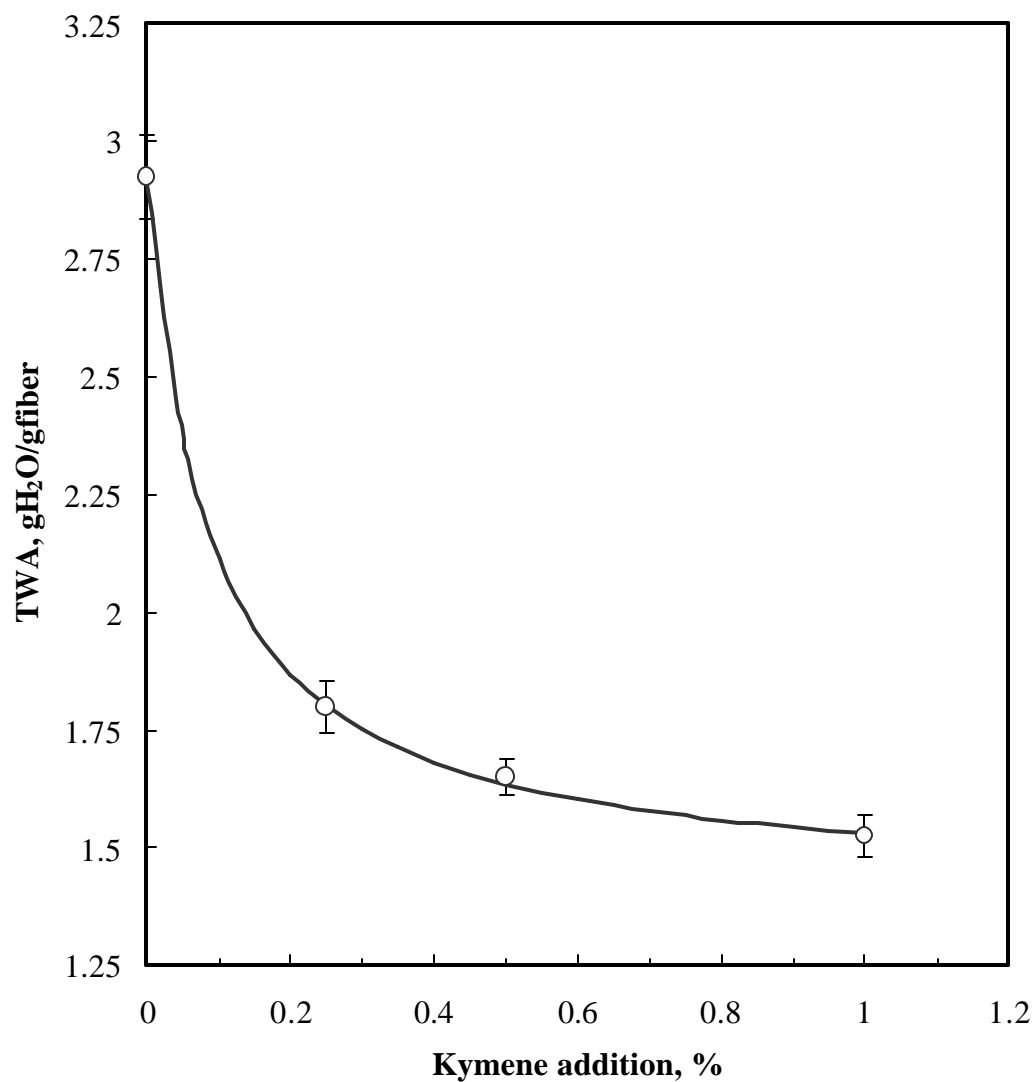


FIGURE 5.9 Effects of Kymene[®]1500 addition on the Total Water Absorbency of the handsheet. All data points represent the average of 3 samples. For each measurement, a 7.62 by 7.62 cm square sample from handsheet was used. The error bars are the 76% confidence interval. The solid curve represents the prediction of Equation 5.4.

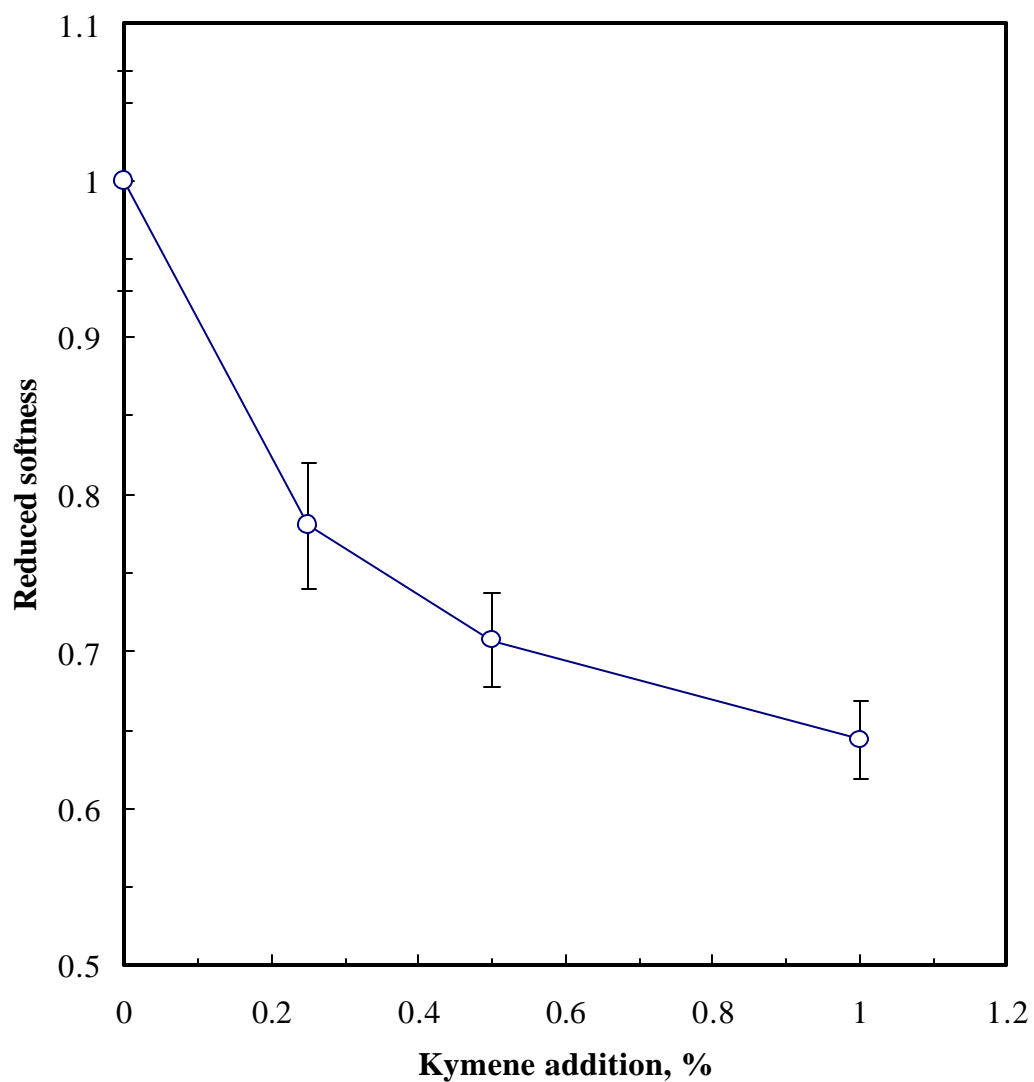


FIGURE 5.10 Effects of Kymene[®]1500 addition on the sheet reduced softness. All data points represent the average of 5 calculations, and the error bars are the 91% confidence interval. The reduced softness is defined as the ratio of softness of handsheet treated with chemical to that of control handsheet. The softness in reduced form presents the additive effect in a quantitative way.

5.2.3.7. Summary

The most noteworthy advantage of Kymene application is the significant improvement on sheet wet strength. The wet strength resin gave the sheet enough strength and ensured its proper function under wet conditions.

Unfortunately, the wet strength resin also incurred some disadvantages for tissue application. Kymene contributed to a moderate increase in sheet dry strength, which would cause the decrease of tissue softness as discussed in Chapter 2. The wet strength resin also made the sheet more rigid, which was reflected on the increase of sheet stiffness measured by the Handle-O-Meter. The sheet bulk was slightly reduced by the addition of the wet strength resin. Because of the wet strength resin addition, sheet total water absorbency capacity was reduced greatly. Finally, due to the increase of tensile strength and stiffness, sheet softness was also adversely affected.

It needs to be pointed out that due to the mechanism of the wet strength resin, the decrease of sheet water absorbency is inevitable. The requirements of improving sheet wet strength and water absorbency are in conflict with one another. Therefore, for specific tissue grades, certain compromises must be made according to the priority of the tissue functionality.

5.2.4. Effects of debonding agent on sheet properties

In this section, the effects of a debonding agent, Softrite[®] 7516, on various sheet properties are presented. The sheet properties considered were wet and dry strength properties, stiffness, bulk, total water absorbency and softness. The pulp stock for making the handsheet was the blend of 65 percent bleached hardwood kraft (BHK) pulp and 35 percent bleached softwood kraft (BSK) pulp. Three debonder concentration levels were applied at 0.25, 0.5 and 0.75 percent. The stock pH was adjusted to 7.5 ± 0.1 , and the experiments were performed at 20°C.

5.2.4.1. Wet strength

The effects of Softrite[®] 7516 on sheet wet strength are shown in Figure 5.11. The wet tensile index for the control was about 1.35 Nm/g. The sheet wet strength was reduced at all Softrite application levels, and the dependence of the sheet wet strength to debonder concentration could be fitted by linear regression as shown in the equation

$$T_w = 1.339 - 0.477 C \quad (5.5)$$

where T_w is the sheet wet tensile index, Nm/g, and

C is the debonder addition amount, percentage.

As pointed out in Chapter 2, most hydrogen bonds between cellulose fibers are lost when the sheet is wet. The results suggest that the debonder, Softrite[®] 7516, destroyed some of the remaining hydrogen bonds. The wet strength reduction by the debonding

agent makes it more difficult for the sheet to maintain its integrity when wet. For this reason, the debonding agent should not be used alone under most circumstances.

5.2.4.2. Dry strength

The effects of Softrite on sheet dry strength are shown in Figure 5.12. The figure indicates that the debonding agent significantly reduced the sheet dry tensile strength at all addition levels. It is interesting to note that the rate of dry strength reduction by Softrite at low concentrations was similar to that at higher concentrations. The dependence of dry tensile strength to Softrite addition can be fitted linearly by the following equation ($R^2=0.973$):

$$T_d = 28.75 - 25.20C \quad (5.6)$$

where T_d is the sheet dry tensile strength, N m/g, and

C is the debonder addition amount, percentage.

From Equation 5.6, the rate of wet tensile reduction by Softrite was 0.477 Nm/g per percent chemical addition. In comparison, the rate of dry tensile reduction was much greater: 25.2 Nm/g per percent Softrite. This difference can be explained by the amount of hydrogen bonds destroyed by the debonder under both wet and dry conditions. The sheet strength is determined by (1) the fiber's intrinsic strength and (2) the inter-fiber bonding, which is mostly hydrogen bonding. The hydrophobic fatty tail of the debonder interrupts the hydrogen bonds among neighboring fibers, which leads to loosened fiber

structure, and thus, lower strength. Under dry conditions, the debonder is able to destroy much more of the hydrogen bonds among fibers than in a wet state. To illustrate this point, the inter-fiber bonding was calculated using the Page Equation [Page, 1969]. The fiber-fiber bonding at the dry state for the control was computed to be 48.21 Nm/g. At highest Softrite concentration, the inter-fiber bonding lost about 75 percent of its value. In comparison, the loss of inter-fiber bonding in absolute value at wet state was merely 0.38 Nm/g, which represented 0.79 percent of the control fiber bonding.

For the debonder-treated sheet, the ratio of the wet to dry tensile index and the reduced tensile index were also calculated. The results showed that the application of Softrite[®]7516 increased the sheet wet to dry tensile ratio. For the control, the ratio was only 0.045. With the addition of 0.25 percent debonder, the ratio was improved to 0.058. At the 0.5 percent addition level, the ratio rose to 0.069. The ratio was further increased to 0.093 at the highest debonder addition level of 0.75 percent.

As discussed in Chapter 4, the hydrophilic head of the debonding agent was adsorbed on the fiber surface and the hydrophobic tail (i.e., the long alkyl fatty chain) was positioned away from the fiber. The hydrophobic part of the debonding agent disrupted the hydrogen bonds between fibers, which led to the loss of sheet strength. At dry conditions, the debonder accounted for all the loss of the dry tensile strength. However, in the presence of water, most of the hydrogen bonds among the fibers were destroyed by water molecules. Therefore, the amount of hydrogen bonds disrupted by the debonder would be much less at the wet state than at the dry conditions.

Figure 5.13 shows the effects of the debonding agent on the reduced wet and dry tensile strength, indicating that the decrease of the reduced dry tensile index was much faster than that of the reduced wet tensile index. The results suggest that the debonding agent was more effective in the sheet dry tensile reduction than the wet tensile reduction.

It is interesting to notice that both the debonding agent and the wet strength resin increased the ratio of sheet wet to dry tensile index; however, the mechanisms were completely different. The wet strength resin formed a polymeric network and reacted with the cellulose fiber, which significantly improved the sheet wet strength. The addition of wet strength resin increased both the dry and wet tensile strength. Since the reduced wet tensile increased much faster than the reduced dry tensile, the ratio of wet to dry tensile was increased. In comparison, the debonding agent reduced the sheet strength at both dry and wet conditions. At wet conditions, the water molecules destroyed most inter-fiber hydrogen bonds and the debonding agent became less effective in strength reduction than at the dry state. Therefore, dry tensile reduction was much more significant than the wet tensile reduction, which resulted in the increase of the wet to dry tensile ratio. The significant reduction in dry strength caused by the debonding agent application is beneficial for the softness improvement as discussed in Chapter 2.

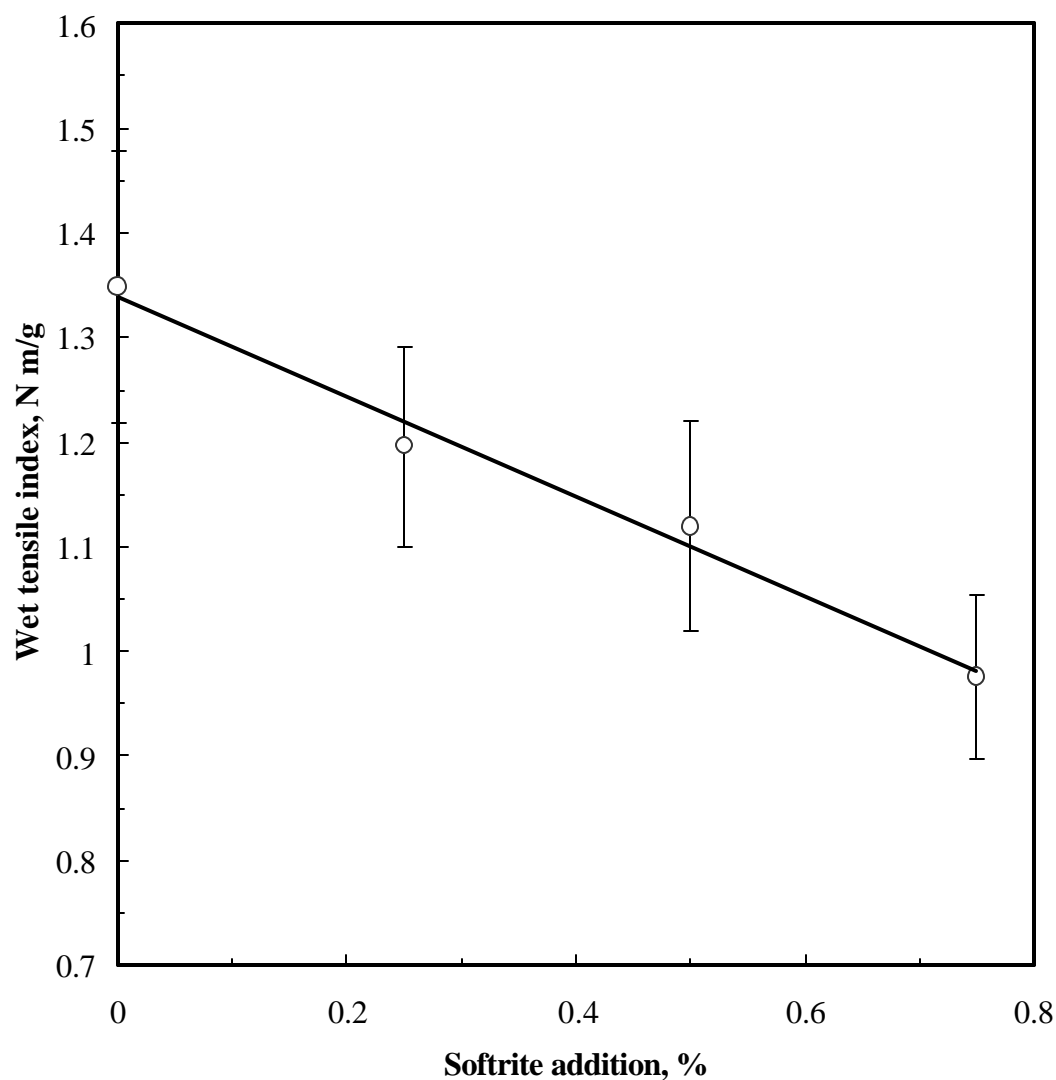


FIGURE 5.11 Effects of Softrite[®]7516 application on the sheet wet tensile index. All data points represent the average of 5 measurements. Points represent experimental data and the error bars are the 91% confidence interval. The solid curve represents the prediction of Equation 5.5.

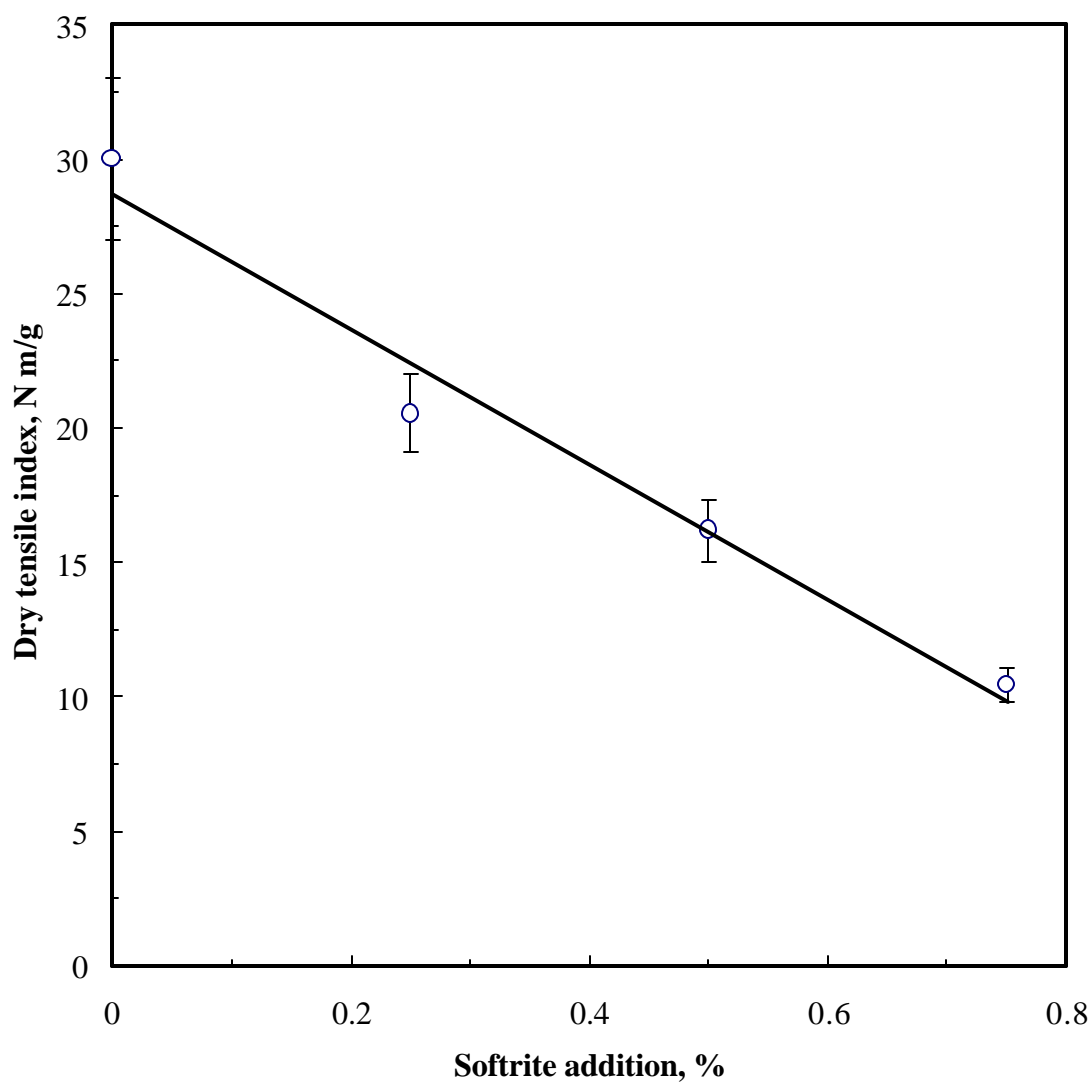


FIGURE 5.12 Effects of Sofrite[®]7516 application on sheet dry tensile index. All data points represent the average of 5 measurements. Points represent experimental data, and the error bars are the 91% confidence interval. The solid curve represents the prediction of Equation 5.6.

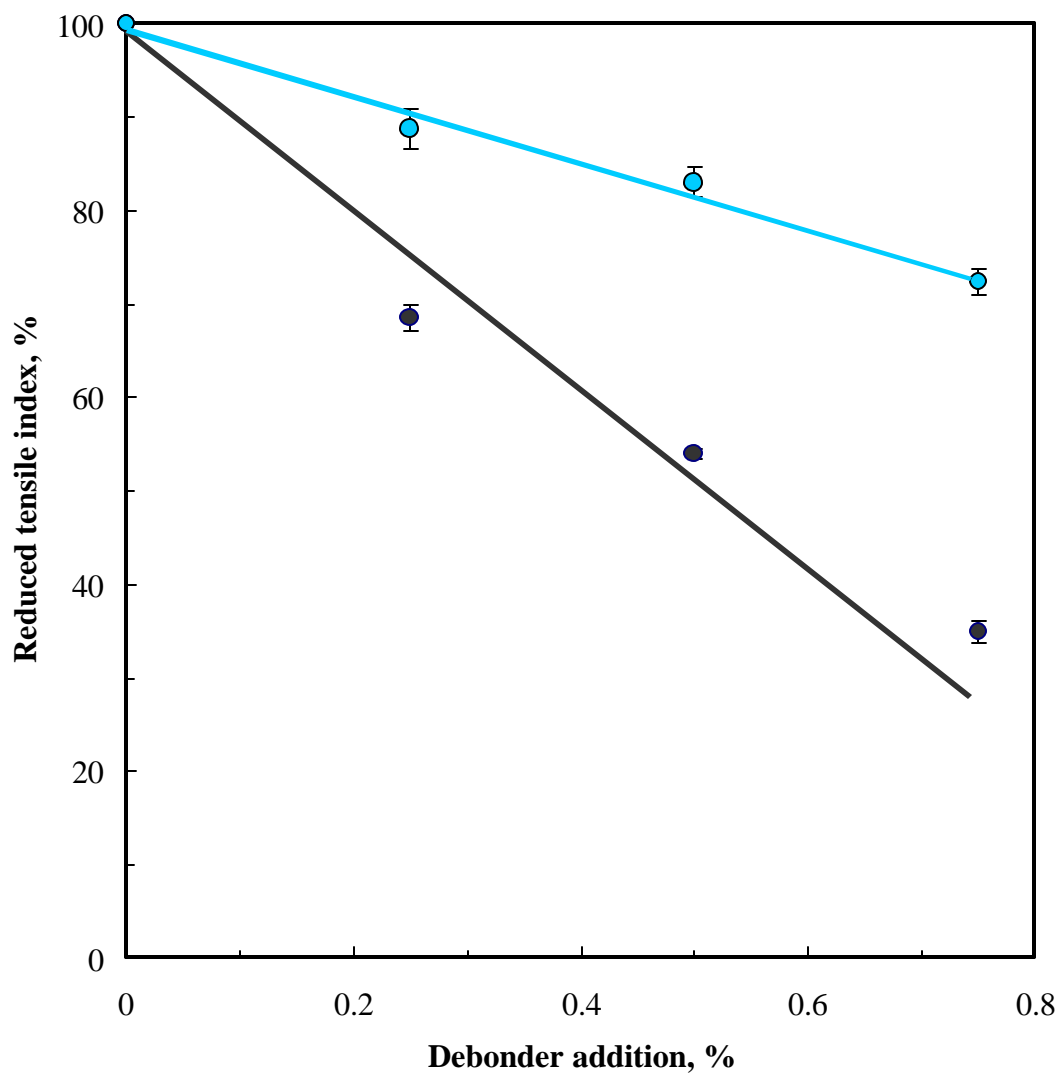


FIGURE 5.13 Effects of Softrite[®]7516 addition on the reduced wet tensile index and reduced dry tensile index. All the points represent the average of 5 calculations, and the error bars are the 91% confidence interval. The black line and the gray line represent the linear correlation fit of the reduced dry tensile index and reduced wet tensile index to debondor application, respectively.

5.2.4.3. Stiffness

The effects of the debonding agent on the handsheet Handle-O-Meter stiffness are shown in Figure 5.10. As the figure indicates, the addition of debonder reduced the sheet stiffness significantly at all concentration levels. The Handle-O-Meter stiffness for the control was 0.23 N. The addition of 0.25 percent Softrite led to 32 percent stiffness decrease and the stiffness lost 56 percent at 0.75 percent Softrite level. The results are in agreement with those of Hollmark et al. [1978], which introduce a correction factor in calculating elastic modulus. As demonstrated in the previous section, the sheet treated with Softrite had a dramatic decrease in its tensile strength. The low tensile suggests fewer inter-fiber crossings per fiber, which decreased the correction factor, and ultimately stiffness. In reference to the results presented in Appendix A, it can be concluded that the stiffness reduction by a debonding agent application leads to an improvement in softness.

5.2.4.4. Bulk

The effects of the debonding agent on sheet bulk are shown in Figure 5.15, which suggests that at all Softrite addition levels, the debonder significantly increased sheet bulk values. The bulk for the control was 1.87 cm³/g. The sheet bulk values increased with increasing amount of Softrite application. The debonding agent weakens the inter-fiber hydrogen bonding; therefore, the sheet fiber structure of the sheet becomes less compact, which leads to the reduced density, and thus, higher bulk.

Observation of the data reveals that bulk increased more quickly at a low debonder concentration than at higher dosages. The dependence of bulk on Softrite addition can be simulated by the following equation:

$$B = B_0 + \frac{0.595C}{1 + 0.531C} \quad (5.7)$$

where B_0 is the bulk of control, $1.87 \text{ cm}^3/\text{g}$.

The equation fit the experimental data well and had a correlation coefficient of 0.99. According to Equation 5.7, at low debonder concentrations, the bulk increase rate was about $0.595 \text{ cm}^3/\text{g}$ per percent chemical and the bulk maximum was predicted to be $3.0 \text{ cm}^3/\text{g}$. The bulk maximum predicted from the data was in agreement of previous work [Liu et al., 1998]. The unpressed handsheet had a bulk value close to the bulk maximum, and it showed that (1) the through-air-dried tissue could be simulated by the unpressed handsheet in the laboratory, and that (2) through-air drying technology is more efficient in improving bulk than the chemical application alone. The debonding agent weakened the inter-fiber hydrogen bonding; therefore, the sheet fiber structure became less compact, which led to the reduced density, and thus, higher bulk.

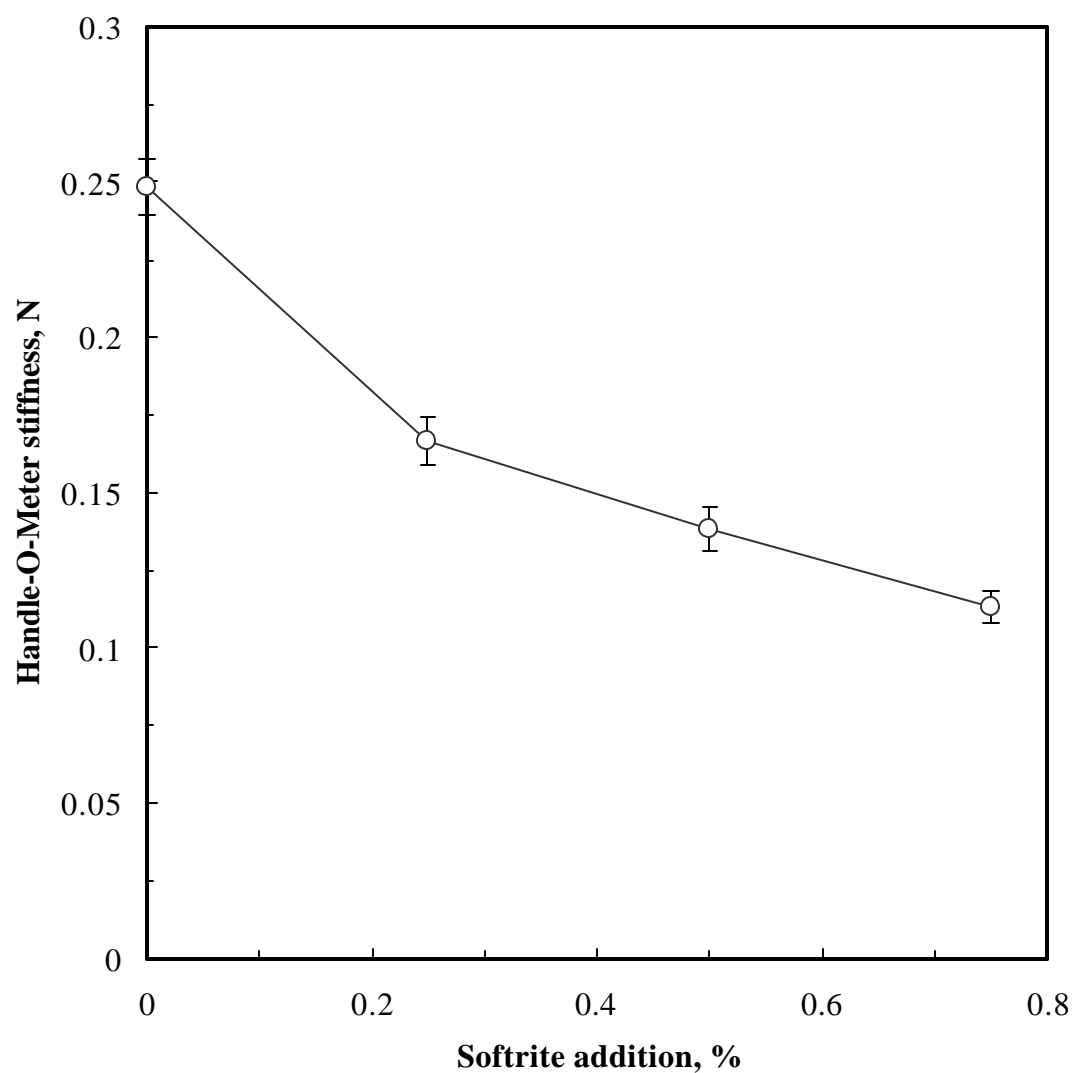


FIGURE 5.14 Effects of Sofrite[®]7516 addition on the sheet Handle-O-Meter stiffness. All data points represent the average of 5 measurements. Points represent experimental data and the curve is hand-drawn to reflect the response of sheet stiffness to the debonding agent addition. The error bars are the 91% confidence interval.

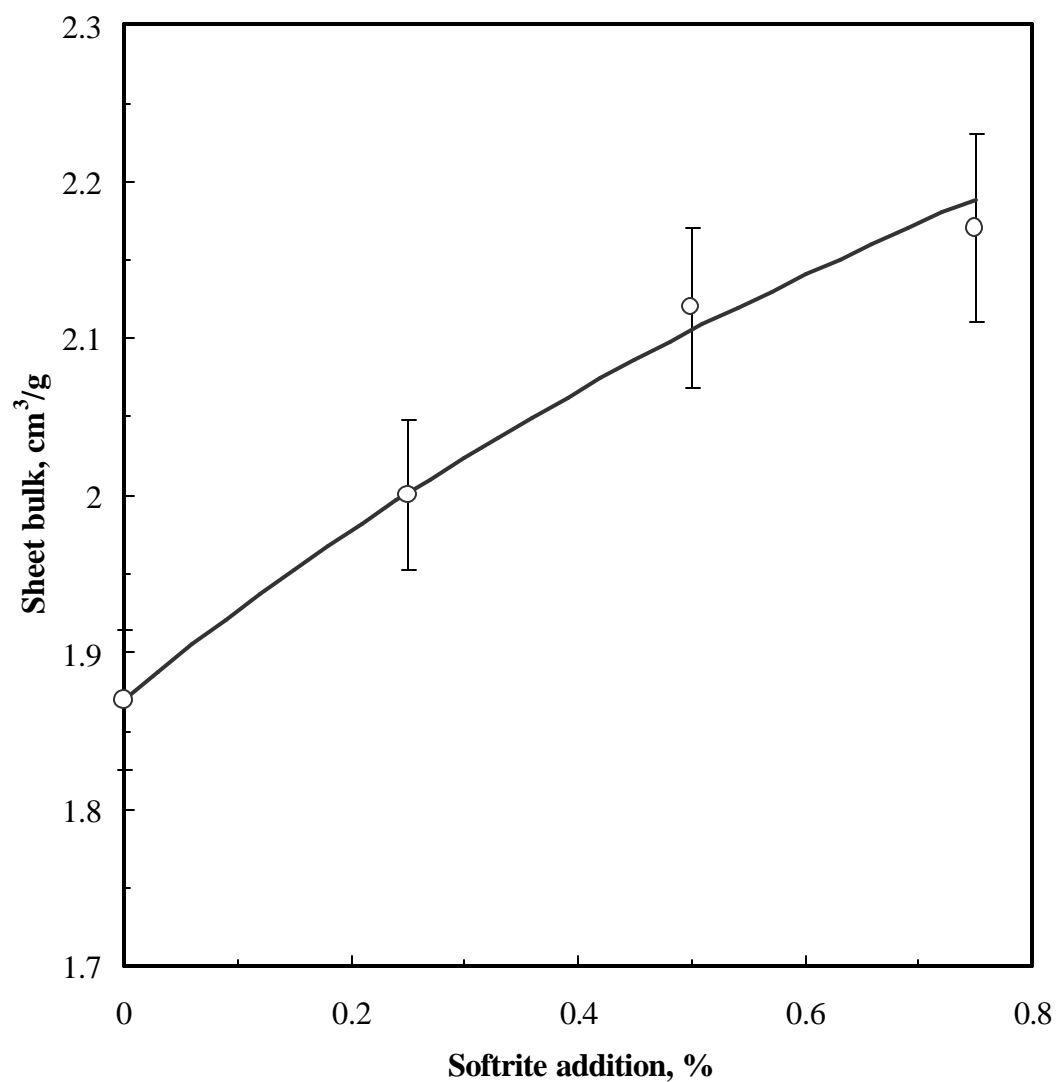


FIGURE 5.15 Effects of Softrite[®]7516 addition on sheet bulk. All data points represent the average of 5 measurements. Points represent experimental data and the error bars are the 91% confidence interval. The black curve represents the predictions of Equation 5.7.

5.2.4.5. TWA (total water absorbency)

The effects of the debonding agent on sheet TWA are shown in Figure 5.16. The data shows that the sheet absorbency capacity was reduced by the application of Softrite. The water absorbency capacity for the control was 2.92 gH₂O/g fiber. With the addition of 0.25 percent Softrite, the TWA was reduced (p -value<0.05). Although absorbency decrease was determined to be statistically insignificant when the Softrite concentration changed from 0.25 to 0.5 percent (p -value>0.1) and from 0.5 to 0.75 percent (p -value>0.1), the decrease over that of control at both 0.5 and 0.75 percent levels was significant (p -value<0.01).

The result is in agreement with the observation of Poffenberger et al. [2000]. They believed that the reduction in TWA could be explained by the presence of the hydrophobic fatty groups. To gain more understanding, the effects of the debonder are considered for capillary and imbibed water, respectively: (A) the debonder molecules effectively reduce water surface tension, which leads to the reduction of capillary water; and (B) debonder produces the sheet with a higher percentage of voids, which provides space for more imbibed water. In addition, the effect of testing method must be taken into consideration: the capillary water is held tight and remained in the sheet capillaries, while a significant portion of imbibed water is removed during the testing. Therefore, the capillary water may carry more weight in the TWA value than the imbibed water. The combined impacts of these factors are the reduced absorbency as the data suggest. In summary, the effects of the debonding agent on the sheet TWA are undesirable.

Comparison of sheet TWA dependence on the wet strength resin and the debonding agent indicates that the water absorbency reduction by the debonder was less than that caused by the wet strength resin.

5.2.4.6. Softness

The effects of debonder addition on the reduced softness are shown in Figure 5.17. In contrast to the effects of wet strength resin, Figure 5.17 indicates that the debonder significantly improved the sheet softness. According to the definition, the reduced softness for the control was one. At a 0.25 percent debonder addition, the reduced softness was improved to 1.6. The softness was further increased to 2.2 and 3.7 at the 0.5 and 0.75 percent Softrite levels, respectively. The increase in softness value was expected, because changes on the critical physical properties were in favor of softness improvement. The two parameters in the reduced softness formula, i.e., tensile strength and stiffness, were decreased by the application of the debonding agent, which led to the increase of the reduced softness. In practice, tensile has been used as a softness indicator where only simple and quick estimation is needed [Carr et al., 1997]. As pointed out by Hollmark [Hollmark, 1983], the reduction in stiffness is beneficial for the bulk softness improvement. The increased bulk by the debonder generates the sense of “being substantial”, which also changes bulk softness favorably. In addition, the fatty chains of the debonder impart a lubricating feel to the fibers; therefore, the surface softness is increased. Sheet softness improvement was also in agreement with the handfeel test

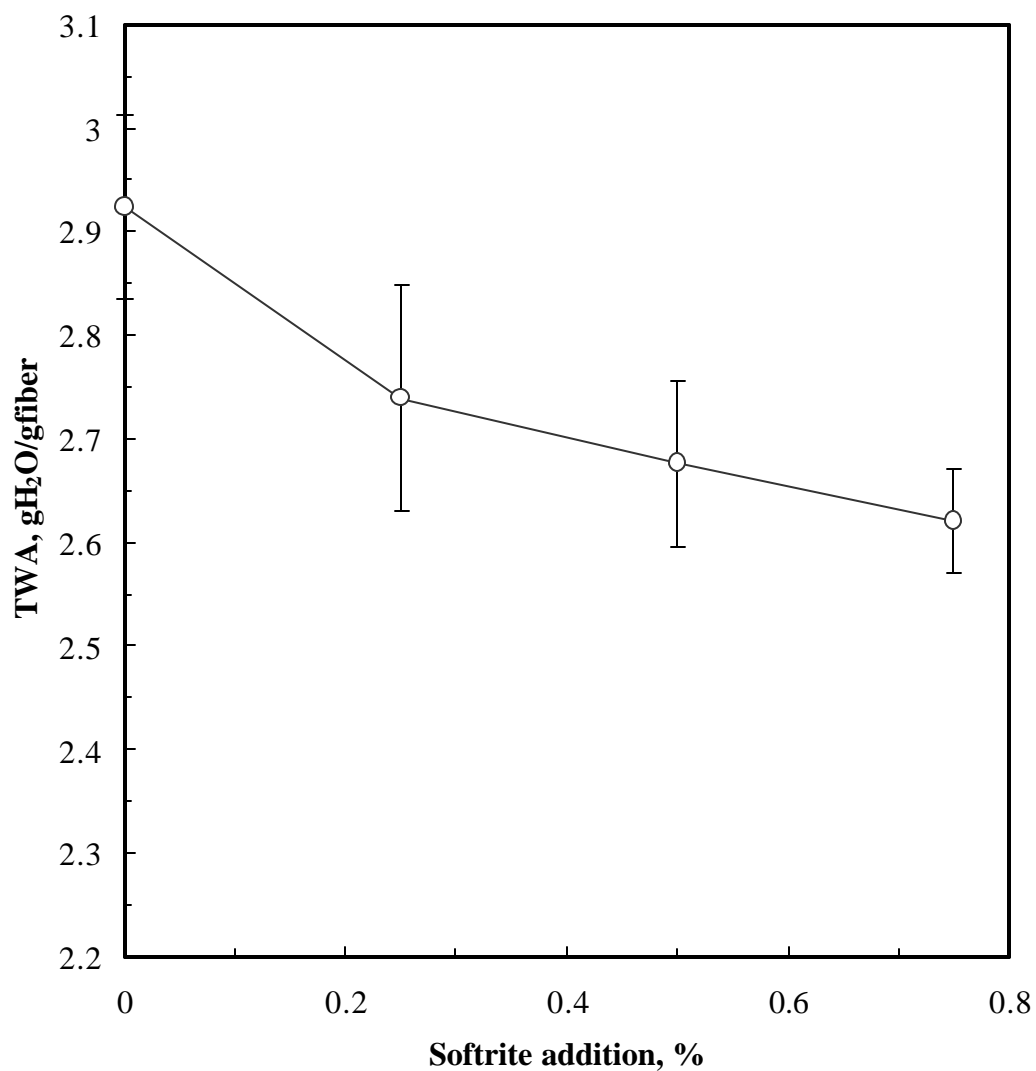


FIGURE 5.16 Effects of Softrite[®]7516 addition on the sheet total water absorbency. All data points represent the average of 3 samples. For each measurement, a 7.62 cm by 7.62 cm square sample from handsheet was used. Points represent experimental data, and the error bars are the 91% confidence interval.

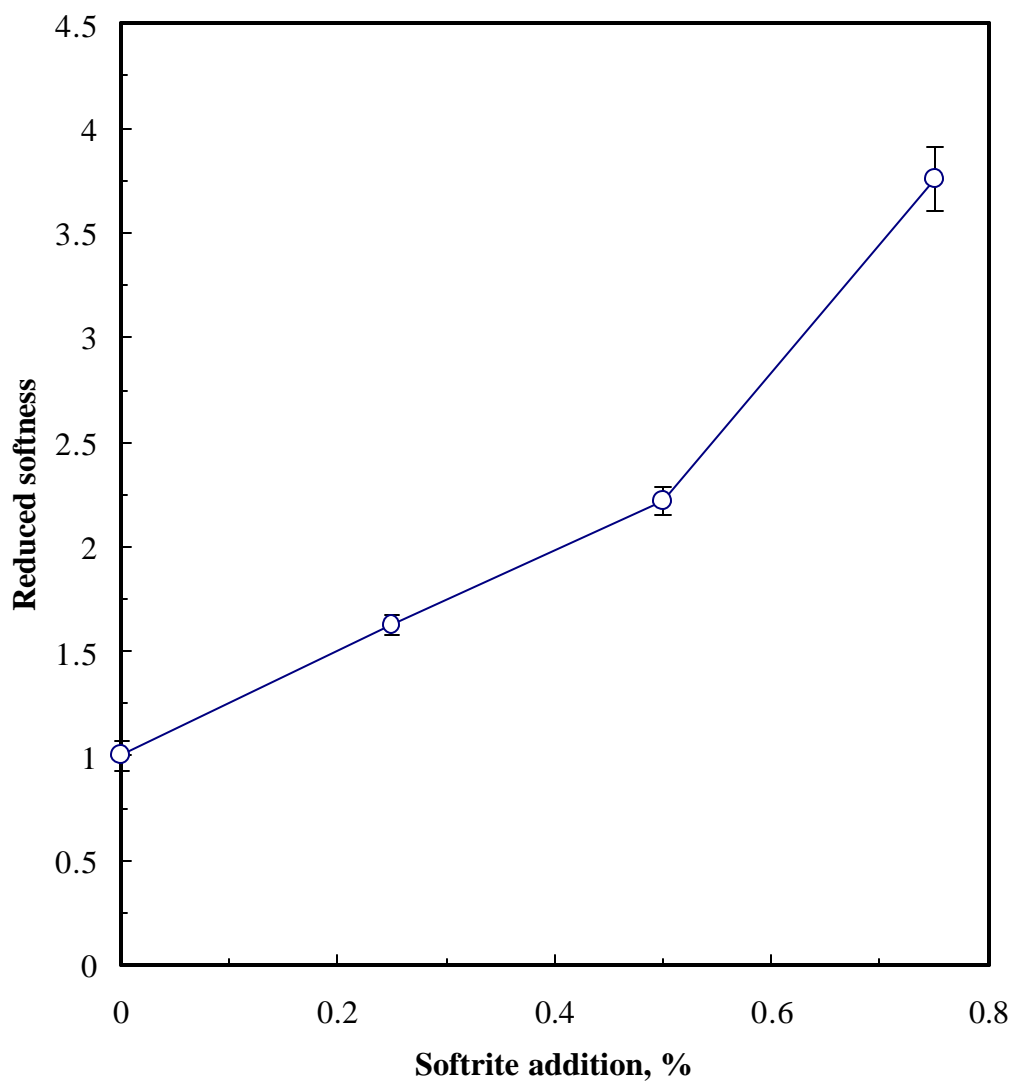


FIGURE 5.17 Effects of Softrite[®]7516 addition on reduced sheet softness. All data points represent the average of 5 calculations, and the error bars are the 91% confidence interval. The reduced softness is defined as the ratio of softness of handsheet treated with chemical to that of control handsheet. The softness in reduced form presents the additive effect in a quantitative way.

conducted in the laboratory. From the above analysis, the debonder changed both components of the softness sensation and was demonstrated to be an effective chemical to increase the sheet softness property.

5.2.4.7. Summary

From the above results, the effects of Softrite on sheet properties are summarized and both the advantages and disadvantages of the debonding agent application are presented. The most important advantage is that the debonding agent improved the sheet softness. The tactile property was improved significantly in terms of reduced softness values. The softness improvement was achieved through debonding agent's effects on important sheet physical properties, i.e., dry tensile strength and stiffness. Another advantage of debonder application is that the sheet bulk was increased. The increased bulk not only contributes to the improvement in softness sensation, but also helps to achieve higher profit margins because fewer raw materials are utilized in the manufacturing process.

The addition of the debonding agent had certain undesired effects on tissue property. The sheet water absorbency capacity was decreased by the application of the debonding agent. The absorbency decrease is undesirable for some tissue grades, especially for paper towels. In addition, the wet strength was further weakened. If the debonding agent were applied alone, it would be quite difficult to use, since the sheet would be too weak

to have any practical applications. The combination of both debonding agent and wet strength resin may overcome some limitations and produce sheets with desired properties.

5.2.5. Effects of wet strength resin and debonding agent on sheet properties

In this section, the effects of dual additive applications on the sheet properties are presented. The pulp stock for making handsheets was the blend of 65% bleached hardwood kraft (BHK) pulp and 35% bleached softwood kraft (BSK) pulp. In the experiment, the addition level of Kymene[®] 1500 was kept at 0.25 percent. Three addition levels of debonder were selected at 0.25, 0.5 and 0.75 percent. The considered sheet properties included sheet wet and dry strength, stiffness, bulk, TWA and softness. The stock pH was adjusted to 7.5 ± 0.1 and the experiments were performed at 20°C.

5.2.5.1. Wet strength

The effects of the combined application of Kymene and Softrite on sheet wet strength are shown in Figure 5.18. For ease of comparison, the data representing Softrite's effects on wet strength were also shown in the figure.

Figure 5.18 suggests that Softrite significantly reduced the sheet wet strength under both conditions. Another observation is that the sheet treated with Kymene and Softrite had significantly higher wet strength than that by Softrite alone. For the sheets treated with both chemicals, the wet strength dependence on debonder concentration can be presented by the following equation (p -value<0.01):

$$T_w = 6.37 - 3.89C \quad (5.8)$$

where T_w is the wet tensile strength, Nm/g, and

C is the Softrite concentration, percentage.

From Equations 5.5 and 5.8, it is shown that for the Kymene treated sheet, the rate of wet tensile reduction by Softrite is much higher than that without wet strength resin. For the Kymene treated sheet, the rate of wet strength decrease was 3.89 Nm/g per percent chemical, while the rate was only 0.477 Nm/g per percent chemical for sheets without wet strength resin addition. The apparent difference in Softrite debonding efficiency could be explained by considering how Softrite affects the mechanism of the wet strength resin. For the wet sheet without Kymene, the debonding efficiency of Softrite is low because most inter-fiber bonds that could have been disrupted by the debonder are destroyed by the attacks of water molecules. For the Kymene-treated sheet, the situation is different. The debonder is deposited on the fiber surface and is able to disrupt the fiber bonds that could have been protected by Kymene and/or the bonds between Kymene polymeric network and cellulose fiber. The proposed explanation is supported by the following observation: at highest Softrite addition level, the wet tensile strength was decreased by 2.92 Nm/g for Kymene treated sheet, while the wet strength of the control was only 1.35 Nm/g. It must be pointed out that despite the reduction caused by the debonder, the sheet wet strength improved significantly through the application of Kymene. For example, at the highest debonder addition rate, 0.75 percent, the remaining wet strength (3.5 Nm/g) was still more than two folds of that of the control. Therefore,

the application of wet strength resin is a must to produce sheets with applicable strength under wet conditions.

5.2.5.2. Dry strength

The effects of the wet strength resin and the debonding agent on sheet dry strength are shown in Figure 5.19. To make the comparison, the data that represent the effects of debonder on dry strength are also shown in the figure.

The data suggest that at the same debonder application level, the dry strength of the Kymene-treated sheet was higher than that without Kymene. In addition, for both types of sheet, the dry strength was shown to decrease with the Softrite application. For the Kymene-treated sheet, the dependence of its dry tensile on Softrite concentration can be simulated with the following linear equation ($R^2=0.99$, p -value<0.01):

$$T_d = 36.1 - 28.2C \quad (5.9)$$

where T_d is the dry tensile strength, N m/g, and

C is the Softrite concentration, percentage.

As discussed in the previous section, in order to retain application sheet strength under wet conditions, wet strength resin must be applied to the sheet. It is shown that Kymene moderately increased dry strength over the applied concentration range. However, it is well recognized that increased strength adversely affects sheet softness [Ampulski et al., 1991]. The results demonstrate that the proper application of debonding

agent could adjust the sheet dry strength to be lower than that of the control, which would contribute to the softness improvement.

The ratio of wet to dry strength was computed for sheets with and without Kymene. In both cases, the ratio response was similar and its value was increased by the Softrite addition. It is shown that the ratio of wet to dry strength was increased by the wet strength resin addition in the previous section. However, the reasons for the ratio increase are different. Kymene significantly increased sheet wet strength and moderately increased its dry strength. For the debonder treated sheet, the dry strength was reduced much more significantly than the wet strength. The mechanisms could also explain the fact that the ratio increase by the debonder was relatively small compared to that by the wet strength resin application.

From the above analysis, it can be demonstrated that the unique properties of wet strength resin and debonder are beneficial in improving sheet wet strength and softness simultaneously. As discussed in Chapter 2, the desired tissue product should have relatively high wet strength, but its dry strength should be low since the tissue softness is adversely affected by high dry strength. The experimental data suggest that the wet strength resin increased the sheet wet strength several times and also enhanced its dry strength, which would have negative impacts on sheet softness property. The application of the debonder significantly decreases the sheet dry strength and is not quite effective to debond at wet conditions. The combined application provides the following benefits: (A)

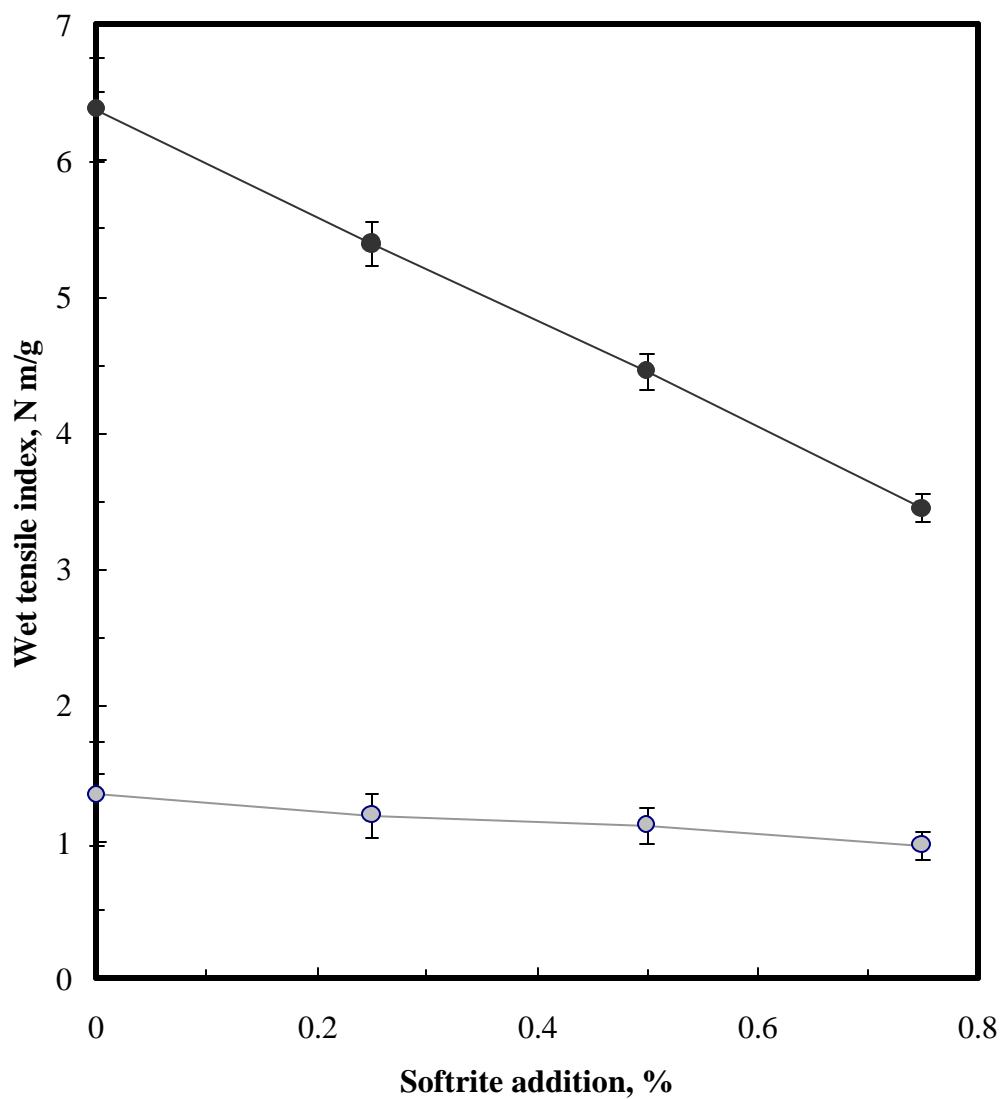


FIGURE 5.18 Effects of combined application of Softrite[®]7516 and Kymene[®]1500 on the sheet wet tensile index. All data points represent the average of 5 measurements, and the error bars are the 91% confidence interval. The solid circle represents for the dual additive application, while the gray circle represents the debonder application alone.

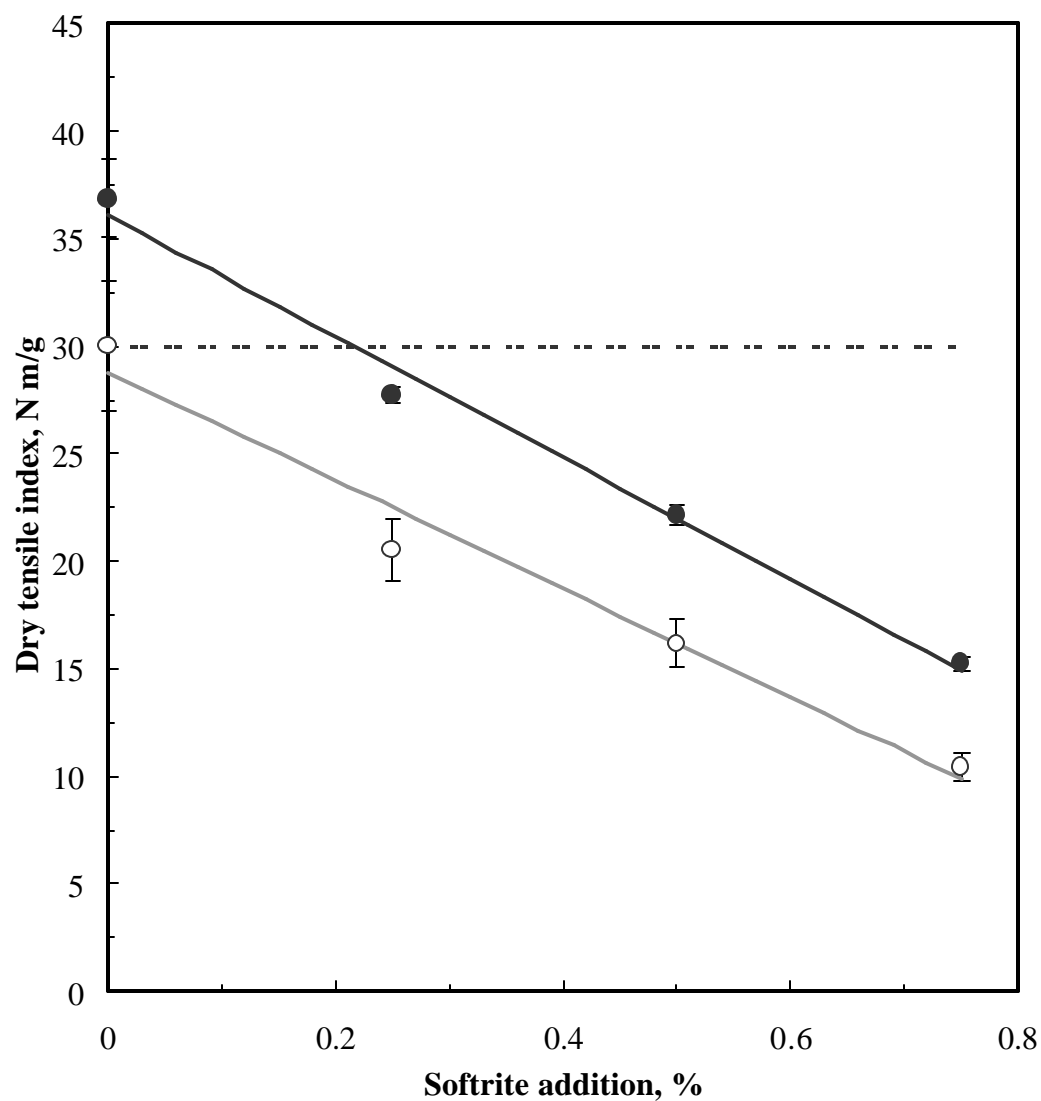


FIGURE 5.19 Effects of combined application of Softrite[®]7516 and Kymene[®]1500 on sheet dry strength. All data points represent the average of 5 measurements, and the error bars are the 91% confidence interval. The solid circle represents for the dual additive application, while the gray circle represents the debonder application alone. The dash line represents the dry strength of the control.

the wet strength is greatly improved compared to that of the control, despite the fact that the debonder reduces a small portion of strength achieved by the wet strength resin application; and (B) the dry strength is reduced to be lower than that of the control. The gain in dry strength from the wet strength resin addition could be offset by the debonder application, and the net result is that the sheet dry strength is reduced, which is necessary for the softness improvement.

5.2.5.3. Stiffness

The effects of the wet strength resin and the debonding agent on sheet stiffness are shown in Figure 5.20. In addition, the figure also shows the effects of the debonder alone on sheet stiffness. Figure 5.20 shows that Softrite reduced Handle-O-Meter stiffness for both cases. The difference was that at same debonder level, the sheet treated with Kymene had higher stiffness. As pointed out in the previous section, the stiffness increase was caused by more intimate fiber contacts within the sheet. The results illustrate that although sheet stiffness was increased by wet strength resin application, the dual chemical application can still be controlled to favor softness improvement by adjusting the debonder dosage.

5.2.5.4. Bulk

The effects of the wet strength resin and the debonding agent on sheet bulk are shown in Figure 5.21. The effects of Softrite on sheet bulk were similar for sheets with Kymene

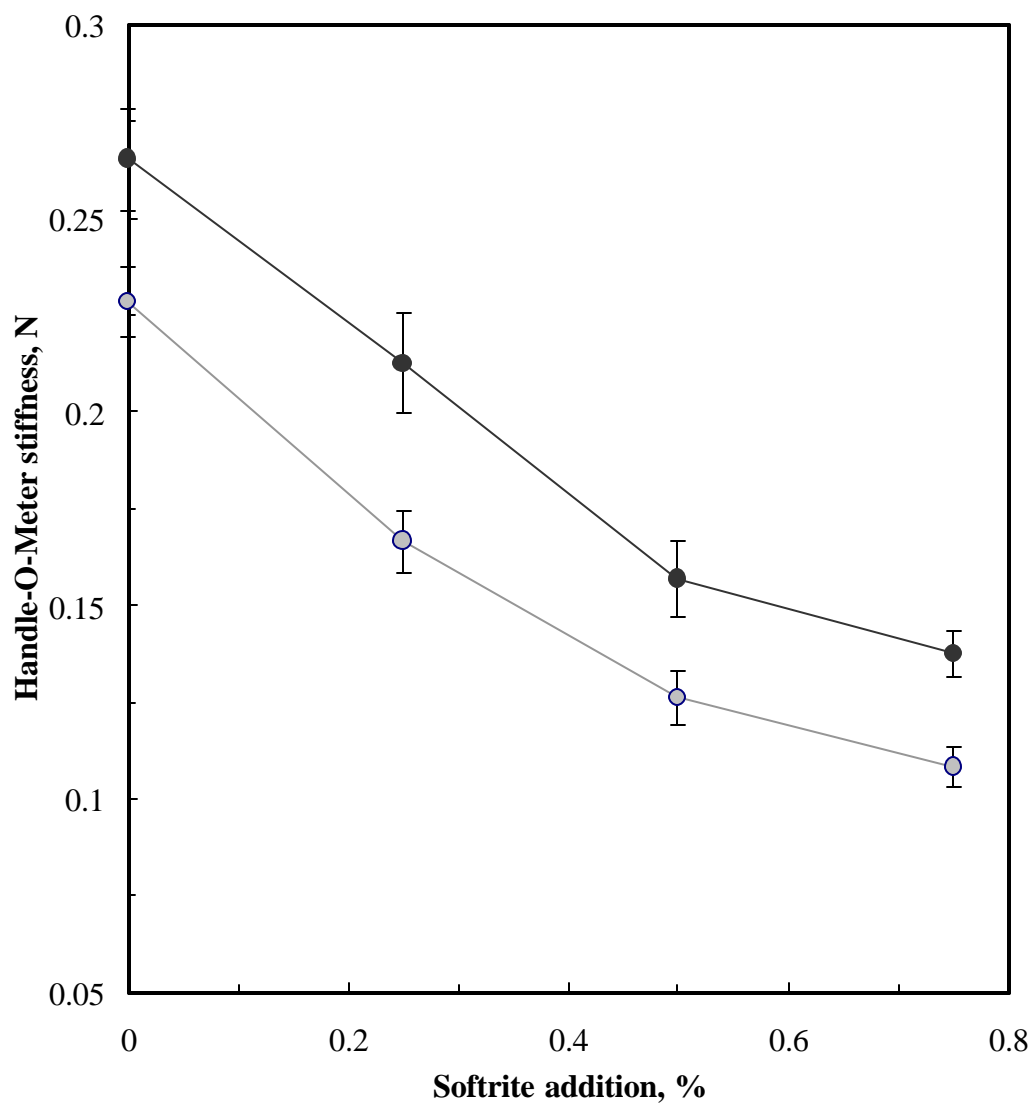


FIGURE 5.20 Effects of combined application of Sofrite[®]7516 and Kymene[®]1500 on sheet Handle-O-Meter stiffness. All data points represent the average of 5 measurements, and the error bars are the 91% confidence interval. The solid circle represents for the dual additive application, while the gray circle represents the debonder application alone.

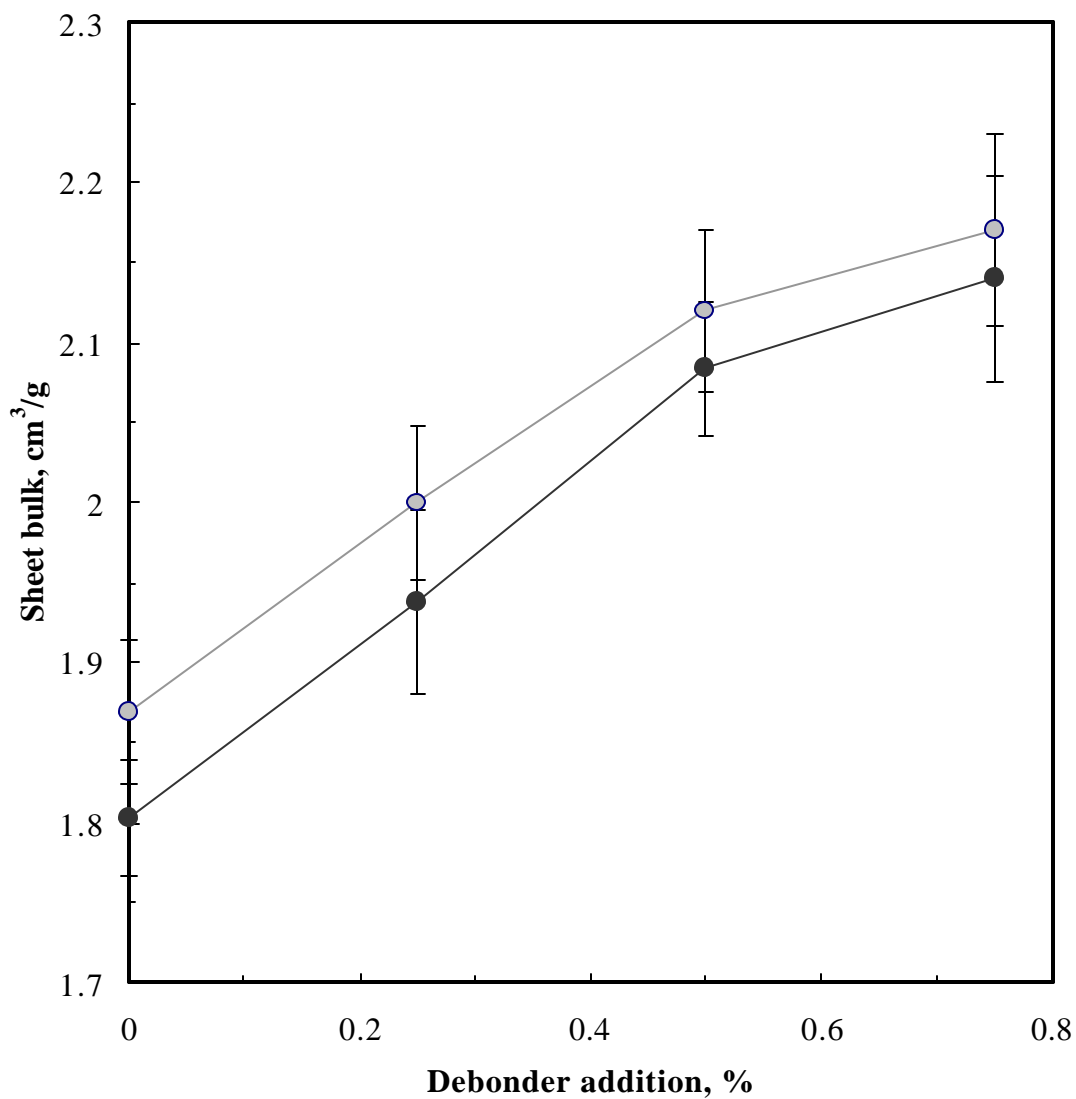


FIGURE 5.21 Effects of combined application of Softrite[®]7516 and Kymene[®]1500 on sheet bulk. The measurement pressure of the electronic bulk tester was 0.687 kPa. All the data points represent the average of 5 measurements, and the error bars are the 91% confidence interval. The solid circle represents for the dual additive application, while the gray circle represents the debondor application alone.

treatment and those without. At both conditions, the dependence of sheet bulk on Softrite concentration was similar. At the same debonder addition level, the sheet treated with wet strength resin seemed to have lower bulk, but the difference was not significant statistically (p -value>0.1).

5.2.5.5. Total water absorbency (TWA)

Figure 5.22 shows the effects of combined application of Kymene and Softrite on sheet TWA. The figure demonstrates that for the dual additive application, the response of total water absorbency to Softrite addition followed a similar trend to that without Kymene. The sheet absorbency decreased with an increasing addition of debonder and the water absorbency of dual additive treated sheet was about 1 gH₂O/gfiber lower than that without Kymene treatment.

The water absorbency was different from other sheet properties in terms of its response to the chemical addition. For properties, such as tensile and stiffness, the dual chemical addition was able to improve the properties over those of control. However, the absorbency was negatively affected by the combined chemical application. The decrease of sheet absorbency capacity could be explained by the fact that both wet strength resin and debonding agent caused the decrease of TWA. The wet strength resin reacts with the carboxyl groups on the fiber surface, and the protective polymeric network formed in the curing process was around or in the inter-fiber bonding area, which retards the loosening of the bonds by water and restrains the cellulose swelling. The reduction of sheet water

absorbency by debonder is due to a different mechanism. The long fatty alkyl groups of the debonding agent have little attraction to each other. Consequently, the surface tension of water is effectively reduced. Since it is the surface tension that causes water to be drawn into the crevices of the fiber interior, the water absorbency is lowered by the addition of the debonding agent [Clark, 1985].

As pointed out in Chapter 1, for certain tissue grades, the water absorbency property is regarded more important than softness. In order for the wet strength resin to be effective, the polymer network must protect the fiber bonding area against the water. The ideal wet strength resin should have the following features: (A) when wet, the fiber structure retains as much strength as possible; and (B) the reduction in the sheet water absorbency is kept as low as possible. The two features represent a pair of conflicts, and the development of new wet strength resin needs to provide a compromise between the two considerations, which is out of the scope of this thesis. To address the issue of decreased sheet water absorbency, alternate approaches to this problem have to be taken. One alternative is to make structural modifications on the debonding agent, which will be presented in Chapter 6.

5.2.5.6. Softness

The effects of the wet strength resin and the debonding agent on sheet softness are shown in Figure 5.23. The effects of the debonder on sheet softness are also shown in the same figure. The addition of 0.25 percent wet strength resin led to the decrease of

reduced softness from one of the control to 0.78. However, it is demonstrated that sheet softness improvement was made possible by the addition of Softrite.

For the Kymene treated sheets, the application of Softrite at all levels significantly increased its reduced softness values ($p\text{-value} < 0.01$). With the addition of 0.25 percent Softrite, the sheet softness was increased to 1.1, which was 10 percent higher than that of the control. At the 0.5 and 0.75 percent addition levels, the sheet softness was increased to 1.5 and 2.3, respectively. The results demonstrate the feasibility of simultaneously improving the sheet wet strength and softness by a combined application of the wet strength resin and the debonding agent.

5.2.5.7. Summary

The advantages of combined chemical application are that the advantages of individual chemical application can be preserved, and the disadvantages of single additive application are overcome at the same time. The experimental data suggested that the application of wet strength resin alone increased the sheet stiffness and strength properties. In comparison, the application of dual additives led to lower sheet dry strength and stiffness.

(A) The advantages of the wet strength resin were kept in the process, and the disadvantages of the debonder were overcome. The application of debonder alone produces weaker sheet and made the sheet lose its practical function under wet

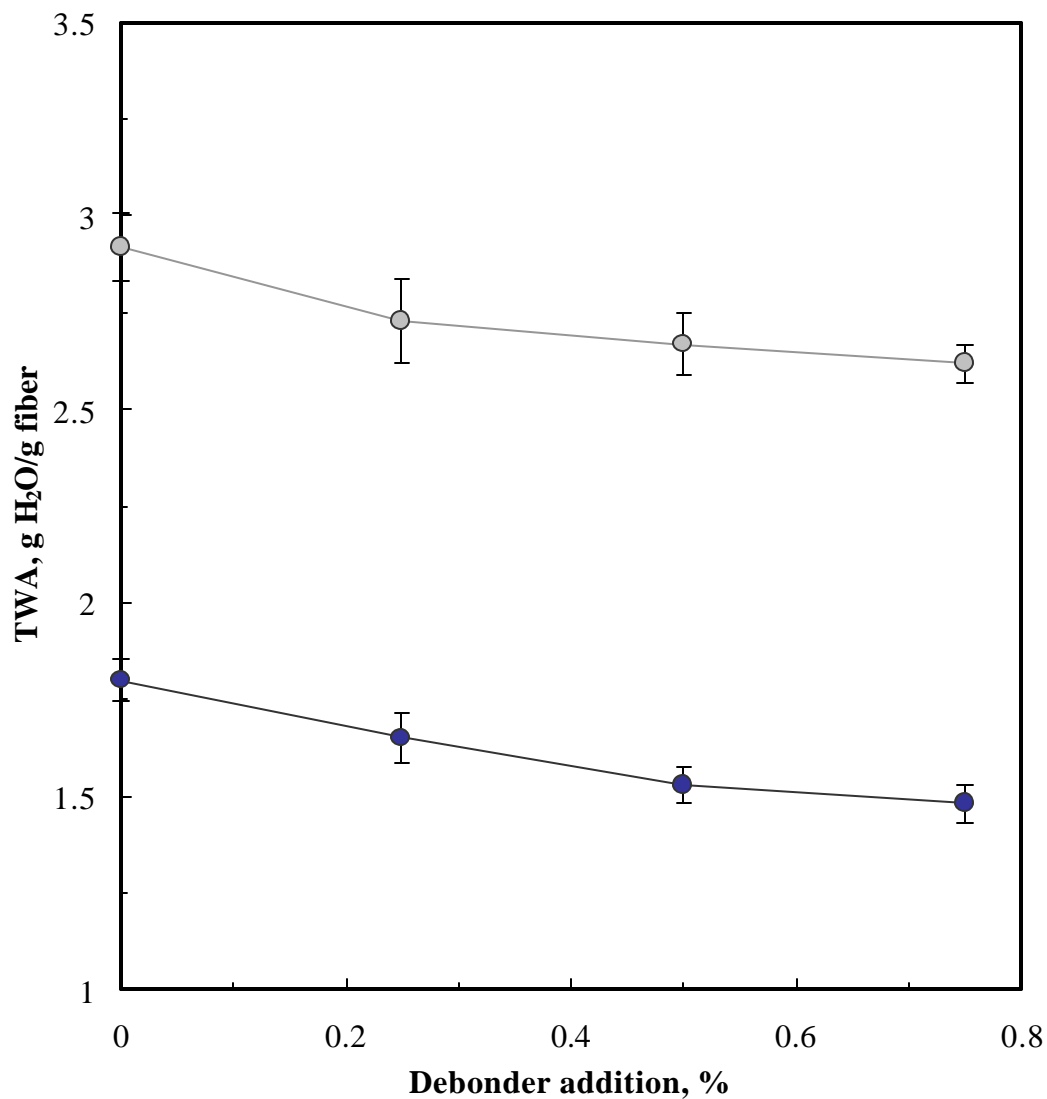


FIGURE 5.22 Effects of combined application of Softrite[®]7516 and Kymene[®]1500 on sheet water absorbency. All data points represent the average of 3 samples, and the error bars are the 76% confidence interval. For each measurement, a 7.62 cm by 7.62 cm square sample from handsheet was used. The solid circle represents for the dual additive application, while the gray circle represents the debonder application alone.

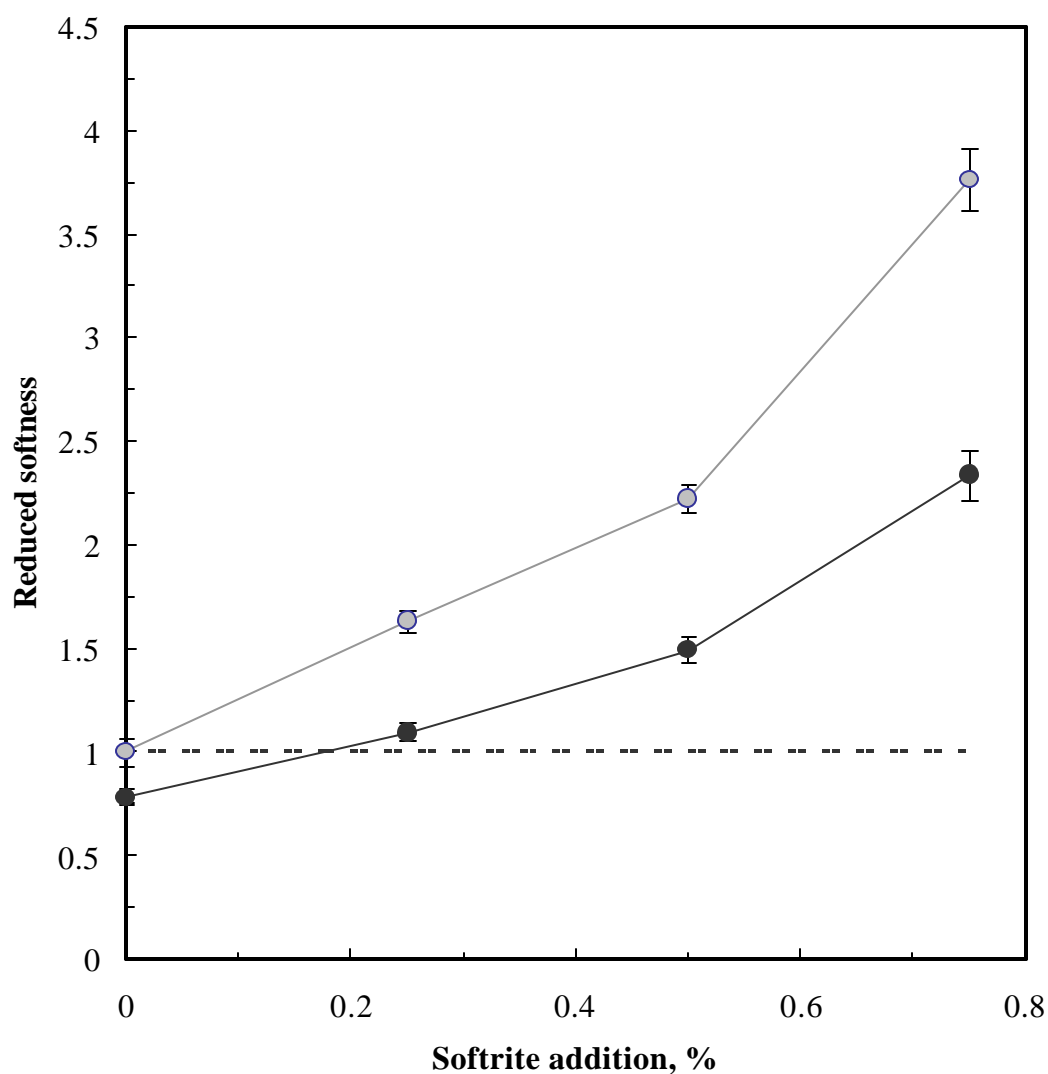


FIGURE 5.23 Effects of combined application of Softrite[®]7516 and Kymene[®]1500 on sheet reduced softness. All the data points represent the average of 5 calculations, and the error bars are the 91% confidence interval. The solid circle represents for the dual additive application, while the gray circle represents the debonder application alone. The dashed line represents the reduced softness of the control.

conditions. Although part of wet strength was lost due to the debonder, the combined application significantly improved sheet wet strength so that the sheet could keep its integrity and function when wet.

(B) The advantages of the debonding agent were kept in the process, and the disadvantages of the wet strength resin were overcome. The sheet gained increase in dry strength, which negatively affects sheet softness. The sheet treated with dual chemical application was shown to have significant improvement in its reduced softness values over control.

(C) The overall benefits for the dual additive application include that the sheet not only functions as wet strength paper, but also has lowered stiffness, increased bulk and improved softness.

The disadvantage of dual chemical application is the decreased sheet water absorbency. To address the issue of reduced water absorbency, one method that can at least partly solve the problem is to develop promising debonding agents by the structural modifications. This method will be discussed extensively in Chapter 6.

5.3. Conclusions

Comprehensive study has been performed on the effects of Kymene[®]1500 and Softrite[®]7516 on various sheet properties. The sheet physical properties considered include wet and dry tensile index, Handle-O-Meter stiffness, bulk, water absorbency and

softness. The results suggest that the application of dual chemical additives is able to combine the advantages of individual additive and produce sheet with high wet strength, low dry strength, low stiffness and high softness. The investigation represents the first reported study on the quantitative effects of combined application of the wet strength resin and the debonding agent on sheet properties. It is shown that the sheet properties can be properly designed by adjusting the addition of the chemical additives. The need to improve the decreased water absorbency property has been addressed. It should provide the researchers in the field with more understanding on mechanisms of the chemical functions and can also serve as a guide for the practical tissue manufacturing.

5.4. References

- Ampulski, R. S., W. U. Spendel, A. H. Sawdai and B. Weinstein, Methods for the measurement of the mechanical properties of tissue paper, *Proceedings of 1991 TAPPI International Paper Physics Conference*, TAPPI Press, Atlanta, GA Vol. 1: 19-30 (1991)
- Bates, N.A., Polyamide-epichlorohydrin wet strength resin, II: a study of mechanism of wet-strength development in paper, *TAPPI Journal*, vol. **52**, no.6: 1162-1168 (1969)
- Carr, C., and P. Knight, How to be objective about softness, *Pulp & Paper Europe* vol. **2**, no. 6: 32-35 (1997)
- Chan, L.L., and P.W.K. Lau, *Wet Strength Resin and Their Application*, TAPPI Press, Atlanta, GA, 3 (1994)
- Clark, J. A., *Pulp Technology and Treatment for Paper*, 2nd edition, Miller Freeman Publications, San Francisco, CA, 1985.

Fredholm, B., Samuelsson, B., Wesfelt, A., and Westfelt, L., Chemistry of paper wet-strength (7) Effect of model polymers on wet-strength, water absorbency, and dry strength, *Cellulose Chem. and Technol.*, vol. **17**, no.3: 279-296 (1983)

Hollmark, H., Evaluation of tissue paper softness, *TAPPI Journal*, vol.**66**, no.2: 97-99, (1983)

Hollmark, H., H. Andersson and R. W. Perkins, Mechanical properties of low density sheets, *TAPPI Journal*, vol.61, No.9, 69-72 (1978)

Liu, J. and J. Hsieh, Interactions of wet strength resin and debonders in tissue manufacturing, *Irving Tissue Inc. Quarterly Technical Conference*, Philadelphia, PA, February 1998.

Liu, J., and J. S. Hsieh, Characterization of facial tissue softness, *TAPPI Journal*, submitted (2001)

Page, D. H., A theory for the tensile strength of paper, *TAPPI Journal*, vol.**52**, no.4: 674-681 (1969)

Phan, D. V., P.D. Trokhan, R.G. Laughlin and T. Trinh, *U.S. Patent 5,543,067*: Waterless self-emulsifiable biodegradable chemical softening composition useful in fibrous cellulosic materials, Aug.6, 1996.

Phan, D. V. and P. D. Trokhan, *U.S. Patent 5,698,076*: Tissue Paper Containing a Vegetable Oil Based Quaternary Ammonium Compound, December 16, 1997.

Poffenberger, C., Yvonne Deac and William Zeman, Novel hydrophilic softeners for tissue and towel applications, *Proceeding of 2000 TAPPI Papermakers Conference and Trade fair*, vol.**1**, 85-93 (2000)

Trokhan, P. D., *U. S. Patent 4,191,609*: Soft absorbent imprinted paper sheet and method of manufacture thereof, March 4, 1980.

Trokhan, P. D. and D. V. Phan, *U.S. Patent 5,575,891*: Soft tissue paper containing oil and a polyhydroxy compound, Nov. 19, 1996.

CHAPTER VI

EFFECTS OF NEW DEBONDING AGENTS ON SHEET PROPERTIES

6.1. Introduction

In Chapter 5, the effects of a wet strength resin, Kymene[®] 1500, and a traditional debonder, Softrite[®] 7516, on various sheet properties were examined. It was shown that the sheet softness was significantly increased by the application of a debonding agent. Additional benefits included increased bulk, reduced stiffness and dry tensile strength. The combined application of wet strength resin and debonding agent was shown to be able to simultaneously improve sheet softness and wet strength property. Although the application of a traditional debonding agent improved many sheet properties for tissue application, it adversely affected the water absorbency.

For certain grades of tissue, water absorbency is the property with the highest priority for the customer [Poffenberger et al., 2000]. In addition to reduced absorbency, traditional debonding agents are not easily biodegradable and can cause environmental problems. Facing increasingly strict environmental regulations, the industry is gradually shifting its debonder consumption to the quaternary ammonium compound with ester

functionality [Phan et al., 1993, 1994, 1995, 1996]. The ester type debonder can be easily degraded into the fatty acids, which are readily biodegradable. The ideal debonding agent should have the following characteristics: (A) it is able to reduce sheet dry tensile strength and improve tissue softness; (B) negative effects on water absorbency are minimized; and (C) the debonder must be environmentally benign.

One approach to overcome the disadvantages of traditional debonding agents is to modify their molecular structure. Recently, a new class of fatty ester quaternary ammonium debonding agent has been developed [Poffenberger et al., 2000]. The new class of debonder contains ester functionality to improve the biodegradability and polyoxyethylene chains to improve the hydrophilicity. The debonder is the esterification product of the ethoxylated primary amine of beef tallow by different fatty acids, such as beef tallow or hydrogenated palm oil. The synthesis of the debonder is illustrated in Figures 6.1 (A), (B) and (C). The new class of debonders is claimed to be environmentally benign and have the balance between water absorbency and debonding functions. Given the continued need for product improvement of premium tissue products and increasingly strict environmental regulations, the future market for the new class of debonders is promising. Despite the promise, to date, there is very little information available on the effects of the new class of debonders on sheet properties. To enhance the capability of designing debonders according to their function requirements, the understanding of the design parameter effects is a must. This chapter addresses the research need on this important topic.

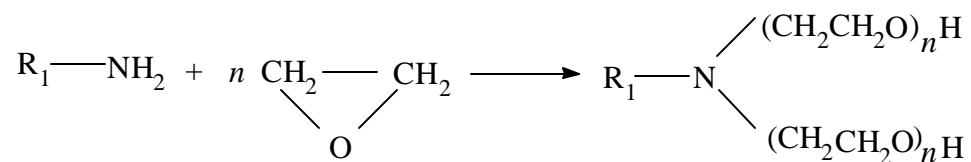


Figure 6.1 (A)

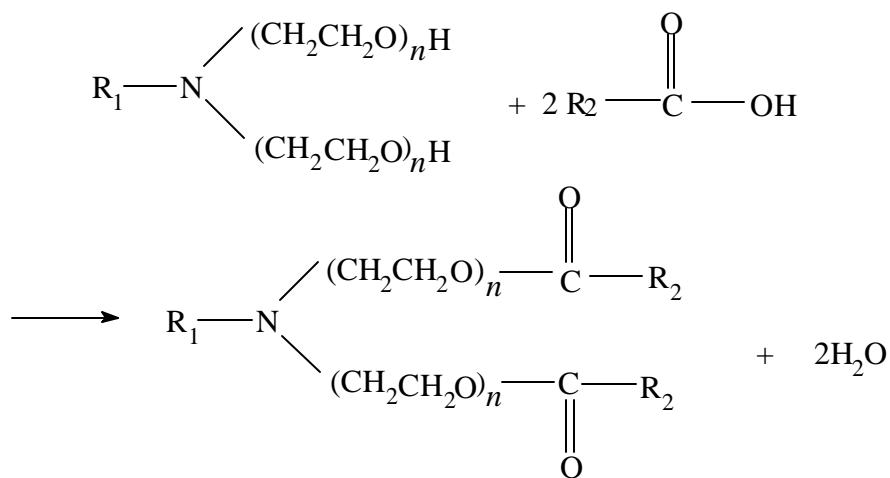


Figure 6.1 (B)

FIGURES 6.1 (A) and (B) The first two steps in synthesizing the new class of debonding agent: (A) The reaction of a primary fatty amine with ethylene oxide produces the intermediate; (B) the product of the step A reacts with fatty acid through estification to produce the diester. R₁ is beef tallow, and R₂ is beef tallow or hydrogenated palm oil.

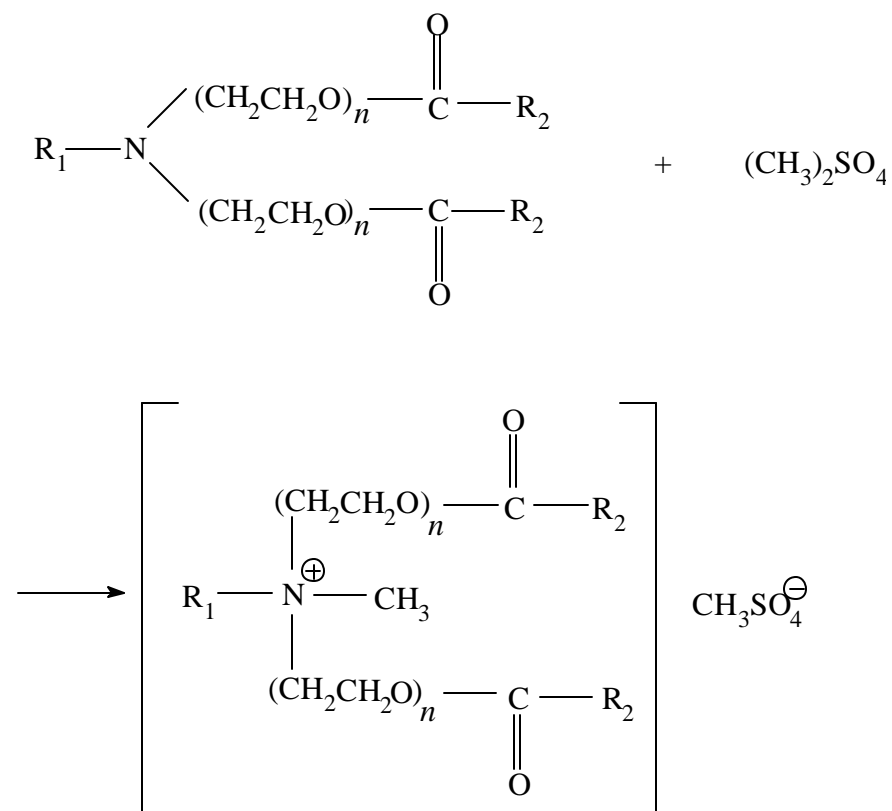


Figure 6.1 (C) The last step of preparation of the new class of debonding agent. The diester is quaternized with the dimethyl sulfate to form a quaternary ammonium salt of the amine ethoxylate ester. R₁ is beef tallow, and R₂ is beef tallow or hydrogenated palm oil.

6.2. Results

6.2.1. Effects of fatty acid on debonder's function

The tallow and palm stearine diesters⁵ (Goldschmidt Chemical Corp., Dublin, Ohio) were used to study the effect of fatty acid on the debonder's function. The degree of ethoxylation for both chemicals was selected to be 15. The pulp for making handsheets was the blend of 65 percent bleached hardwood kraft (BHK) and 35 percent bleached softwood kraft (BSK). Two debonder addition levels were applied at 0.25 and 0.5 percent. The stock pH was adjusted to 7.5 ± 0.1 and the experiments were performed at 20°C. In the following section, effects of fatty acids on various sheet properties will be presented.

6.2.1.1. Total water absorbency (TWA)

Figure 6.2 shows the effects of fatty acid in the debonder on the sheet TWA property. As the figure indicates, the application of both palm stearine and tallow diesters increased the water absorbency at both addition levels. The results of Chapter 5 showed that the absorbency capacity of control was 2.92 gH₂O/g fiber. The data indicate that the application of both debonders significantly improved sheet water absorbency at the

⁵ Tallow diester: diester di (tallowyl-oxy-ethyl) tallow methyl ammonium methylsulfate. Palm stearine diester: diester di (C16-18 and C18-unsaturated alkyl-oxy-ethyl) tallow methyl ammonium methylsulfate.

addition levels and that the absorbency increased with increasing debonder concentration (p -value<0.01). The experiment results demonstrate that effects of the debonders with polyoxyethylene chains on absorbency are remarkable since the traditional debonder tends to reduce the water absorbency. In order to compare the effectiveness of a debonder from different fatty acids, t -tests were performed over the data and the conclusion was that the sheet absorbency treated with tallow diester was higher than that of stearine diester treated sheet (p -value<0.01). This study shows that the introduction of polyoxyethylene chains in fatty acid diesters could effectively enhance water absorbency. The oxyethylene units improved debonder's hydrophilicity and the water absorbency decrease by traditional cationic debonders was avoided.

6.2.1.2. Strength

Figure 6.3 illustrates the effects of fatty acid in the debonder structure on sheet tensile strength. It is shown that the sheet dry strength was greatly reduced by the application of debonding agents. At 0.25% addition level of palm stearine diester, the tensile was reduced to 21.4 Nm/g, a 28.7 percent decrease from 30 Nm/g of the control. Higher application levels of palm stearine diester reduced the sheet strength further down to 17.4 Nm/g, which was a 42 percent tensile reduction from that of control. The strength reduction was determined statistically significant through the use of linear regression (p -value<0.01). For the tallow diester, the sheet strength reduction versus the chemical addition gave a regression slope that was also statistically significant (p -value<0.01). A t -

test was used and it was found that the tensile strength of the tallow diester treated sheets was statistically higher than those of palm stearine diester treated sheets (p -value<0.02 for 0.25 percent addition level, and p -value<0.05 for 0.5 percent level). The data showed that the diesters of both fatty acids could be used to effectively reduce sheet tensile strength and that tallow diester treated sheets exhibited statistically higher strength than those treated with palm stearine diester.

6.2.1.3. Bulk

Figure 6.4 shows the effects of fatty acid in the debonder structure on sheet bulk. It suggests that both palm stearine and tallow diesters slightly increased sheet bulk. For palm stearine diester, a 0.25 percent application improved the sheet bulk from 1.87 cm³/g of the control to 1.91cm³/g, which represented a 2.1 percent increase. At a 0.5 percent palm stearine addition level, the sheet bulk was further improved to 1.95 cm³/g, a 4.3 percent increase. For the tallow diester application, the sheet bulk increased with the increasing diester concentration. At the 0.25 and 0.5 percent application levels, the sheet bulk was increased to 1.90 and 1.92 cm³/g, respectively. The bulk data suggests that the sheets treated with palm stearine diester seemed to have higher bulk than those treated with tallow diester at the 0.5 percent level (p -value<0.1).

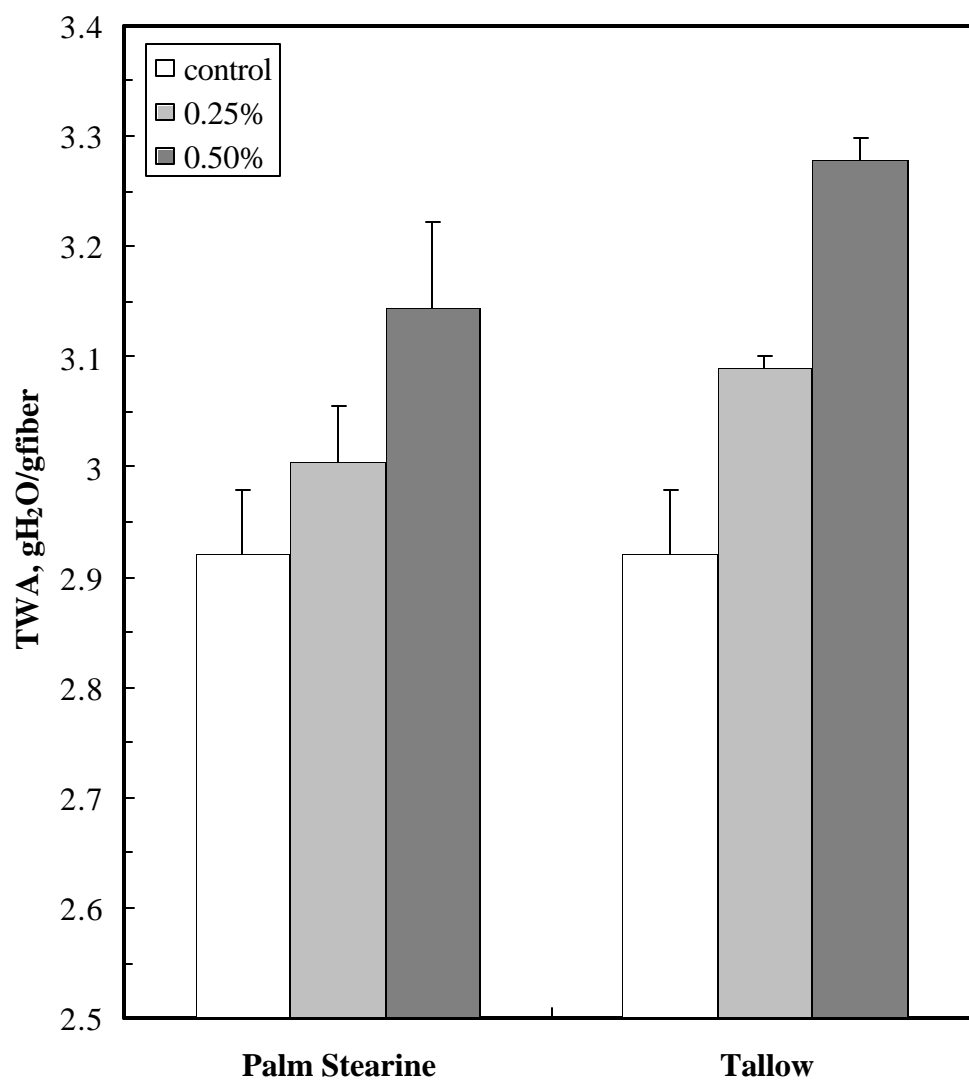


FIGURE 6.2 Effects of fatty acid on the sheet TWA (total water absorbency) property. All data points represent the average of three samples, and the error bars are the 76% confidence interval. For each experiment, a sample of 7.62 cm by 7.62 cm from handsheet was used.

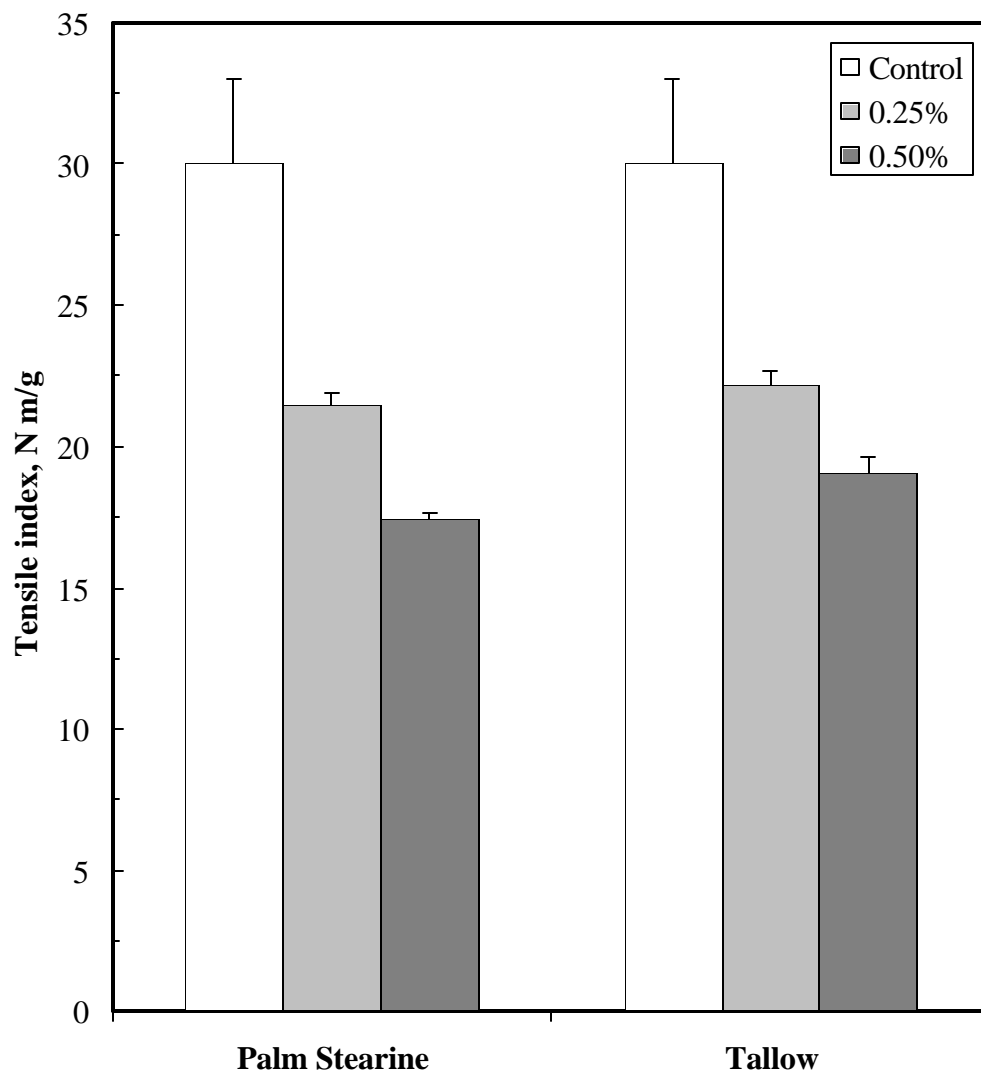


FIGURE 6.3 Effects of fatty acid in the debonder structure on the tensile strength of sheet. All data points represent the average of three measurements, and the error bars are the 76% confidence interval.

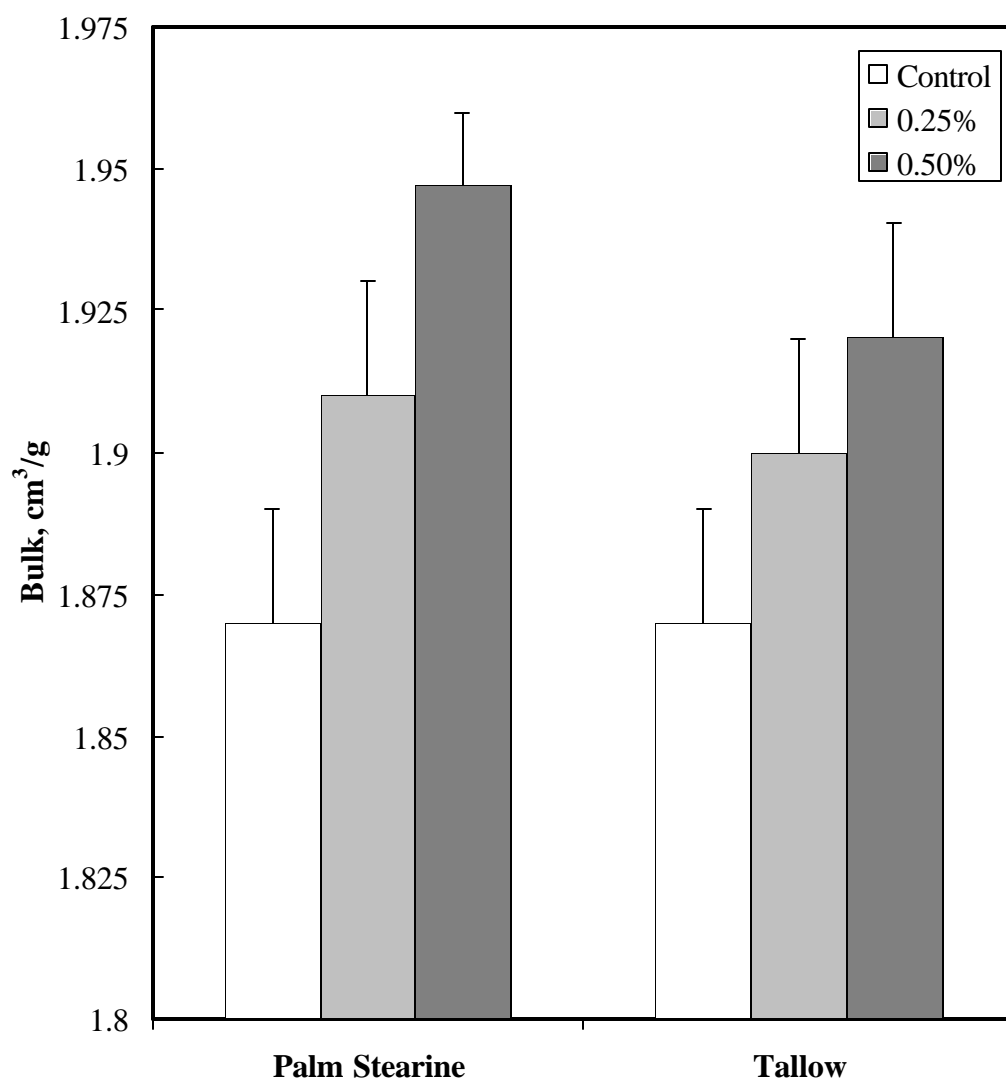


FIGURE 6.4 Effects of fatty acid in the softener structure on the sheet bulk. All data points represent the average of three measurements, and the error bars are the 76% confidence interval. The measurement pressure of the electronic bulk tester was 0.687 kPa.

6.2.1.4. Stiffness

Figure 6.5 demonstrates the effects of fatty acid in the debonder structure on sheet Handle-O-Meter stiffness. The figure indicates that the application of palm stearine and tallow diesters greatly reduced sheet Handle-O-Meter stiffness. For palm stearine diester, the stiffness was reduced to 0.18 N at the 0.25 percent level, which represented a 28 percent decrease from 0.25 N of control. The sheet stiffness was further reduced to 0.146 N when the concentration was increased to 0.5 percent. The statistical significance of sheet stiffness reduction by palm stearine diester was confirmed by linear regression (p -value <0.01).

For the tallow diester treated sheet, its stiffness was reduced to 0.19 N and 0.16 N at the 0.25 and 0.5 percent levels, respectively. Similarly, the significance of stiffness reduction by tallow diester was determined by regression (p -value <0.01). In order to compare the effectiveness of stiffness reduction by the diesters, t-test was used to determine whether stiffness values were significantly different at same diester level. At 0.25 percent, sheet treated with palm stearine diester showed statistically higher stiffness reduction than that with tallow diester treatment (p -value <0.05). A similar conclusion was also drawn at the 0.5 percent application level (p -value <0.01).

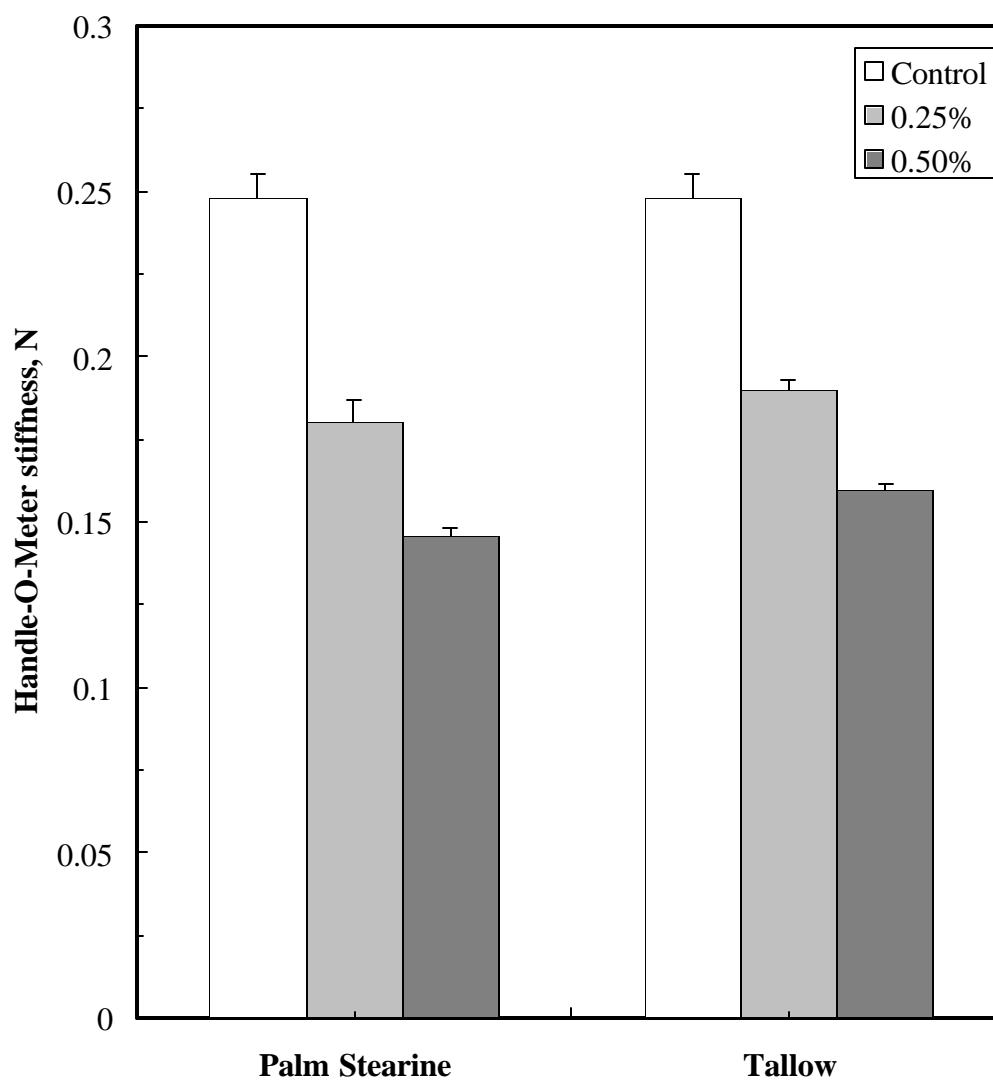


FIGURE 6.5 Effects of fatty acid in the debonder on the sheet Handle-O-Meter stiffness. All data points represent the average of three measurements, and the error bars are the 76% confidence interval.

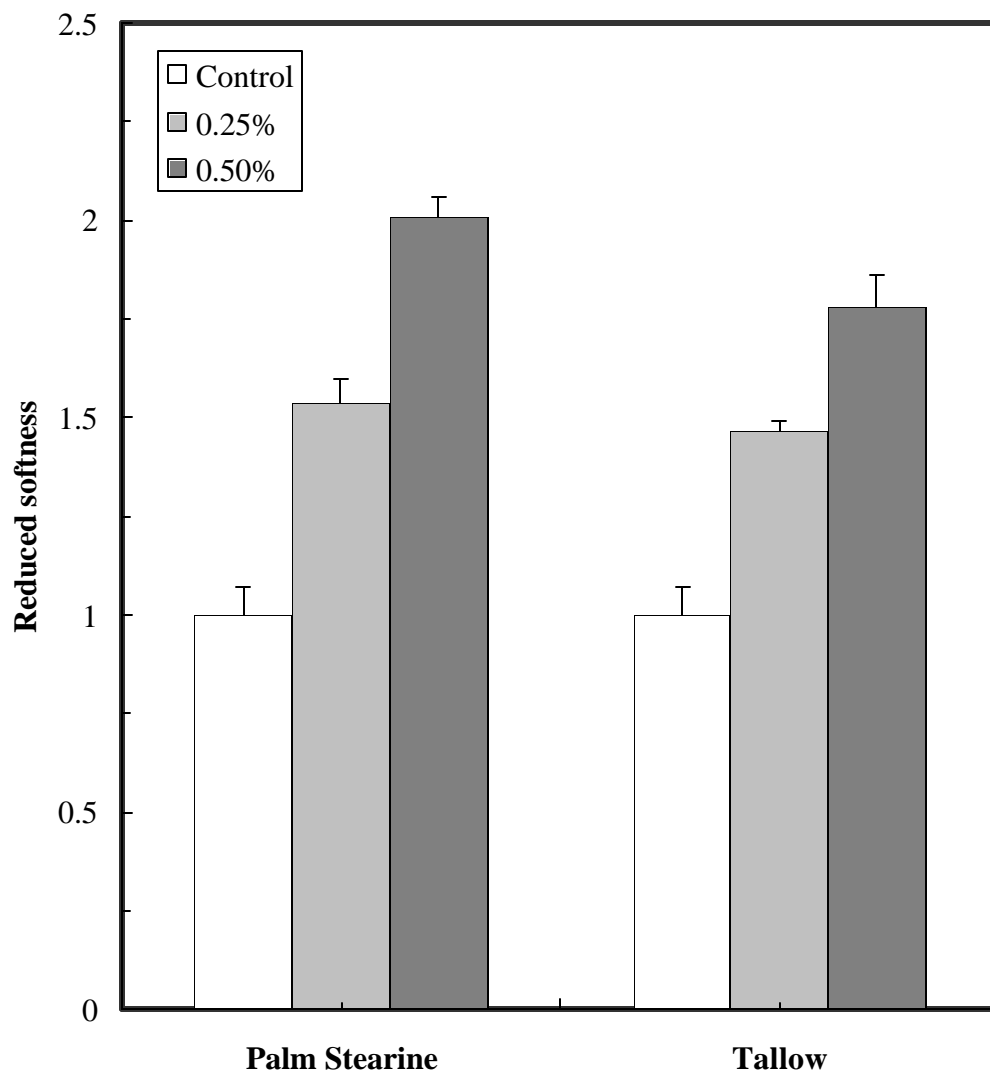


FIGURE 6.6 Effects of fatty acid in the debonder on sheet reduced softness. All data points represent the average of three calculations, and the error bars are the 76% confidence interval.

6.2.1.5. Reduced softness

The effects of fatty acid in the debonder on sheet reduced softness are shown in Figure 6.6. As discussed in Chapter 5, reduced softness can facilitate interpretation of sheet physical properties and give quantitative predictions on handsheet softness. According to the definition, the reduced softness of control is one. Figure 6.6 indicates that both diesters greatly improved sheet reduced softness. For palm stearine diester, at the 0.25 percent level, the reduced softness was improved to 1.54 from one of control. The application of 0.5 percent palm stearine diester resulted in a reduced softness of 2.01. The softness increase by palm stearine diester was determined to be significant by regression (p -value<0.01). A similar trend was observed for the tallow diester-treated sheets and the significance of softness improvement was confirmed (p -value<0.01). It needs to be pointed out that the two diesters did not improve sheet softness to the same extent. The t -test results showed that at both the 0.25 and 0.5 percent application levels, reduced softness values of palm stearine diester-treated sheets were higher than those of tallow diester-treated sheets (p -value<0.01).

6.2.2. Effects of degree of ethoxylation on debonder's function

Tallow diesters were synthesized with different degrees of ethoxylation (Goldschmidt Chemical Corp., Dublin, Ohio) and were used to study the effects of ethoxylation on the function of debonder. In this portion of the experiment, the fatty acid was chosen to be tallow. The pulp stock for making handsheets was the blend of 65

percent bleached hardwood kraft (BHK) and 35 percent bleached softwood kraft (BSK). Two debonder addition levels were applied at 0.25 and 0.5 percent. The stock pH was adjusted to 7.5 ± 0.1 and the experiments were performed at 20°C . In the following section, effects of degree of ethoxylation on various sheet properties will be presented.

6.2.2.1. Total water absorbency (TWA)

Figure 6.7 shows the effects of degree of ethoxylation on sheet water absorbency. The figure clearly indicates that the water absorbency was improved by the application of debonders with polyoxyethylene chains. The water absorbency of the control was $2.92 \text{ gH}_2\text{O/g fiber}$. At the degree of ethoxylation of 10, the TWA of the sheet treated with 0.25 percent tallow diester remained the value of the control ($p\text{-value} < 0.01$). At 0.5 percent application level, the sheet TWA was improved and the statistical analysis showed that the absorbency increase was significant ($p\text{-value} < 0.01$). As the number of oxyethylene unit increased to 15, the sheet absorbency was increased at all the debonder addition levels as discussed in the previous section. The effects of the degree of ethoxylation of the debonder were investigated by comparing the absorbency data at the two levels of the ethoxylation. The t-test result suggests that the debonder with higher degree of ethoxylation ($n = 15$) produces sheets with higher absorbency ($p\text{-value} < 0.01$).

6.2.2.2. Strength

Besides water absorbency, the debonder must be capable of effectively modifying sheet tensile strength. Figure 6.8 shows the effects of debonder ethoxylation on sheet tensile strength. It suggests that at the application levels, the debonders with ethoxylation greatly reduced sheet tensile strength. At the degree of ethoxylation of 10, the dry tensile index was reduced to 20.8 Nm/g at the 0.25 percent level from 30 Nm/g of control. The sheet dry tensile was further reduced to 16.8 Nm/g at 0.5 percent level. Linear regression was performed and the significance of strength reduction by the debonder application was confirmed (p -value<0.01). When the degree of ethoxylation was increased to 15, the sheet tensile strength was reduced to a lesser degree (p -value<0.01). The results suggest that the ethoxylated debonder was effective in reducing sheet strength and that increasing degree of ethoxylation seemed to lead to less strength reduction.

6.2.2.3. Bulk

Figure 6.9 shows the effects of the degree of ethoxylation of debonder on sheet bulk. The figure indicates that the debonders at both degrees of ethoxylation increased sheet bulk. The bulk of the control was 1.87 cm³/g. At the degree of ethoxylation of 10, the sheet bulk treated with 0.25 percent debonder was increased to 1.95 cm³/g, which was determined to be statistically significant (p -value<0.01). Further increase of the debonder dosage only slightly improved the sheet bulk and the increase was not significant. In the previous section, the effects of the debonder ($n=15$) on sheet absorbency were discussed.

Comparison of bulk data for n at 10 and 15 showed that the debonder with a lower degree of ethoxylation produced a sheet with higher bulk (p -value<0.01).

6.2.2.4. Stiffness

Figure 6.10 illustrates the effects of degree of ethoxylation on sheet Handle-O-Meter stiffness. The figure shows that the application of debonders with exothylation significantly reduced sheet stiffness. At the degree of ethoxylation of 10, the stiffness of a sheet treated with 0.25 percent debonder was reduced to 0.174 N, which was a 30.4 percent decrease. The stiffness was further reduced to 0.142 N at 0.5 percent level. The stiffness decrease was determined to be statistically significant by regression (p -value<0.01). As the ethoxylation degree was increased to 15, the sheet stiffness was reduced to 0.19 N and 0.16 N at 0.25 and 0.5 percent, respectively. Comparing the stiffness at 0.25 percent application showed that the stiffness of the sheet treated by the debonder with two ethoxylation degrees was not statistically different (p -value>0.1). However, at the 0.5 percent level, the stiffness of the sheet treated by tallow diester with an ethoxylation degree of 15 was higher than that of the sheet treated by the diester with an ethoxylation degree of 10 (p -value<0.01).

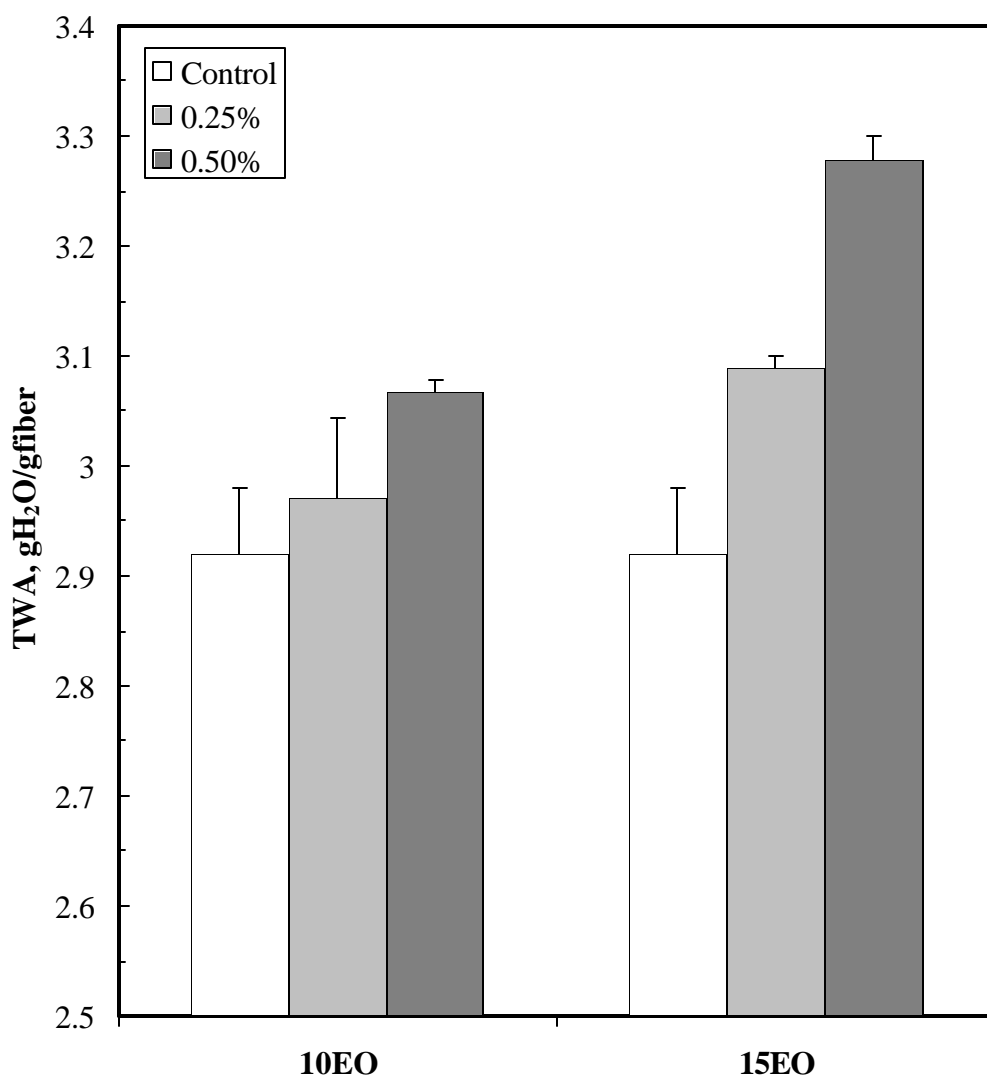


FIGURE 6.7 Effects of degree of ethoxylation of debonder on sheet total water absorbency property. All data points represent the average of three samples, and the error bars are the 76% confidence interval. For each experiment, a sample of 7.62 cm by 7.62 cm squared from the handsheet was used.

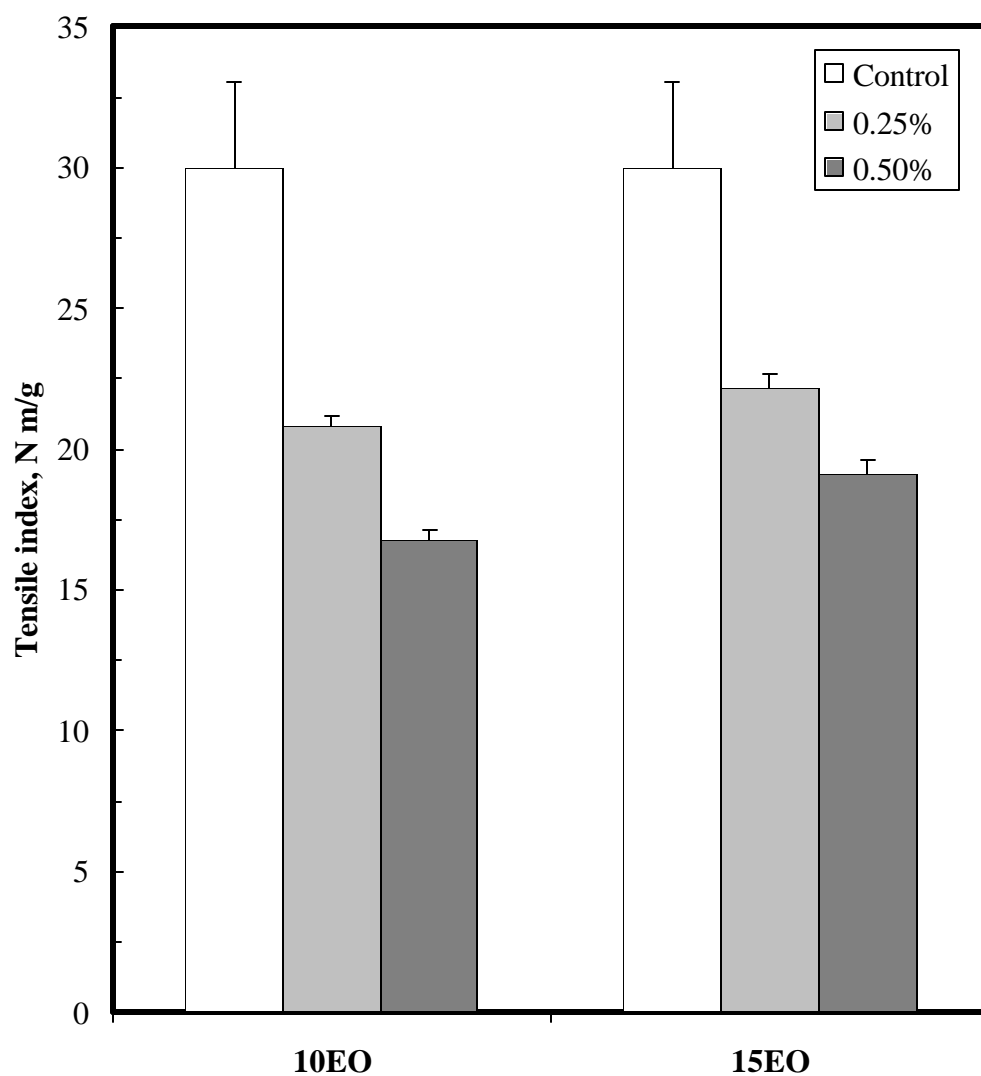


FIGURE 6.8 Effects of degree of ethoxylation of debonder on sheet tensile strength. All data points represent the average of three measurements, and the error bars are the 76% confidence interval.

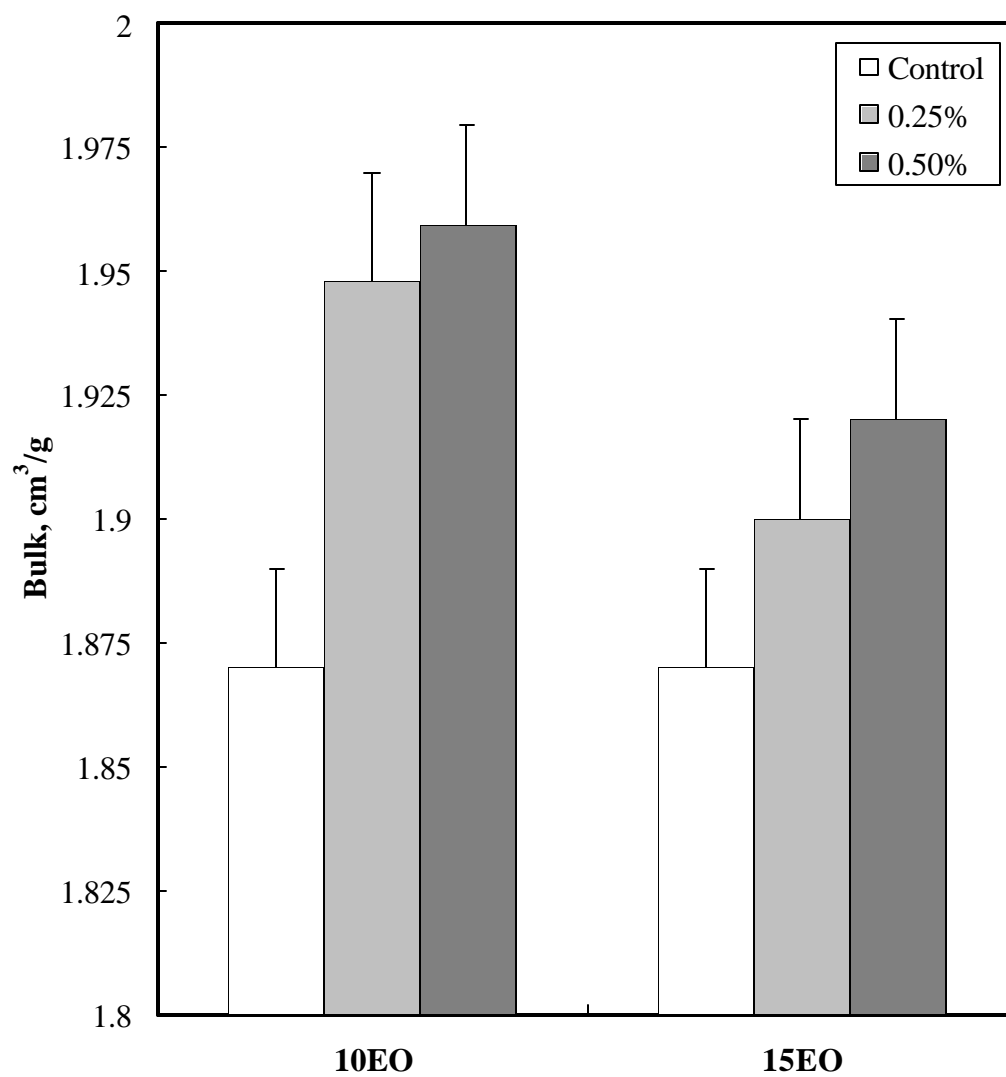


FIGURE 6.9 Effects of degree of ethoxylation of debonder on the sheet bulk. All data points represent the average of three measurements and the error bars are the 76% confidence interval. The measurement pressure of the electronic bulk tester was 0.687 kPa.

6.2.2.5. Reduced softness

The effects of the degree of ethoxylation on reduced softness are shown in Figure 6.11. As discussed before, reduced softness was developed to characterize the handsheet softness change by various technologies. For tallow diester with the degree of ethoxylation of 10, the increase of sheet softness was determined to be significant by regression and t-test (p -value <0.01). When the degree of ethoxylation was increased to 15, the reduced softness was increased to 1.47 at the 0.25 percent application level, and was further increased to 1.78 at the application level of 0.5 percent. The statistical significance of softness increase at an ethoxylation degree of 15 was also validated (p -value <0.01). In order to compare the effectiveness of softness improvement by tallow diesters with different ethoxylations, a t-test was performed. The results suggested that softness values were statistically higher for the sheets treated with tallow diester with an ethoxylation degree of 10 (p -value <0.01). In addition, a “handfeel” test was performed and confirmed that the handsheets treated with the diesters had higher softness compared to that of the control.

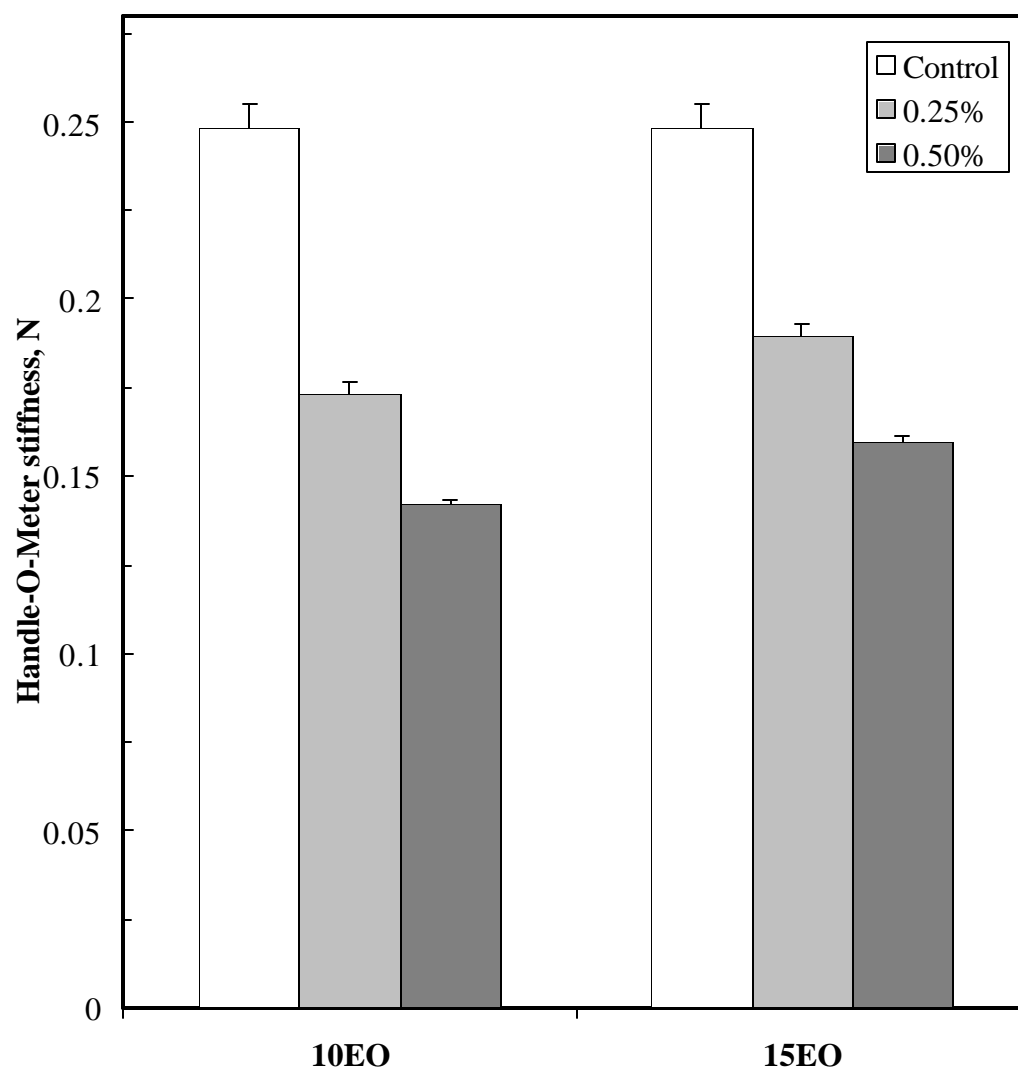


FIGURE 6.10 Effects of degree of ethoxylation on the sheet Handle-O-Meter stiffness. All data points represent the average of three measurements, and the error bars are the 76% confidence interval.

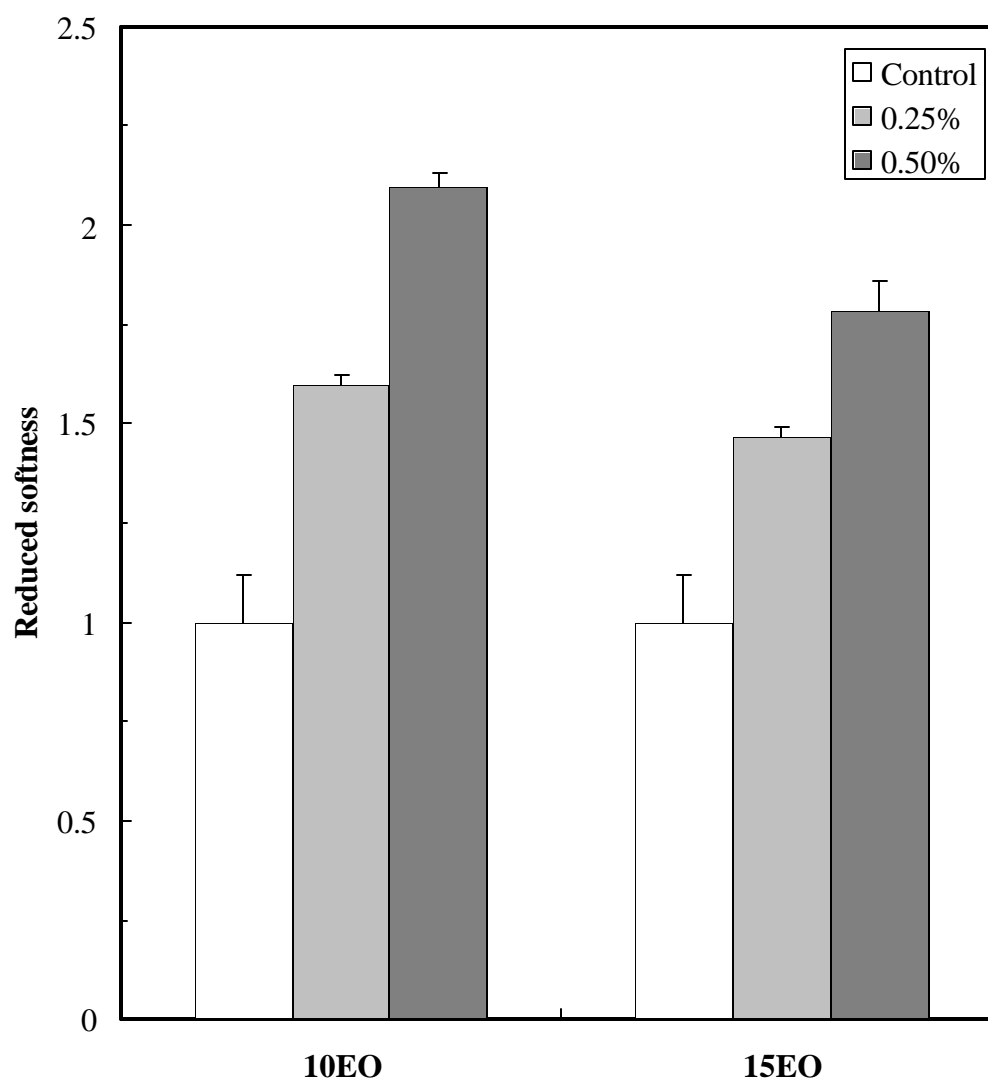


FIGURE 6.11 Effects of degree of ethoxylation of debonder on the sheet reduced softness. All data points represent the average of three calculations, and the error bars are the 76% confidence interval.

6.3. Discussion

In summary, a series of experiments were conducted to provide an understanding of the effects of design parameters of debonders: two levels of fatty acids, two levels of the degree of ethoxylation, and three levels of concentration. In previous sections, the effects of fatty acids and the degree of ethoxylation were discussed. To summarize the effects of the variables on the debonder's function, an analysis of variance was performed using the General Linear Model from Minitab[®]. The ANOVA results for sheet absorbency are included in Table 6.1 and the results for other properties are provided in Tables 6.2-6.5.

The results show that the debonder concentration played the most significant role in affecting all sheet properties. The highest concentration level used in the study was 0.5 percent, which corresponded to the upper limit in practical application [Conte et al., 1992]. It is not surprising to see that various sheet properties were significantly changed. Among the three factors, the second most significant factor in changing sheet properties was the degree of ethoxylation. From Tables 6.1 to 6.5, the sheet property changes due to the debonder ethoxylation are all shown to be significant (p -value <0.001). In contrast, the fatty acid factor only statistically changed some sheet properties. This is in agreement with the conclusion of Berg [Berg, 1985], which states that the differences in surfactant properties are generally more responsive to the hydrophile than to the hydrophobe type. The introduction of the polyoxyethylene chain to the softener may add another mechanism for its adsorption on the pulp fiber surface. It is pointed out that surfactants

containing a polyoxyethylene chain could be adsorbed onto the substrate with groups such as OH and COOH by hydrogen bonding [Rosen, 1989]. Due to the mechanisms of electro-static adsorption and hydrogen bonding, the adsorption of the synthesized debonders is expected to be fast, which is confirmed by the previous experimental study [Poffenberger et al., 2000]. The polyoxyethylene chain is thought to take the form of a coil in the aqueous phase and its cross sectional area increases with the number of C_2H_4O (EO) units in the debonder [Schick, 1962]. The strong interaction between the polyoxyethylene and water has been also confirmed by experimental work [Courval, et al., 1983] and theoretical calculations [Kambe et al., 1983]. Theoretically, the hydration of the ether oxygen atoms by hydrogen bonding should result in binding two moles of water per mole of C_2H_4O group. However, the hydration numbers are generally found to be 2-4 [Foster et al., 1982; Nilsson et al., 1983]. Various experimental evidences support the proposal that water molecules are either physically bound or entrapped by the polyoxyethylene chains [Attwood, 1968; El Eini et al., 1976; Elworthy et al., 1962; Muller et al, 1969, 1971].

One fact that contributes to the sheet absorbency increase is the hydration of the polyoxyethylene chain. However, the hydration alone could not account for all the increase in absorbency. To illustrate this point, the case of the 0.5 percent debonder application is considered. If the hydration number is assumed to be 4, the hydrated water on the EO chains will be less than 0.12 gH₂O/g fiber, far less than the increase in absorbency. Another factor that helps the absorbency improvement may be that the

surface tension reduction is less for the cationics with polyoxyethylene chains. As the length of the polyoxyethylene chain increases, the effectiveness of the surfactant surface tension reduction decreases [Rosen, 1989]. There is a trade-off between debonding ability and absorbency. It is shown from the data that when the number of EO units increased, the debonder's ability in strength reduction was decreased. Despite the decrease, the new debonders were shown to debond effectively and significantly improve sheet softness. In summary, the debonder with ethoxylation is shown to be effective in maintaining hydrophilicity and balancing its debonding capabilities.

The effects of the hydrophobic group on sheet properties were not as significant as those of ethoxylation. Tallow and palm oil are natural fatty acids and are mainly comprised of different percentages of various saturated C16-C18 and unsaturated C18 fatty acids [Woollatt, 1985]. Table 6.6 compares the typical compositions of beef tallow and palm oil. The mole averaged carbon numbers for beef tallow and palm oil are calculated to be about the same, 17.1. Palm stearine refers to the hydrogenated palm oil with the Iodine Value (IV) less than 6, while the beef tallow has an IV about 50 [Poffenberger, 2001; Zeman, 2001]. Since Iodine value is an indicator of the average degree of unsaturation of a fatty material, palm stearine is obviously more saturated than tallow. The experimental results show that the sheets treated with palm stearine have lower strength than tallow treated sheets, which is in agreement with previous studies [Rosen, 1989]. Although statistically significant, sheet strength differences were small.

TABLE 6.1 ANOVA results for sheet water absorbency property

| Source | DF ⁶ | F ⁷ | P ⁸ |
|---------------|-----------------|----------------|---------------------|
| Fatty acid | 1 | 13.16 | 0.002 |
| Degree of EO | 1 | 43.92 | $<5 \times 10^{-4}$ |
| Concentration | 2 | 93.36 | $<5 \times 10^{-4}$ |

TABLE 6.2 ANOVA results for sheet tensile strength

| Source | DF | F | P |
|---------------|----|--------|---------------------|
| Fatty acid | 1 | 3.51 | 0.079 |
| Degree of EO | 1 | 23.63 | $<5 \times 10^{-4}$ |
| Concentration | 2 | 171.80 | $<5 \times 10^{-4}$ |

⁶ DF is the degree of freedom.

⁷ F is the F variance statistic (F ratio).

⁸ P is the significance level from the multivariate F-test.

TABLE 6.3 ANOVA results for sheet bulk

| Source | DF | F | P |
|---------------|----|-------|-------|
| Fatty acid | 1 | 2.99 | 0.103 |
| Degree of EO | 1 | 16.53 | 0.001 |
| Concentration | 2 | 12.23 | 0.001 |

TABLE 6.4 ANOVA results for sheet stiffness

| Source | DF | F | P |
|---------------|----|--------|---------------------|
| Fatty acid | 1 | 5.67 | 0.030 |
| Degree of EO | 1 | 16.63 | 0.001 |
| Concentration | 2 | 391.53 | $<5 \times 10^{-4}$ |

TABLE 6.5 ANOVA results for sheet reduced softness

| Source | DF | F | P |
|---------------|----|--------|---------------------|
| Fatty acid | 1 | 10.95 | 0.004 |
| Degree of EO | 1 | 82.22 | $<5 \times 10^{-4}$ |
| Concentration | 2 | 199.38 | $<5 \times 10^{-4}$ |

Table 6.6 Typical compositions of beef tallow and palm oil [Woollatt, 1985].

| Saturated acids ^a | | | Unsaturated acids | | |
|------------------------------|-------------------|----------------------|--------------------------|-------------------|----------------------|
| | Palm oil Wt. % | Beef tallow Wt. % | | Palm oil Wt. % | Beef tallow Wt. % |
| C ₁₂ | ----- | 1 | Oleic ^b | 40 | 42 |
| C ₁₄ | 1 | 5 | Linoleic ^c | 10 | 3 |
| C ₁₆ | 44 | 27 | Palmitoleic ^d | ----- | 5 |
| C ₁₈ | 5 | 16 | ---- | ----- | ----- |
| C ₂₀ and above | ----- | 1 | ---- | ----- | ----- |

^a For saturated fatty acid, C_{n+1} is C_nH_{2n+1}-COOH

^b C₁₇H₃₃COOH (one double bond)

^c C₁₇H₃₁COOH (two double bonds)

^d C₁₅H₂₉COOH (one double bond)

The debonder containing tallow is found to produce a more absorbent sheet than that of palm stearine, which could be explained by higher effectiveness of surface tension reduction by the palm containing debonder. The data in this study suggest that the animal oil based (tallow) debonder can be substituted by vegetable oil based (palm) cationics in the regions where the application of tallow is a sensitive issue due to cultural or religious reasons. In addition, the tissue made with a vegetable oil based softener is claimed to have improved odor compared to tissue made with animal oil based debonding agent [Phan et al., 1994].

6.4. Conclusions

The effects of a new class of debonder with polyoxyethylene chains on sheet properties were investigated. The new type of debonder has two distinct features: (1) ester functionality, which makes the softener readily biodegradable; and (2) polyoxyethylene chains, which help to overcome the absorbency loss caused by traditional cationics. Two key debonder design parameters, i.e., ethoxylation degree and type of fatty acids, are illustrated to change various sheet properties. The degree of ethoxylation is demonstrated to play a critical role in improving sheet absorbency while maintaining the debonding capability of the softener. The higher the content of the polyoxyethylene chain, the greater the sheet absorbency increase can be achieved. The change in the hydrophobic groups is found to have small impacts on the ability of

cationics to de-bond, but the softener with more saturated hydrophobic groups (vegetable oil based) is less favorable for the absorbency. The flexibility introduced by incorporating the polyoxyethylene chain into the debonder structure allows promising commercial application in the regions where the use of animal oil based softener is restricted.

6.5. References

Attwood, D., A light-scattering study of the effect of temperature on the micellar Size and shape of a nonionic detergent in aqueous solution, *J. Phys. Chem.* **72**, 339 (1968)

Berg, J. C., Chapter V: The role of surfactants, in *Absorbency* (edited by P. K. Chatterjee), 149-195, Elsevier Science Publishers B.V., Amsterdam, the Netherlands (1985)

Conte, J.S. and G. W. Bender, Chapter 13: Softening and Debonding Agents, in *Chemical processing Aids in Papermaking: A practical Guide*, TAPPI Press, Atlanta, GA (1992)

Courval, G. J., and D. G. Gray, Gas chromatographic evaluation of thermodynamic interaction parameters for the water-poly(ethylene Oxide) system, *Polymer* **24**: 323 (1983)

El Eini, D. I. D., B. W. Barry and C. T. Rhodes, Micellar size, shape, and hydration of long-chain polyoxyethylene nonionic surfactants, *J. Coll. Interf. Sci.* **54**, 348 (1976)

Elworthy, P. H., and C. B. Macfarlane, *J. Chem. Soc.* 537 (1962)

Foster, K. R., B. R. Epstein, P. C. Jenin and R. A. Mackay, Dielectric studies on nonionic microemulsions, *J. Coll. Interf. Sci.* **88**, 233 (1982)

Kambe, Y. and C. Honda, Dynamic light scattering from aqueous solutions of poly(ethylene oxide), *Polymer Commun.* **24**: 208 (1983)

Muller N. and T. W. Johnson, Investigation of micelle structure by Fluorine Magnetic Resonance. III. Effect of organic additives on sodium 12,12,12-Trifluorododecyl sulfate solutions, *J. Phys. Chem.* **73**, 2042 (1969)

Muller N., and H. Simsohn, Investigation of micelle structure by Fluorine Magnetic Resonance V. Sodium Perfluorooctanoate, *J. Phys. Chem.* **75**, 942 (1971)

Nilsson, P. G., and B. Lindman, Water self-diffusion in nonionic surfactant solutions: hydration and obstruction effects, *J. Phys. Chem.* **87**, 4756 (1983)

Phan, Dean V. and Paul D. Trokhan, *U.S. Patent 5,264,082*: Soft absorbent tissue paper containing a biodegradable quaternized amine-ester softening compound and a permanent wet strength resin, November 1993.

Phan, Dean V., Paul D. Trokhan and Toan Trinh, *U.S. Patent 5,312,522*: Paper products containing a biodegradable chemical softening composition, May 1994.

Phan, D. V., Paul D. Trokhan, *United States Patent: 5,405,501*, Multi-layered tissue paper web comprising chemical softening compositions and binder materials and process for making the same, April 11, 1995.

Phan, D. V. and P. D. Trokhan, *U.S. Patent 5,510,000*: Paper products containing a vegetable oil based chemical softening composition, April 23, 1996.

Poffenberger, C., Y. Deac and W. Zeman, Novel hydrophilic softeners for tissue and towel applications, *Proceedings of 2000 TAPPI Papermaker Conference*, vol. **1**, 85-93 (2000)

Poffenberger, C., personal communication (2001)

Rosen, M. J., Chapter 5: Reduction of surface and interfacial tension by surfactants, *Surfactants and interfacial phenomena*, John Wiley & Sons, Inc. (1989)

Schick, M. J., Surface films of nonionic detergents-1. Surface tension study, *J. Colloid Sci.*, **17**, 801 (1962)

Woollatt, E., *The Manufacture of Soaps, Other Detergents and Glycerine*, Ellis Horwood Limited, Chichester, England, 118-125 (1985)

Zeman, W., personal communication (2001)

CHAPTER VII

CONCLUSIONS AND RECOMMENDATIONS

7.1. Conclusions

This thesis focused on the tissue properties improvement through the application of chemical additives. A softness model based on a power relationship was developed for the conventional facial tissue and showed excellent prediction capability. The softness model not only quantifies tissue softness offline with high precision, but also opens the prospect of on line application empowered by emerging enabling technologies. From the softness characterization of commercial tissue, a softness model was derived for the handsheet, which facilitated the interpretation of handsheet physical properties in the laboratory.

An experimental apparatus was developed so that the kinetic data of chemical additive adsorption onto the cellulose fibers could be collected real-time. The experimental setup represents the very first development in the field. The adsorption of a wet strength resin, Kyemene[®]1500 and a debonding agent, Softrite[®]7516, on cellulose fiber was studied and the adsorption mechanisms proposed. At the 0.6 percent fiber

consistency, the adsorption of Softrite[®]7516 on the fiber was fast and complete within 2 minutes. The rate-limiting step in the whole adsorption process seemed to be diffusion through the boundary layer. Kymene[®]1500's adsorption could be divided into two stages; the first, rapid stage of adsorption corresponded to the electrostatics-favored situation and the rate-limiting stage was the diffusion through the boundary layer, while the slower adsorption at the second stage might be the result of disfavored electrostatic repulsion. Kymene's adsorption was not complete at long time and could be simulated by the format of a reversible adsorption. The simultaneous competitive adsorption was also studied, and it showed that the adsorbed amount of each additive was reduced in the presence of a competing species. At higher fiber consistencies, the individual and the competitive adsorption of the two additives were much faster and more complete than at lower consistencies.

The study shows that the sheet properties can be properly designed by chemical modification. The effects of Kymene[®]1500 and Softrite[®]7516 on various sheet properties were studied and a better understanding of chemical application was provided. The addition of Kymene[®]1500 significantly improved sheet wet strength, but made the sheet more stiff and less water absorbent. The softness was also negatively affected by the application of the wet strength resin. Softrite[®]7516 reduced a high percentage of the sheet dry tensile strength and stiffness and increased the sheet bulk. The sheet softness was improved by the addition of a debonding agent. The data suggest that the application of dual chemical additives can combine the advantages of individual additives and produce

sheets with high wet strength, low dry strength, low stiffness and high softness. The disadvantage is that the sheet TWA property is negatively affected.

To address the need of improving sheet absorbency, a new class of debonding agents with ester functionality was designed and applied to the sheet. The effects of the two design parameters, i.e., fatty acid and degree of ethoxylation, on sheet properties were investigated. The palm stearine based debonder produced sheets with slightly less water absorbency capacity and lower tensile strength and stiffness than those of the tallow based debonder. The investigation of the effects of ethoxylation degree for the tallow based debonder shows that the debonder with the higher degree of ethoxylation produced sheets with higher absorbency, but the increase in the sheet absorbency was achieved at the expense of less strength reduction and sheet softness improvement.

7.2. Recommendations

The thesis has systematically studied the tissue property improvement through chemical additive treatment and provides valuable information for researchers in the field. The following recommendations are given so that a better understanding of the additive effects on tissue making can be achieved and the results can be more readily applied to the commercial production.

The softness models for other tissue grades are needed. The model should still assume the power form but it may involve different physical properties and have different

exponents. The softness models developed for the conventional facial tissue need to be tested on the manufacturing site. Ideally, the physical properties involved in the model can be measured on line; therefore, tissue softness can be monitored in real-time. The promising technologies, such as acoustical and optical methods, need to be further explored so that the on-line facial tissue softness monitoring can be realized in the future. Because the softness model is tissue grade sensitive, different sets of studies need to be performed on other grades, such as bath tissue and paper towels, although the methodology is similar to this investigation. In this study, a convenient softness model derived from commercial tissue had been directly applied to quantify handsheet softness. Therefore, the validity of the reduced softness needs to be tested. A whole different set of standard samples has to be made, and the softness scores need to be obtained from the panelist. A softness model that is specific to handsheets may need to be developed.

This study designed the instrumentation for the study of adsorption kinetics of chemical additives onto cellulose fibers. The method is proved to be fast and accurate in the chemical analysis, and its limitation is that it could not handle the system with consistency higher than 0.6 percent. Therefore, other nontraditional alternatives should be explored so that the adsorption study under higher consistency can be easily performed.

In the laboratory, the efficiency of making handsheets is quite low and labor intensive. The M/K automatic sheet former can greatly reduce the time in producing sheets and improve the experiment efficiency. Although the general steps of making the handsheets and automatic sheets are similar, different instrument setups of the two

systems will lead to sheets with different properties. The comparison needs to be made for sheets made by different systems. To better simulate the tissue making system, which is close to complete closure, the water used in the sheet making process need to be collected and recycled. Effective methods need to be established to analyze the chemical concentrations in the white water. Under different degrees of water closure, the effects of chemical additives on sheet properties tend to be different. With little information available, the study in this area is of great value to the paper industry, which is striving to meet increasingly strict environmental regulations. To address this issue, the automatic sheet former must be used since the experiment would be extremely tedious if performed simply on the TAPPI sheet mold.

Though valuable in providing quantitative information, the sheets by the TAPPI handsheet mold and the M/K automatic sheet former are fundamentally different from the commercial tissue, because they do not have directionality. Pilot tissue machines must be constructed and utilized to introduce sheet directionality and generate results more relevant to the manufacturing. In addition, the tissue machine needs to have the capabilities of performing “Creping” and “Through-Air-Drying”, so that the physical properties of sheets made by the pilot machine can better represent those produced commercially. The effects of the chemical additives in the more complex system will enable researchers to have more realistic predictions for the commercial application of paper additives.

APPENDIX A

CHARACTERIZATION OF TISSUE SOFTNESS

A1. Fundamentals of physiology of human tactile sensory response

In this part, the fundamentals of the physiology of the human tactile sensory response are reviewed. Although the physiology of human sensory responses seems to provide little direct applicable information to the tissue softness characterization, it provides the physiological basis for the understanding of the effects of important tissue physical attributes over softness.

A1.1 Signal conductions of nerve cells

The neuron is the basic unit of the nervous system. In addition to common cellular structures, a neuron has two types of special extensions (processes): dendrites and axons. Dendrites are those that receive and transmit signals inward to the cell body, and axons are those that conduct signals away from the cell. One unique characteristic of nerve cells is that they are electrically excitable. A resting cell is in a state of polarization with the resting membrane potential. Certain types of stimuli can trigger a sequence of changes in the neuron membrane potential (action potential). The action potential of a nerve cell is generated by the sequential opening and closing of sodium and potassium ion channels on the membrane. The action potential represents a transient depolarization process, and the membrane depolarization is conducted passively to an adjacent region on the membrane.

When the polarization of the adjacent region reaches its threshold, it will also generate an action potential. The process repeats until the action potential is propagated to the base of the axon (axon hillock). From there, the action potential (nerve impulse) moves along the axon at a velocity in the order of 100 m/s and without amplitude decrease in the process. The nerve impulse eventually reaches a synapse, which is the junction structure to transmit the signal from one neuron to the next. According to the mechanism of the synaptic signal transmission, the synapse is of either electrical or chemical type.

The electrical synapse allows the ion and small molecules to pass freely from the cytosol of neuron to the next, and provides the transmission without delay. In the chemical synapse, the axon terminal of the pre-synaptic neuron and the dendrite membrane of the post-synaptic neurons are separated by synaptic cleft (a gap of 20-50nm). The electrical signals are first converted into the chemical signals of neurotransmitter in the pre-synaptic neuron. The next two steps are that the neurotransmitter is released and diffuses across the synaptic cleft. Finally, the chemical signals are converted back to electrical signals in the post-synaptic neuron.

A1.2. Temporal and spatial summation

A single action potential from the pre-synaptic neuron can cause the depolarization of the post-synaptic neuron membrane, but usually the depolarization may not be enough to

fire an action potential. For excitatory stimuli, the excitatory post-synaptic potential (EPSP) must build up to reach the threshold of firing an action potential.

The action potential is an all-or-none event, and the neurons produce the action potential with the same value. The intensity of a stimulus is encoded in the fire frequency of the action potential. A single action potential only produces a temporary EPSP. If two action potentials from the pre-synaptic neuron arrive at the post-synaptic neuron in a very short time (or at high frequency), the second EPSP will be added to the first EPSP before it completely fades away. If the frequency in which the action potentials are encoded is high enough, the EPSPs will be summed up over time, and the threshold of the post-synaptic neuron can be reached. This is called the temporal summation.

Another mechanism for the neural signal integration is the spatial summation. As mentioned above, neurons can receive thousands of synaptic inputs from other neurons. In the mechanism of spatial summation, the depolarization effects caused by the individual synaptic input are combined to produce to a large EPSP.

A1.3 Tactile nerve endings

The human skin has specialized nerve endings embedded in it so that the skin can be stimulated in a variety of ways to mediate different sensations. About 95 percent of human skin is covered with hairs, and the rest is hairless (also called glabrous). The glabrous skin can be found on palms, fingers and certain facial areas.

The skin consists of several layers, including the epidermis, dermis and subcutaneous tissue. Two kinds of nerve fiber endings are found in the skin, i.e., free nerve endings and the corpuscular receptors. The free nerve endings are located in the dermal and epidermal layers of the skin and around hair follicles. Three types of corpuscular receptors are commonly described in the literature: (a) Merkel's corpuscles, (b) Meissner's corpuscles and (c) Pacinian corpuscles.

Merkel's corpuscles can be found in almost all areas of human skin, and can sense the tactile stimuli. Merkel's corpuscles consist of a specialized basal epidermal cell and a disk-shaped nerve terminal [Cauna, 1966]. In the glabrous skin, Merkel's corpuscles are found in the papillary ridges where they are sheltered from thermal and painful stimuli, but are sensitive to the mechanical stimulation through the leverage of the overlying epidermis.

Meissner's corpuscles are only contained in the dermis of glabrous skin and responsible for the touch and pressure sensation. Meissner's corpuscles consist of stacks of laminar cells interleaved with nerve endings, and are found to be associated with the papillary ridges. Each Meissner's corpuscle is supplied by two to six nerve fibers, and surrounded by an elastic capsule attached to the epidermis and the dermis.

The Pacinian corpuscles are contained in subcutaneous tissue, which is mainly fatty and vascular. With typical length of 1mm and width of 0.5mm, the Pacinian corpuscles are the largest of the specialized nerve endings [Quilliam, 1966]. The Pacinian corpuscle consists of more than 50 concentric layers of tissue and fluid surrounding its sensory

nerve. The Pacinian corpuscle does not respond to sustained pressure and only fires at the onset or offset of brief tactile stimulus.

A1.4. Mechano-receptive fibers

In the human glabrous skin, four groups of mechano-receptive fibers have been identified: (a) rapidly adapting (RA) fibers; (B) type I, slowly adapting (SA I) fibers; (c) type II, slowly adapting (SA II) fibers; and (d) Pacinian corpuscle (PC) fibers [Johansson et al., 1979]. The Pacinian corpuscle and type II slowly adapting fibers have large receptive fields that lack distinct borders, while the receptive field for the rapidly adapting fibers and type I slowly adapting fibers is smaller and better defined. In addition, these mechano-receptive fibers have different capacities to respond to the vibratory stimuli of specific frequency ranges.

Corresponding to the four mechano-receptive fibers, four information channels, i.e., P, NP I, NP II, and NP III, have been shown to mediate tactile sensation [Bolanowski et al., 1988]. The four information channels have their own physiological substrate: P channel and PC fibers, NP I channel and RA fibers, NP II channel and SA II fibers, and NP III channel and SA I fibers. The channels also have their corresponding receptor: P channel and Pacinian corpuscle, NPI and Meissner corpuscle, NP II and Ruffini cylinder, NP III and Merkel receptor.

The P channel usually operates over the vibratory frequency range of 40-800Hz, and has a “U” shaped threshold-frequency characteristic with a maximum sensitivity near 300

Hz [Verrillo, 1975]. It is observed that increases in both the size and duration of a vibratory stimulus activating the P channel produces decreasing threshold [Craig, 1968]. Therefore, the P channel is capable of both spatial and temporal summation. In addition, the P channel is found to be highly sensitive to changes in the skin-surface temperature [Bolanowski et al., 1988]. The non-Pacinian I (NP I) channel has a typical operating range of vibration frequencies between 10 and 100 Hz [Gescheider et al., 1985] and has a relatively flat response throughout the vibratory frequencies. The NP I channel is not sensitive to the temperature variations, and it does not display temporal or spatial summation. The second non-Pacinian channel, NP II, is shown to operate in the vibratory-frequency range of 15-400 Hz that is similar to that of P channel, but the sensitivity of NP II is much lower [Gescheider et al., 1985]. NP II is temperature sensitive and also capable of temporal summation. The third non-Pacinian channel, NP III, operates in the vibratory frequency range between 0.4 and 100 Hz. The NP III has a similar sensitivity to that of the NP I channel and does not possess spatial summation. NP III is affected by the variation of the skin-surface temperature.

At a particular frequency, the information channel with the lowest threshold usually determines the absolute psychophysical sensitivity. The threshold between 35 and 500 Hz is determined by the P channel [Verrillo, 1968]. The channel NPI has its highest sensitivity in the range of 3-100 Hz. Compared with P channel, the NP I is much less sensitive to the frequencies higher than 35Hz; therefore, it does not actively mediate threshold in this range. The NP II's sensitivity is much less than that of the P channel

though the two channels operate at similar vibratory frequencies. Finally, the NP III operates from very low frequencies to more than 100Hz. It is pointed out that at the relatively low frequencies, e.g., 4.0-35 Hz, more than one channel may be stimulated at the same time, even at threshold-level intensities [Bolanowski et al., 1988]. The reason is that at those frequencies, two or more channels have roughly the same threshold. The complex stimuli, such as pulse and noise, have the broadband spectra and will simultaneously activate more than one channel. Therefore, the full and complete understanding of certain perceptual phenomena demands the consideration of each channel's response individually.

A2. Background

The study of tactile sensation falls into the category of psychophysics. Psychophysics studies the relationships between the perceived constructs and the physical attributes of the external source. The psychophysical laws generalize the relations between the physical and subjective magnitudes of stimuli. Weber's law was discovered by Ernst Weber in the mid-nineteenth century [Luce, 1958]. The law states that the increase in stimulus intensity required to produce a just noticeable difference divided by the stimulus intensity is constant as shown in Equation A2.1

$$\frac{\Delta S}{S} = K \quad (A2.1)$$

where DS is the just noticeable difference,

S is the stimulus intensity, and

K is a constant.

In the 1950's, Stevens developed the power law, which is widely referred and applied [Stevens, 1957]. The Power law states that the psychological magnitude of a stimulus is an exponential function of its physical magnitude:

$$R = KS^n \quad (\text{A2.2})$$

where R is the psychological magnitude of a stimulus,

S is the physical magnitude of a stimulus, and

K and n are constants depending on the nature of the stimulus.

In Table A2.1, the power function exponents from the group-averaged subjective magnitude estimation are listed. The power function implies that equal sensation ratios correspond to equal stimulus ratios.

TABLE A2.1 Power function exponents from the group averaged subjective magnitude estimation [Stevens, 1959].

| Continuum | Exponent | Conditions |
|-------------|----------|------------------------|
| Temperature | 1.0 | Cold on arm |
| Temperature | 1.6 | Warm on arm |
| Loudness | 0.6 | Binaural |
| Loudness | 0.55 | Monaural |
| Vibration | 0.95 | 60 c. p. s. on finger |
| Vibration | 0.6 | 250 c. p. s. on finger |
| Smell | 0.55 | Coffee order |
| Smell | 0.6 | Heptane |
| Duration | 1.1 | White noise |

A3. Experimental

A3.1. Sample selection

19 facial tissue samples were purchased from local market. 14 facial samples made of creping technology were used for the softness model development, and the other 5 samples were used to test the prediction accuracy of the model.

A3.2. Tissue softness ranking

The softness of the labeled tissue sample was evaluated by an experienced panelist using the “direct comparison” method. In this process, two pads of tissue samples were needed; one pad was the standard sample with a known softness score, and the other pad was the tissue sample to be tested. The panelist determined the softness by holding each pad in the palm of the hand with the thumb being pressed down on the sample and simultaneously being moved over the sample surface. With one pad in the left hand and the other in the right hand, the panelist compared the softness sensation with that of standard tissue sample, and a softness score was assigned to the tissue. For each sample, the softness score was the average of the 5 softness evaluations. All the hand feel determinations were made on samples conditioned in TAPPI standard environment.

A3.3. Measurement of tissue physical property

After purchase, the tissue samples were placed in a conditioning room overnight. The room was kept at $50.0\% \pm 2.0\%$ relative humidity and 23.0 ± 1.0 °C (73.4 ± 1.8 ° F) as required by TAPPI standard 402 om-88. The mass of each tissue sample was measured using Ohaus electronic balance (model GT 210, Precision Advanced, Florham Park, New Jersey) before physical testing. Since most physical properties were done on both directions, the machine direction (MD) and cross machine direction (CD) of tissue were identified. The measured tissue physical properties included:

A3.3.1. Tensile

For each tissue sample, 10 test specimens in both machine direction and cross machine direction were cut with the width of 25.4 ± 1 mm (1.00 ± 0.04 in.). The length of the strips was no more than 180 mm. The test strips were free of wrinkles, creases and etc.

The specimen was first aligned and clamped in the upper jaw of the QC-1000 Tensile tester (Thwing-Albert Instrument Company, Philadelphia, PA). After carefully removing noticeable slack, specimen was clamped in the lower jaw. The purpose of the proper specimen alignment was to prevent the jaw tear type breaks. The tensile and percent of elongation were recorded when the strip was broken.

A3.3.2. Tissue surface profile

The tissue surface profile was obtained by using the HommelWerke LV-50 Surface Profilometer (Alte Tuttlinger, Western Germany) equipped with a TKL300-3312 diamond probe. The diameter of the probe was 5 μm . The data was collected and analyzed using the Turbo Roughness for Windows 2.17a software package. This data was arranged as an array with two columns, i.e., scan distance and the surface profile, respectively. The profilometer parameters used in this study are given in Table A3.1.

Table A3.1 Parameters used in the tissue profile scanning by the HommelWerke LV-50 Surface Profilometer.

| Parameter | Setting | Parameter | Setting |
|---------------------------------|---------|-----------------------|-------------------|
| L _t , Trace length | 48mm | H, Maximum altitude, | 300 μm |
| L _c , Cutoff length, | 8mm | Number of measurement | 8000 |
| V, Probe velocity, | 1mm/sec | ----- | ----- |

The sample was placed on the Hommelwerke LV-50 scanning block and the edges of the sample were weighted so that the tissue sample surface was kept tight and free of waviness. The probe was lowered until it almost touched the sample surface. The test screen was brought up in the software package by pressing F5. The probe was then put into position by manually adjusting the screw, until the probe altitude value was between

-7 and +7 μm . The F5 key was pressed to start the scan. Once the test was complete, the data was converted to ASCII text (CPG.DAT) using the CONVERT.EXE program.

The computer screen was refreshed and the converted files could appear by pressing the F5 key. The CPG.DAT file was then renamed using an appropriate title. The file was then saved to the computer hard drive for further treatment.

A3.3.3. Coefficient of friction

The coefficients of friction of tissue samples were measured using Amontons I (Mu Measurement, Madison, WI). The Amontons instruments effectively controlled the variables in the measuring process and eliminated variations caused by the operator. Both the table and sled were covered with a soft, foam-rubber backing material. Two pieces of tissue sample were cut to the size of 2" by 2". One piece was put "face up" on the table, and the other piece was put "face down" unto the surface of the lower piece. The sled (measuring arm) was then placed onto the tissue samples. A steady normal force (700 grams force) was applied, and the static coefficient of friction was measured. For each tissue sample, 10 measurements were taken.

A3.3.4. Handle-O-Meter stiffness

The Handle-O-Meter (Thwing-Albert Instrument Company, Philadelphia, PA) consisted of a penetrating arm pivoted to ride on an eccentric cam engaging the test specimen and forcing it into a slot. In this study, the slot width was adjusted to 6.35 mm (0.25 in.). A square of 3.5 inch by 3.5 inch was cut from the tissue sample and placed across the platform over the slot. The Handle-O-Meter was turned on to set the

penetration arm in motion and the force necessary to push the specimen into the slot to form a “U” shaped strip was recorded.

A3.3.5. Thickness

Tissue thickness was measured using an Electronic Thickness Tester (Model 89-100, Thwing-Albert Instrument Company, Philadelphia, PA). The thickness tester was capable of measuring tissue bulk at various pressures. The pressure was altered by a series of stainless steel rings added onto the tester’s pressure foot. Table A3.2 lists the settings of the thickness tester. The electronic bulk tester was calibrated by pressing the “ZERO” button. For each sample, the thickness of ten sheets was measured. A TAPPI standard micrometer (E. J. Cady Co., Wheeling, IL) was used to measure the thickness of tissue samples at 50 kPa. The pressure foot was lowered at the speed of approximately 0.8mm per second. The thickness readings were taken 3 seconds after the pressure foot exerted steady pressure on tissue surface.

Table A3.2 Settings of TA Model 89-100 electronic thickness tester

| Diameter of pressure foot: 5.08cm P ₀ : 0.689kPa | | | | | | |
|--|----------------|----------------|----------------|----------------|----------------|----------------|
| P # | P ₁ | P ₂ | P ₃ | P ₄ | P ₅ | P ₆ |
| Pressure, kPa | 1.168 | 1.648 | 2.129 | 2.610 | 3.091 | 3.571 |

A.3.3.6. Thermal conductivity

Thermal conductivity of tissue samples was measured using Thermal Conductivity Probe (Mathis Instruments Ltd., Fredericton, New Brunswick, Canada). Before the test, the instrument was calibrated with standard samples provided by the manufacturer. The test time was set to be 30 seconds. Since the sensor's heating element absorbed a certain amount of the heat that the TC Probe sensor emits, the data gathered at the first two seconds were not used for final data analysis. The instrument's sampling frequency was set at 10 Hz. At the end of sample testing, a summary graph was plotted and the sample's thermal bulk value (square root of the product of thermal conductivity, density and heat capacity) was provided. The cooling period of the instrument was set to be 10 minutes. For each tissue sample, five repetitions were performed.

A4. Results and discussion

A4.1. Multiple regression analysis

Previous study suggests that the psychological magnitude of a stimulus is an exponential function of its physical magnitude [Stevens, 1957]. In this study, the power law regression was performed between tissue softness and physical properties. The multiple regression analysis was used to determine the following:

- Tissue physical properties that significantly contribute to human tactile sensation.

- A mathematical model to establish the relationship between various physical properties and the softness sensation.

Assume the power relationship exists between softness S and n tissue physical properties (x_1, \dots, x_n) as shown in Equation A4.1. Taking the logarithm of both sides of Equation A4.1 led to Equation A4.2

$$S = a \prod_{i=1}^n x_i^{k_i} \quad (\text{A4.1})$$

$$\ln(S) = b + \sum_{i=1}^n k_i \ln(x_i) \quad (\text{A4.2})$$

where S is the panel softness score,

x_i is the measured tissue physical property,

k_i is the exponent of x_i by regression, and

a and b are the constants in the regression relationship.

A4.2. Correlation of tissue physical properties with softness

In this section, various properties of the creped facial tissue were correlated with the softness. The correlation coefficient of the power relationship as well as F and P values served as the criteria for identifying statistically significant predictors of tissue softness.

A4.2.1. Tensile index

The correlation results of softness with tensile strength are listed in Table A4.1. The tensile index is the tensile strength (N/m) normalized by tissue basis weight (g/m^2). R is defined as the tensile index ratio (cross machine direction to the machine direction). Among various tensile properties, the tensile index at the machine direction had the highest degree of correlation among various tensile properties with adjusted R^2 of 52.5%. Figures A4.1 (A) and (B) show the correlation of tissue softness with tensile index in machine direction and tensile strength ratio, respectively.

TABLE A4.1 Correlation between measured physical properties and softness ranking

| Properties | b | k | $R^2_{\text{(adj)}}$, % | F | P |
|------------------------------|-------|-------|--------------------------|-------|-------|
| Tensile index (MD), N m/g | 51.6 | -0.75 | 52.5 | 15.35 | 0.002 |
| Tensile index (CD), N m/g | 0.298 | 3.98 | 7.2 | 2.01 | 0.182 |
| Mean tensile index, N m/g | 5.16 | -1.50 | 52.5 | 15.35 | 0.002 |
| R, Tensile index CD/MD ratio | 4.50 | 0.428 | 48.7 | 13.32 | 0.003 |

As the regression equation indicates, the tissue softness decreased as the machine direction tensile index increased and increasing the tensile strength ratio tended to improve the softness.

A4.2.2. Tissue modulus

The correlation of the tissue softness with the elastic modulus in both machine and cross machine directions was performed using the power law relationship. The tensile stiffness E_t was also computed and correlated with the tissue softness. The results were summarized in Table A4.2.

The elastic modulus in the machine direction had significant correlation with the tissue softness as shown in Figure 4.2 with the adjusted R^2 of 65.6%. The mean Elastic modulus was also significant with an F value of 5.56 ($p < 0.05$).

TABLE A4.2 The correlation results of the tissue softness with tissue modulus

| Properties | b | k | $R^2_{(adj)}$, % | F | P |
|---------------------------|------|--------|-------------------|-------|-------|
| Elastic modulus (MD), MPa | 5.91 | -0.451 | 65.6 | 25.78 | 0.000 |
| Elastic modulus (CD), MPa | 4.53 | -0.093 | 0.0 | 0.81 | 0.387 |
| Mean elastic modulus, MPa | 5.32 | -0.290 | 26.0 | 5.56 | 0.036 |
| Elastic modulus ratio | 4.09 | -0.139 | 4.3 | 1.59 | 0.231 |
| Tensile stiffness, N/m | 6.24 | -0.284 | 15.1 | 3.32 | 0.093 |

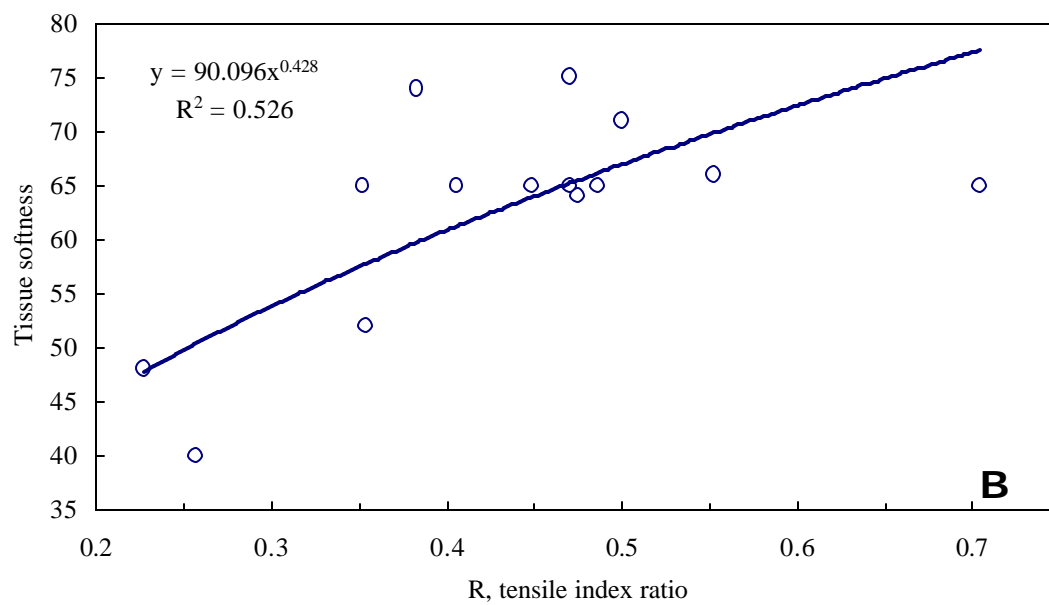
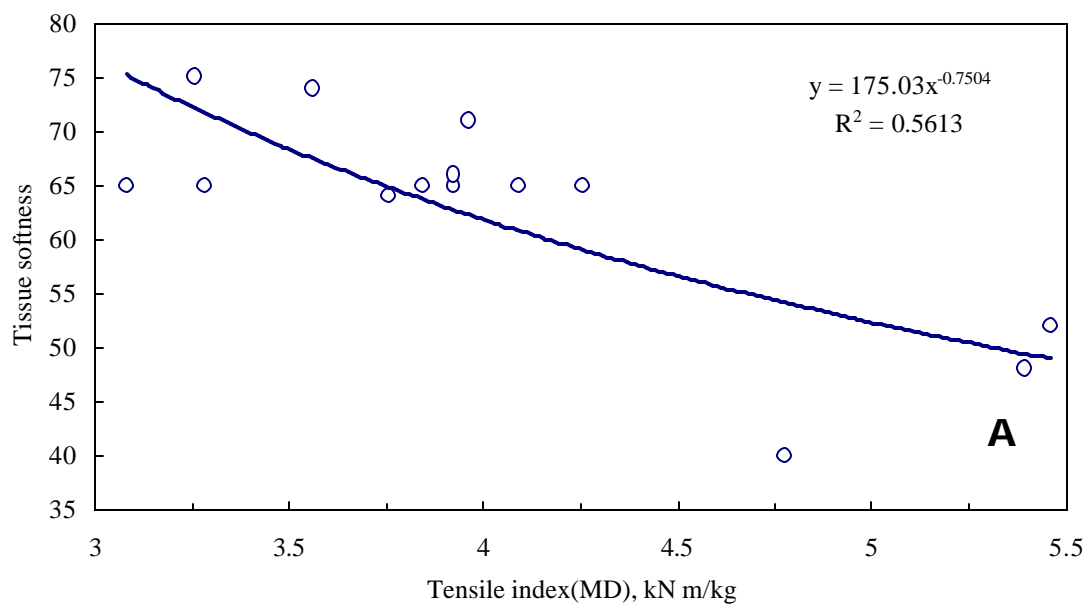


FIGURE A4.1 (A) Tissue softness correlation with the tensile index in the machine direction; (B) tissue softness correlation with the tensile index ratio (cross machine direction to the machine direction)

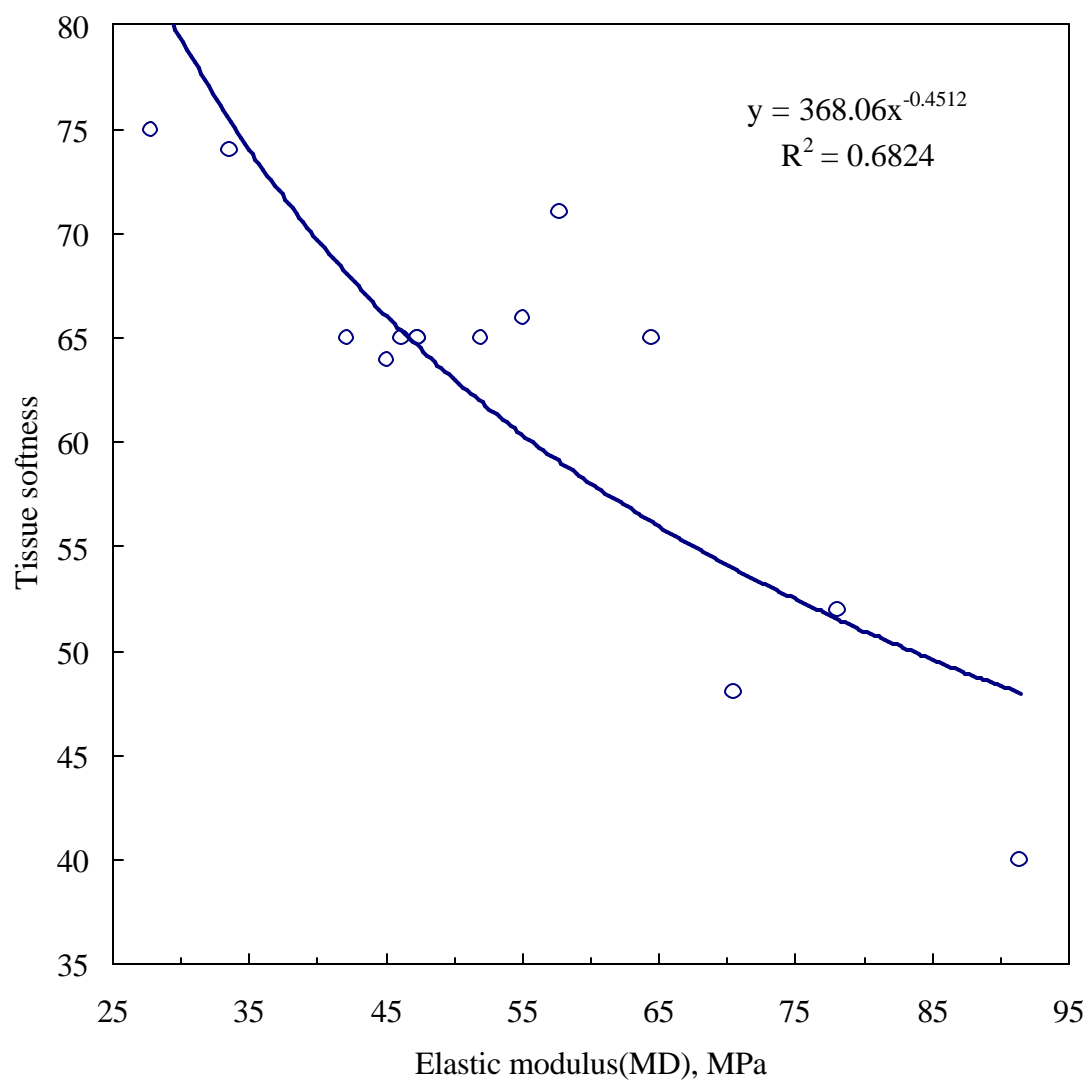


FIGURE A4.2 The power law correlation of tissue softness with elastic modulus in the machine direction ($R^2=0.6824$).

The softness correlation with tensile stiffness only had the adjusted R^2 of 15.1%. In comparison, a high degree of correlation of tensile stiffness with bulk softness of tissue and towel was found [Hollmark, 1983]. The fact that tissue stiffness had a high degree of correlation with tissue bulk softness and a low correlation with facial softness suggests surface softness played an important role in the tactile sensation of facial tissue products.

A4.2.3. Tissue surface texture

The tissue surface texture was measured by stylus profilometry. Figure A4.3 (A) shows the tissue surface profile over the scanned distance of 32mm. The total scanned distance was 48mm, and the data on the first and last 8mm of each scan were discarded. The profile treated with a second order digital elliptic filter with the cut off frequency [13, 82] Hz, 0.5dB of ripple in the pass band and 40dB of attenuation in the stop band. The signals with frequencies below 13Hz and above 82 Hz were filtered. The filtered tissue profile is shown in Figure A4.3 (B). The Matlab program used in the data processing is enclosed in Appendix B. For each tissue profile, the arithmetic mean roughness and the root mean square roughness were computed by Equations A4.3, A4.4

$$R_a = \frac{1}{l_m} \int_0^{l_m} |z(x)| dx \quad (A4.3)$$

$$R_q = \sqrt{\frac{1}{l_m} \int_0^{l_m} z^2(x) dx} \quad (A4.4)$$

where R_a is the arithmetic mean roughness, μm ,

R_q is the root mean square roughness, μm ,

L_m is the scanned distance, mm, and

$Z(x)$ is the adjusted z direction amplitude (deviation from the least-square fit mean line of data).

The R_a and R_q values of the tissue samples were used to correlate with the tissue softness. Figures A4.4 (A) and (B) give the power function correlation results.

The filtered profiles of two tissue samples are given in Figure A4.5 (A) and (B). The two samples had dramatically different softness scores: 40 and 71, respectively. The surface profiles of the two samples also had noticeable differences. The profile of the sample with a softness score of 40 had more dramatic changes; the height differences between the peaks and valleys were larger than those of the sample with a softness score of 71. The feature differences between tissue profiles were reflected in the quantities such as R_a and R_q . Within the range of R_a and R_q , the tissue softness score decreased with increasing surface roughness values.

The PAAREA factor was also considered in this study. The amplitude (square root of power) frequency spectrum was obtained and integrated over the frequency from 0 to 10 cycles per millimeter, and the integration result was the PAAREA of the tissue sample. HTR was obtained by integrating the amplitude frequency spectrum from 0.394 to 1.969 cycles per mm (10 to 50 cycles per inch) and above the $2.54\mu\text{m}$ base amplitude. The PAAREA and HTR were correlated with the tissue softness. The adjusted R^2 of the

power correlation of softness with HTR and PAAREA was 30.9 and 31.5 percent, respectively. PAAREA_EQ, a similar factor to PAAREA, was defined as the integration over the frequencies from 0.67 to 1.5 cycles/mm, which had a good correlation with softness with an adjusted R^2 of 58.1%. Figure A4-6 shows tissue softness correlation with PAAREA_EQ. In summary, the correlation results with the surface profile parameters are summarized in Table A4.3.

TABLE A4.3 The correlation results of the tissue softness with surface profile parameters

| Properties | b | k | $R^2_{(adj)}$, % | F | P |
|------------|------|-------|-------------------|-------|-------|
| R_a | 7.00 | -1.01 | 34.5 | 7.85 | 0.016 |
| R_q | 7.23 | -1.01 | 35.3 | 8.08 | 0.015 |
| PAAREA | 3.91 | -2.57 | 31.5 | 6.53 | 0.027 |
| HTR | 2.45 | -1.32 | 30.9 | 6.37 | 0.028 |
| PAAREA_EQ | 1.00 | -1.68 | 58.1 | 17.62 | 0.001 |

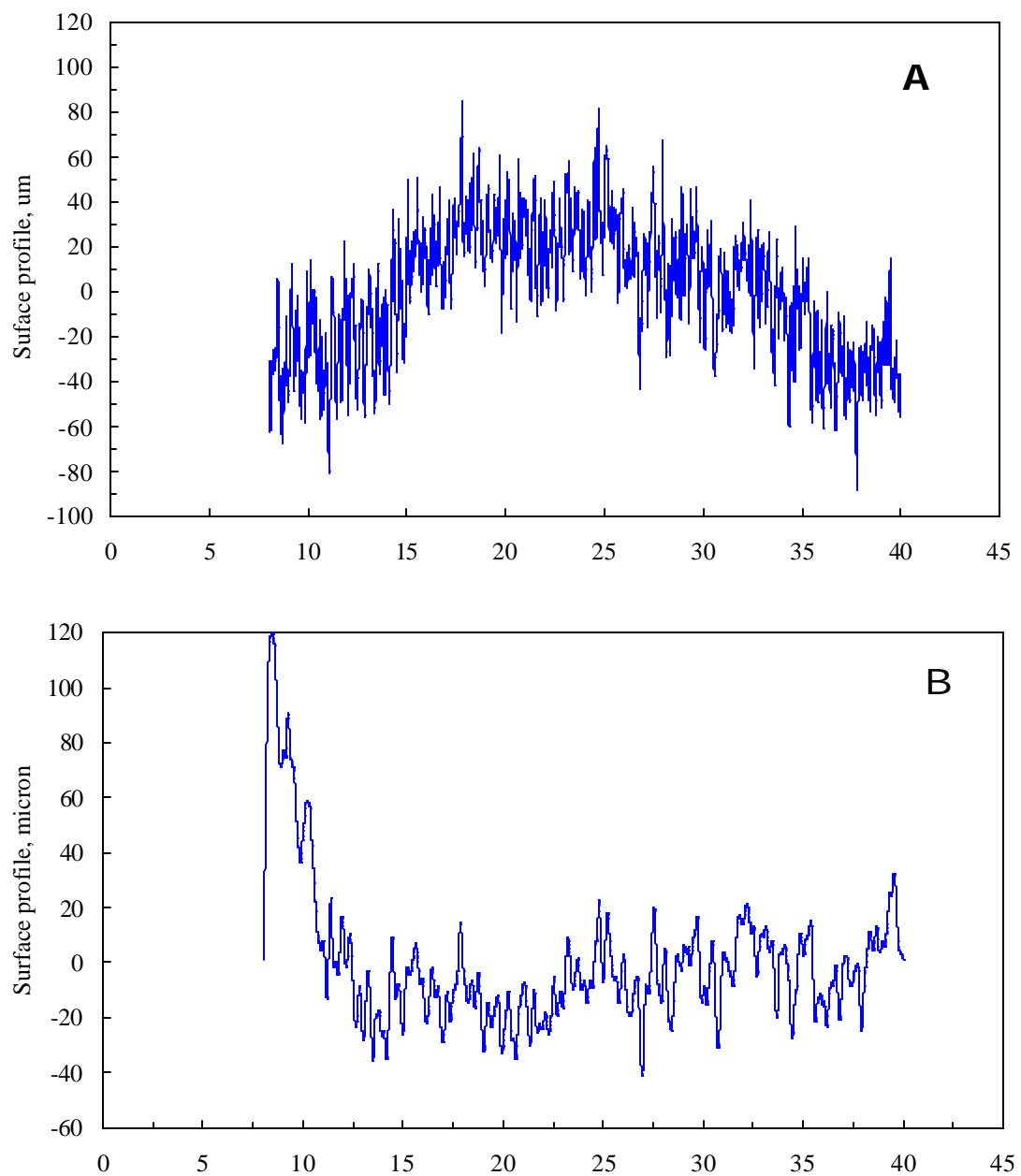


FIGURE A4.3 (A) The facial tissue surface profile obtained by stylus profilometry. (B) The facial tissue surface profile with pass band filtering. The signals with frequency lower than 13Hz, higher than 82Hz were filtered out.

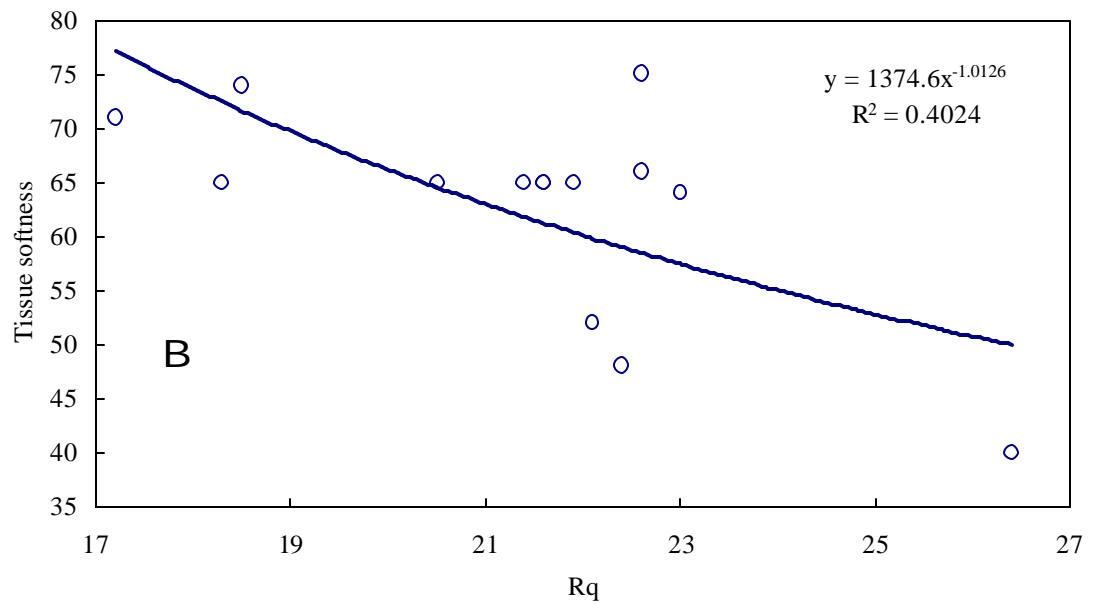
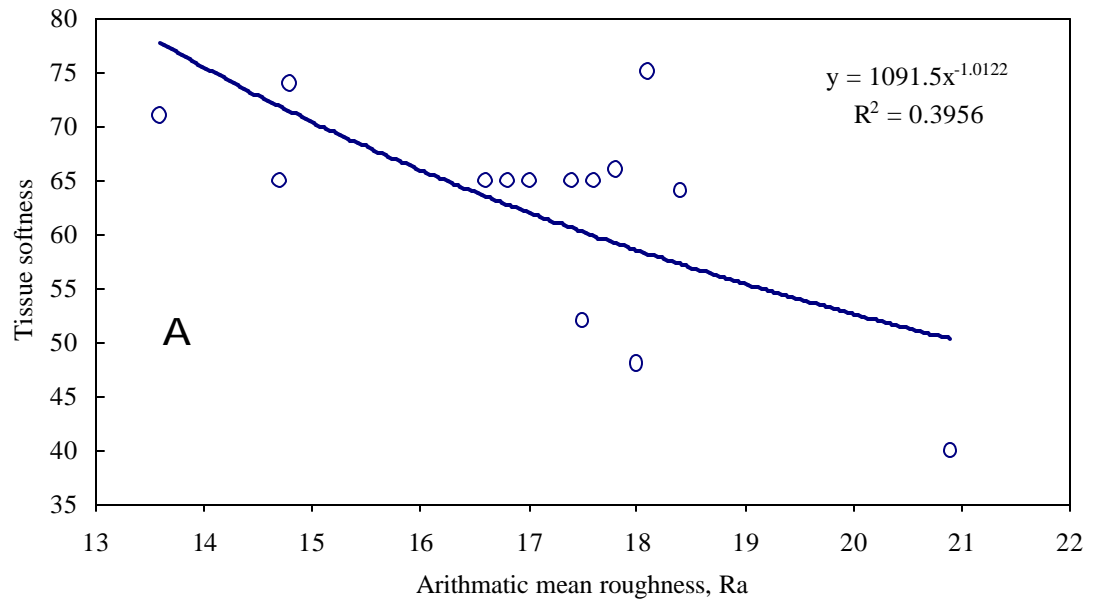
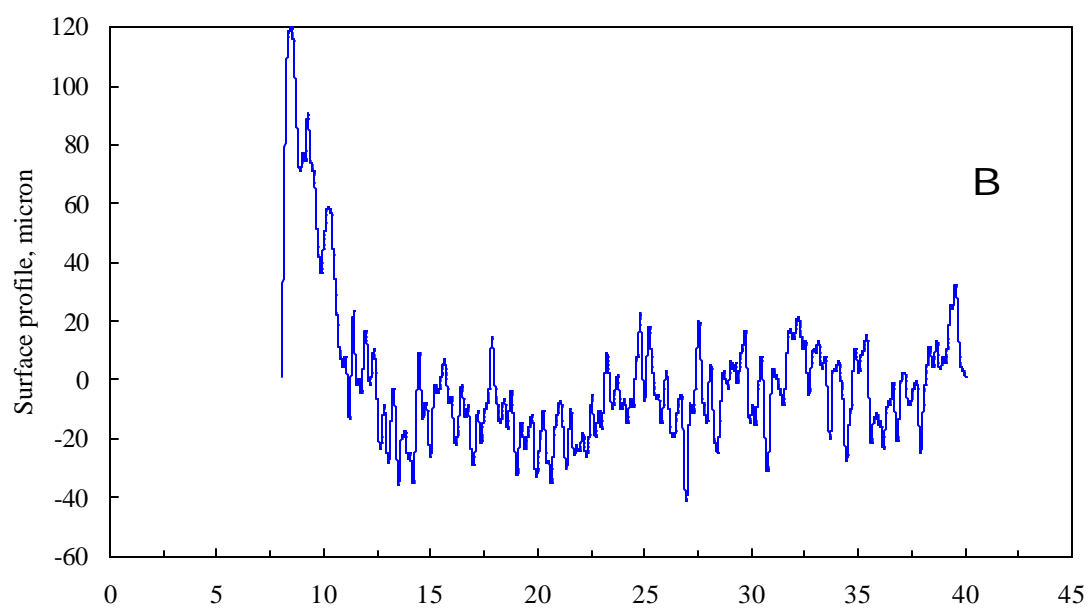
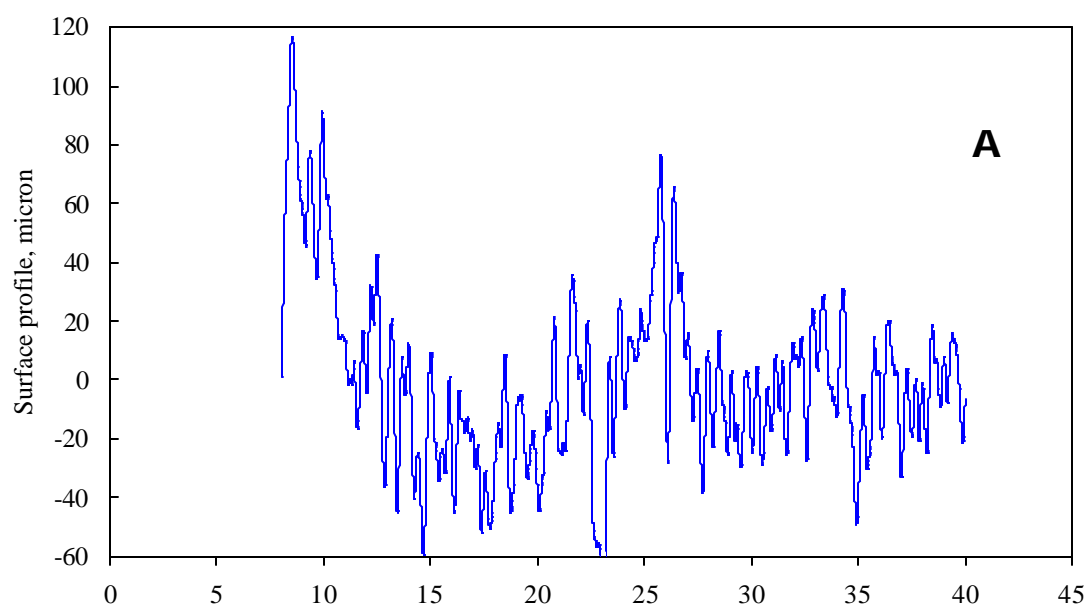


FIGURE A4.4 (A) The power law correlation of tissue softness with arithmetic mean roughness; (B) the correlation of softness with mean square roughness.



FIGURES A4.5 (A) A facial tissue surface profile with filtering treatment. The softness of the sample was 40; and (B) A facial tissue surface profile with filtering treatment, and the softness score was 71.

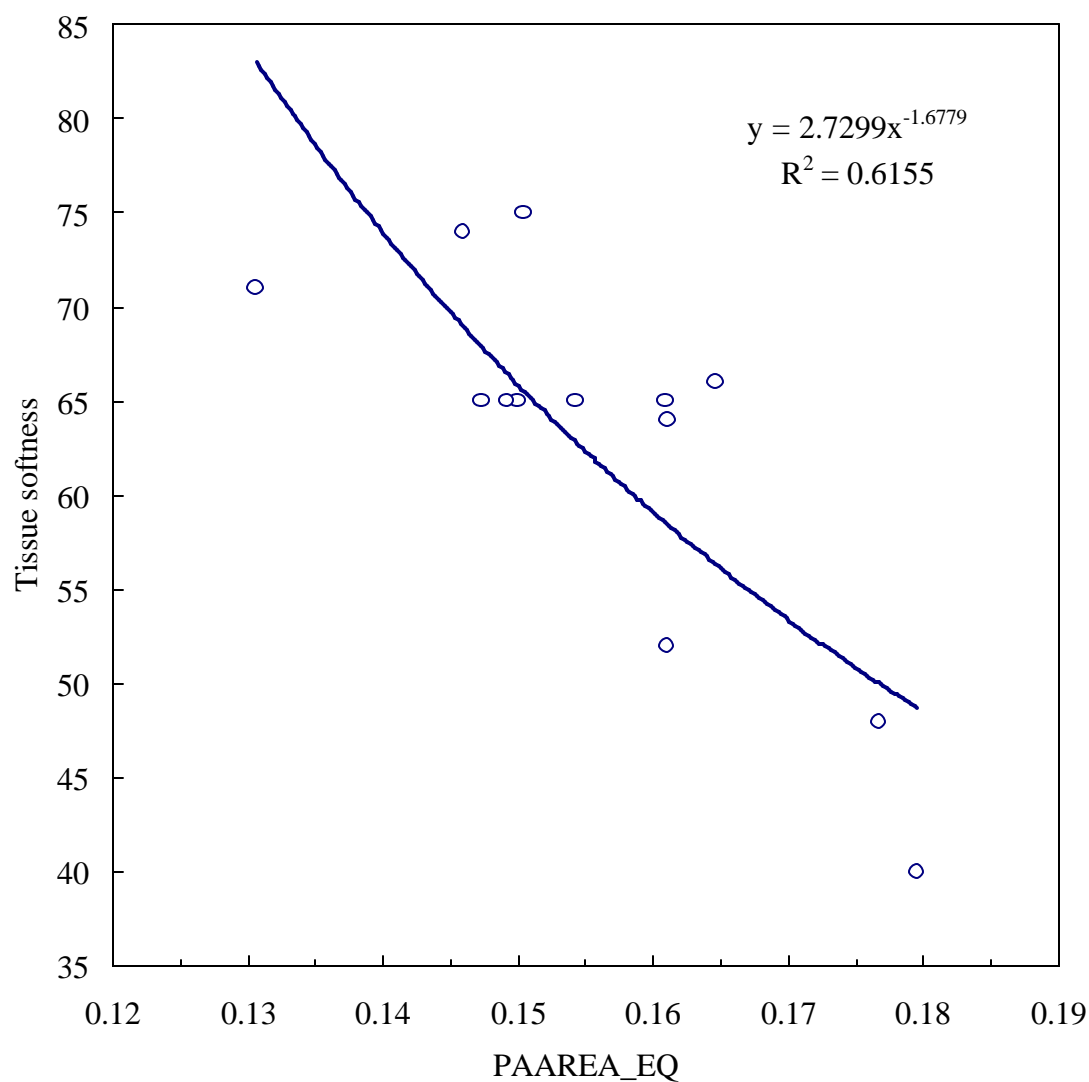


FIGURE A4.6 The power law correlation of tissue softness with PAAREA_EQ. The softness correlation with PAAREA_EQ was found to be better than those with the surface texture factors defined in the literature.

A4.2.4. Coefficient of friction

The tissue static coefficient of friction was measured by Amontons I (Mu Measurement, Madison, WI). As Equation A4.5 defines, the static coefficient of friction is the ratio of the frictional force to the normal force asserted to the tissue sample by the measuring arm

$$\mu = \frac{f}{N} \quad (\text{A4.5})$$

where μ is the coefficient of friction,

f is the minimum frictional force needed to move the sample, gf, and

N is the normal force applied by the sled, gf.

The static coefficient of friction was found to be irrelevant to the softness generation. The adjusted R^2 for the power correlation was only 1.3%. The F and P values for the correlation were 1.18 and 0.299, respectively.

The reason for the irrelevance of the coefficient of friction with softness sensation is probably two fold. The normal force applied by Amontons I was 700 gf. The applied pressure by the sled on the tissue sample was about 2.66 kPa. This pressure may not be the optimum pressure to measure the coefficient of friction. More importantly, the customer either brushes his finger on the tissue surface or crumbles the tissue in his hand, in which process the relative displacement between the finger and the sample usually occurs.

In fact, Nafe et al. were not able to relate the static aspects of mechanical stimulus with the tactile sensations [Nafe et. al., 1941]. Lindblom put forward the concept of critical slope, which is the minimum rate of displacement that will produce a neural response [Lindblom, 1966]. His study shows the critical slopes of the monkey glabrous skin ranges from 0.08 to 3.5 mm per second. As the displacement rate decreases toward the critical slope, the displacement thresholds increase exponentially. Given the above reasons, the dynamic coefficient of friction may be more suitable in the softness prediction.

A4.2.5. Handle-O-Meter stiffness

Both flexibility and the surface friction of the sample affect the instrument's final reading. Tissue with a higher flexibility or coarser surface usually results in higher reading. The Handle-O-Meter stiffness was measured at tissue machine and cross-machine directions.

The Handle-O-Meter readings at the cross machine direction were found to be more sensitive to the softness than those at the machine direction. The average Handle-O-Meter reading and H_{MD}/H_{CD} are statistically significant in the softness correlation. The result of the power relationship correlation is given in Table A4.4.

TABLE A4.4 The correlation results of the tissue softness with tissue Handle-O-Meter readings

| Properties | b | k | $R^2_{(adj)}, \%$ | F | P |
|---------------------------------|------|--------|-------------------|-------|-------|
| H_{MD} | 4.06 | -0.288 | 24.5 | 5.21 | 0.041 |
| H_{CD} | 3.91 | -0.333 | 46.1 | 12.13 | 0.005 |
| $(H_{MD} \bullet H_{CD})^{0.5}$ | 3.98 | -0.325 | 36.8 | 8.58 | 0.013 |
| H_{MD}/H_{CD} | 3.81 | 0.718 | 27.4 | 5.90 | 0.032 |

A4.2.6. Thickness

Tissue thickness at different pressures was correlated with the softness. The lowest measurement pressure was 0.687 kPa, above which the pressure was increased at the interval of 0.481 kPa until 3.571 kPa. The highest measurement pressure was 50 kPa specified in the TAPPI standard for the paper thickness measurement.

Tissue thickness values at all pressures failed to contribute to tissue softness in a significant way. The correlation results are included in Table A4.5.

The positive k values for thickness under all pressures indicate that softness increases with the tissue thickness. The above correlation shows that the tissue thickness values measured at 1.168 kPa have about 90.4% possibility to be relevant to the tissue softness sensation. The thickness values measured at higher pressures, however, show decreasing correlation coefficients and P values, and therefore, are more irrelevant.

TABLE A4.5 The correlation results of the tissue softness with thickness values

| Properties | b | k | $R^2_{(adj)}$, % | F | P |
|----------------------------|------|-------|-------------------|------|-------|
| B ₀ (0.687 kPa) | 2.20 | 0.424 | 13.9 | 3.09 | 0.104 |
| B ₁ (1.168 kPa) | 2.21 | 0.429 | 14.9 | 3.27 | 0.096 |
| B ₂ (1.648 kPa) | 2.24 | 0.428 | 14.1 | 3.13 | 0.102 |
| B ₃ (2.129 kPa) | 2.31 | 0.414 | 12.5 | 2.85 | 0.117 |
| B ₄ (2.610 kPa) | 2.32 | 0.415 | 11.8 | 2.74 | 0.124 |
| B ₅ (3.091 kPa) | 2.38 | 0.405 | 10.4 | 2.51 | 0.139 |
| B ₆ (3.571 kPa) | 2.54 | 0.370 | 7.7 | 2.09 | 0.174 |
| B _f (50.0 kPa) | 2.76 | 0.342 | 3.9 | 1.53 | 0.24 |

A4.2.7. Compressibility

The compressibility was defined to describe thickness changes versus handling pressures, as shown in Equation A4.6

$$Compressibility = \frac{T_i}{T_f} \quad (A4.6)$$

where T_i is the thickness value measured at P_i , and

T_f is the thickness measured at 50 kPa.

A high compressibility value indicated high tissue deformability (a sense of cushion).

The tissue under the pressure of 50 kPa was in the most condensed state since the loading

pressure was highest. According to the definition, it is obvious that tissue compressibility is bigger than 1 under low pressures. Table A4.6 lists the correlation results using the compressibility factors.

As Table A4.6 indicates, tissue softness increased with compressibility factors. It is interesting to notice that the compressibility factor at the 1.168kPa gave best correlation with the softness ($P=0.014$).

TABLE A4.6 The correlation results of compressibility factors with tissue softness

| Properties | b | k | $R^2_{(adj)}$, % | F | P |
|------------|------|------|-------------------|------|-------|
| B_0/B_f | 3.05 | 1.98 | 24.6 | 5.23 | 0.041 |
| B_1/B_f | 3.01 | 2.41 | 35.7 | 8.21 | 0.014 |
| B_2/B_f | 3.17 | 2.30 | 29.8 | 6.51 | 0.025 |
| B_3/B_f | 3.23 | 2.37 | 25.9 | 5.55 | 0.036 |
| B_4/B_f | 3.29 | 2.39 | 22.4 | 4.76 | 0.050 |
| B_5/B_f | 3.15 | 3.00 | 23.3 | 4.95 | 0.046 |
| B_6/B_f | 3.36 | 2.57 | 11.3 | 2.65 | 0.129 |

This observation agrees with the finding by Eperen et al. [1965] that when the measurement load was increased from 0.0207 kPa to 0.207 kPa, the thickness measured at a higher pressure gave better correlation with softness. It is pointed out that the loading pressure for the thickness measurement needed further optimization. In another study [Eperen, 1965], the thickness measurement pressure was set to be 8.620 kPa.

It is found that the thickness and compressibility measured at 0.207 kPa correlated with the tissue softness better. Under usual application conditions, the pressure used on a paper towel to wipe water is about 1.380 kPa, and facial tissue is handled at the pressure of no higher than 3.447 kPa [Bates, 1965]. Therefore, the thickness values and the compression factors measured under the pressure of 8.620 kPa may not realistically reflect the softness evaluation process.

This study shows that the adjusted correlation coefficient decreases when the thickness measurement pressure is beyond about 1.65 kPa. The tissue thickness measured by TAPPI standard method (at the pressure of 50 kPa) had the poorest softness correlation coefficient, i.e., 3.9%. It seems that the tissue thickness measured at 1.65 kPa gives the best correlation within the applicable pressure range.

A4.2.8. Thermal effects

The thermal conductivity of tissue samples was measured. A heat capacitor of 32°C was put in contact with one side of the tissue. The condition for the other side of the tissue was treated as being thermally insulated. Assuming that the tissue temperature was

the function of time and the thickness (x), the following heat conduction equation was set up to describe the distribution of temperature $u(x, t)$:

$$\frac{\partial^2 u}{\partial x^2} = \frac{1}{k} \frac{\partial u}{\partial t} \quad 0 \leq x \leq a, \quad t > 0 \quad (\text{A4.7})$$

$$u(0, t) = T_0 \quad t > 0 \quad (\text{A4.8})$$

$$\frac{\partial u(a, t)}{\partial x} = 0 \quad t > 0 \quad (\text{A4.9})$$

$$u(x, 0) = T_1 \quad 0 \leq x \leq a \quad (\text{A4.10})$$

where the u is the tissue temperature, K,

K is the tissue thermal diffusivity, $10^{-7} \text{ m}^2/\text{s}$,

A is the tissue thickness, m, and

T_0 and T_1 are the temperatures of heat capacitor (32°C) and room temperature (20°C).

The tissue temperature at time t and the thickness x was given in the following Equation A4.11

$$u(x, t) = 32 - \sum_{n=1}^{\infty} \frac{48}{(2n-1)\mathbf{p}} \sin \left[\frac{(2n-1)\mathbf{p}}{2a} x \right] \exp \left[-\frac{(2n-1)^2 \mathbf{p}^2}{4a^2} kt \right] \quad (\text{A4.11})$$

The thermal flux at time t was calculated by taking the derivative of the temperature profile at $x = 0$; its form was given in Equation A4.12

$$q = \frac{24k}{a} \sum_{n=1}^{\infty} \exp \left[-\frac{(2n-1)^2 \pi^2}{4a^2} kt \right] \quad (\text{A4.12})$$

For each sample, the thermal flux q at 0.2, 1, 1.5, 2, 3, 5, and 10 seconds was calculated using Equation A4.12. The thermal flux higher than 10 seconds is not of practical use and not considered here. The correlation using the power relationship was done. At the any above time, the thermal flux correlated poorly with tissue softness. Among the thermal flux quantities, the thermal flux at 3 seconds had the highest degree of correlation with adjusted R^2 of 8.4% ($p>0.1$). As the correlation equations indicated, the tissue softness seemed to be independent of the thermal flux.

TABLE A4.7 The correlation results of the thermal flux with tissue softness

| Thermal flux, kW/m ² | b | k | R ² _(adj) , % | F | P |
|------------------------------------|-------|-------|-------------------------------------|------|-------|
| Q _{t=0.2} | -1.36 | 1.83 | 4.0 | 1.55 | 0.238 |
| Q _{t=1} | -0.03 | 1.89 | 4.9 | 1.67 | 0.221 |
| Q _{t=1.5} | 0.33 | 1.90 | 4.9 | 1.67 | 0.220 |
| Q _{t=2} | 0.47 | 1.98 | 5.6 | 1.77 | 0.208 |
| Q _{t=3} | 1.04 | 1.90 | 8.4 | 2.20 | 0.164 |
| Q _{t=5} | 3.43 | 0.551 | 3.6 | 1.48 | 0.247 |
| Q _{t=10} | 4.07 | 0.145 | 2.2 | 1.29 | 0.279 |

A4.3. Multi-variable softness model

In the correlation of tissue softness with individual physical property, the elastic modulus at the machine direction gave the highest degree of correlation with adjusted R^2 of 65.6 and F of 25.78.

In order to improve the model's prediction accuracy, the multi-variable regression technique was used to construct multi-variable softness models. The correlation was done between $\ln(S)$ and $\ln(x_i)$ by the least square method. Table A4.8 summarizes the multi-variable power correlation results.

TABLE A4.8 The correlation results of multi-variable softness correlation

| No. of predictors | Predictors | $R^2(\text{adj})$ | F | P |
|-------------------|---------------------------------|-------------------|--------|-------|
| 1 | E_{MD} | 65.6 | 25.78 | 0.000 |
| 2 | E_{avg} , R | 91.4 | 69.75 | 0.000 |
| 3 | E_{avg} , R, R_a | 99.5 | 825.02 | 0.000 |
| 4 | E_{avg} , R, R_a , H_{CD} | 99.6 | 825.17 | 0.000 |

With two predictors (i.e., E_{avg} and R), the accuracy of the model was greatly improved, and its adjusted correlation coefficient was 91.4%. By incorporating tissue surface arithmetic roughness R_a , the adjusted correlation coefficient of softness model

was further increased to 99.5%. The model's degree of correlation was not improved by adding the fourth predictor, the Handle-O-Meter reading at the cross machine direction, H_{CD} .

The 2-predictor softness model takes the form shown in Equation A4.13

$$S = 354.25 \left(\frac{R}{E_{avg}^{0.706}} \right)^{0.463} \quad (A4.13)$$

The softness model predicted by three predictors, i.e., R , E_{avg} and R_a , is given in Equation A4.14

$$S = 1164.4 \left(\frac{R}{R_a^{1.220} E_{avg}^{0.793}} \right)^{0.387} \quad (A4.14)$$

In Figure A4.7, the softness values predicted by the 3-predictor models are compared with the tissue softness scores given by the panelist.

This model is developed to predict the softness of conventional facial tissue. Five creped facial tissue samples that were not included in the model development were used to test the validity of the model. Figure A4.8 represents the results, which showed a high degree of correlation between the softness scores by the model and those by the panelist, with an adjusted R^2 of 96%.

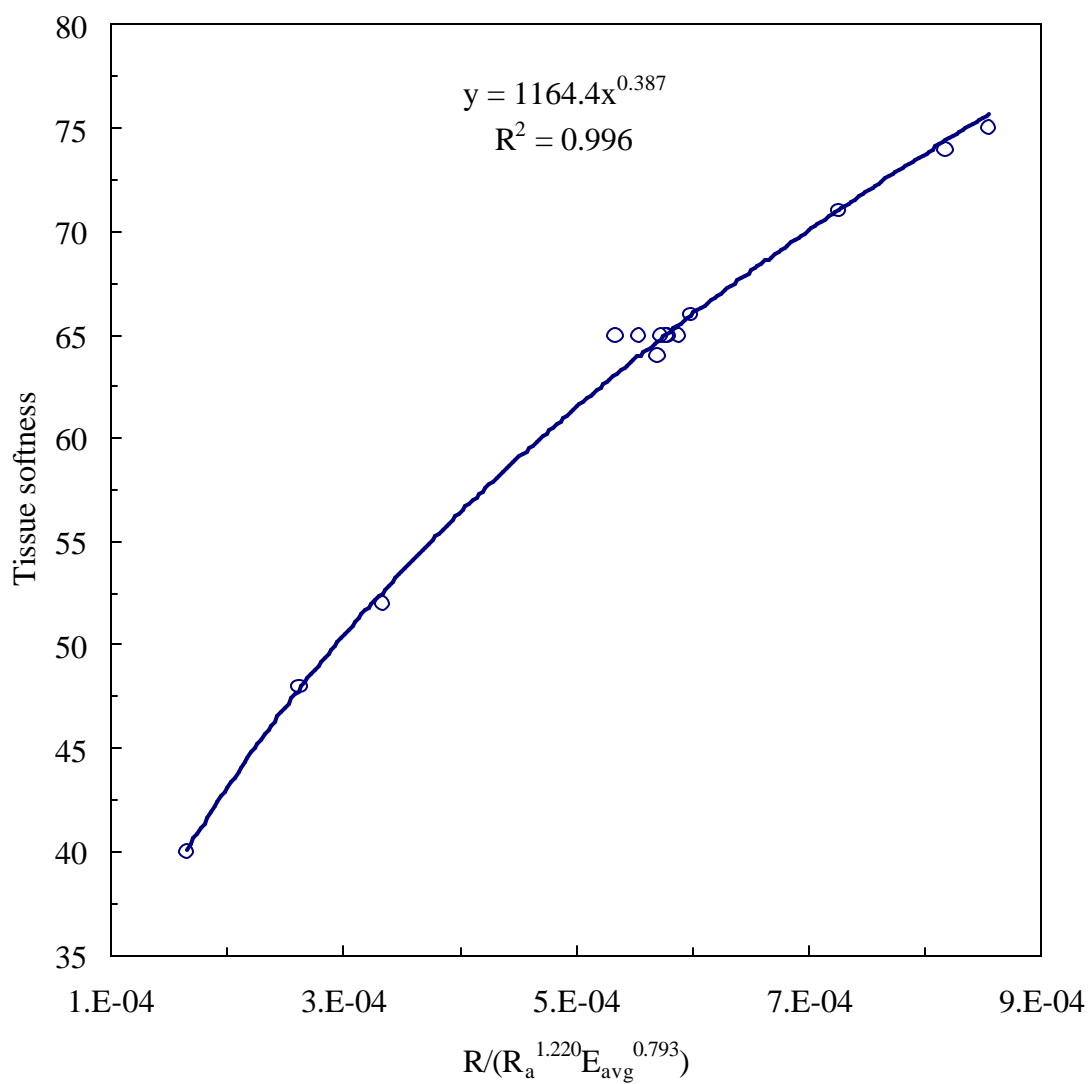


FIGURE A4.7 Comparison of tissue softness by the panelists and the 3-parameter softness model. The softness value by the model is represented by the curve.

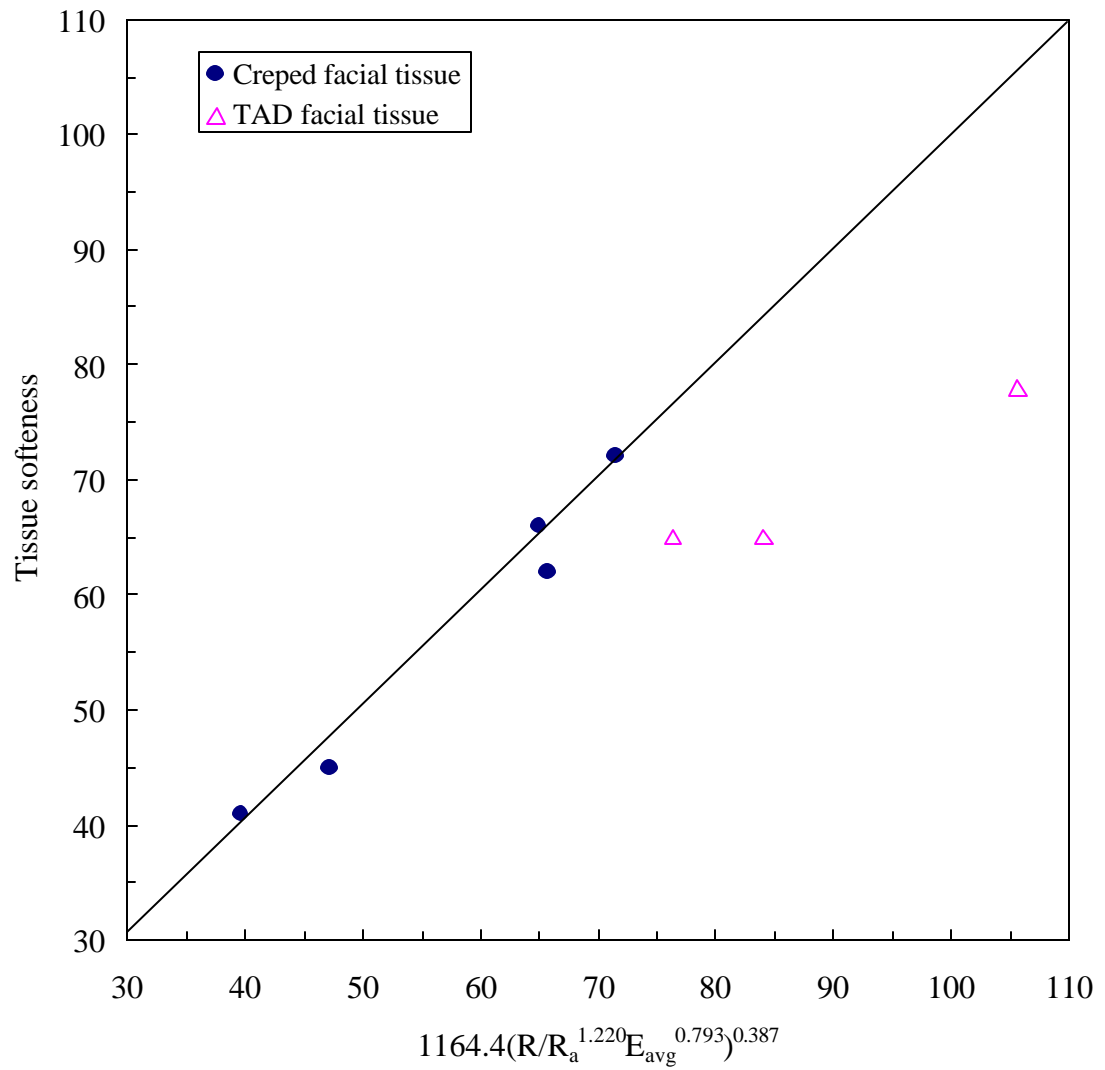


FIGURE A4.8 Testing of softness model for five facial tissue samples by conventional creping technology and three tissue samples by through-air-drying technology. The creped facial tissue samples were represented by •, and the through-air-dried tissue samples were represented by Δ.

A5. Conclusions

The physical properties that contribute to human tactile sensation of conventional tissue have been extensively investigated in this study. The low degree of correlation of tensile stiffness with softness in this study combined with the high percentage of its contribution to the tissue bulk softness suggests that the surface softness plays an important role in the human tactile sensation of facial tissue. Various parameters describing the tissue surface textures, such as the arithmetic roughness, the root mean square roughness, the PAAREA and the HTR were correlated with tissue softness. Tissue surface roughness had comparable softness correlation degree to PAAREA and HTR. A new parameter PAAREA_EQ was defined, which integrated the amplitude frequency spectrum from 0.67 to 1.50 cycles/mm. In this study, the PAAREA_EQ correlated with facial tissue softness better than similar parameters defined in the literature.

Elastic modulus at the machine direction and the PAAREA_EQ were found to be the most important single factors that contributed to tissue softness. The adjusted R^2 for PAAREA_EQ and elastic modulus at machine direction was 58.1 and 65.6 percent, respectively. The tensile index at the machine direction as well as Handle-O-Meter stiffness at the cross machine direction correlated with the tissue softness in the power law relationship with adjusted coefficients of correlation at 52.5% and 46.1%, respectively.

The tissue thickness measured at various low pressures did not correlate with the facial softness in a significant way. The correlation degree decreased as the loading pressure increased. The compressibility at certain pressures had better correlation with softness than thickness itself. The regression indicated that the tissue softness increased with compressibility. Among the compressibility and thickness values measured at various pressures, those at 1.168kPa had the highest coefficient of correlation.

The static coefficient of friction had minimal effects on the tissue softness, which seems to suggest that the kinetic coefficient of friction might be of more interest. The thermal effect was considered in this study, and the thermal flux to the tissue at different contact time was calculated. From the regression, it seems that the thermal flux was irrelevant to softness sensation.

Finally, a softness model was developed based on the cross machine direction to machine direction tensile index ratio, arithmetic surface roughness and the mean elastic modulus. This model was shown to be able to predict the softness of creped facial tissue with high accuracy, and opened the prospect of on-line monitoring of tissue softness.

A6. References

Bates, J. D., Softness Index: Fact or Mirage, *TAPPI Journal*, vol.**48**, no.4: 63-64 (1965)

Bolanowski, S. J., Jr., Gescheider, G. A., Verrillo, R. T. and Checkosky, C. M., Four channels mediate the mechanical aspects of touch, *J. of Acoust. Soc. Am.*, vol.**84**, no.5, 1680-1694 (1988)

- Cauna, N. Fine Structure of the receptor organs and its probable functional significance, *Ciba Foundation Symposium*, 117-127, Boston, MA (1966)
- Craig, J. C., Vibrotactile spatial summation, *Percept. Psychophys.*, vol.**4**: 351-354 (1968)
- Eperen, V., Winck, W. A., *IPCProject 2220*, Report 5, The Institute of Paper Chemistry, Appleton, Wis. (1965)
- Gescheider, G. A., B. F. Sklar, C. L. Van Doren, and R. T. Verrillo, Vibrotactile forward masking: Psychophysical evidence for a triplex theory of cutaneous mechanoreception, *Journal of Acoustical Society of America* **74**: 534-543 (1985)
- Hollmark, H., Evaluation of tissue paper softness, *TAPPI Journal*, vol.**66**, no.2: 97-99, (1983)
- Johansson, R. S., and Vallbo, A. B., Tactile sensitivity in the human hand: Relative and absolute densities of four types of mechanoreceptive units in glabrous skin, *J. Physiol.*, **286**: 283-300 (1979)
- Lindholm, U., The relationship of skin displacement to receptor activation, *Ciba Foundation Symposium*, 145-157, Boston, MA (1966)
- Luce, R. D., and Edwards, W., The derivation of subjective scales from just noticeable differences, *Psychol. Rev.*, **65**, no. 4: 222-241 (1958)
- Nafe, J. P., and Wagoner, K. S., The nature of sensory adaptation, *J. Gen. Psychol.*, **25**:295-321 (1941)
- Quilliam, T. A. Unit design and array patterns in receptor organs, *Ciba Foundation Symposium*, 86-112, Boston, MA (1966)
- Stevens, S. S., On the psychophysical law, *Psychol. Rev.*, vol.**64**: 153-181 (1957)
- Stevens, S. S., Tactile vibration: Dynamics of sensory intensity, *Journal of Experimental Psychology*, vol.**57**, no.4: 210-218 (1959)
- Verrillo, R. T., Specificity of a cutaneous receptor, *Perception and Psychophysics*, vol. **5**: 149-153 (1968)
- Verrillo, R. T., A duplex mechanism of mechanoreception, in *The skin Senses*, edited by D. R. Kenshalo, Thomas, Springfield, IL, 39-159 (1975)

APPENDIX B

MATLAB CODE FOR TISSUE SURFACE PROFILE


```

%rliul.m-----filtered profile (80 to 1000) and filtered
spectrum(amp.~freq)
%-----sample information:48mm evaluation length,y1 is the scan
distance, y2 is the amplitude-----
y=load('F.dat');
    y1=y(:,1);
y2=y(:,2)*25.4;
%-----unit: mm-----
plot(y1,y2)
%-----original measurement data plot-----
%subplot(3,1,2)
fss=48.0e-3/8000.0;
fs=1.0/fss;
%-----fs is the space-sampling frequency-----
rp=0.5;
%----ripple decibel-----
rs=40;
%-----cut off db-----
f1=78.0;
f2=1000.0;
%-----f2-f1 is the bandwidth-----
wn=[f1 f2]*2/fs;
[b,a]=ellip(2,rp,rs,wn);
%----elliptical filter design, 2 is the filter's order--
y3=filter(b,a,y2);
%----filtered profile, b, a are the filter parameters, y2
original profile-----
av=mean(abs(y3))
rms=sqrt(mean(abs(y3.*y3)))
subplot(2,1,1)
plot(y1*25.4,y3)

```

```

subplot(2,1,2)
pxx=abs(fft(y3));
%----get the amplitude spectrum by fft of y3-filtered profile by
elliptical filter-----
for i=1:length(pxx)/100
    kx(i)=i/48.0;
    %-----1.5 is the length of sample in mm, kx is the space
    frequency, unit:rad/mm-----
end
ppxx=pxx(1:length(kx));
l=48.0;
%-----length of Scanned distance-----
n=8000;
plot(kx,ppxx*l/n)
% -----the unit of the y axis is the mm^2-----
%subplot(3,1,3)
qxx=abs(fft(y2));
for j=1:length(qxx)/100
    mx(j)=j/48.0;
end
qqxx=qxx(1:length(mx));
plot(mx,qqxx*48/8000)
%-----this is the plot of spectrum(amp., frequency)-----

```

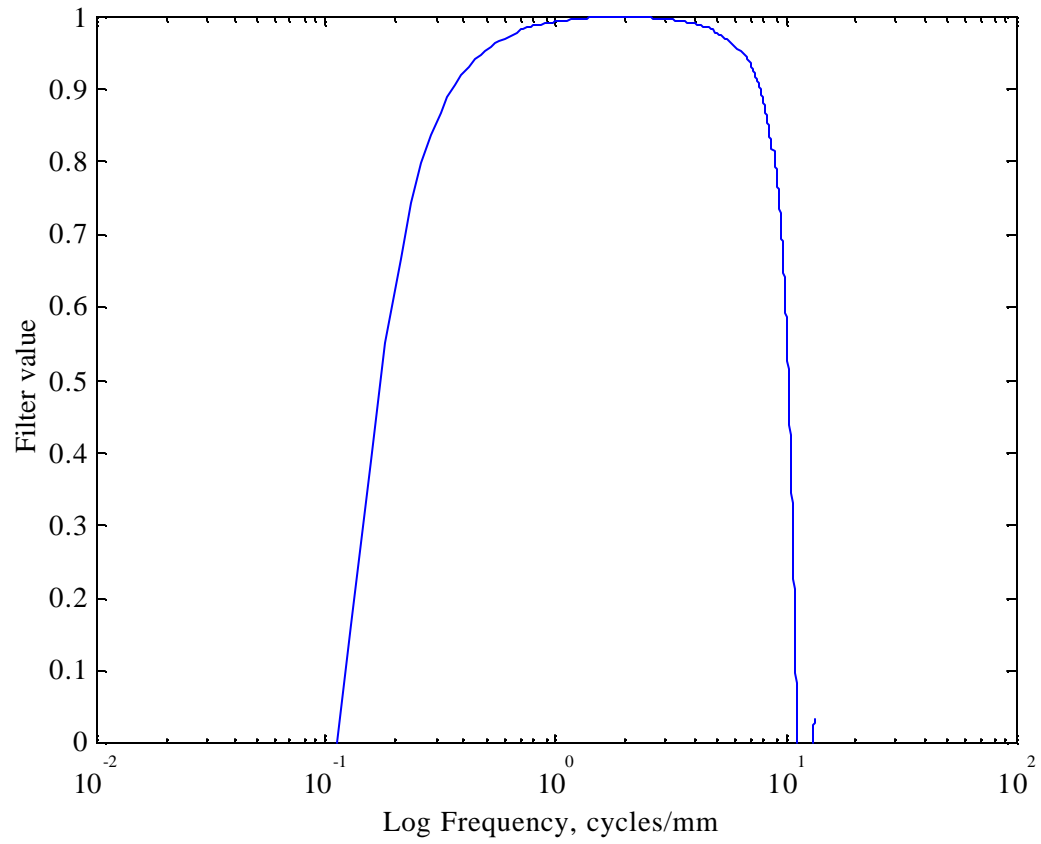


Figure B.1 The filter values as a function of the finger motion frequency. In this particular chart, a second order elliptical filter was used.

APPENDIX C

FIBER QUALITY ANALYSIS RESULTS

The fiber properties of hardwood and softwood pulp were measured by the Fiber Quality Analyzer (Econotech, Delta, BC, Canada). The pulp was disintegrated at the consistency of 4mg/L. The pulp slurry then passed through the cytometric flow cell, which oriented the fibers for precise measurement of length and shape.

The following fiber parameters were provided by the FQA:

1. The fiber length distribution. The fiber length measured is the fiber contour length rather than the end-to-end length.
2. The fiber curl index mean and distributions. The fiber curl is the gradual and continuous curvature and the curl index is defined as the ratio of fiber contour length to the end-to-end length minus one.

The testing results of two types of pulp are shown in Figures C1-4.

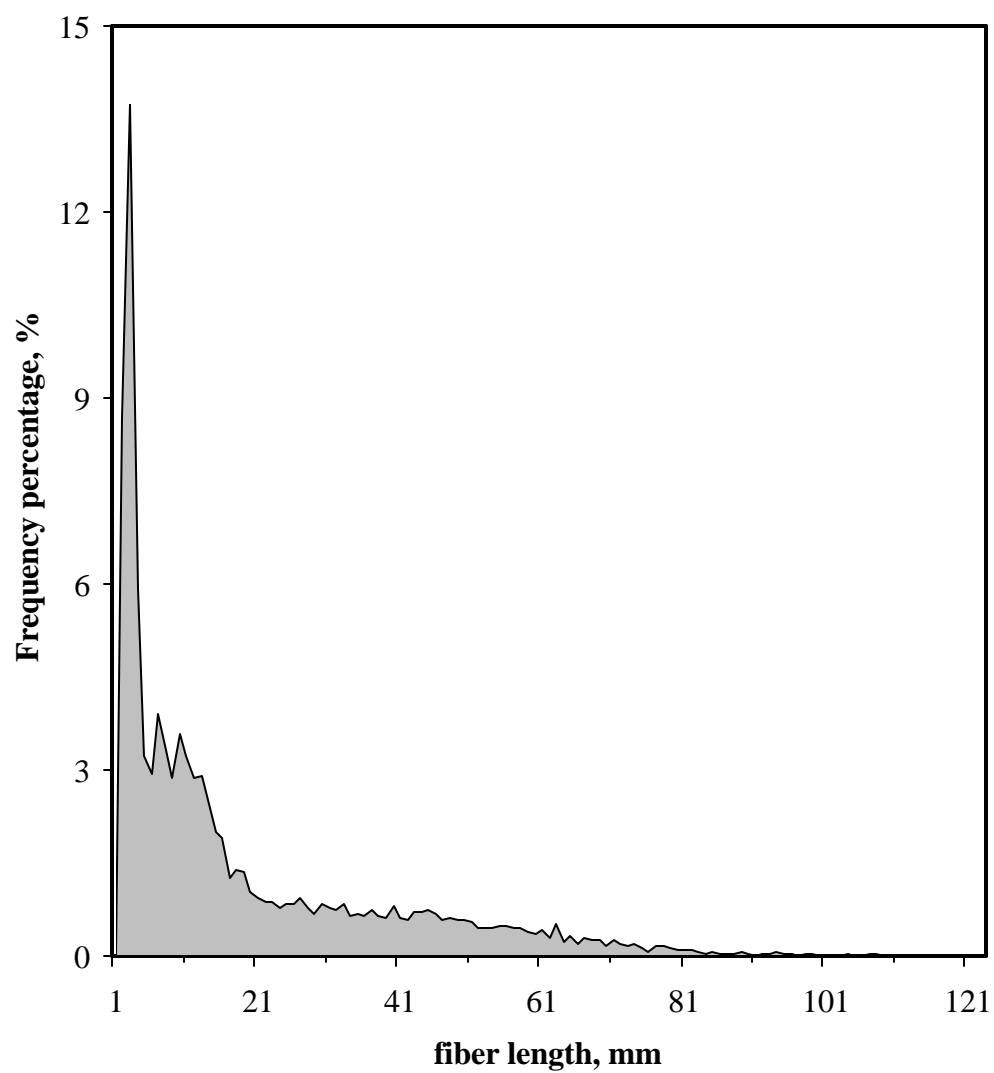


FIGURE C.1 Softwood fiber length histogram

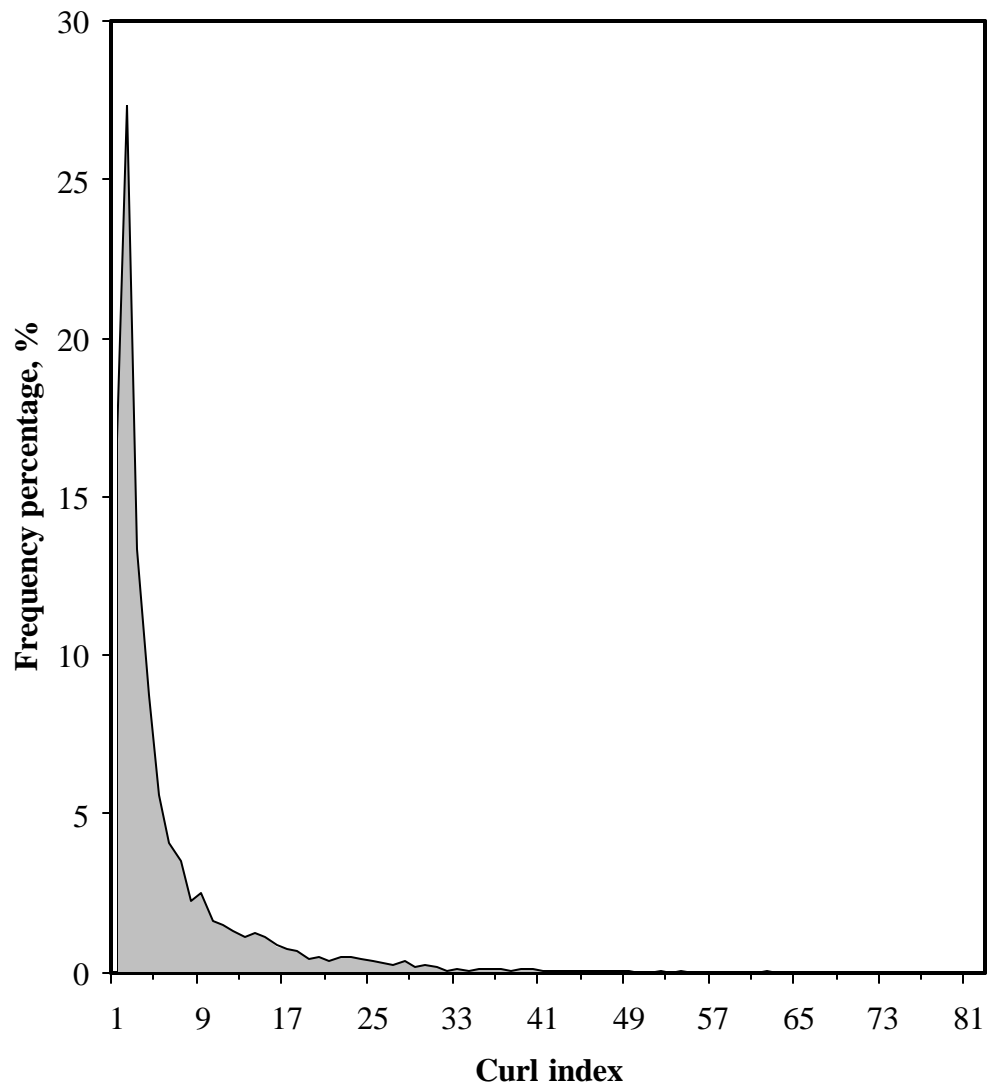


FIGURE C.2 Softwood fiber curl index histogram

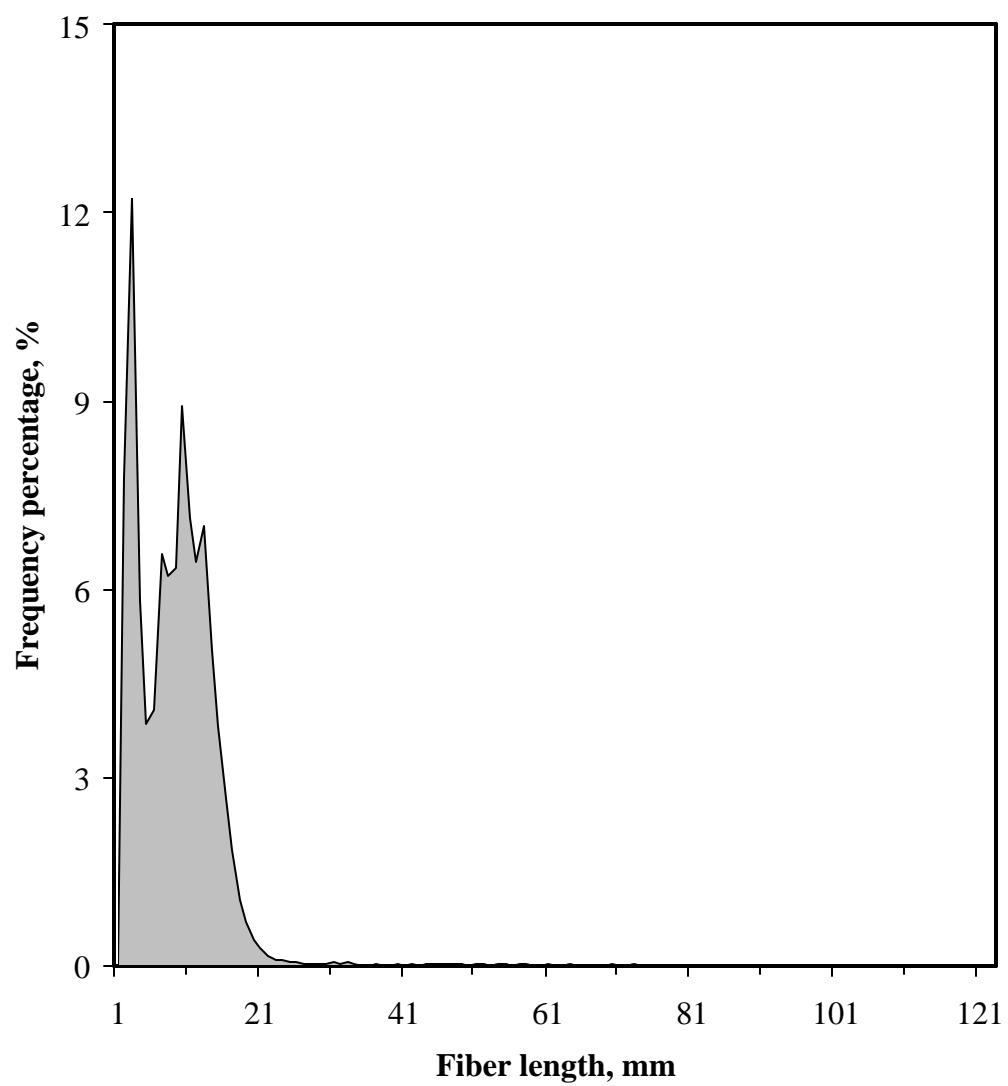


FIGURE C.3 Hardwood fiber length histogram

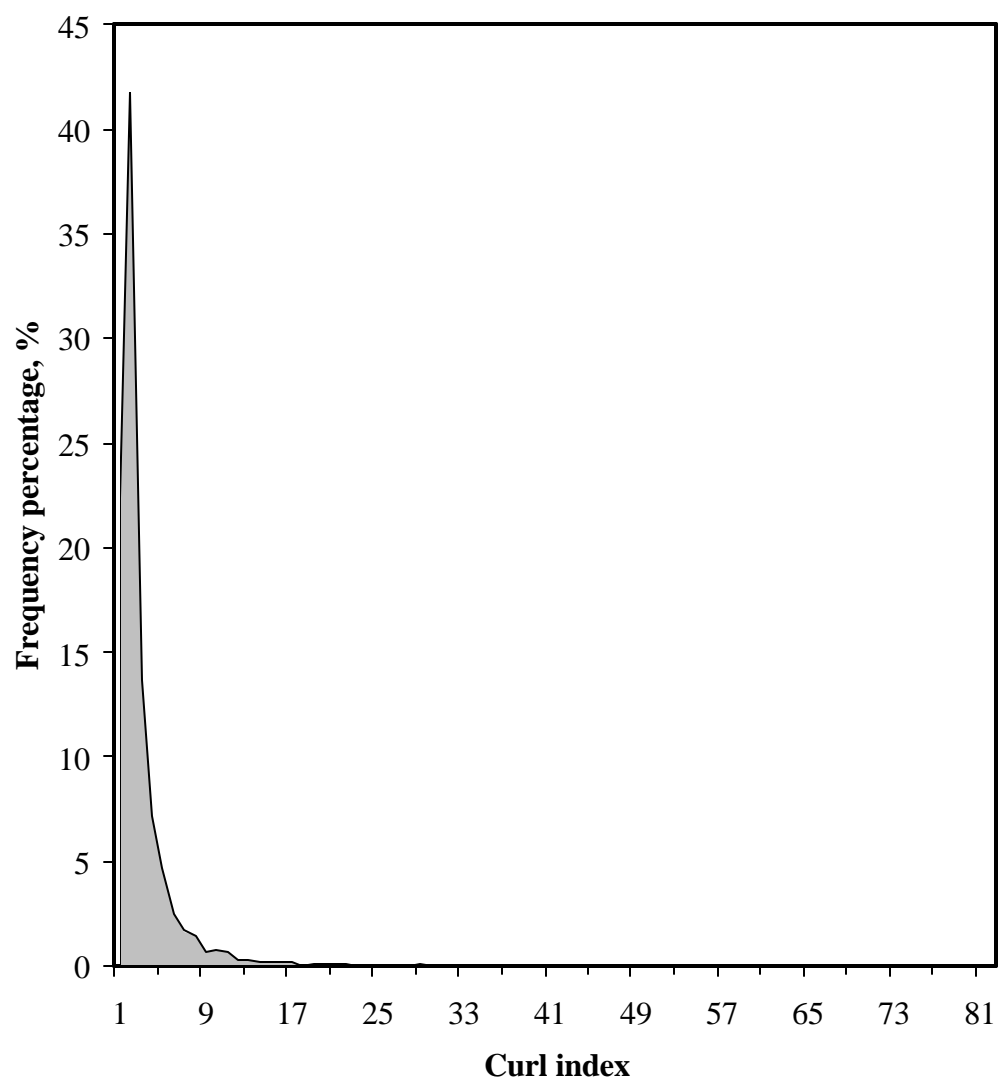


FIGURE C.4 Hardwood fiber curl index histogram

APPENDIX D

EFFECTS OF PULP QUALITY VARIATION ON TISSUE PRODUCT PROPERTIES

D1. Introduction

The paper manufacturers are facing fierce competition in the market of almost all paper grades, and most paper companies have to deal with the challenge of an unsatisfactory return of investment to the stockholders. Various total quality management programs have been established within the industry to improve product quality, gain cost savings and customer satisfaction. A survey conducted by *Pulp & Paper* shows that 58 percent of mills were required by customers to have a quality program in 1994, while in 1992 only 40 percent of mills were required to do so [Ferguson, 1991, 1994]. Deming's philosophy about quality control has been a great inspiration for the more intensive and systematic application of statistical methods [Deming, 1986].

Probably the best example of a process control concept is the Six Sigma technique. The term "Six Sigma" was first coined by Motorola in 1980's as a production management strategy. Recently, this technique has gained attention and has been implemented by some major world-class companies, such as General Electric, Texas Instrument and Sony among many others [Breyfogle, 1999]. Enormous production savings have been achieved; for example, General Electric has reported over \$1 Billion savings during the period from 1995 to 1998, and the estimated annual savings is projected to be \$6.6 Billion by the year 2000.

It has been estimated that most companies operate between Three and Four Sigma, which means approximately from 6,200 to 67,000 defective products per million. In contrast, the Six Sigma companies only produce 3.4 defects per million. In the implementation of the strategy, key issues are identified, data are measured, and the statistical tools are used in a methodical and systematic way to improve product quality, reduce manufacturing cost, and increase operation efficiency.

In the paper industry, the endeavor to further improve quality control and management strategy will no doubt help the papermaker to achieve remarkable production savings. The partnership between pulp supplier and paper producer is vitally important for high quality paper production. It is often the case that the control on the raw material quality is the starting point for a quality program.

In this paper, the effects of market pulp from different suppliers on tissue manufacturing were investigated and the effects of key pulp properties on various tissue qualities were quantified.

D2. Experimental

Two kinds of pulp variations, i.e., inter-lot variations and within-a-lot variations, were investigated. Inter-lot variations are the changes that occur when different lots of pulp are used, while the within-a-lot variations reflect the pulp property changes when a single lot

of pulp is used. In the investigation, three groups of pulp, Hardwood A, Softwood A and Hardwood B, were studied.

The pulp samples were collected at a tissue mill during the period of one month. For inter-lot variation study, 39 lots of Hardwood pulp A, 19 lots of Softwood pulp B and 7 lots of Hardwood pulp B were tested. 5 lots of Hardwood pulp A, Softwood pulp A, and Hardwood pulp B were selected respectively for the within-a-lot variation study, and 5 samples from each lot were tested. Tissue product samples were collected on the mill site and tested.

Inter-lot pulp data (one-month period) were analyzed. The parameters used in the data analysis are listed in Table 1, and the meaning and the unit of each parameter are also given there. The best subset regression technique was used to correlate the tissue product quality with the pulp data and process variables in the statistical data analysis.

D3. Results and discussion

(I) Within-a-lot pulp variation

- Figure D.1 shows the tensile strength variations for Softwood pulp A, Hardwood pulp A and Hardwood pulp B. For all three kinds of pulp, the within-a-lot variations were around 20 percent. In terms of the tensile strength variation ($\Delta \text{Tensile} = \text{Tensile}_{\max} - \text{Tensile}_{\min}$), the Hardwood pulp B had the lowest value. The tensile strength order was the following:

$\text{Tensile}_{\text{Softwood A}} \gg \text{Tensile}_{\text{Hardwood A}} \gg \text{Tensile}_{\text{Hardwood B}}$.

- The pulp freeness variations are shown in Figure D.2. The freeness variation percentages for all three pulps were below 10 percent. The order of freeness values of the three pulp was the following:

$\text{Freeness}_{\text{Softwood A}} > \text{Freeness}_{\text{Hardwood B}} > \text{Freeness}_{\text{Hardwood A}}$.

- Among the 3 kinds of pulp, Hardwood pulp B consistently had the highest bulk. The within-a-lot bulk variation for the Softwood pulp A was 11.2 percent, but the bulk variations for both Hardwood pulp A and Hardwood pulp B were far below 10 percent. The order of bulk values of the three kinds of pulp was the following:

$\text{Bulk}_{\text{Hardwood B}} > \text{Bulk}_{\text{Softwood A}} > \text{Bulk}_{\text{Hardwood A}}$.

(II) Inter-lot pulp variation

- In terms of tensile strength, Hardwood pulp B samples consistently had the lowest strength values. The absolute tensile strength variations in Hardwood pulp B were significantly lower than those of Softwood pulp A and Hardwood pulp A (*See Figure D.4*).
- Hardwood pulp B showed much stable freeness values than Hardwood pulp A and Softwood pulp A. The freeness value of Hardwood pulp B was consistently higher than that of Hardwood pulp A and close to the freeness value of Softwood pulp B (*See Figure D.5*).

- Hardwood pulp B gave highest bulk values among the three kinds of pulp, and also showed the best inter-lot bulk stability (*See Figure D.6*). The bulk variation for Hardwood pulp B was only 6.6 percent, while the bulk variations for both Hardwood A and Softwood pulp A were beyond 12 percent.

(III) Statistical analysis

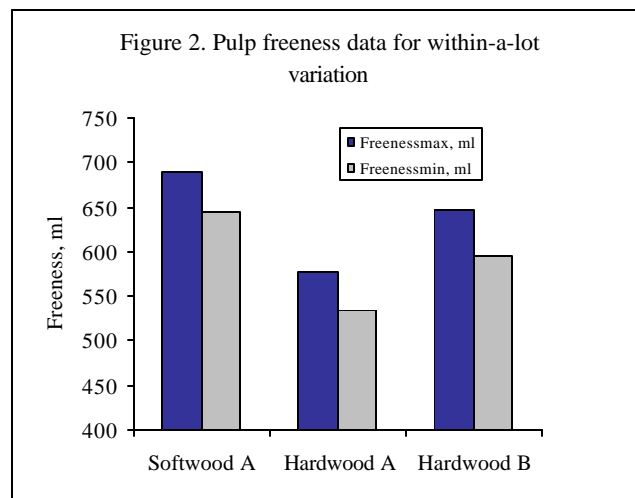
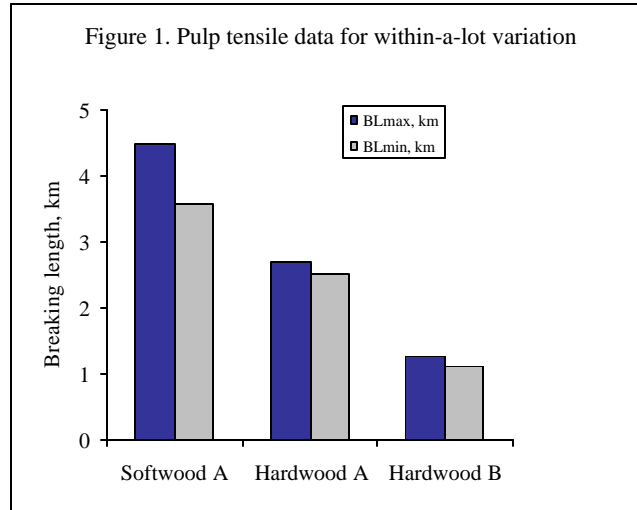
In the statistical analysis, the best subset regression technique was used. This method gives the highest degree of regression (characterized by adjusted correlation coefficient, R^2) for a response with a given set of regression factors. Three studies on the data were done:

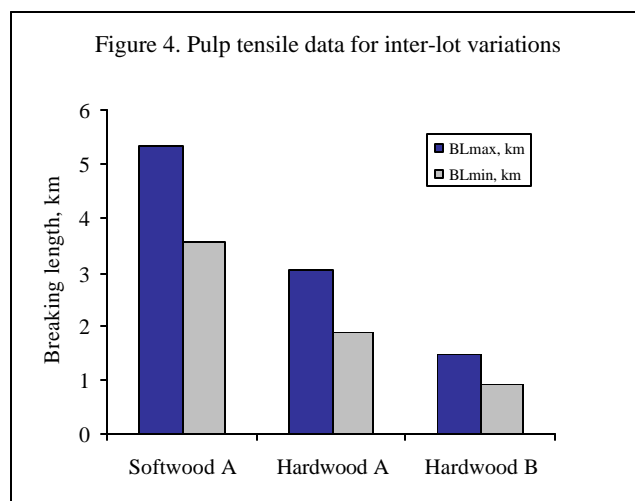
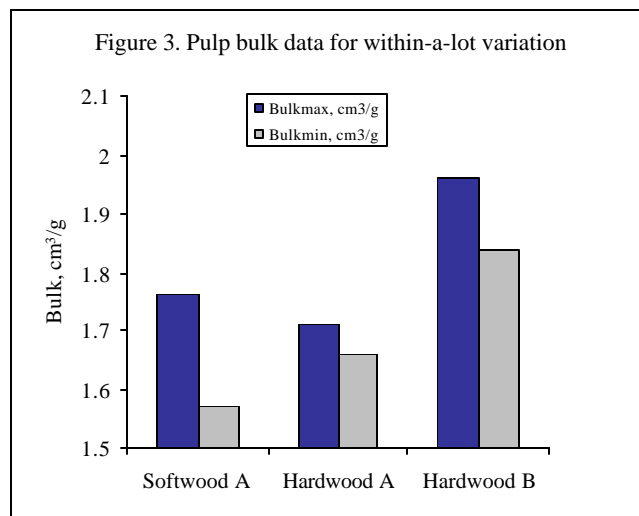
- (A): Correlation of tissue product property data with pulp testing data only,
- (B): Correlation of tissue product property data with all data available, including both pulp testing data and important process data, and
- (C): Correlation of tissue product property data with pulp property data, which were selected in the best subset regression of study (B).

The results of regression (A), (B) and (C) are given in Tables D.2, D.3 and D.4. In the papermaking process, there are as many as 300 process parameters. In our data analysis, only 9 process data were both available and important. For each kind of pulp, 3 pulp properties (tensile, freeness, bulk) were used for the analysis. Therefore, it is not

surprising that among the three studies, the best correlation achieved about 62% correlation (for CD wet tensile).

The study (B) had consistently higher correlation coefficients than the study (A), which showed clearly that pulp property variations were only part of the sources that contributed to tissue product property variations. However, it is important to investigate the relative percentage of the pulp factor's contribution to a specific product property. The pulp factor weight for each paper property was obtained through the comparison of the correlation coefficients of study (B) and (C).





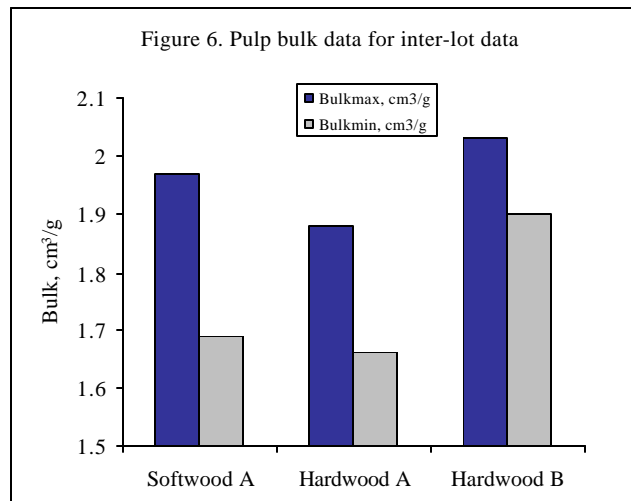
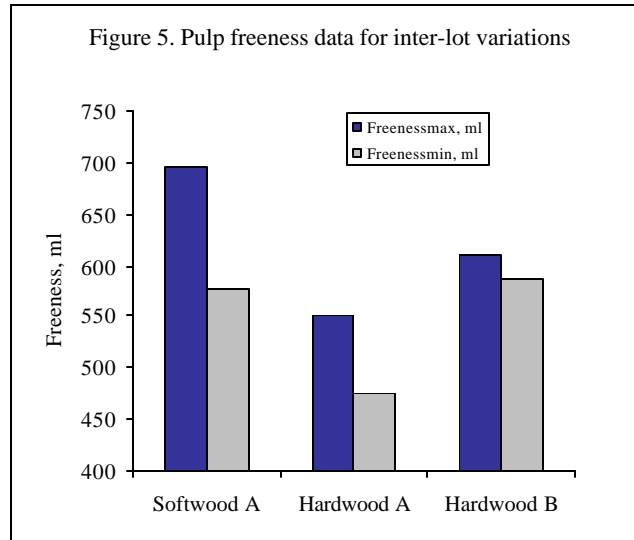


TABLE D.1 Parameters used in the data statistical analysis

| Product Property | | Pulp data | | Process data | |
|----------------------|----------------------|------------|------------------------------|-------------------|------------------------------|
| MDT | MD tensile, g/in | HAT | HWA tensile, km | RF | Recycle fiber flow rate, GPM |
| CDT | CD tensile, g/in | SWT | SW tensile, km | Broke | Broke flow rate, GPM |
| CDWT | CD wet tensile, g/in | HBT | HWB tensile, km | DD current | DD refiner current, Amps |
| MDS | MD stretch, % | HAF | HWA freeness, ml | Press | Top press roll load, psi |
| Bulk | As it is, .001 in | SWF | SW freeness, ml | Adhesion | Adhesion chemical rate, GPM |
| BW | Basis weight, lb./rm | HBF | HWB freeness, ml | Release | Release chemical rate, GPM |
| HF | Hand feel rating | HAB | HWA bulk, cm ³ /g | WSR | Wet strength resin rate, GPM |
| MDT/ CDT | As it is | SWB | ISW bulk, cm ³ /g | Blade P | Creping blade pressure, ply |
| CDWT/ CDT | As it is | HBB | SW bulk, cm ³ /g | Blade life | Creping blade life, hours |

TABLE D.2 Correlation of tissue properties with pulp testing data only

| Product properties | Correlation equations | R ² (adj, %) |
|--------------------|---|----------------------------|
| CDT | CDT = 463 - 12.3 HAT - 5.25 SWT - 19.3 HBT - 0.0950 SWF - 71.6 HAB - 33.9 SWB | 12.9 |
| CDWT | CDWT = 135 - 8.60 HAT - 9.45 SWT + 0.0601 HAF - 0.266 HBF - 54.2 HAB + 112 HBB | 36.2 |
| MDS | MDS = 53.0 + 1.91 HAT - 1.53 SWT - 3.25 HBT + 0.0148 HAF - 0.101 HBF + 8.40 HAB + 6.65 SWB | 26.4 |
| Bulk | Bulk = 121 + 2.87 HAT - 1.68 SWT - 12.0 HBT + 23.6 HAB + 21.8 SWB - 47.4 HBB | 25.8 |
| BW | BW = 10.1 + 0.097 HAT - 0.417 HBT + 0.000780 SWF + 0.800 SWB - 1.09 HBB | 25.1 |
| HF | HF = 67.8 + 2.24 HAT - 0.0456 HAF + 0.0313 SWF | 13.5 |
| MDT/CDT | MDT/CDT = 5.51 + 0.125 SWT + 0.00394 SWF - 0.0123 HBF + 1.05 SWB | 12.0 |
| CDWT/ CDT | CDWT/CDT = -1.65 - 0.054 SWT + 0.172 HBT + 0.000451 HAF + 0.102 SWB + 0.897 HBT | 17.5 |

TABLE D.3 Correlation of tissue properties with pulp and process data

| Product properties | Correlation equations | R ² (adj, %) |
|--------------------|---|----------------------------|
| CDT | CDT = 462 - 0.692 DD current - 139 Adhesion + 2.20 Blade life - 11.0 HAT - 6.08 SWT - 34.9 HBT - 0.0510 SWF - 71.2 HAB | 26.2 |
| CDWT | CDWT = 326 - 0.331 RF + 0.435 Broke - 0.0245 Press + 327 WSR + 28.1 Release - 0.00660 HAT - 0.00560 SWT - 23.1 HBT - 60.8 HAB - 53.0 HBB | 61.7 |
| MDS | MDS = 74.9 + 0.0280 RF + 0.0584 DD current - 0.00757 Press + 26.6 WSR - 0.205 Blade life + 1.82 HAT - 1.37 SWT - 4.95 HBT + 0.122 HAF - 0.131 HBF + 7.92 HAB + 6.95 SWB | 39.5 |
| Bulk | Bulk = 142 + 19.7 SWB + 18.2 HAB - 0.190 HBF + 0.0190 HAF - 6.52 HBT - 1.72 SWT - 24.8 Release + 28.0 Adhesion | 31.6 |
| BW | BW = 11.4 - 0.00490 DD current - 0.000169 Press + 2.44 WSR - 1.40 Release - 0.108 HAT - 0.240 HBT - 0.687 HWB + 0.306 SWB | 36.9 |
| HF | HF = 102 + 31.7 Adhesion + 0.310 Blade P - 1.09 Blade life - 0.0294 HAF - 16.8 SWB | 16.3 |
| MDT/CDT | MDT/CDT = -2.77 + 0.00956 RF + 0.0321 DD current + 4.59 Adhesion + 8.57 HBB + 1.50 SWB - 0.0369 HBF + 0.00533 SWF + 1.49 HBT | 44.5 |
| CDWT/ CDT | CDWT/CDT = 0.497 - 0.00232 RF + 0.00417 Broke + 0.00342 DD current + 1.57 WSR + 0.673 Adhesion + 0.700 HBB + 0.222 SWB - 0.181 HAB - 0.00383 HBF + 0.000496 SWF + 0.118 HBT - 0.03 SWT | 52.9 |

TABLE D.4 Correlation of tissue properties with pulp testing data selected in the best subset regression of study (B)

| Product properties | Correlation equations | R ² (adj, %) |
|--------------------|---|----------------------------|
| CDT | CDT = 372 - 11.5 HWT - 6.74 SWT - 17.6 HBT - 0.0591 SWF - 64.9 HAB | 11.7 |
| CDWT | CDWT = 18 - 8.40 HAT - 9.82 SWT + 12.0 HBT - 66.5 HAB + 110 HBB | 33.5 |
| MDS | MDS = 53.0 + 1.91 HAT - 1.53 SWT - 3.25 HBT + 0.0148 HAF - 0.101 HBF + 8.40 HAB + 6.65 SWB | 26.4 |
| Bulk | Bulk = 107 + 23.7 SWB + 14.2 HAB - 0.118 HBF + 0.0158 HAF - 7.38 HBT - 2.28 SWT | 22.6 |
| BW | BW = 8.70 + 0.091 HAT - 0.189 HBT - 0.150 HAB + 0.648 SWB | 22.2 |
| HF | HF = 104 - 0.0315 HAF - 9.98 SWB | 6.9 |
| MDT/CDT | MDT/CDT = -2.04 + 4.09 HBB + 1.73 SWB - 0.0167 HBF + 0.00491 SWF + 0.707 HBT | 11.3 |
| CDWT/ CDT | CDWT/CDT = -0.892 + 1.23 HBB + 0.229 SWB - 0.155 HAB - 0.00237 HBF + 0.000426 SWF + 0.171 HBT - 0.052 SWT | 14.6 |

$$\mathbf{c} = \frac{R^2_{adj,study(C)}}{R^2_{adj,study(B)}} \quad (1)$$

Important observations were made on the pulp factor weight value. Among various process data (9 process data) and pulp data, the pulp data as a whole contributed almost 72 percent to bulk value, 67 percent to MD stretch, 54 percent to CD wet tensile, 60 percent to basis weight, and 42.3 percent to handfeel. Figure D.7 shows pulp factor weight for each product property.

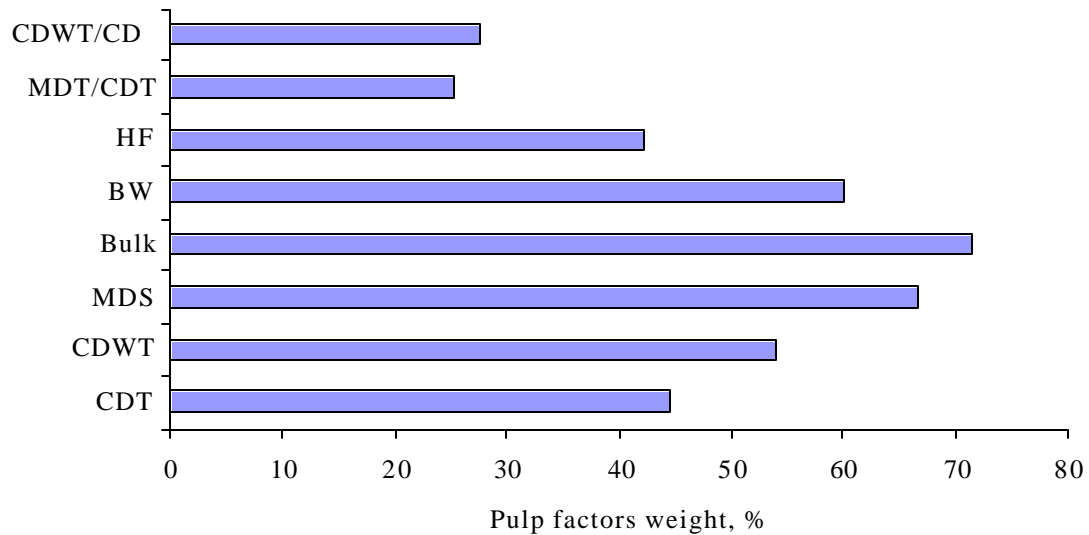


Figure D.7 Pulp factor weight for tissue product properties

D4. Conclusions

- Statistical analysis has shown that in various processes and pulp data, pulp data were shown to contribute a relatively big part of important tissue product property, such as bulk, MD stretch, CD wet tensile and hand feel. This shows that the tissue product quality is heavily dependent on the pulp properties. Therefore, it is important to use pulp from reliable sources and to maintain an on-going pulp quality-monitoring program.
- The pulp quality variation can be significant from one manufacturer to another, from one lot to another, and even within a single lot of pulp. For both within-a-lot variation and inter-lot variation, the following pulp property orders were observed:

$\text{Tensile}_{\text{Softwood A}} \gg \text{Tensile}_{\text{Hardwood A}} \gg \text{Tensile}_{\text{Hardwood B}}$

$\text{Freeness}_{\text{Softwood A}} > \text{Freeness}_{\text{Hardwood B}} > \text{Freeness}_{\text{Hardwood A}}$

$\text{Bulk}_{\text{Hardwood A}} > \text{Bulk}_{\text{Softwood A}} > \text{Bulk}_{\text{Hardwood A}}$

- High tensile strength variation was noticed for both within-a-lot variation and inter-lot variations. Among three pulp properties monitored, i.e., tensile, freeness and bulk, tensile strength fluctuation was highest. For the inter-lot tensile value monitoring, all three kinds of pulp got variations higher than 40 percent, while for the within-a-lot tensile value, all the pulp got variations around 20 percent.

- The contrast between Hardwood pulp A and Hardwood pulp B was sharp. Hardwood pulp A was superior to Hardwood pulp B in all three important pulp properties. It had lower tensile, higher freeness, and higher bulk.

D5. Reference

Ferguson, K. H., Customer Demands, Tighter Markets Drive Mills' Quality Control, *Pulp & Paper* March: 71-77 (1991)

Ferguson, K. H., Customer Focus, Fight Markets Drive Industry's Quality Emphasis, *Pulp & Paper* June: 65-71 (1994)

Deming, W. E., *Out of Crises*, MIT Press, Cambridge, MA (1986)

Breyfogle III, F. W., *Implementing Six Sigma: Smarter Solutions using Statistical*, Wiley, New York, NY (1999)

APPENDIX E

M/K 9000 FULLY AUTOMATIC SHEETFORMER OPERATION PROCEDURE

M/K automatic sheet former (M/K Systems, Denver, MA) is capable of producing sheet automatically in the laboratory and significantly improves the experimental efficiency. The M/K 9000 Fully Automatic Sheetformer is the most advanced model and consists of three sections, i.e., sheet forming, press and drying as shown in Figure E.1. This section describes the operation procedure of the M/K automatic sheet former. The operation of the sheet former consists of the preparation of the pulp slurry and chemical additives, the warm up of the dryer, setting up the operating parameters with M/K Automatic Sheet Former software, and the automatic sheet making by the machine.

E1. Stock feed tanks

The individual Stock Tank holds about 30 gallons of stock. According to the M/K Systems Inc.'s recommendation, the consistency of the stock tank should be about 0.15%. When the 0.15% fiber consistency is used, 20 sheets, each weighing 5.12g (60 g/m^2), can be formed from a full tank. The consistency of the stock tank can also be increased so that a full tank of stock can last longer. The consistency can be as high as 0.3%, and no problems have been encountered.

Consistency higher than 0.3% is not recommended. When the slurry consistency gets too high, the pulp fibers tend to flocculate, and it is becoming more difficult to control the variation of the basis weight from one sheet to another.

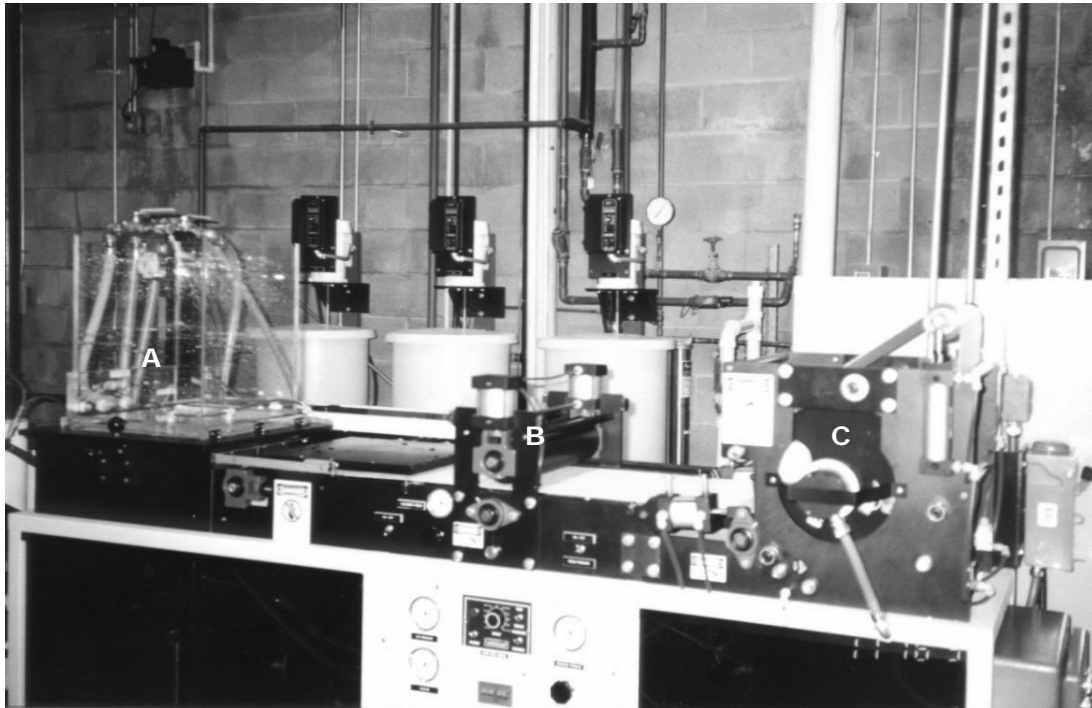


FIGURE E.1 M/K 9000 Fully Automatic Sheet-former. The instrument consists of three sections: (A) deckle tank. The pulp slurry is ejected from the stock tank, diluted with water, agitated by compressed air, after which water is drained and sheet is formed on the fabric. The sheet is transferred to the felt. (B) Press section. Extra water in the sheet is dewatered by vacuum and by the mechanical press of this section. (C) Dryer section. The sheet is finally dried by the dryer and comes out from this section to be conditioned.

In order to keep the stock in each tank agitated, each tank is equipped with a mixer with a variable speed control. Proper mixing is required in order to maintain uniform basis weight for the entire contents of the tank.

Note: Each mixer is equipped with two propellers. The lower propeller could not agitate the pulp slurry under it. Therefore, it is suggested that when the pulp slurry level is below the lower propeller, the stock in that stock tank should not be used to make sheet unless more pulp is added to the tank or the stock is transferred to another tank with good stock mixing.

E2. Chemical addition tanks

The chemical addition tank holds about 2 1/2 liters of a liquid chemical additive. M/K Systems Inc. suggests that if particulate additives such as clay suspensions are to be employed, the mixing motor should be used. In making low-basis weight sheet, the chemicals such as wet strength resin or debonding agents should also be mixed with the mixers.

The addition rate of additives is controlled by the stroke length and pulse frequency adjustments on the pumps. When the system works, the chemicals should be added to the deckle with momentum. If the chemical additive flow rate is too low, it is possible that air bubbles are entrapped in the plastic tube. The plastic tubing can be disconnected, and make sure that the air bubbles are driven out of the tube.

Each time when the sheet making is completed, the tubing must be cleaned with water. The reason is that when another chemical is to be tested, the old chemicals left from previous test will be added to the sheets.

Manual addition of the chemical additives can also be done. The chemicals can then be added directly to the deckle right after the addition of the pulp slurry and before the air agitation starts.

E3. Dryer warming up

The dryer usually requires about one hour to heat up to the designated temperature. The light on the heater housing on the dryer drum periodically flashes on and off when the dryer reaches the temperature. Be sure the drum is turning whenever the dryer is on; otherwise the felt could be damaged.

In case the dryer temperature needs to be adjusted, turn the thermostat screw on the front end plate of the dryer in the counter-clockwise direction to increase the temperature, and vice versa to decrease it. (There are two wires leading from the thermostat to the Dryer's heater housing.) Temperature is pre-set at the factory to 100°C. It is recommended to operate at this temperature.

When the dryer is at the pre-set temperature, the pressing pressure is set around 40psi. The manufacturer suggests that the press pressure ranges from 40 to 70 psi. The specific pressure used depends upon the sheet density desired, and it must be determined by trial

and error. It must be noted that high press pressure will leads to the felt marks (wavy shape) on the light weight paper and may cause the loss of dryer coating. If the dryer rotates, but the press felt does not, check the “press” button on the front panel of the sheet former. During the sheet making process, the button should be “on”. The dryer drives the press section to movement. If the Dryer is turning too fast to dry a sheet, or too slowly and over-dries the sheet, the speed should be adjusted by changing the setting of the speed controller. The dryer felt tension should be approximately from 20 to 30 psi.

E4. Setting the operating parameters of the setup menu

Enter the “Setup Menu” by selecting “Change Run Settings” from the “Settings” menu of the Sheet Former Menu bar if the Setup Menu is not already open. The setup menu consists of four menu pages: variables, recipes, chemicals, and save and load settings.

E4.1. Variables menu

The five primary variables of forming a sheet are shown in the left-hand column of the Setup menu under the heading "Variables". All have a maximum value of 999.9. Again, use the cursor keys to alter the original values of these variables. Stock addition can also be set with the method described below. The times entered here will be employed in all of the recipes unless altered during the course of sheet making.

Seven other operating variables displayed on the monitor have to be set as well. Check the box next to the function with the mouse (or keyboard using the tab and space keys), to turn the particular function on. When one exits the setup menu, any functions that selected as “ON” will appear as red on the main screen.

These seven functions are:

1. Setting "Change White Water" to ON will drain the white water tank after each sheet from a given tank is completed.
2. "Flush stock lines" is the same instruction for cleaning the stock lines with fresh water after each sheet. If this function is selected, the three-way valve should be open before the stock addition; after the addition of the stock (strictly speaking, before the wet sheet is pressed onto the press felt), the valve needs to be open to the stock tank. In the sheet-making process, after the wet sheet is pressed onto the press felt, the “flush stock lines” function starts. The fresh water will flush the stock to the stock tank. If the three-way valve is open to the deckle at that moment, the stock in the stock lines will be flushed to the drain. In order to save pulp, the “Flush stock lines” function is strongly recommended to use. If multiple sheets are made using one recipe, there is no need to open the three-way valve to the stock tank until the last sheet is made.
3. Setting "White Water Heater" to ON will turn on the heater in the white water tank. The heater will be turned off when the tank is drained. Usually this function is not selected unless a particular temperature is needed for the sheet-making process.

4. Setting "Continuous Sheet" to ON will create one continuous sheet by stopping the felt once the sheet has almost cleared the couch.
5. Setting "Hold on Agitate" to ON will automatically place the program in "hold" mode until the Resume button is depressed. It is observed that short time agitation leads to poor chemical retention on fiber. This function allows the operator to make the agitation as long as needed. The maximum of agitation time in the "Setup" menu is 99 seconds. Another alternative to the "hold on agitate" function is to add the chemical additive into the stock tank, and increase the contact time between the chemical and the pulp. The effect of longer chemical-pulp mixing time for the sheets made later in the process needs to be considered.
6. Setting "Drainage Assist" to ON will apply vacuum to the sheet mold to speed up the forming process. Line vacuum is employed for this purpose.
7. Turn on pH Control if desired and set the pH Lower Limit and pH Upper Limit variables to the desired range. Proper operation of the dosing depends on acid/base concentrations and the difference between the pH Lower and pH Upper Limits in order to prevent undershoot or overshoot of the pH reading. This machine is not equipped with automatic pH control capability; therefore, the addition of HCl or NaOH is manual.

Generally speaking, the most commonly used functions out of the above-mentioned seven are "flush stock lines", "drainage assist" and "hold on agitate".

E4.2. Recipes menu

This menu controls the addition of stock to the sheet former. Initially, recipe #1 calls for a sheet to be made entirely from the stock in tank #1. The pulp can come entirely from any of the three stock tanks.

The user may enter the combination of stocks to be employed for the sheet. The "recipe" is edited by locating the cursor on each variable using the mouse or the tab key of the computer. The new settings are then selected or typed.

As an example, the first sheet might be produced entirely from tank #1. In this case, enter "100" next to "% Stock tank #1". Alternatively, if this sheet is to be made from a 50/50 mixture of the stocks in tanks #1 and #3, type 50 next to these two lines. The total for each Recipe must always be 100%.

A maximum of three Recipes to produce three different sheet recipes can be entered at one time. Up to 99 sheets may be produced from each recipe. Once the Stock Recipes are entered you may return to the Variables menu to accept the settings or continue to the Chemicals menu.

If a mistake is made in the recipe menu, such as having the sum of the stocks in one Recipe total more or less than 100, a warning indicating the type of error made will appear. It is not possible to proceed as long as there is an error in the recipe menu.

E4.3. Chemicals menu

You may set the times of chemical additions from the chemical addition tanks under chemicals in the setup menu. These times can be set between 0 and 999 seconds.

The times of addition shown in the "Chemicals" column are employed for every sheet unless the "Inc. Chem. Times" is set. If the amount of additive per sheet is to be incremented, the variation is set in this column. The chemical times will be incremented by the amount set at the end of each sheet.

E4.4. Save/load settings menu

Once all of the settings have been programmed as you want them, you can save the settings in a file. There is virtually no limit to the number of different setups you can save. Be sure to give every different setup a different name.

Once all of the desired settings have been programmed, the operator should press the "Accept Settings" button to proceed.

E5. Set basis weight

This function can facilitate the adjustment of the sheet basis weight. Once the first sheet has been produced and weighed, the Stock Addition time is reset to produce sheets of the desired weight in the following manner.

Select the Set Basis Weight item from the Functions menu of the Sheet Former Menu Bar, type the weight of the last sheet produced (m_1) and press the RETURN key. Then, type the desired weight (m), and press RETURN. The Monitor will now display and set

the proper Stock Addition time (t) as well as the basis weight of the sheet being produced in both English and Metric units. Note that the Set Basis Weight function is only allowed when the Setup Menu is not open.

The calculation the program used to calculate the desired stock addition time is as the following, and the unit of the sheet mass is in gram

$$t = \frac{m}{m_1} t_1 \quad (E5.1)$$

$$BW = 9.92m \text{ (g/m}^2\text{)} \quad (E5.2)$$

$$BW = 6.09m \text{ (lb/3,000ft}^2\text{)}. \quad (E5.3)$$

Although the sheet former provides the “set basis weight” function, it has been found that hand calculation often will not take longer time than the computer program. The operator is free to choose the method he prefers.

E6. Running the sheet former

Once all of the variables have been accepted, the Sheet Former is ready to begin making sheets. Press the Start Run button to initiate the process. The computer program will instruct the sheet former to make sheets automatically. If all the parameters have been set properly, no further operator intervention is needed.

The sheet forming process begins with the cleaning of the wire. While in progress, each operation and its remaining time are indicated in the lower status bar. In addition, the date and time at which sheet formation was initiated are displayed. White water, stock, chemical additives and, lastly, pH (if so equipped) is adjusted accordingly. The mixture is agitated, allowed to settle, and sheet formation takes place by the automatic opening of a ball valve below the sheet mold.

During Stock Addition the number of the Tank from which stock is currently being taken is displayed. When the sheet is being formed, the total time of formation, i.e., Drainage Time, is indicated in the status bar. The Drainage Time is also recorded for each sheet and can be printed out along with all of the operating variables and conditions. Until the formation of a sheet proceeds, the Drainage Time indicated on the monitor refers to the previous sheet formed.

Once the Sheet Former has produced all of the sheets called for by the RECIPE MENU, it shuts itself down automatically, leaving water in the deckle to keep the screen moist. Prior to shutting down, it will perform the cleaning functions called for by the Setup menu.

E7. Shut down the sheet former

When the operation of the sheet former is finished, empty all the stock tanks, otherwise the pulp may cause plugging in the stock lines if the stock is left for a

prolonged period of time. Turn off the mixers equipped for the stock tanks. Exit the “M/K Automatic Sheetformer” program. Stop the vacuum pump. Turn off the “press” on the front panel of the sheet former frame so that the press felt is disengaged from the dryer. Turn off the dryer heater switch and the main power switch. The compressed air should be left on all the time.

VITA

Jin Liu was born in Henan, People's Republic of China. He graduated from Luoyang No.1 Senior High School in 1989, and received his B.S. degree in Chemical Engineering from Tianjin University with distinguished honor in 1993. In 1995, he came to Atlanta, Georgia for advanced studies at the School of Chemical Engineering at Georgia Institute of Technology.

In 1997, he was awarded M.S. degree in Chemical Engineering at Georgia Tech under the direction of Dr. Mark R. Prausnitz. His work with Dr. Prausnitz led to a US/internal patent on ultrasound mediated drug delivery and a technical paper award from Science Application International Corporation (SAIC). In the fall of 1997, he joined the research group of Dr. Jeffery S. Hsieh to pursue the Ph.D. study.

He is a member of American Institute of Chemical Engineers, American Chemical Society and Technical Association of Pulp and Paper Industry. On August 30, 1998, he was baptized in Christ Church Presbyterian in Atlanta, GA, and has been a member of that church since. On March 8, 2001, he became a permanent resident of United States.